

FINAL REPORT
ADVANCED SUPERSONIC TECHNOLOGY
CONCEPT STUDY-
HYDROGEN FUELED CONFIGURATION

by G.D. Brewer

JANUARY 1974

Distribution of this report is provided in the interest of
information exchange. Responsibility for its contents
resides in the author or organization that prepared it.

Prepared under Contract NAS 2-7732

for
AMES RESEARCH CENTER
NATIONAL AERONAUTICS AND
SPACE ADMINISTRATION

by
LOCKHEED - CALIFORNIA COMPANY
 **BURBANK, CALIFORNIA**

A DIVISION OF LOCKHEED AIRCRAFT CORPORATION

(NASA-CR-114718) ADVANCED SUPERSONIC
TECHNOLOGY CONCEPT STUDY: HYDROGEN
FUELED CONFIGURATION Final Report, Jul.
- Dec. 1973 (Lockheed-California Co.)
326 p

N75-10943

Unclas

CSC 21D G3/07 02714

Reproduced by
NATIONAL TECHNICAL
INFORMATION SERVICE
US Department of Commerce
Springfield, VA. 22151

175-10943

1. Report No. NASA CR 114718		2. Government Accession No.		3. Recipient's Catalog No.	
4. Title and Subtitle FINAL REPORT - ADVANCED SUPERSONIC TECHNOLOGY CONCEPT STUDY - HYDROGEN FUELED CONFIGURATION				5. Report Date January 1974	
				6. Performing Organization Code	
7. Author(s) G. D. Brewer				8. Performing Organization Report No. LR 26323	
9. Performing Organization Name and Address LOCKHEED-CALIFORNIA COMPANY P.O. Box 551 Burbank, California 91520				10. Work Unit No.	
				11. Contract or Grant No. NAS 2-7732	
12. Sponsoring Agency Name and Address National Aeronautics and Space Administration Ames Research Center Moffett Field, California 94035				13. Type of Report and Period Covered Contractor Report	
				14. Sponsoring Agency Code	
15. Supplementary Notes					
16. Abstract <p>Conceptual designs of hydrogen fueled supersonic transport configurations for the 1990 time period were developed and compared with equivalent technology Jet A-1 fueled vehicles to determine the economic and performance potential of liquid hydrogen as an alternate fuel.</p> <p>Parametric evaluations of supersonic cruise vehicles with varying design and transport mission characteristics established the basis for selecting a preferred configuration which was then studied in greater detail.</p> <p>An assessment was made of the general viability of the selected concept including an evaluation of costs and environmental considerations, i.e., exhaust emissions and sonic boom characteristics. Technology development requirements and suggested implementation schedules are presented.</p> <p style="text-align: center;">PRICES SUBJECT TO CHANGE</p>					
17. Key Words (Suggested by Author(s)) Hydrogen, supersonic, propulsion, aerodynamics, arrow-wing, cryogenics, structures, costs, weight, noise, emissions.				18. Distribution Statement	
19. Security Classif. (of this report) Unclassified		20. Security Classif. (of this page) Unclassified		21. No. of Pages 320	
				22. Price*	

*For sale by the National Technical Information Service, Springfield, Virginia 22151

FINAL REPORT
ADVANCED SUPERSONIC TECHNOLOGY
CONCEPT STUDY-
HYDROGEN FUELED CONFIGURATION

by G.D. Brewer

JANUARY 1974

Distribution of this report is provided in the interest of
information exchange. Responsibility for its contents
resides in the author or organization that prepared it.

Prepared under Contract NAS 2-7732

for
AMES RESEARCH CENTER
NATIONAL AERONAUTICS AND
SPACE ADMINISTRATION

by
LOCKHEED - CALIFORNIA COMPANY
 **BURBANK, CALIFORNIA**

A DIVISION OF LOCKHEED AIRCRAFT CORPORATION

u-a

ERRATA TO NASA CR 11418
FINAL REPORT, ADVANCED SUPERSONIC TECHNOLOGY CONCEPT STUDY -
HYDROGEN FUELED CONFIGURATION

- Page iii - Correct spelling of R. Sessing
- Page 16 - The graphic illustrations of Figures 4 and 5 should be interchanged
- Page 58 - Figure 31 - DTAM callout should read DTAM = 15C (27F)
- Page 68 - Figure 40 DTAM callout should read DTAM = 15C (27F). Also - engine identification should read, LH₂TJ-2 STD + 15C T/O
- Page 172 - Reference to Table 18 in line 10 of Para. 4.2.1 - should be Table 13
- Page 177 - Figure 86 - Point design symbol should be relocated on an extension of each curve to the 4200 NM range mark
- Page 179 - Figure 90 - Curve identification labels should be interchanged
- Page 186 - 6th line - Fuel function should be "fuel fraction"
- Page 197 - Table 23 should read -
DOC Cents/seat kilometer (cents/S n. mi.) 1.111(1.78) 1.012(1.629)
IOC Cents/seat kilometer (cents/Sn. mi.) 0.498(0.801) 0.497(0.799)
- Page 242 - Table 33 - insert additional technology development item.
"o A flight demonstration program involving conversion of existing subsonic aircraft to LH₂ fuel and use in simulated airline operation."
- un*

FOREWORD

This is the final report of a study of Hydrogen Fueled Advanced Supersonic Technology aircraft performed under contract NAS 2-7732 for NASA-Ames Research Center, Moffett Field, California. The report presents documentation of the substance of the work performed during the six months period, July through December 1973.

The work was accomplished in two phases. Phase I was a parametric analysis to determine the effect of different vehicle configurations and design concepts on performance, weight, and cost as a function of design range. Phase II was a study of a single point-design airplane at a level of depth sufficient to afford a credible basis for comparison with a Jet A-1 fueled vehicle designed for the same mission.

The study was performed within the Science and Technology Branch of the Lockheed-California Company at Burbank, California, under the direction of G. Daniel Brewer as study manager. Robert E. Morris was project engineer. Other principal investigators were:

C. F. Ehrlich	aerodynamics
E. L. Bragdon	propulsion
H. E. Young	design
C. W. Lindblom	
R. N. Jensen	weights
R. D. Mijares	
L. A. Vaughn	cost
R. Johnston	
R. Sessign	stress
I. F. Sakata	
R. S. Peyton	vehicle synthesis
T. G. Vanderbrug	thermodynamics
E. F. Versaw	fuel systems

Mr. Charles Castellano, of the Advanced Vehicle Concepts Branch of NASA-Ames Research Center, was technical monitor for the work.



TABLE OF CONTENTS

	Page
SUMMARY	ix
LIST OF ILLUSTRATIONS	xi
LIST OF TABLES	xvii
NOMENCLATURE	xix
1.0 INTRODUCTION	1
2.0 TECHNICAL APPROACH	3
3.0 PHASE I - EXPLORATORY ANALYSIS	7
3.1 BASIC DATA GENERATION	7
3.1.1 Preliminary Sizing Estimate	7
3.1.2 Aerodynamic Parametric Data	9
3.1.3 Propulsion Data	33
3.1.3.1 Mach 2.7 Turbofan	39
3.1.3.2 Mach 2.7 Turbojet	55
3.1.3.3 Mach 2.2 Turbojet	67
3.1.4 Materials Selection	76
3.1.4.1 Requirements	76
3.1.4.2 Candidate Materials	76
3.1.5 Weight Parameters	84
3.1.5.1 Basis for Weight Estimates in Phase I	84
3.1.5.2 Fuel Volume Available	85
3.1.6 Cost Parameters	87

Preceding page blank

TABLE OF CONTENTS(CONT)		Page
3.1.6.1	Development	87
3.1.6.2	Investment	89
3.1.6.3	Operations	90
3.2	PARAMETRIC VEHICLE STUDY.	93
3.3	RESULTS OF PHASE I PARAMETRIC STUDY	97
3.3.1	Design Trends	97
3.3.2	Cost Trends	104
3.3.3	General Conclusions	107
3.3.4	Candidate Vehicle Selection	108
4.0	PHASE II: VEHICLE POINT DESIGN STUDY	111
4.1	VEHICLE DESCRIPTION	111
4.1.1	Design Requirements	112
4.1.2	Design Evolution	113
4.1.3	Configuration Description	124
4.1.3.1	Vehicle Description	143
4.1.3.2	Aerodynamic Characteristics	150
4.1.3.3	Propulsion System Description	162
4.1.3.4	Fuel System Description	162
4.1.4	Mass Properties	166
4.1.4.1	Weight Statement	166
4.1.4.2	Materials Utilization	169
4.1.4.3	Vehicle Balance and Moment of Inertia	169

TABLE OF CONTENTS(CONT)

	<u>Page</u>
4.2 VEHICLE PERFORMANCE	172
4.2.1 Design and Performance Characteristics	172
4.2.2 Sensitivity Analysis	174
4.2.3 Environmental Summary	186
4.2.3.1 Airport Noise and Footprint	186
4.2.3.2 Sonic Boom Signatures	186
4.2.3.3 Emissions	194
4.3 VEHICLE COST	196
4.3.1 Summary of Vehicle Cost	196
4.3.2 System Cost Sensitivities	199
4.4 STRUCTURES	202
4.4.1 Design Load Conditions	202
4.4.2 Structural Analysis	209
4.4.2.1 Wing Structure	210
4.4.2.2 Fuselage Structure	213
4.4.2.3 Empennage Structure	217
4.4.2.4 Fuel Tanks	217
4.5 INSULATION EVALUATION	223
4.5.1 Approach	223
4.5.2 Design Configuration	223
4.5.3 Thermal Environment	225
4.5.4 Analysis Method	226
4.5.5 Results	227

TABLE OF CONTENTS(CONT)

5.0	CONCEPT VIABILITY	<u>Page</u> 235
5.1	CRITICAL EVALUATION	235
5.1.1	Comparison with Equivalent Jet A-1 Vehicle	235
5.1.2	Community Acceptance	239
5.1.3	Level of Technical Risk	241
5.1.4	FAA Regulation Compatibility	243
5.2	MAJOR TECHNOLOGY DEVELOPMENT REQUIRED	244
5.3	CONCLUSIONS	245
6.0	RECOMMENDATIONS	247
	REFERENCES	249
	APPENDICES	
	A. Cost Model Description	A-1
	B. Computer Printout of Point Design Vehicle	B-1
	C. Tank Structure Calculations	C-1

SUMMARY

This study has examined the feasibility of supersonic transport aircraft which use liquid hydrogen as the fuel. In Phase I a parametric analysis was carried out to determine a preferred configuration among the wide variety of possibilities that were examined. In Phase II, one vehicle of the selected configuration was studied to establish an acceptable basic design concept for the vehicle structure, the cryogenic fuel tanks, and the tank thermal protection system. The size, weight, and cost of this design of hydrogen fueled AST aircraft were then determined as required for the following mission capability:

Cruise speed	Mach 2.7
Range	7778 km. (4200 n.mi.)
Payload	22,226 kg. (49,000 lb.) (234 passengers)

Design tradeoffs, and performance and cost sensitivities were then evaluated.

An analysis was made of the environmental compatibility of the hydrogen fueled aircraft in terms of noise, sonic boom overpressure, and exhaust emissions. The design was then compared with that of a conventionally fueled AST airplane designed to the same criteria. The hydrogen fueled aircraft was found to provide advantages in nearly every category of comparison:

		Jet A-1	LH ₂
Gross Weight	(lb.) kg.	(750,000) 340,194	(368,000) 166,922
Operating Empty Weight	(lb.) kg.	(309,700) 140,478	(223,100) 101,196
Fuel Weight	(lb.) kg.	(391,300) 177,491	(95,900) 43,500
Engine Thrust	(lb.) newtons	(89,500) 398,100	(46,000) 204,600
Cost			
RDT & E	\$ x 10 ⁹	4.28	3.32
Production Aircraft	\$ x 10 ⁶	67.33	47.97
Noise			
Sideline	EPNdB	108	106.1
Flyover	EPNdB	108	104.2
Sonic Boom Overpressure	(psf) newton/m ²	(1.86) 89.1	(1.32) 63.2
Energy per Seat Mile	(Btu/seat n.mi.) joule/seat m	(6102) 3479	(4274) 2437
Emissions			
		CO	None
		HC	None
		NO _x	Minimal
		H ₂ O	~ Twice as much
		Noxious Odor	None

SUMMARY(CONT)

A comparison of direct operating cost and/or return on investment is strongly dependent on the cost of fuel. Analysis has shown the DOC of the two vehicles to be approximately equal when the cost of liquid hydrogen, in \$/Btu, is not more than 1.75 times that of Jet A-1 fuel. At current prices being paid for petroleum based fuels, this ratio is well within the cost estimated by several authorities for making liquid hydrogen from coal and water.

A program for developing technologies required for designing, building, and operating liquid hydrogen fueled supersonic transport aircraft is described and recommended for implementation. One of the urgent items is a recommendation to carry out a flight demonstration program using existing, subsonic transport aircraft converted to liquid hydrogen, to provide practical, operational experience in establishing design requirements and handling specifications for the new fuel.

FIGURES

FIGURE	PAGE
1. Configuration Variables	10
2a. Wing Definition for $S_W = 743.2$ sq. m (8000 sq. ft.)	11
2b. Wing Definition for $S_W = 1005.4$ sq. m (10,822 sq. ft.)	12
2c. Wing Definition for $S_W = 13006$ sq. m (14,000 sq. ft.)	13
3. Wing Thickness Ratio	14
4. Fuselage Area Distribution	16
5. Fuselage Section Definition	16
6. Drag-Due-to Lift Parameters	18
7a. Wave Drag Coefficients $S_W = 743.2$ sq. m (8000 sq. ft.)	20
7b. Wave Drag Coefficients $S_W = 975.5$ sq. m (10,500 sq. ft.)	21
7c. Wave Drag Coefficients $S_W = 1300.6$ sq. m (14,000 sq. ft.)	22
8. Component Wave Drag Data	23
9a. Low Speed Lift Characteristics - In Ground Effect	24
9b. Low Speed Lift Characteristics - Out of Ground Effect	25
10a. Low Speed Drag Polars - In Ground Effect	26
10b. Low Speed Drag Polars - Out of Ground Effect	27
11. Skin Friction Drag Increment for Body-Wing Combination	28
12a. Low Speed Lift - In Ground Effect	29
12b. Low Speed Lift - Out of Ground Effect	30
13a. Low Speed Drag Polars - In Ground Effect ($M_D = 2.2$)	31
13b. Low Speed Drag Polars - Out of Ground Effect ($M_D = 2.2$)	32
14. Engine Thrust/Weight Ratio Trends	35
15. Turbine Inlet Temperature Trends	36
16. Inlet Recovery	37
17. Spillage and Drag Coefficients	38
18. Nozzle Velocity Coefficients	40
19. D-B Turbofan Engine Cycle Selection	41
20. Installed Flight Performance (Thrust)	42
21. Installed Flight Performance (Thrust)	43
22. Installed Flight Performance (Fuel Consumption)	44
23. Installed Flight Performance (SFC)	45

FIGURES (CONT)

FIGURE	PAGE
24. Installed Flight Performance (SFC)	46
25. Installed Flight Performance (SFC)	47
26. Duct Burning Turbofan Schematic	49
27. Dry Turbojet LH2TJ-2 Nacelle Dimensions and Scaling Data	50
28a. Sideline Suppressed Duct Jet Noise (Augmented)	51
28b. Jet Noise Conversion to EPNL	52
28c. Jet Noise Suppressor Performance	53
29. AST Jet Noise Suppressor Performance	54
30. Turbojet Engine Cycle Selection - OPR Varied	56
31. Installed Flight Performance - Thrust	58
32. Installed Flight Performance - Thrust	59
33. Installed Flight Performance - SFC	60
34. Installed Flight Performance - SFC	61
35. Installed Flight Performance - SFC	62
36. Installed Flight Performance - SFC	63
37. Turbojet vs. Turbofan Performance Comparison	64
38. Hydrogen Fueled Dry Turbojet LH2TJ-1 (Mach 2.7)	65
39. Mach 2.7 Hydrogen Fueled Dry Turbojet Nacelle Dimensions and Scaling Data	66
40. Installed Flight Performance - Thrust	68
41. Installed Flight Performance - Thrust	69
42. Installed Flight Performance - Fuel Consumption	70
43. Installed Flight Performance - SFC	71
44. Installed Flight Performance - SFC	72
45. Installed Flight Performance - SFC	73
46. Hydrogen Fueled Dry Turbojet LH2TF-2 (Mach 2.2)	74
47. Mach 2.2 Hydrogen Fueled Dry Turbojet LH2TJ-2. Nacelle Dimensions and Scaling Data	75
48. Candidate Aluminum Alloys Comparison	78
49. ASSET Synthesis Cycle	94
50. ASSET Program Schematic	94
51. Data Presentation and Reduction	96

FIGURES (CONT)

FIGURE		PAGE
52.	Wing Area and t/c vs. Gross Weight (Constant Range)	98
53.	Weight Fractions and Cruise L/D vs. Wing Area	99
54.	Effect of t/c and W/S on Gross Weight	100
55.	Vehicle Range - Weight and Engine Comparison	102
56.	Comparison of Off-Mission Performance - Turbojet vs Turbofan	103
57.	DOC Cost Comparison	105
58.	Candidate Payload/Tank/Structural Arrangements	114
59.	Passenger Compartment Arrangements	117
60.	1975 Technology - Non-Integral Tank Concept	120
61.	Integral Tank Concepts	121
62.	General Arrangement - Liquid Hydrogen Fueled Phase II Design Aircraft	125
63.	General Arrangement - Jet A-1 AST	127
64.	Interior Arrangement - Phase II Point Design Aircraft	131
65.	Interior Arrangement - Jet A-1 AST	133
66.	Main Landing Gear Arrangement - LH_2 Fueled AST	137
67.	Inboard Power Plant Installation - LH_2 Fueled AST	141
68.	Low Speed Lift Characteristics	144
69.	Low Speed Drag Polars	145
70.	Skin Friction Drag	146
71.	Wave Drag	147
72.	Trim Drag	148
73.	Drag-due-to-Lift Parameters	149
74.	Wing Camber Drag	151
75.	Range vs Duct Burning Temperature	152
76.	Mach 2.7 Hydrogen Fueled Duct Burning Turbofan Nacelle Dimensions and Scaling Data	154
77.	Installed Flight Performance - Noise Limited Takeoff Power (Augmented)	155
78.	Installed Flight Performance - Augmented Max Climb	156
79.	Installed Flight Performance - Augmented Max Climb	157
80.	Installed Flight Performance - Non-Augmented Part Power	158

FIGURES (CONT)

FIGURE	PAGE
81. Installed Flight Performance - Non-Augmented Part Power	159
82. Installed Flight Performance - Augmented Part Power	160
83. Fuel System Schematic	163
84. Mass Properties vs. Aircraft Gross Weight	171
85. Noise and Gross Weight vs. T/W and W/S	176
86. Gross Weight, W/S, T/W, and T.O. Field Length vs. Range	177
87. Empty Weight Change vs. Gross Weight (Constant Range)	178
88. Empty Weight Change vs. Range (Constant Gross Weight)	178
89. Specific Fuel Consumption vs. Range	179
90. Effect of Subsonic Cruise Leg on Total Range	179
91. Payload vs. Range (Point Design)	180
92. Gross Weight vs. Engine Noise	182
93. Range vs. Drag Level	183
94. Gross Weight vs. Landing Field Length	184
95. Engine Takeoff Power Setting vs. Takeoff Distance and Noise	185
96. Takeoff Noise Contours	187
97. Area Contained Within Constant Noise Level Contour Lines vs. Effective Perceived Noise Levels	188
98. Sonic Boom Overpressure Signature - Weight = 356K LB.	189
99. Sonic Boom Overpressure Signature - Weight = 351K LB.	190
100. Sonic Boom Overpressure Signature - Weight = 344K LB.	191
101. Sonic Boom Overpressure Signature - Weight = 287K LB.	192
102. DOC/ROI vs. Utilization	200
103. ROI vs. Load Factor	200
104. DOC/ROI vs. Stage Length	201
105. ROI vs. Fare Level	201
106. DOC/ROI vs. Fuel Cost	203
107. Production Cost vs. Production Quantity	203
108. DOC/ROI vs. Production Quantity	204
109. Fuselage and Contents Shear - Gear Up	206
110. Forebody Shear and Bending Moments (Lim.)	207

FIGURES (CONT)

FIGURE	PAGE
111. Afterbody Shear and Bending Moments (Lim.)	208
112. Structural Arrangement - Sheet 1	211
113. Structural Arrangement - Sheet 2	215
114. Boiloff Summary for Non-Integral AST LH ₂ Tankage	228
115. Non-Integral Tank - Interface Temperature	229
116. Non-Integral Tank - Mission Boiloff	229
117. Non-Integral Tank - Total Insulation + Boiloff	230
118. Integral Tank - Interface Temperature	230
119. Integral Tank - Mission Boiloff	231
120. Integral Tank - Total Insulation + Boiloff	231
121. DOC vs. Cost of Fuel	240
122. LH ₂ AST Conceptual Development Schedule	244
A-1 Aircraft Flyaway Cost Model	A-6

LIST OF TABLES

<u>Table</u>		<u>Page</u>
1	Vehicle Mission and Configuration Parameters	4
2	Basic Guidelines	4
3	Changes in Basic Guidelines for Phase II	6
4	Preliminary Vehicle Sizing	7
5	Tail Volume Coefficients	15
6	Propulsion Technology Forecast	34
7	Liquid Hydrogen Turbojet and Turbofan Cycle Characteristics (SLS, Uninstalled)	57
8	Composite Material Properties	79
9	Physical Properties of Films	82
10	Vehicle LH ₂ Capacity Estimate	86
11	Phase I Production Cost Comparison	106
12	Characteristics of Selected Vehicles from Phase I	109
13	Changes in Basic Guidelines for Phase II	113
14	Tankage/Thermal Protection Concept Comparison	122
15	Liquid Hydrogen Duct Burning Turbofan Cycle Characteristics (SLS, Uninstalled)	153
16	Weight Statement	168
17	Materials Utilization	170
18	Point Design Vehicle Characteristics	173
19	Sideline Noise Level Matrix for Plotting Footprint Contours	193
20	Sonic Boom Table	194
21	Emissions - Jet A-1 vs LH ₂ Fuel	195
22	Investment Cost Summary	196
23	System Cost Summary (4,200 n.mi. Stage Length)	197
24	System Cost Summary (2,200 n.mi. Stage Length)	198
25	Fuselage Loads - LH ₂ AST	205
26	Weight Breakdown: Non-Integral Tanks	219
27	Weight Breakdown: Integral Tanks	222

Preceding page blank

LIST OF TABLES (Continued)

<u>Table</u>		<u>Page</u>
28	Insulation Thermodynamic Properties	225
29	Comparison of Non-Integral vs Integral Insulation Systems	233
30	Comparison of Jet A-1 and LH ₂ Fueled Supersonic Transports of Advanced Design	236
31	Cost Comparison: Jet A-1 vs LH ₂ AST's	238
32	Community Acceptance Parameters	241
33	Major Technology Development Required for LH ₂ Fueled AST Aircraft	242
A-1	Asset Cost Input	A-7

TABLE OF NOMENCLATURE

A	= Fuselage Cross Sectional Area
A_C	= Capture Area
APU	= Auxiliary Power Unit
AR	= Aspect Ratio
AST	= Advanced Supersonic Technology
α	= Angle of Attack
α_{WPR}	= Angle of Attack - Wing Reference Plane
BL	= Buttock Line
C_D	= Drag Coefficient
$C_{D\pi}$	= Drag Coefficient based on Frontal Area
$C_{D_{CAMBER}}$	= Wing Camber Drag Coefficient
C_{D_F}	= Friction Drag Coefficient
$C_{D_{HT}}$	= Drag Coefficient - Horizontal Tail
C_{D_i}	= Induced Drag Coefficient
C_{D_K}	= Wing Camber Drag Coefficient
C_{D_R}	= Roughness Drag Coefficient
$C_{D_{TRIM}}$	= Trim Drag Coefficient
$C_{D_{VT}}$	= Drag Coefficient - Vertical Tail
C_{D_W}	= Zero Lift Wave Drag Coefficient
$C_{D_{WING}}$	= Drag Coefficient - Wing
C_L	= Lift Coefficient
C_{L_K}	= Lift Coefficient for Minimum Drag
C_p	= Specific Heat
C_v	= Nozzle Velocity Coefficient
CO	= Carbon Monoxide
CO ₂	= Carbon Dioxide
D _{COMP}	= Compressor Diameter

TABLE OF NOMENCLATURE (Continued)

D_{MAX}	=	Nacelle Diameter
D_{NOZ}	=	Nozzle Diameter
DOC	=	Direct Operating Cost
D/B	=	Duct Burning
Δ	=	Increment
δ_{TE}	=	Flap Deflection - Trailing Edge
E_C	=	Compressive Modulus of Elasticity
E_t	=	Tensile Modulus of Elasticity
F_{CU}	=	Compressive Ultimate Strength
F_{CY}	=	Compressive Yield Strength
F_n, F_N	=	Net Thrust
F_{TU}	=	Tensile Ultimate Strength
F_{TY}	=	Tensile Yield Strength
FAA	=	Federal Aviation Authority
$FN_{L.O.}$	=	Net Thrust at Lift-off
FN_{SLS}	=	Uninstalled Thrust at Sea Level Static
FPR	=	Fan Pressure Ratio
FR	=	Body Fineness Ratio
F.S.	=	Fuselage Station
h	=	Altitude
H_2O	=	Water
HP	=	High Pressure
IOC	=	Indirect Operating Cost
I_{XX}	=	Moment of Inertia - X axis
I_{YY}	=	Moment of Inertia - Y axis
I_{ZZ}	=	Moment of Inertia - Z axis
k	=	Thermal Conductivity
K	=	Induced Drag Parameter
K_{CI}	=	Fracture Toughness
K_g	=	Kilogram
km	=	Kilometer
l, L	=	Fuselage Length
LA	=	A parameter used in sonic boom analysis. Arbitrarily assumed to be 800 ft. for present study.

TABLE OF NOMENCLATURE (Continued)

L_{ENG}	=	Engine Length
L_{INLET}	=	Inlet Length
LH_2	=	Liquid Hydrogen
LP	=	Low Pressure
L/D	=	Lift/Drag
M	=	Mach
m	=	meter
M_Y	=	Moment - Y axis
MAC	=	Mean Aerodynamic Chord
MEW	=	Manufacturers Empty Weight
MLG	=	Main Landing Gear
n_z	=	Load Factor - Z axis
NLG	=	Nose Landing Gear
N.M., n.m.	=	Nautical Mile
NO_X	=	Oxides of Nitrogen
OEW	=	Operating Empty Weight
p	=	Tank pressure
R	=	Range
R_B	=	Body Radius
ROI	=	Return on Investment
ρ	=	Density
SFC	=	Specific Fuel Consumption
S_{REF}	=	Reference Wing Area
S_W	=	Wing Area
S_Z	=	Shear - Z axis
t/c	=	Wing Thickness Ratio
TF	=	Turbofan
TIT	=	Turbine Inlet Temperature
TJ	=	Turbojet
T.O.	=	Take-off
TOGW	=	Take-off Gross Weight
T/W	=	Thrust/Weight

TABLE OF NOMENCLATURE (Continued)

\bar{V}	=	Tail Volume Coefficient
V_E	=	Equivalent Air Speed
W	=	Weight
W_G	=	Gross Weight
WF	=	Fuel Flow Rate
W/S	=	Wing Loading
ZFW	=	Zero Fuel Weight

1.0 INTRODUCTION

This is the final report of a study performed by Lockheed-California Company for NASA-Ames Research Center. The NASA Request for Proposal (RFP 2-19866, HK-94) dated March 29, 1973, sought promising new ideas for advanced technology supersonic transport concepts. The intent was to complement the existing AST studies (References 1, 2, 3, and 4) and provide feasibility information for new, different concepts. The contemporary AST studies were all based on use of conventional (kerosene) type fuel (Jet A-1).

The approach proposed by Lockheed, reported herein, was to investigate the feasibility of using liquid hydrogen as the fuel in a supersonic transport of advanced design. This approach was suggested as a result of recognition of the impending energy crisis and the fact that the world's supply of petroleum will be significantly diminished by 1990, according to recent projections (References 5, 6, and 7). The prospects of having the demands of a fleet of SST's, with their prodigious appetite for fuel, imposed on the dwindling reserves of crude oil in that time period could very well be the cause for rejection of America's bid to build such aircraft.

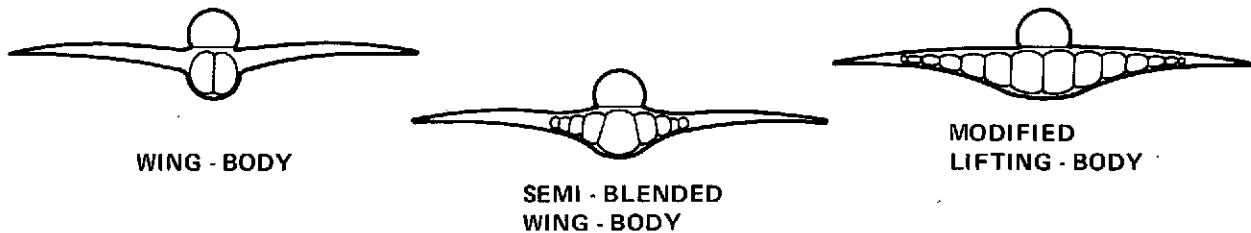
Preliminary conceptual analyses performed by Lockheed had indicated that use of hydrogen as the fuel in supersonic commercial transport aircraft could conceivably lead to the following advantages:

- Significantly lower gross weight
- Reduced pollution
- Lower sonic boom overpressure
- Lower engine noise
- Decreased costs

Accordingly, the subject study was proposed to investigate the economic and performance potential of liquid hydrogen (LH_2) fueled AST aircraft and to discover the extent to which these significant advantages might be realized.

2.0 TECHNICAL APPROACH

The study was conducted in two phases. Phase I was an exploratory analysis, conducted to parametrically identify the potential of a large number of different configurations of LH_2 fueled AST aircraft, and to determine a preferred design concept, as well as a set of design requirements, for more specific analysis in Phase II. Table 1 is a list of the mission and vehicle configuration parameters and their values which were studied in every viable combination during Phase I. These established the scope of the configuration investigation; namely, vehicles whose cross-sectional shape ranged from a conventional wing-body, through semi-blended wing-bodies, to modified lifting-bodies as illustrated:



Aircraft representing this wide range of potential configurations were parametrically designed and evaluated in accordance with the list of guidelines shown in Table 2.

Phase I involved, first, a preliminary sizing investigation to establish approximate sizes for various example aircraft representing the scope of the configurations involved in the study. Next, aerodynamic, weight, and cost parameters were generated to appropriately represent the candidate vehicles in the ASSET (Advanced System Synthesis and Evaluation Technique) computer program, described in section 3.2. Engine decks were generated to represent the performance of hydrogen fueled versions of both turbojet and turbofan engines for Mach 2.7 cruise aircraft, and of a turbojet for a Mach 2.2 aircraft. ASSET runs were then made to determine performance capability, weight, costs and significant design tradeoffs for aircraft representing the full scope of the candidates from the matrix of design variables. These results were analyzed to determine the four most attractive vehicle configurations

Preceding page blank

TABLE 1
VEHICLE MISSION AND CONFIGURATION PARAMETERS

CRUISE MACH	M	= 2.2 AND 2.7
WING AREA m^2 (ft^2)	S_W	= 743.2 , 1021.9 AND 1300.6 (8000) (11,000) (14,000)
WING THICKNESS RATIO (PERCENT) t/c		= 3, 5 AND 7
FUSELAGE SECTION AREA m^2 (ft^2)	A_B	= 13.66 , 19.17 , 23.05 AND 27.22 (147) (206) (248) (293)
THRUST/WEIGHT N/kg	T/W	= 0.5, 0.6, 0.7 AND 0.8
ENGINE TYPES		TURBOFAN AND TURBOJET
GROSS WEIGHT kg (lb)	W_G	= 124,738 to 317,515 (275,000) (700,000)
RANGE km (n.mi.)	R	= 5926 , 7408 , 9260 AND 10,186 (3200) (4000) (5000) (5500)

TABLE 2
BASIC GUIDELINES

Fuel - liquid hydrogen
 Planform - NASA Arrow - wing
 IOC - 1990

Use of advanced materials and technology postulated to be developed by 1985. (Data available from Lockheed AST studies (References 1 and 4)).

Certification - FAR Part 25 and SST White Book

Noise - FAR Part 36 minus 5 EPNdB

Fuel Reserves - FAR Part 121.648

Runway Length Determination - FAR Part 25 for 305.6°K (90°F) day and 304.8 m (1000 ft) airport altitude.

Operability - compatible with Air Traffic Control Systems and general operating environment envisioned for 1990, including capability for Category III-A operations.

Aircraft Design Life - 50,000 flying hours

Sonic Boom - no boom at ground level over populated areas

Stability - control configured aircraft

Cost - production up to 600 aircraft. Use modified ATA formulas for DOC evaluation at passenger load factor = 0.55. Use 1972 dollars for direct comparison with AST results. LH_2 available at airports.

Payload - 28,032 kg (61,800 pounds) (258 to 300 passengers, depending on class mix).

for consideration leading to selection of the one preferred vehicle for more detailed study in Phase II. The final event of Phase I was the Mid Term Oral Review on 17 October 1973, following which NASA specified the design and performance requirements of the Phase II airplane.

Phase II consisted of an analysis to provide design, performance, and cost information for the selected configuration of LH_2 fueled aircraft at a greater level of detail. The design basis and criteria were selected so as to provide a direct comparison of the cost, performance, and design characteristics of the LH_2 fueled supersonic transport with those of an equivalent design based on use of conventional Jet A-1 (sometimes called JP) fuel. The Jet A-1 airplane selected to provide this comparison was one being evolved in a concurrent study by Lockheed for NASA-Langley Research Center under contract NAS 1-12288 titled, "Study of Structural Design Configuration." (Reference 4). Thus, the following mission requirements were established:

Cruise speed	Mach 2.7
Range	7778 km (4200 n.mi.)
Payload (234 passengers)	22,226 kg (49,000 lb.)

To assure equivalency in design and evaluation between the Jet A-1 and LH_2 aircraft being evolved in the two separate NASA studies, several changes from the basic guidelines used in Phase I of the subject study were made for Phase II. Table 3 lists the differences from those presented in Table 2.

Using these criteria, and the duct-burning turbofan engine shown to be preferred in Phase I, preliminary size and performance relationships for the Phase II point design aircraft were established. Aerodynamic data were rechecked and analyses were made of significant structural areas and of the cryogenic tanks and their thermal protection system. Based on these results, new weight and cost relationships were established for input to ASSET. A series of ASSET runs were made to determine the most advantageous set of values for parameters such as thrust-to-weight ratio (T/W) and wing loading (W/S) which would produce an airplane that would perform the desired mission with the best combination of lowest gross weight, lowest fuel weight, and

TABLE 3
CHANGES IN BASIC GUIDELINES FOR PHASE II
(Refer to Table 2)

	<u>Phase I</u>	<u>Phase II</u>
Materials and Technology State-of-the-Art	1985	1981 *
* technology level defined per agreement for contract NAS 1-12288		
Noise	FAR 36 minus 5	FAR 36
Cost	1972 dollars	1973 dollars
Payload	28,032 kg (61,800 lb.) (300 passengers)	22,226 kg (49,000 lb.) (234 passengers)

minimum cost. The result was definition of the point design LH₂ fueled AST airplane. Design tradeoffs and sensitivities to various parameters were then established to provide information about the importance of each of the significant design and cost variables.

Finally, an assessment was made of the general viability of the concept, including an evaluation of environmental considerations such as exhaust emissions and sonic boom characteristics. Major technology development requirements were enumerated, along with suggested schedules for their implementation. Recommendations were made for follow-on development activity.

For convenience, some characteristic properties of Jet A-1 and liquid hydrogen are listed:

	<u>Jet A-1</u>	<u>Hydrogen</u>
Nominal Composition	CH _{1.94}	H ₂
Molecular Weight	120	2.016
Heat of Combustion(Btu/lb.)	18,400	51,590
Liquid Density(lb/ft. ³)	47 (at 50°F)	4.43 (at boiling point)
Boiling Point (°F) (@ one atmosphere)	400 to 500	-423
Specific Heat (Btu/lb.°F)	.48	2.22

3.0 PHASE I: EXPLORATORY ANALYSIS

The purposes of Phase I were to 1) explore the potential of advanced design concepts of supersonic transport aircraft fueled with liquid hydrogen, 2) determine four preferred configurations, and 3) generate a set of design requirements for a specific aircraft which would be examined in greater detail in Phase II.

As outlined in Section 2.0, the exploratory analysis was conducted parametrically to evaluate every viable combination of mission and vehicle configuration values listed in Table 1. The following sections describe how the basic data was generated, how the vehicle synthesis was conducted, the general design and cost results that were obtained, and the general conclusions that were reached. Finally, the characteristics of the four vehicles that were selected as the most promising candidates for the Phase II Point Design refinement study are described.

3.1 BASIC DATA GENERATION

In this section the basis for generating the data required to perform the vehicle synthesis study is described by technical discipline.

3.1.1 Preliminary Sizing Estimates

The starting point for preliminary sizing of the hydrogen vehicle was the basic Mach 2.7 hydrocarbon fueled AST with a payload of 28,032 kg (61,800 lbs.) and a gross weight of 340,193 kg. (750,000 lb.). The arrow wing configuration, payload, and low speed characteristics were retained because of the data background available. A series of systematic hand calculations were made by modifying the weights, aerodynamics, and propulsion data to identify the probable range of gross weights, engine sizes, wing areas, and volumes required for liquid hydrogen (LH_2) aircraft in order to guide the data generation for the initial parametric studies. The hydrogen fuel was assumed to be contained in the lower fuselage lobe and in a thickened wing root. The fuselage lower radius was expanded as required to contain the fuel volume.

The ground rules followed in this initial investigation are those already described in Section 2.0, above. Typical characteristics of a hydrogen fueled

vehicle with a range of 9649 km. (5,210 n.mi.) are given in Table 4 as an example of the output of the preliminary sizing work.

TABLE 4
PRELIMINARY VEHICLE SIZING
(EXAMPLE LH₂ VEHICLE CHARACTERISTICS)

Performance		Weights	
Engine	Turbofan		
Cruise Mach	2.7	Structures -	Kg 76,158 (167,900)
Range - (n.mi.)	9,649 (5,210)	Propulsion -	Kg 18,035 (39,760)
Payload - (lbs.)	kg. 28,032 (61,800)	Sys., Furn. & Equip. -	Kg 13,054 (28,780)
Block Time - hr.	4.0	MEW -	Kg 107,247 (236,440)
Block Fuel - (lbs.)	kg 44,225 (97,500)	OP + Std. Items -	Kg 5,107 (11,260)
Wing Loading - (lbs/ft ²)	kg/m ² 244 (50)	OEW -	Kg 112,354 (247,700)
Thrust/Weight	0.55	Payload -	Kg 28,032 (61,800)
FAR T.O. Fld. Length - (ft)	m 2,195 (7,200)	ZFW -	Kg 140,386 (309,500)
Approach Speed (KEAS)	m/s 78.2 (152)	Fuel -	Kg 53,297 (117,500)
L/D - Cruise	7.71		
SFC - Cruise (lbs/hr/lb)	kg/hr/daN 0.571 (0.56)	TOGW -	Kg 193,683 (427,000)

3.1.2 Aerodynamic Parametric Data

The basic philosophy employed during the development of data for the study of the Phase I parametric series of configurations was to retain the geometric relationships of the AST Systems/Structures Study vehicles (References 1 and 4) (herein noted as "original") as much as possible. In this light, then, the aerodynamic performance of the present study vehicles could be developed from that of the earlier studies, thus fully utilizing the detailed analyses of analytical and experimental data already performed.

The matrix of the parametric configuration variables - wing area (S), wing thickness ratio (t/c), and body cross-sectional area (A_B) - is depicted in Figure 1. Twenty-seven possible combinations (solid lines) were evaluated initially, while an additional six (dashed lines) were added later to provide additional range (fuel volume) capability.

This section details the scaling methods employed to develop the study configuration and the aerodynamic data provided for the Phase I parametric analyses of the present study. Aerodynamic data for the Phase II Point Design vehicle configuration are presented in Section 4.1.3.

3.1.2.1 Geometry Development

Wings

The original wing planform shape and section was retained for all vehicles to maintain the low speed lift characteristics. Planform and camber dimensions for the 743.2 (8,000) and 1300.6 sq.m. (14,000) (sq ft) wings were scaled from the original 1005.4 sq.m. (10,822 sq ft) dimensions by the ratio $\sqrt{S_{\text{study}}/S_{\text{orig}}}$. The wing 0.45 MAC station was located at the same relative body location (0.56 body length) to maintain the basic airframe CG (to the first order).

The high aspect ratio wings ($AR = 2.0$) for the $M = 2.2$ cruise mission were developed from the $M = 2.7$ cruise vehicles by scaling the wing dimensions by $\sqrt{AR_{M=2.2}/AR_{M=2.7}}$. Wing sweep was defined so as to retain an equal value of Mach number normal to the leading edge.

The wings so developed are delineated in Figure 2a, b, c with the pertinent dimensions indicated.

Wing thickness ratios were increased at the root airfoil from the original 3 percent (nominal) to values of 5 and 7 percent; the incremental variations outboard of the root airfoil were decreased linearly to zero at the tip (the original thickness ratio). Typical spanwise variations at the 50 percent chord line are shown in Figure 3. No effects on low speed performance were assessed, such effects being observed only in increased wing supersonic wave drag.

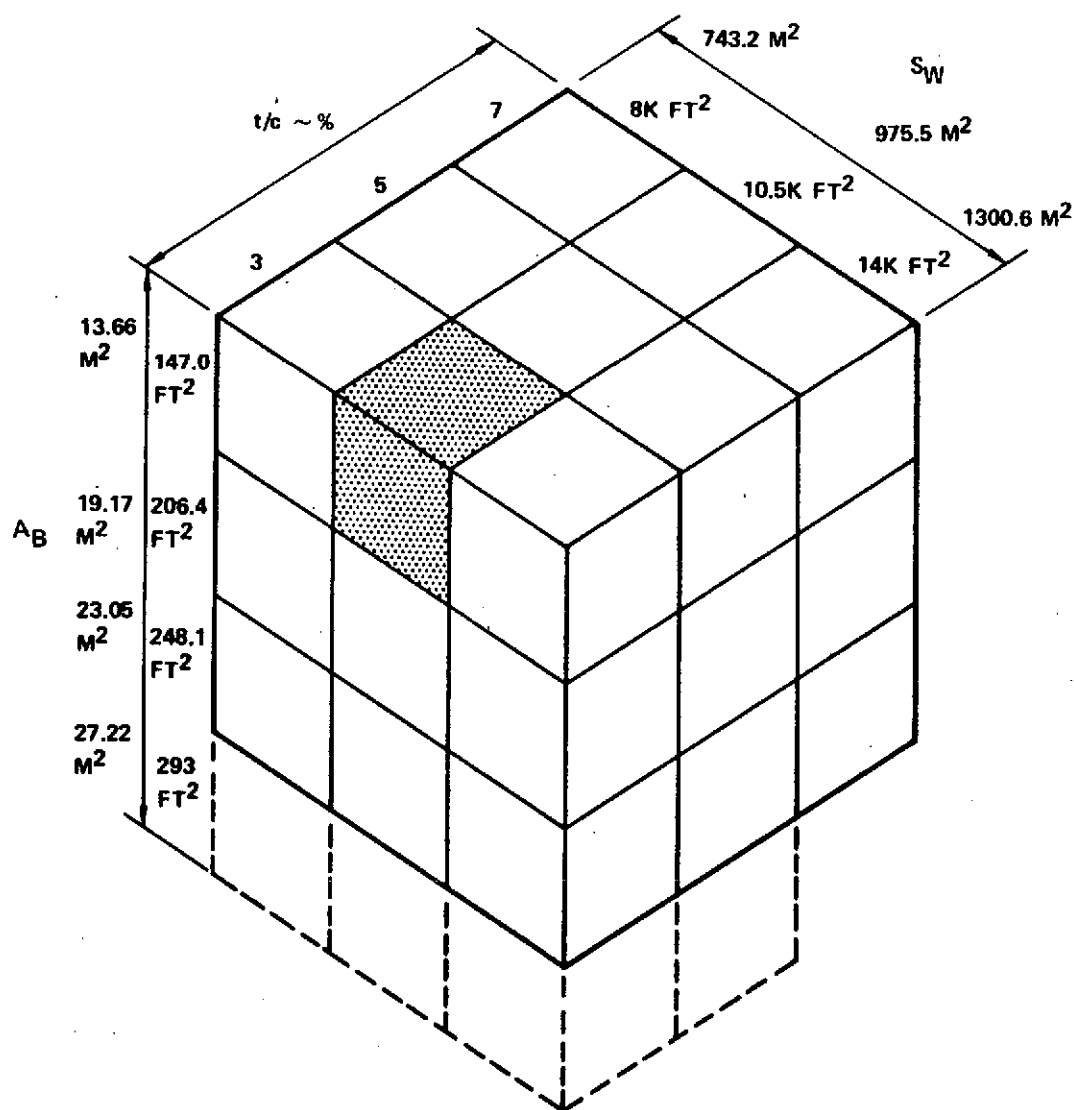


Figure 1. Configuration Variables

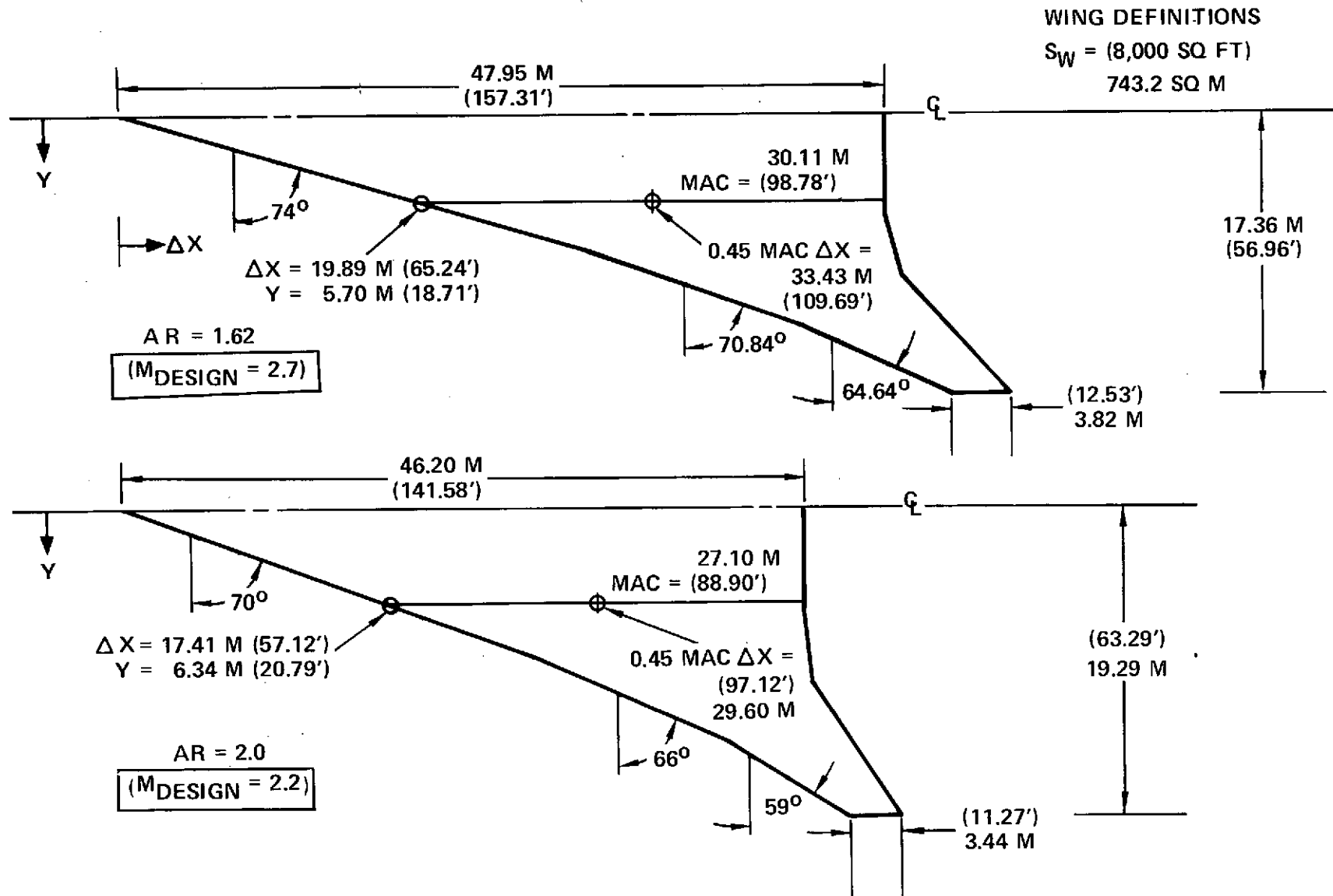


Figure 2a. Wing Definition for $S_W = 743.2 \text{ sq. m}$ (8000 sq. ft.)

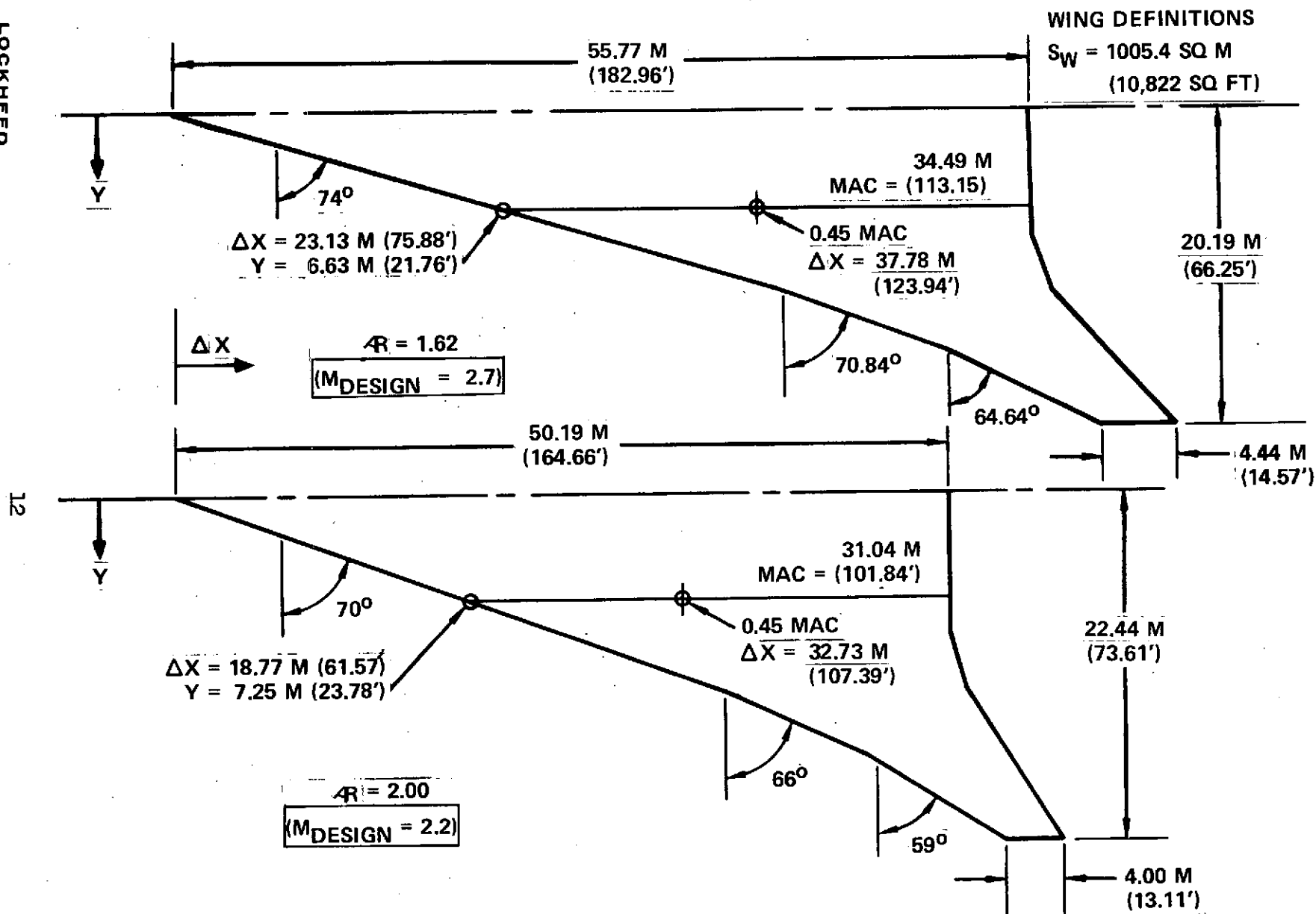


Figure 2b. Wing Definition for $S_W = 1005.4 \text{ sq. m}$ (10,822 sq. ft.)



13

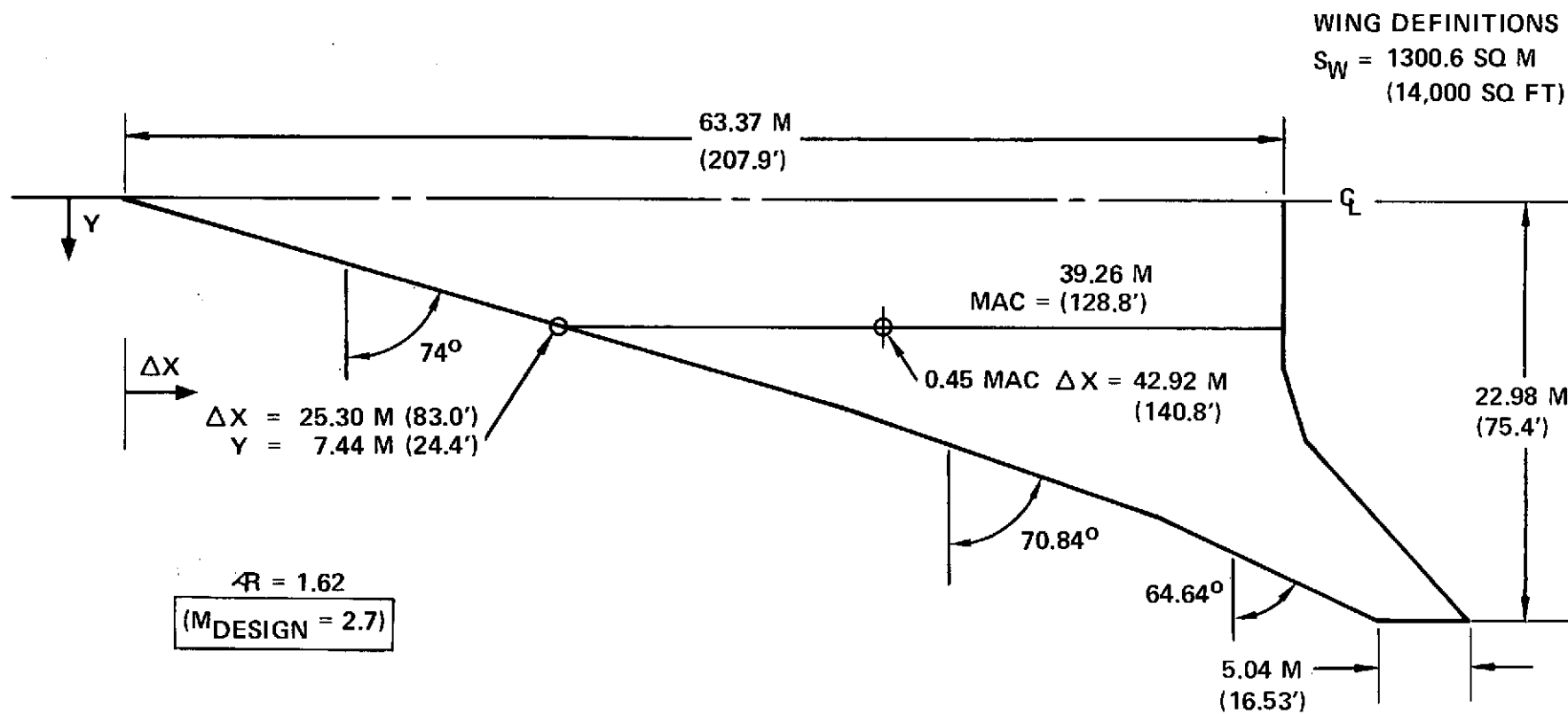


Figure 2c. Wing Definition for $S_W = 13006 \text{ sq. m}$ (14,000 sq. ft.)

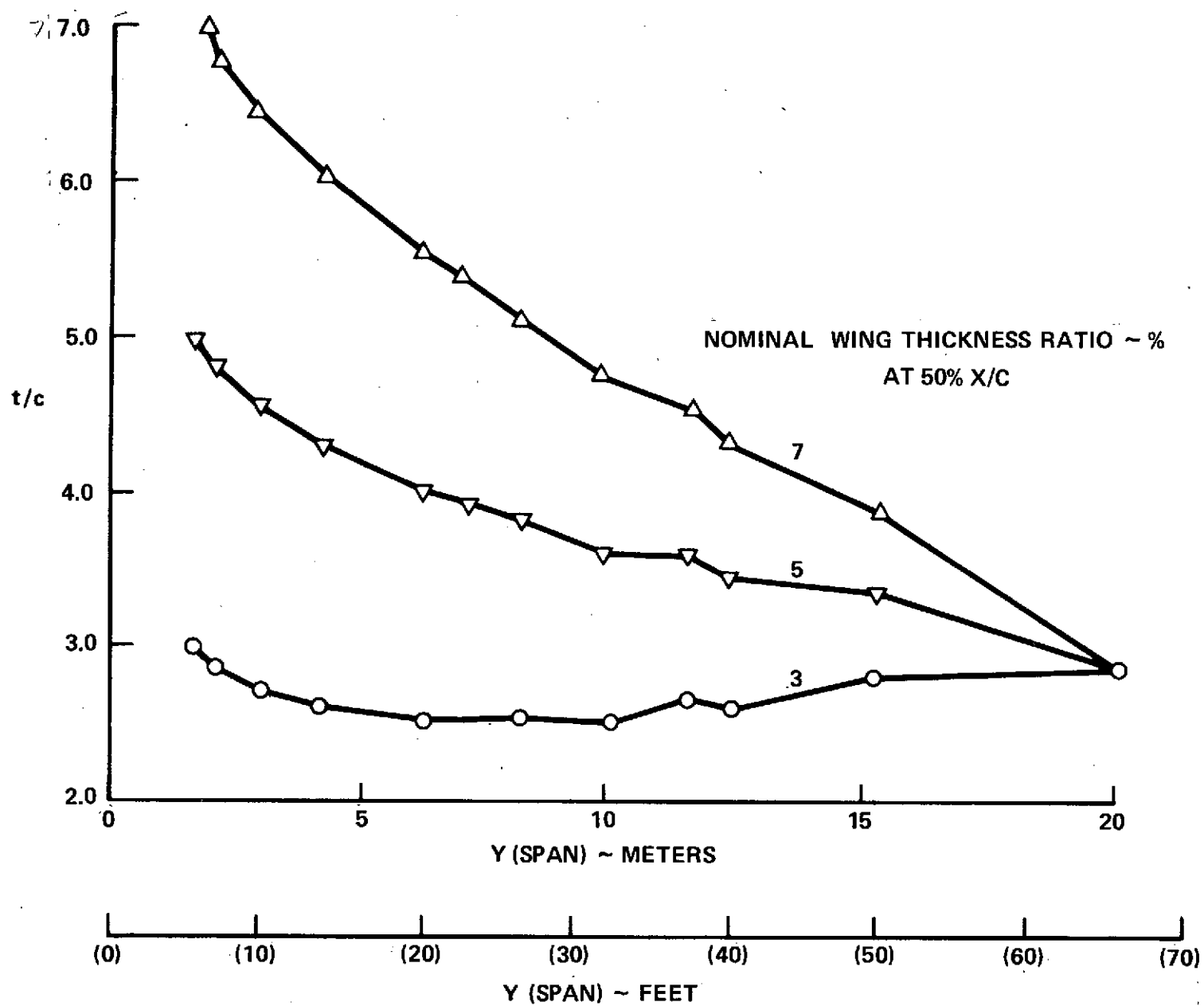


Figure 3. Wing Thickness Ratio

Fuselages

The fuselage retained the cross-sectional area ratio distribution and camber of the original vehicle. The area ratio distribution is shown in Figure 4. Maximum cross-sectional areas of 13.66 (147.0), 19.17 (206.4), 23.05 (248.1), and 27.22 (293.0) sq.m. (sq ft), and nominal overall length of 108.5 m (356 ft) were employed to develop the parametric fuselage geometries. The basic fuselage section concept from which these areas were derived is shown in Figure 5; the upper (passenger) lobe is identical to the original and retained throughout, while the lower lobe (fuel tankage) was varied as indicated.

Horizontal and Vertical Tails

As in the case of the wing, the vertical and horizontal tail planform geometries were retained throughout. The original thickness ratio (3 percent) was retained and held constant. Tail areas were defined by tail volume coefficients retained at their original magnitudes (Table 5).

TABLE 5
TAIL VOLUME COEFFICIENTS

Surface	Volume Coefficient
fuselage vertical	0.023
wing verticals (two)	0.022
horizontal	0.07

This approach is feasible since in each case (vertical and horizontal), the dominant designing characteristics were low speed effects - vertical tail: two engines out at takeoff; horizontal tail: control power to rotate at takeoff. Longitudinal tail moment arms were scaled by the overall fuselage length ratio (108.5/90.5) (356 ft/297 ft). The resulting surface areas were then calculated accordingly. Linear theory suggests an increase in the resulting vertical tail areas to compensate for the increased lateral fuselage area. In many cases, however, such theory represents a substantial oversimplification of the real world; a more detailed analysis is beyond the scope of the present study and would have no effect on the outcomes of the major conclusions derived therefrom. The areas, therefore, were not modified.

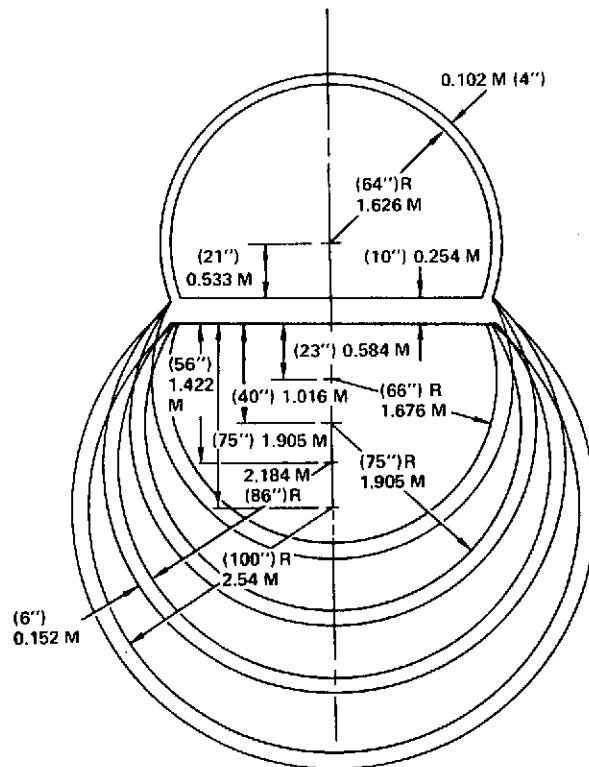


Figure 4. Fuselage Area Distribution

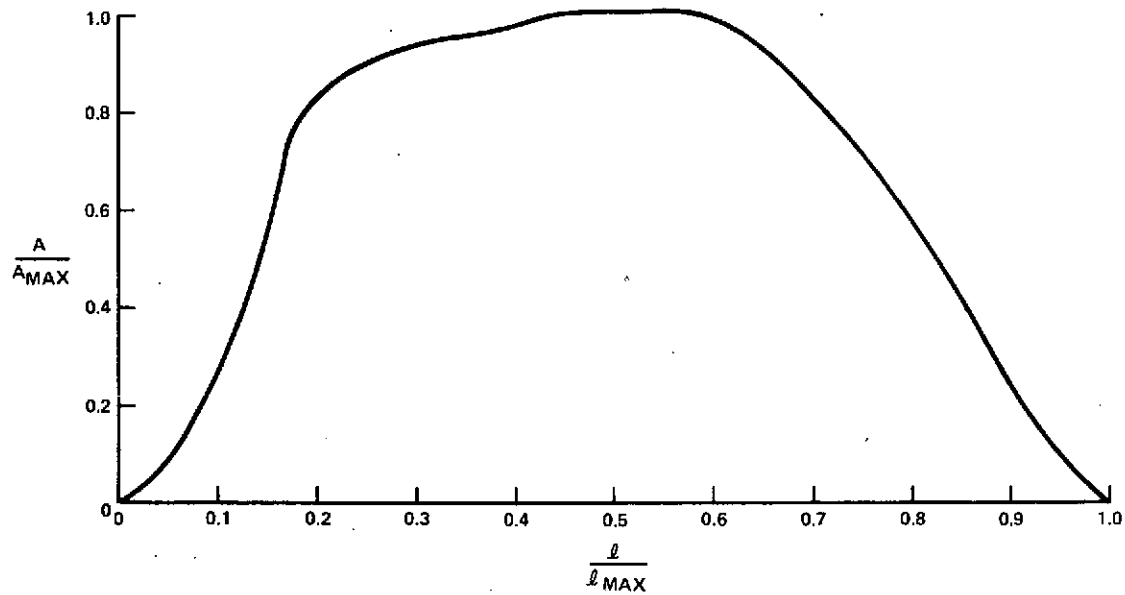


Figure 5. Fuselage Section Definition

Engine Pods

The centerlines of the engine pods were located at the same percent spanwise locations as the original. Similarly, the pod inlets were located at the same relative chordwise location. Pod diameters were defined for nominal engines sized for each wing and nominal mission requirements.

3.1.2.2 Aerodynamic Development

The aerodynamic characteristics developed for the Phase I parametric series of configurations were tailored to the requirements and capabilities of the ASSET Program utilized for the tradeoff studies (see Section 3.2 for a description of that program). That program, as configured for the present study, calculated clean configuration lift (1 g flight assumed), skin friction (based on component wetted surface area and reference length), and parasite drag. Hence, for the cruise configuration (gear and flaps retracted), input requirements included only the drag-due-to-lift parameter variation with Mach number, and wave drag. For the takeoff and landing configurations, lift-drag polars were provided which included gear, flap, and ground effect increments. As noted earlier, the Systems/Structures Studies (Reference 1 and 4) provided the primary data base.

Drag-Due-to-Lift

The drag-due-to-lift parameters are presented in Figure 6. These are identical to the original values for the $M = 2.7$ airplane, since the wing aspect ratios are equal and the span efficiency factor may be considered identical for the purpose of the present study. The parameters were used to develop the drag-due-to-lift as below:

$$C_{D_i} = K(C_L - C_{L_K})^2$$

The higher aspect ratio of the $M = 2.2$ aircraft required that the "K" parameter be modified by $AR_{M=2.7}/AR_{M=2.2}$ to reflect the inherent induced drag reduction.

Wave Drag

The wave drag for each of the 27 possible combinations of parametric configuration elements was computed at four Mach numbers ($M = 1.2, 1.6, 2.2, \text{ and } 2.7$).

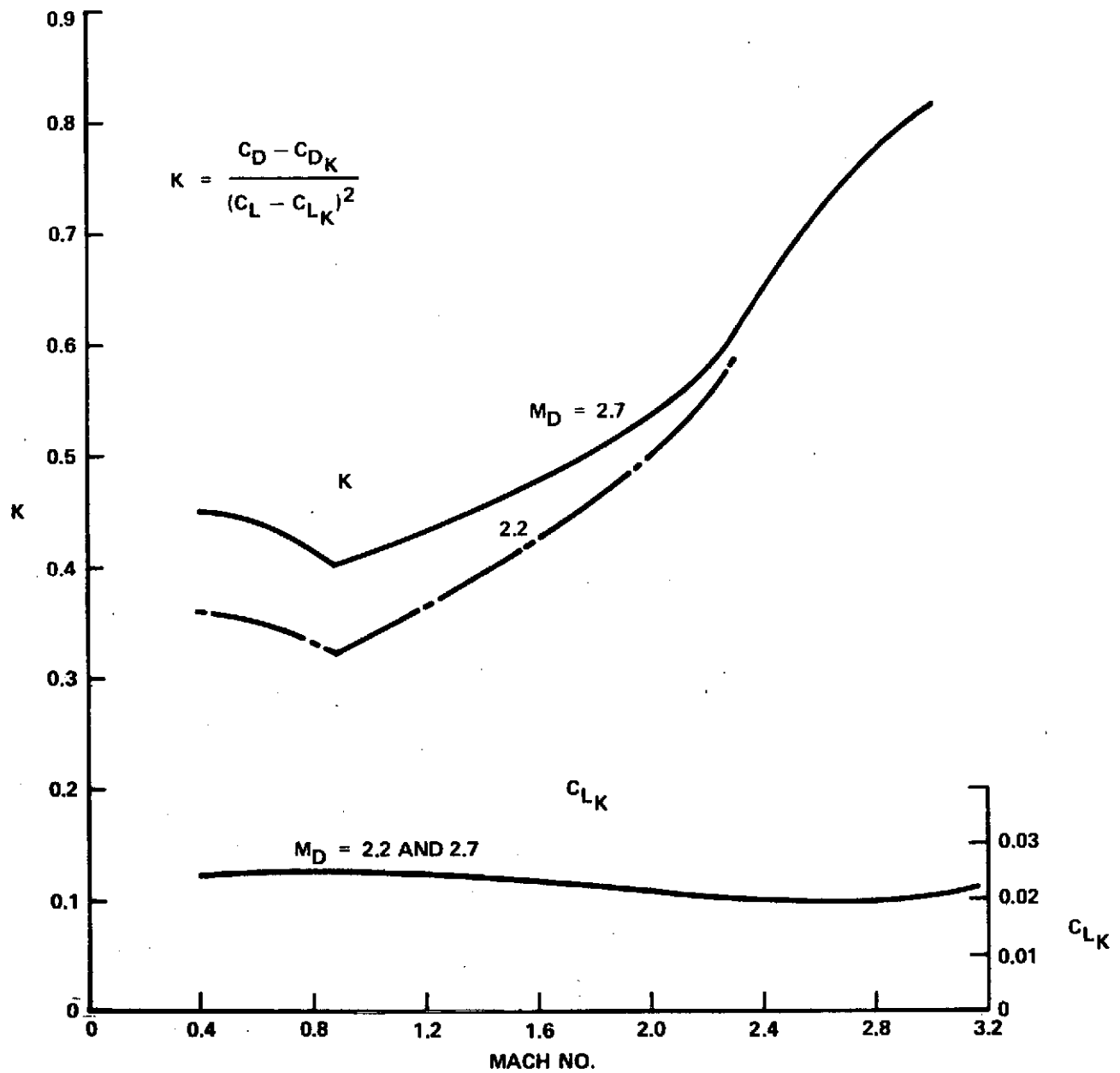


Figure 6. Drag-Due-to Lift Parameters

The NASA/Langley wave drag program, P 7120, (Reference 15) was used for this analysis. Since this program can accept only circular uncambered fuselages and uncambered symmetrical wing airfoils, spot checks were made for comparison purposes, on the effects of a more accurate representation of the configurations using NASA/Langley program D2500 (Reference 16). Negligible differences were noted at high and low supersonic Mach numbers, and therefore, the P7120 results were considered acceptable for this study. The configuration wave drag data so calculated are presented in Figures 7a, b, and c, and the component wave drag data are presented in Figure 8.

Low Speed Characteristics

The low speed lift characteristics of the original $M = 2.7$ configuration (in and out of ground effect) were adopted without change (Figure 9a and b). This was made possible by the utilization of the original wing geometric arrangement without change (except for total area). The possible variation in body-wing interference is considered negligible since the body radius/wing semi-span ratio does not vary significantly. Lift-drag polars were also adopted (Figure 10a and b), but required the calculation of an additional zero-lift drag increment for each configuration due to significant variations in body-wing wetted area ratios, Figure 11.

Similar arguments prevailed in developing the low speed characteristics of the $M = 2.2$ configuration. In this case, the lift characteristics were modified to reflect the increased aspect ratio (Figures 12a and b and 13a and b).

AST HYDROGEN FUEL STUDY

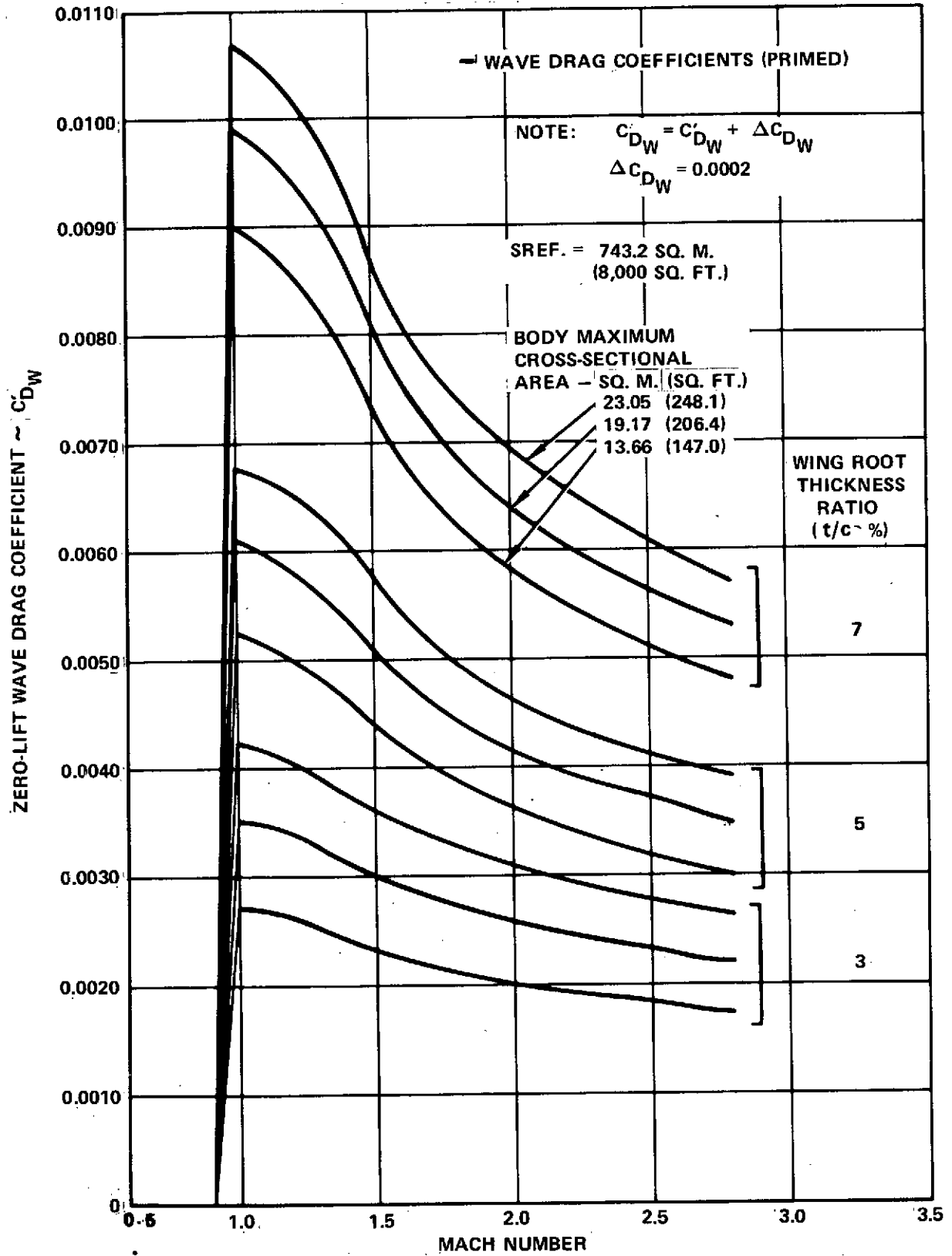


Figure 7a. Wave Drag Coefficients $S_W = 743.2$ sq. m (8000 sq. ft.)

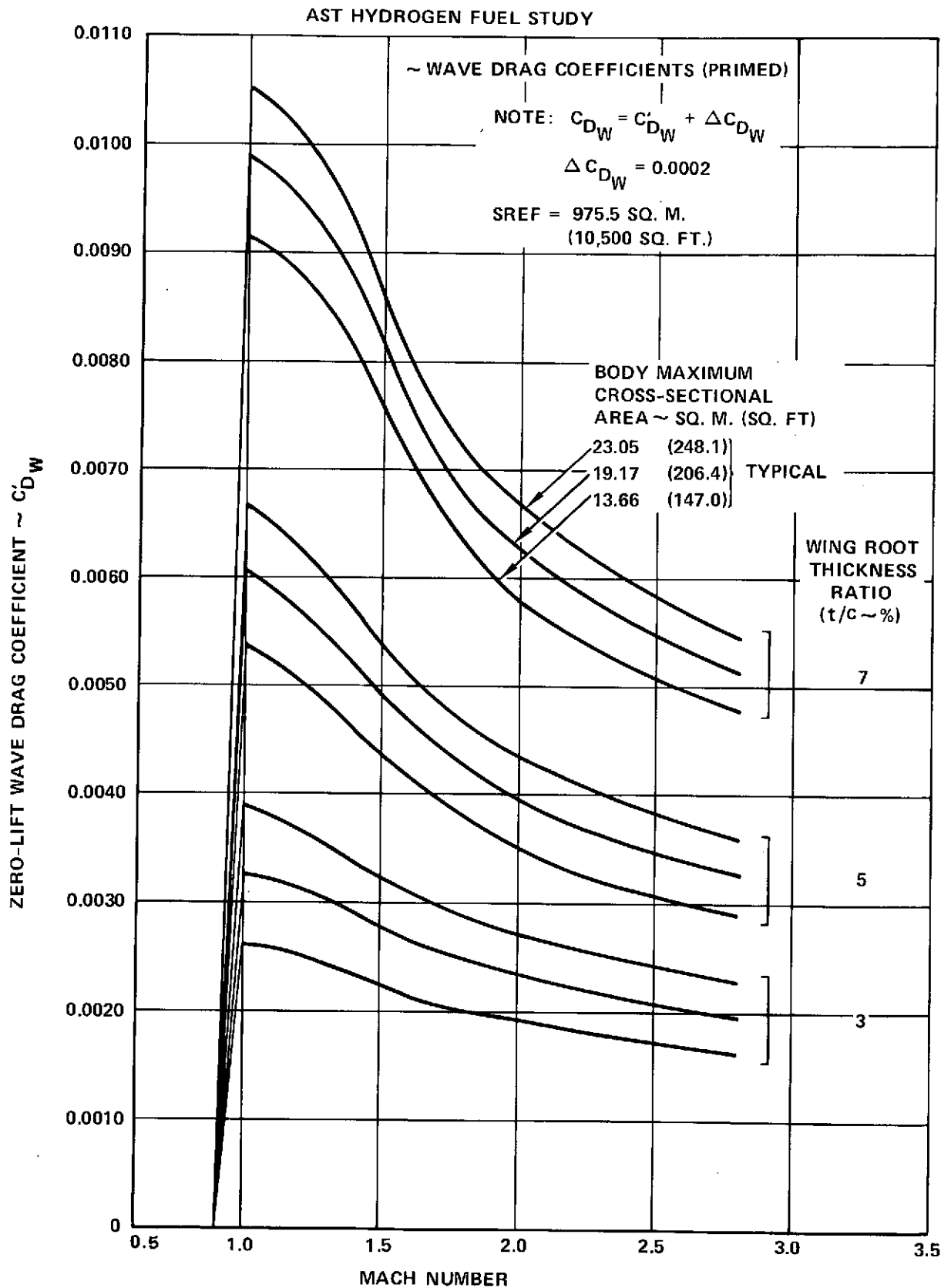


Figure 7b. Wave Drag Coefficients $S_W = 975.5$ sq. m (10,500 sq. ft.)

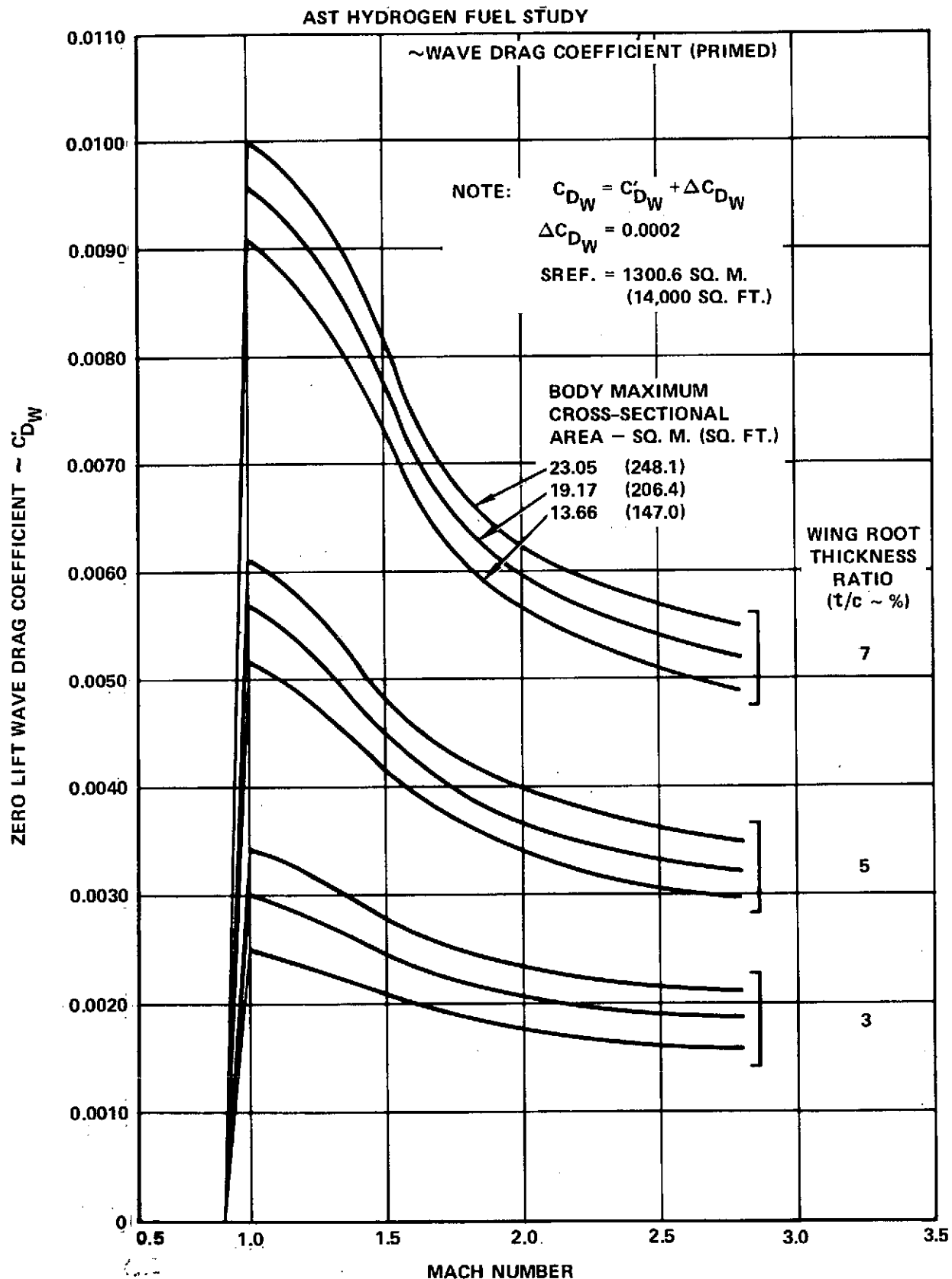


Figure 7c. Wave Drag Coefficients $S_W = 1300.6$ sq. m (14,000 sq. ft.)

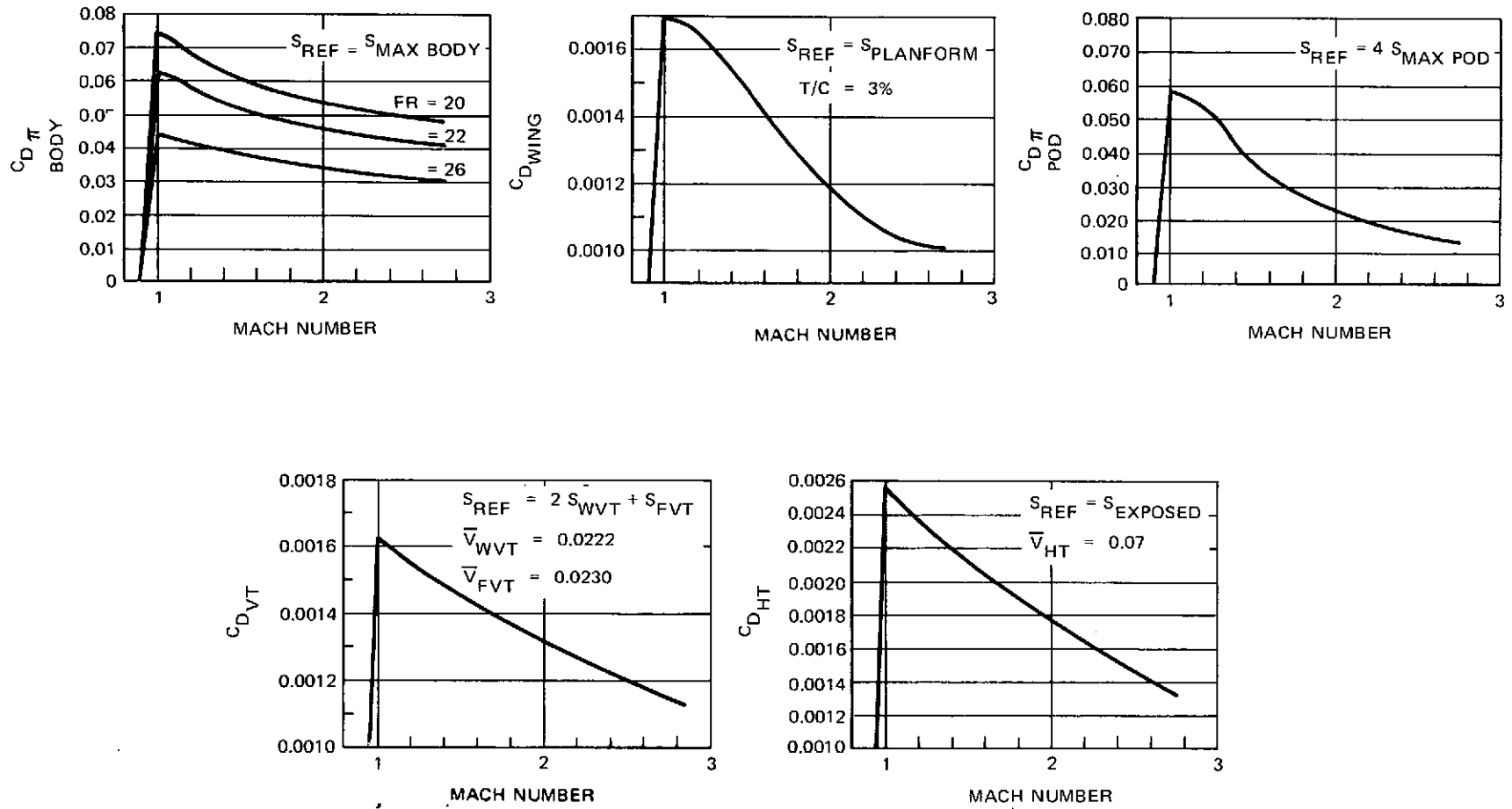
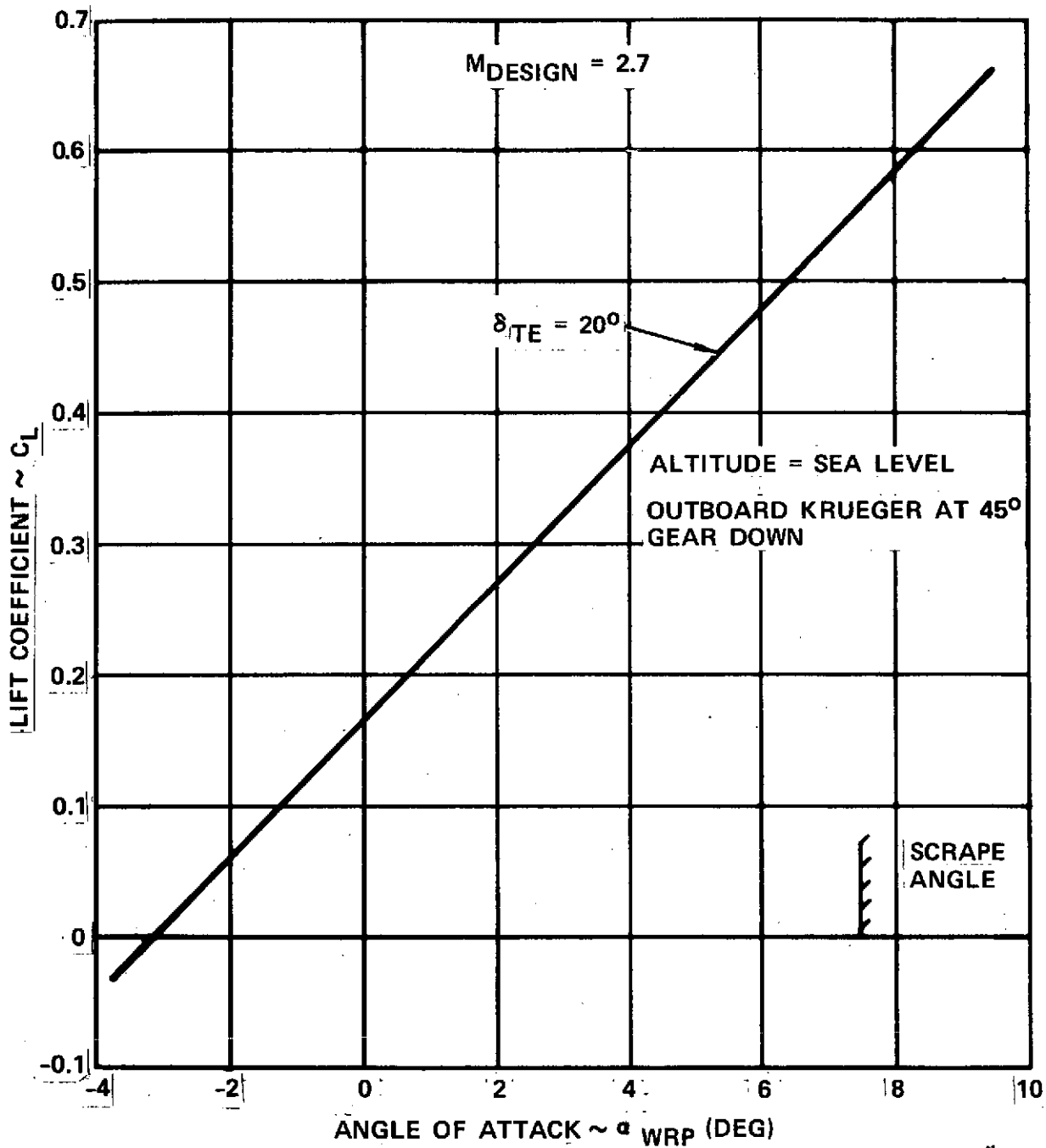


Figure 8. Component Wave Drag Data



LOW SPEED LIFT CHARACTERISTICS ~ IN GROUND EFFECT

Figure 9a. Low Speed Lift - In Ground Effect

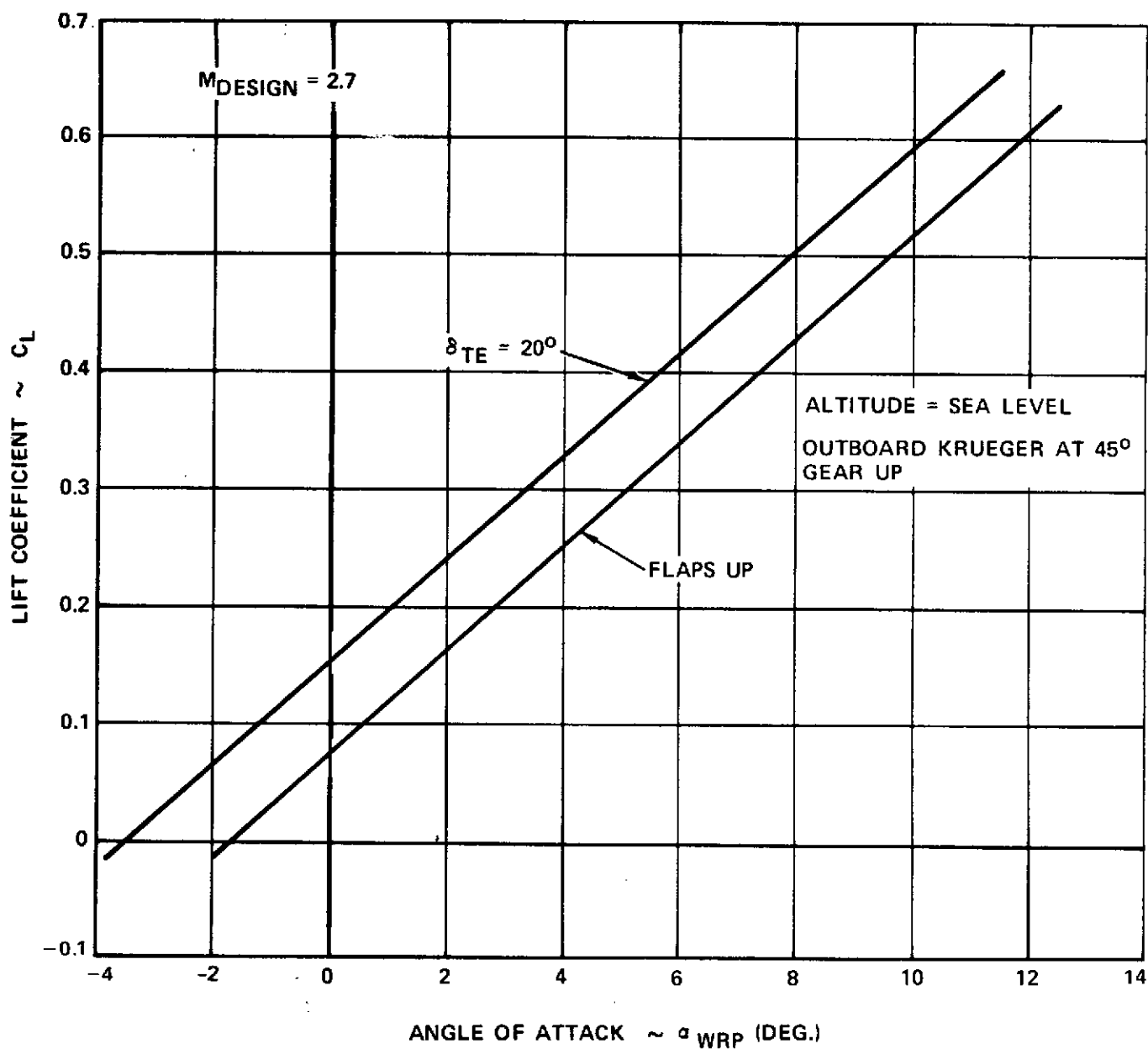


Figure 9b. Low Speed Lift Characteristics - Out of Ground Effect

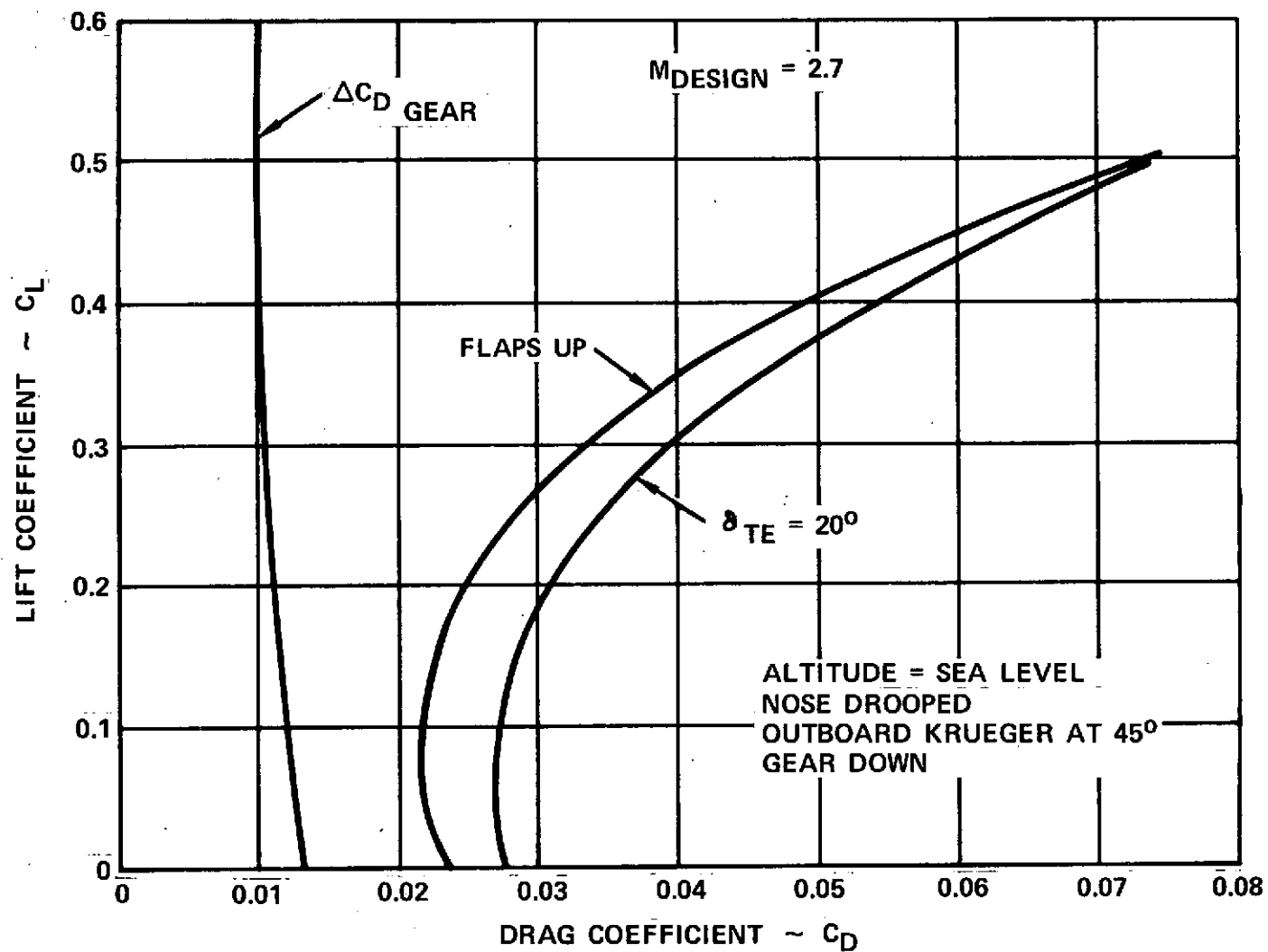


Figure 10a Low Speed Drag Polars - In Ground Effect.

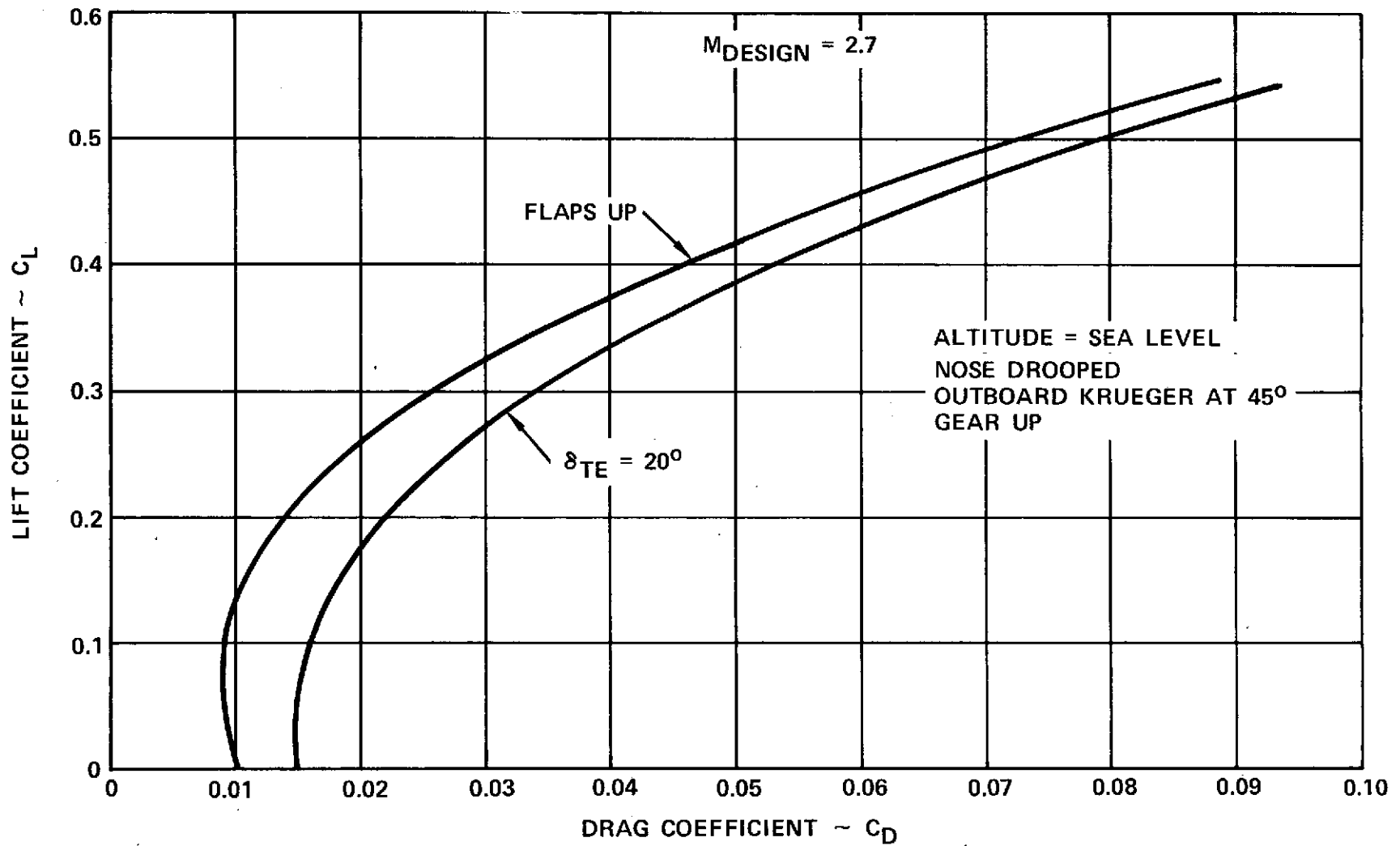


Figure 10b. Low Speed Drag Polars - Out of Ground Effect

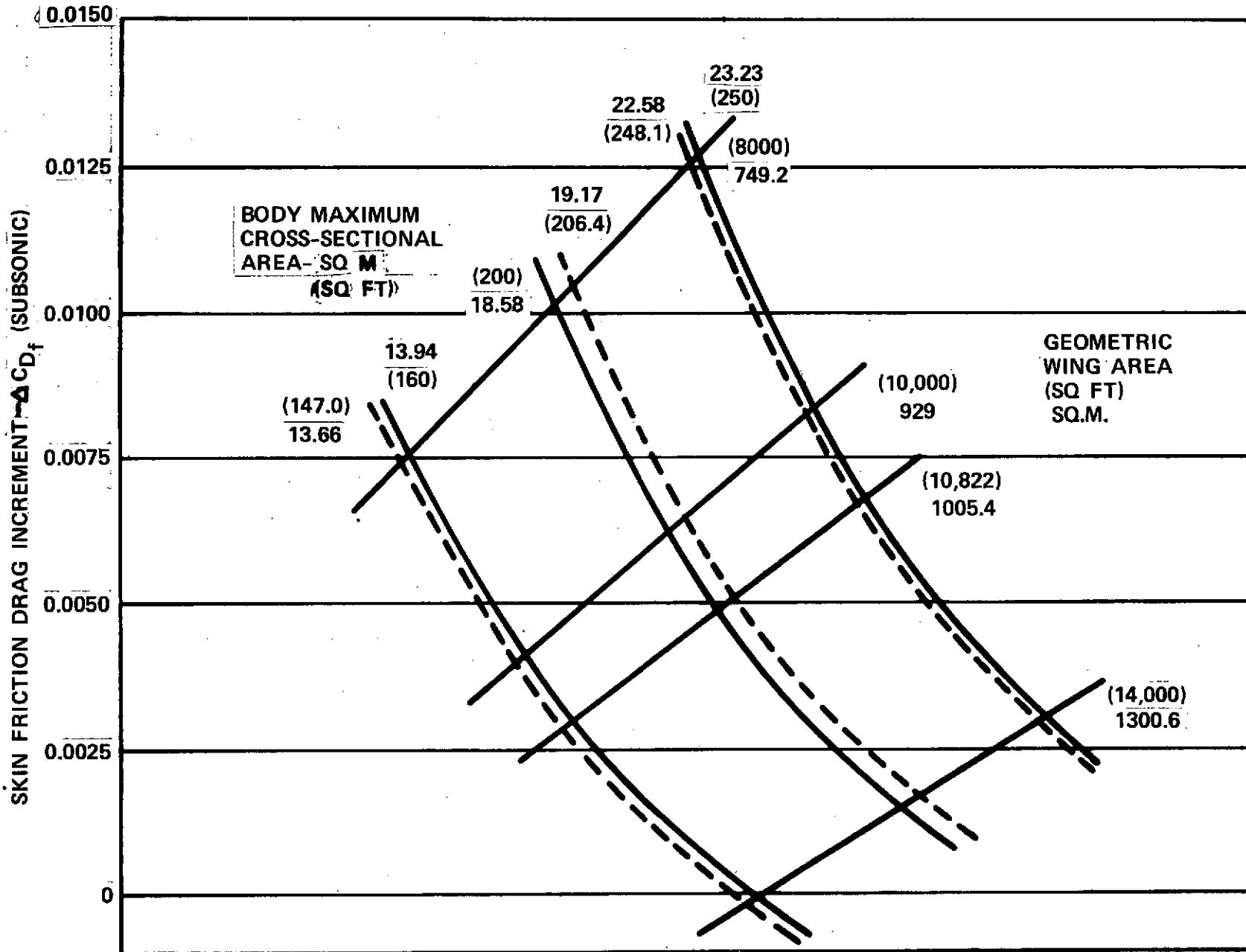


Figure 11. Skin Friction Drag Increment for Body-Wing Combination

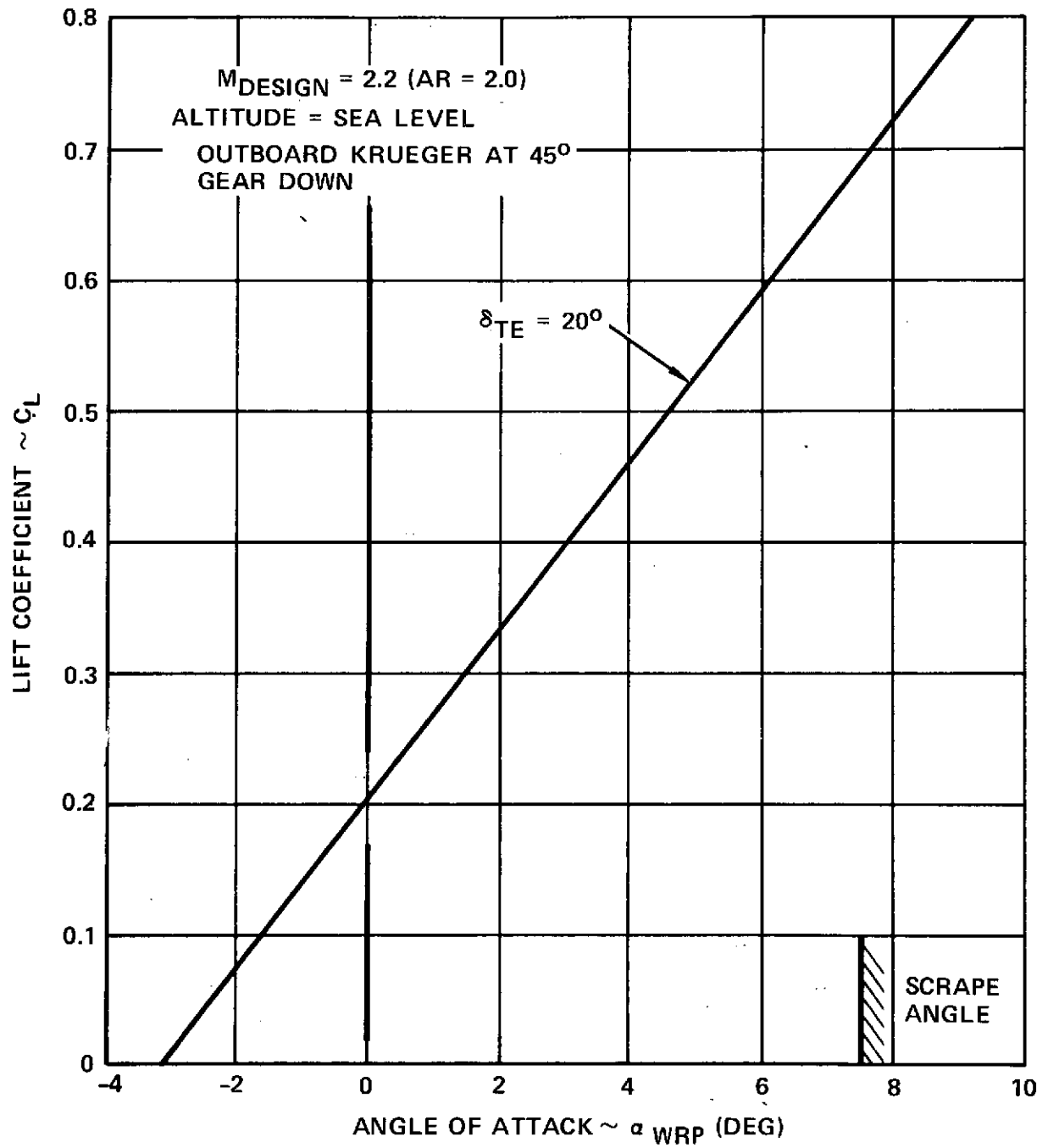


Figure 12a Low Speed Lift Characteristics - In Ground Effect

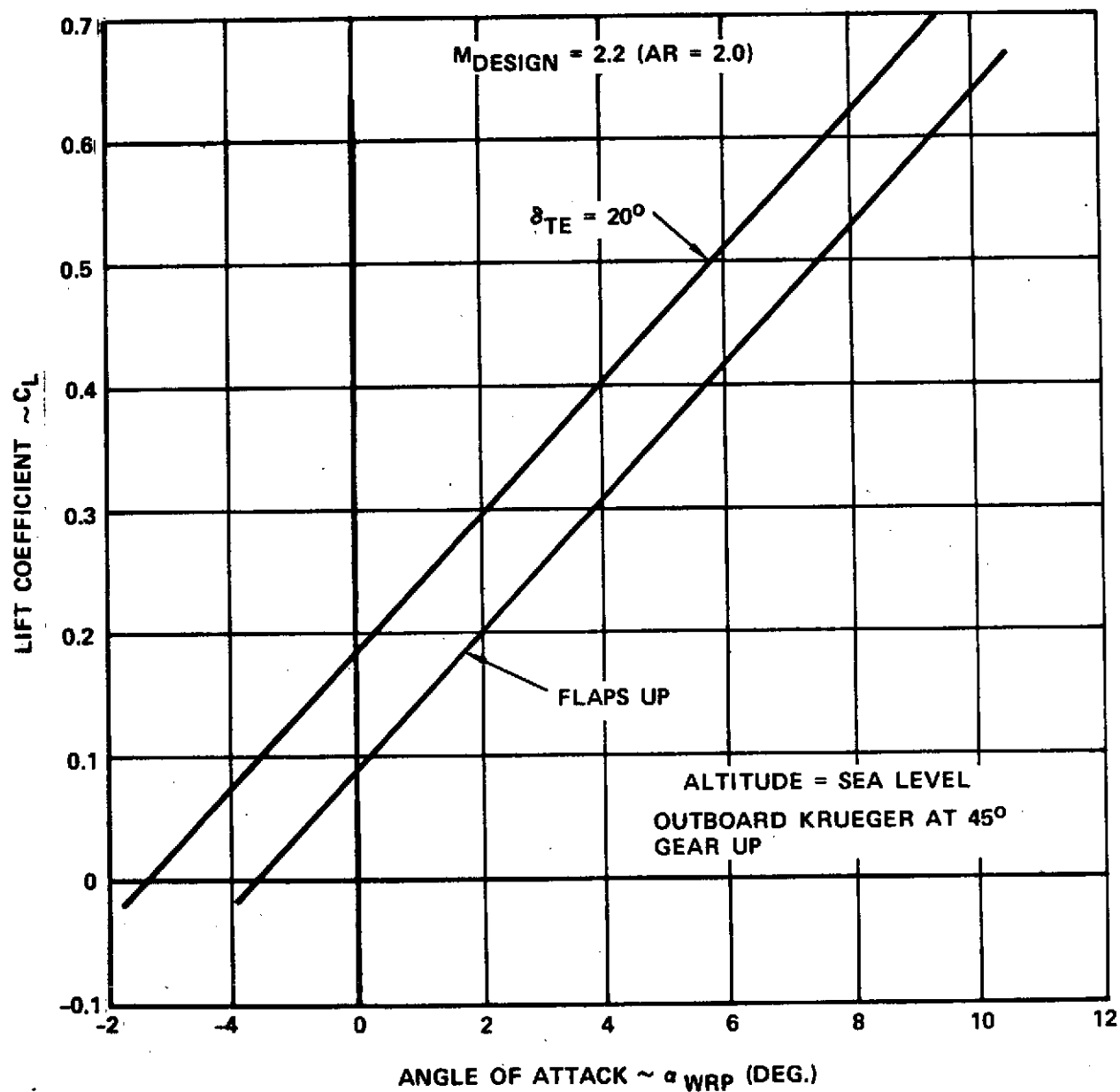


Figure 12b. Low Speed Lift - Out of Ground Effect

AST HYDROGEN FUEL STUDY

$M_{\text{DESIGN}} = 2.2$ (AR = 2.0)

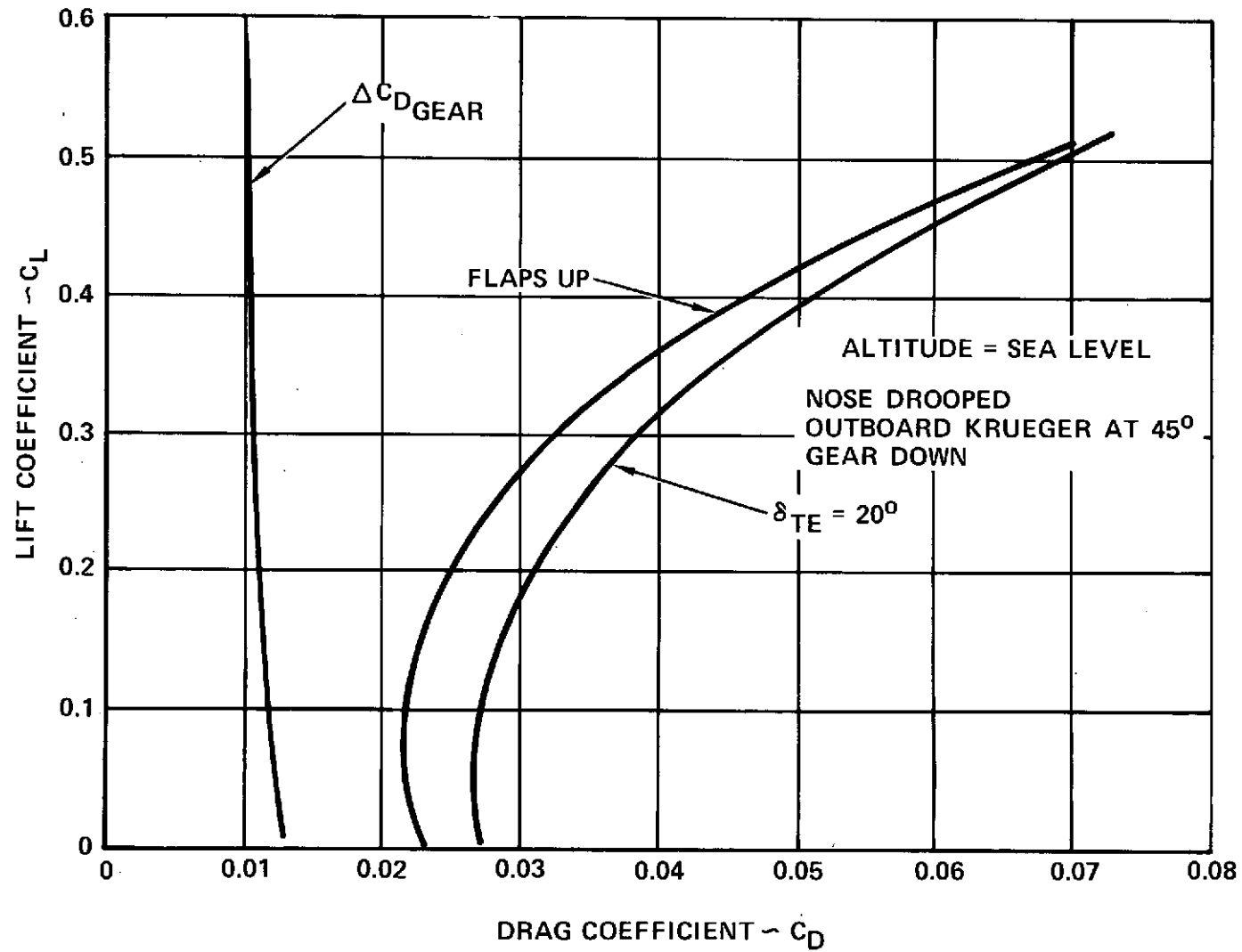


Figure 13a. Low Speed Drag Polars - In Ground Effect

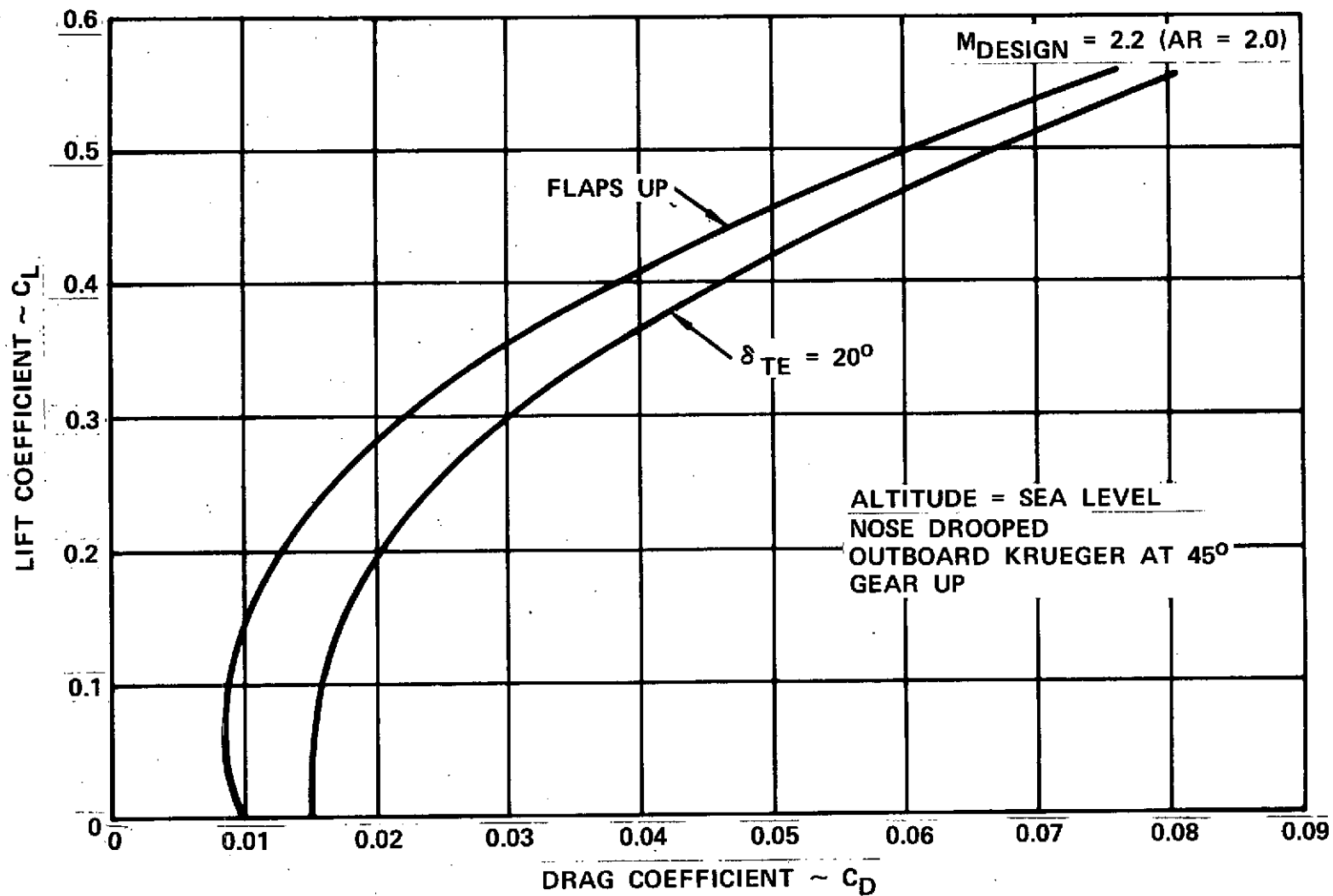


Figure 13b. Low Speed Drag Polars - Out of Ground Effect

3.1.3 Propulsion Data

The propulsion requirements of a liquid hydrogen (LH_2) fueled supersonic transport aircraft are similar to those of more conventional hydrocarbon fueled aircraft, except that the LH_2 aircraft designed for an equivalent mission will be significantly lighter, therefore the thrust required will be less, and the specific fuel consumption (SFC) will be much lower. Engine cycles considered for the subject study were non-augmented turbojet and duct augmented turbofan engines.

Although LH_2 and JP fueled supersonic transports require the same types of turbine propulsion systems, in hydrocarbon fueled aircraft turbine engine design the temperature of the air conveniently available to cool the turbines is essentially the temperature of the final compressor stage air. Maximum metal temperature restrictions and the compressor discharge air heat sink potential thus restricts both the maximum compression ratio and the maximum turbine temperature available for engine design. In the hydrogen-fueled aircraft turbine engine the cryogenic hydrogen can be used to precool the air or other medium used for turbine cooling and therefore, within certain bounds, the hydrogen-fueled engine's compression ratio and turbine temperature can be independently selected for optimum overall propulsion performance.

Practical limits of overall compression ratios and turbine inlet temperatures appear to be 40:1 and 2093°C (3800°F), respectively, for engines which might be developed in the 1980's. However, determination of the best cycle parameters for a particular aircraft design depends on parametric evaluation related to the aircraft requirements. Although both Pratt & Whitney and General Electric were contracted to NASA-Lewis for hydrogen engine studies, sufficient LH_2 engine data for either parametric studies or aircraft studies were not available from either company at the time information was needed for this study. Lockheed therefore generated the propulsion cycle optimization study data and the propulsion flight performance data for aircraft evaluation using Lockheed's propulsion installation subroutines in conjunction with the SYNTHA engine cycle program. Component efficiency and technology forecasts were made based on the data and trends discussed below.

Forecasted component performance data are shown in Table 6. Also shown are an engine supplier's projections made available to Lockheed for another study. Engine thrust/weight ratios are shown in Figure 14, where the trend data were derived from a combination of existing production engines and engine supplier's projections. Turbine temperatures are shown in Figure 15 where the trends were also derived from a combination of existing production engines and engine supplier projections.

The three basic methods available for cooling the turbine of a LH_2 fueled engine are: (1) aircooling; (2) aircooling, with a H_2 /air heat exchanger to chill the turbine cooling air; and (3) liquid metal cooling used in a closed loop with a H_2 /liquid metal heat exchanger. In the interest of cycle analysis

TABLE 6
PROPULSION TECHNOLOGY FORECAST

	LOCKHEED LH_2 STUDY	ENGINE SUPPLIER PROJECTED TECH LEVEL 1980 - 1985
Fan Polytropic Efficiency (max)	90%	85 - 91%
Compressor Polytropic Efficiency (max)	91.5%	92.5%
Turbine Adiabatic Efficiency	91-92%	90 - 92%
Primary Combustion Efficiency	100%	100%
Combustion Pressure Loss	6%	6%
Fan Duct Pressure Loss	2%	1%
Primary Exhaust Pressure Loss	0.5%	1%

simplification, Lockheed assumed the use of a liquid metal turbine cooling cycle for all the parametric cycle and flight performance data generated.

The following preliminary propulsion system installed performance data were used to develop all the study flight performance data. Figure 16 presents the inlet ram recovery. The data shown are based on Lockheed and Boeing FAA SST test experience (References 8, 9 and 10). Figure 17 presents inlet spillage drags for Mach 2.7 and Mach 2.2. The drag data are based on Lockheed, Boeing, and NASA test data. There is no inlet bypass drag curve because it

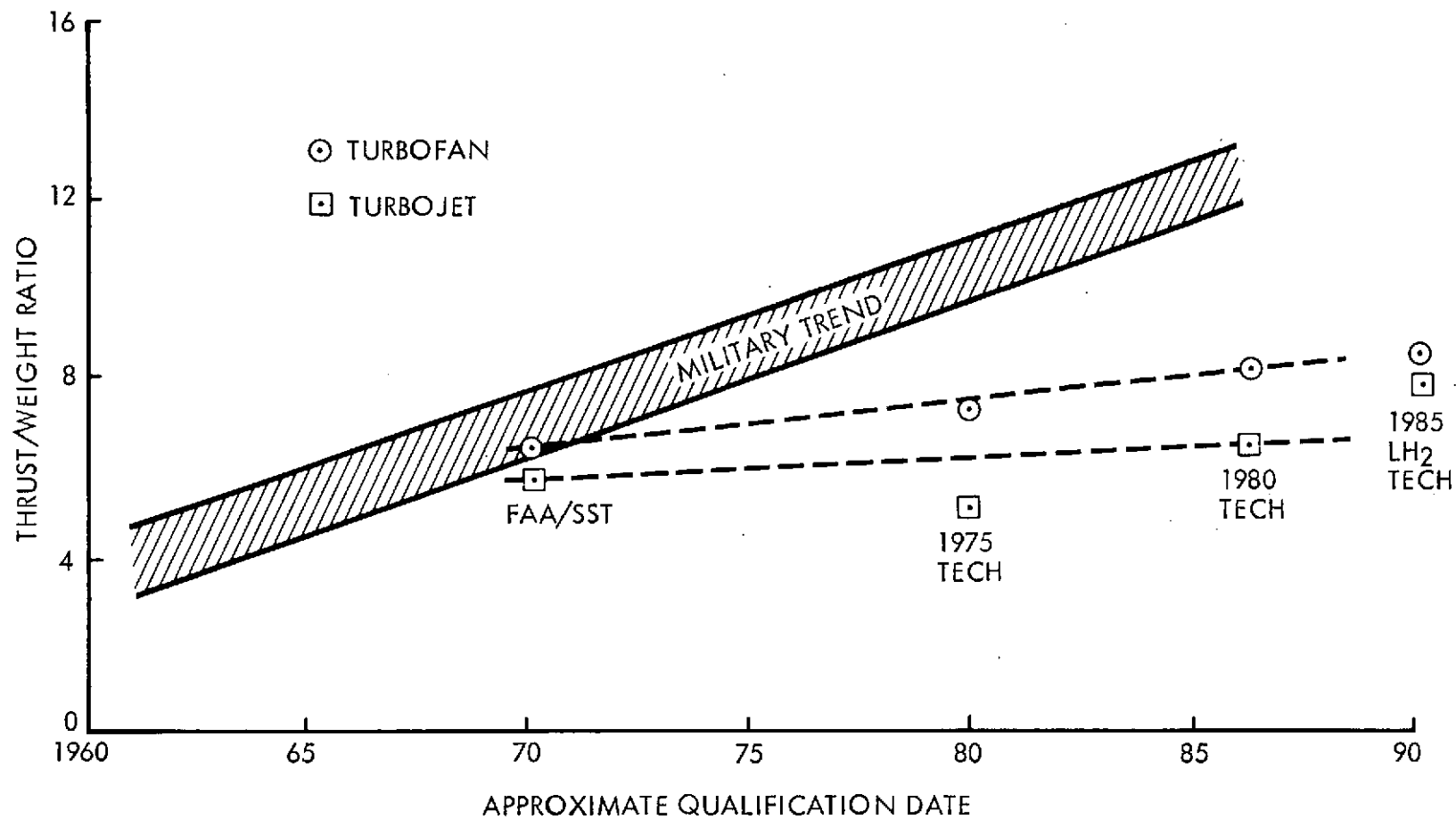


Figure 14. Engine Thrust/Weight Ratio Trends

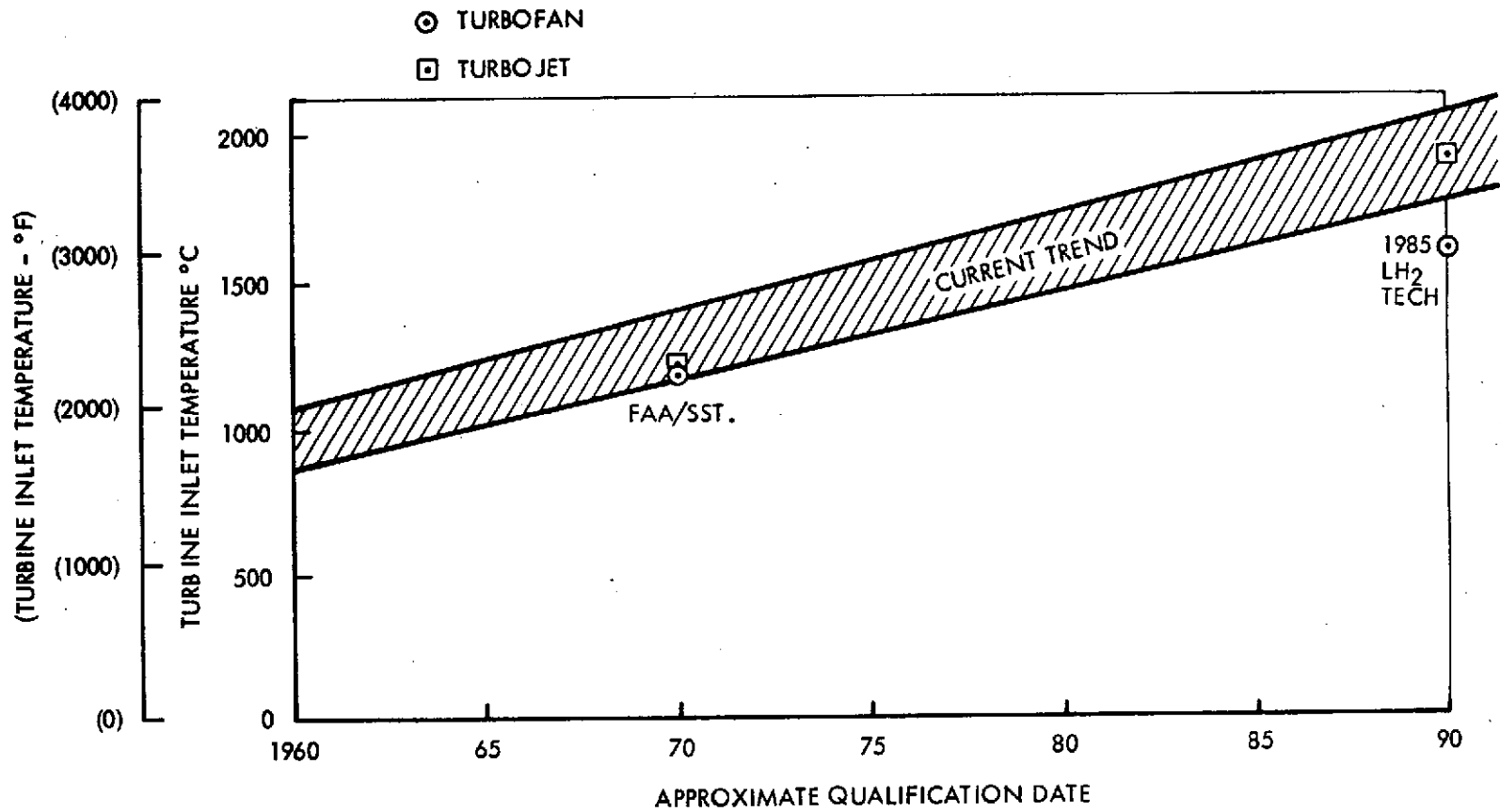


Figure 15. Turbine Inlet Temperature Trends

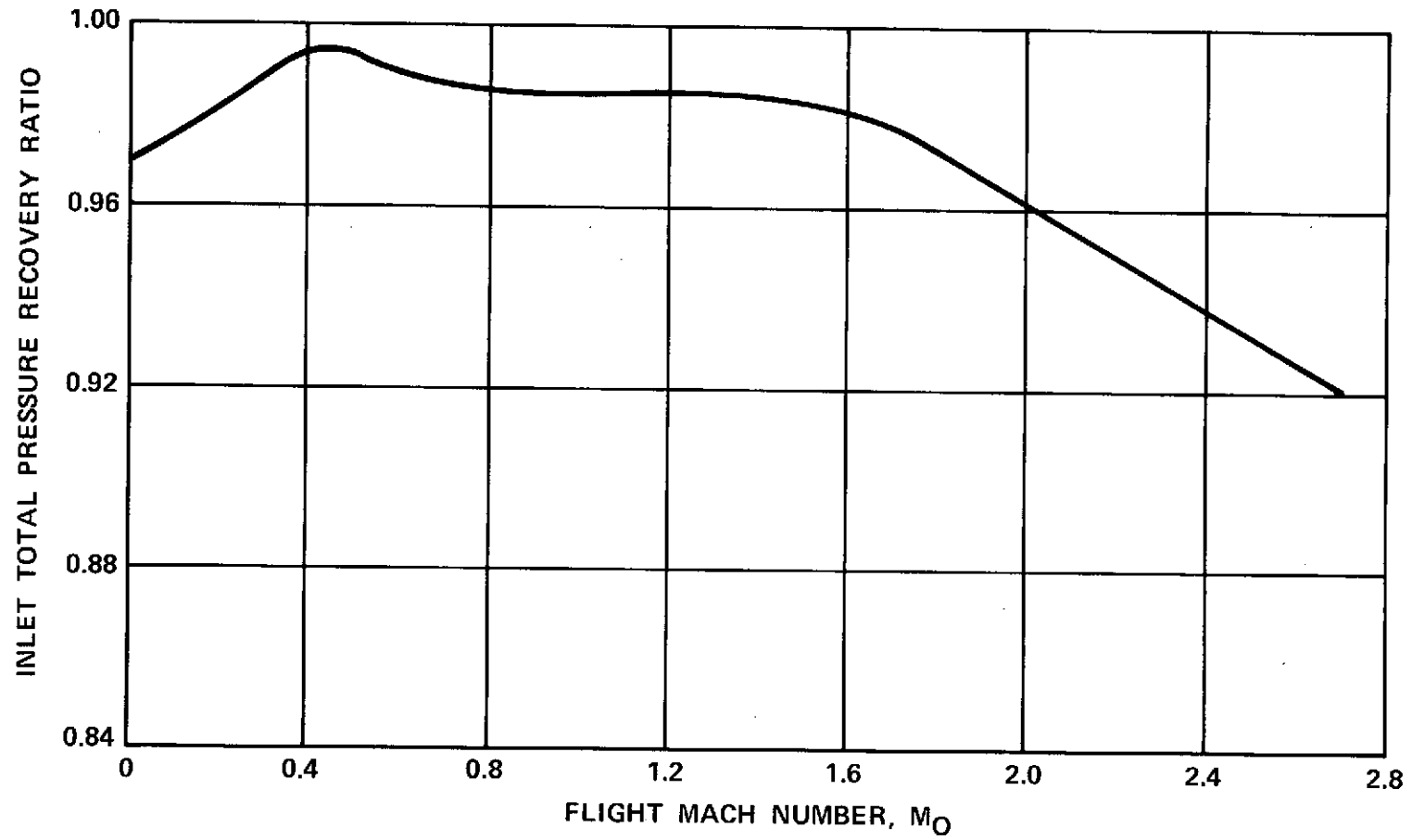


Figure 16. Inlet Recovery

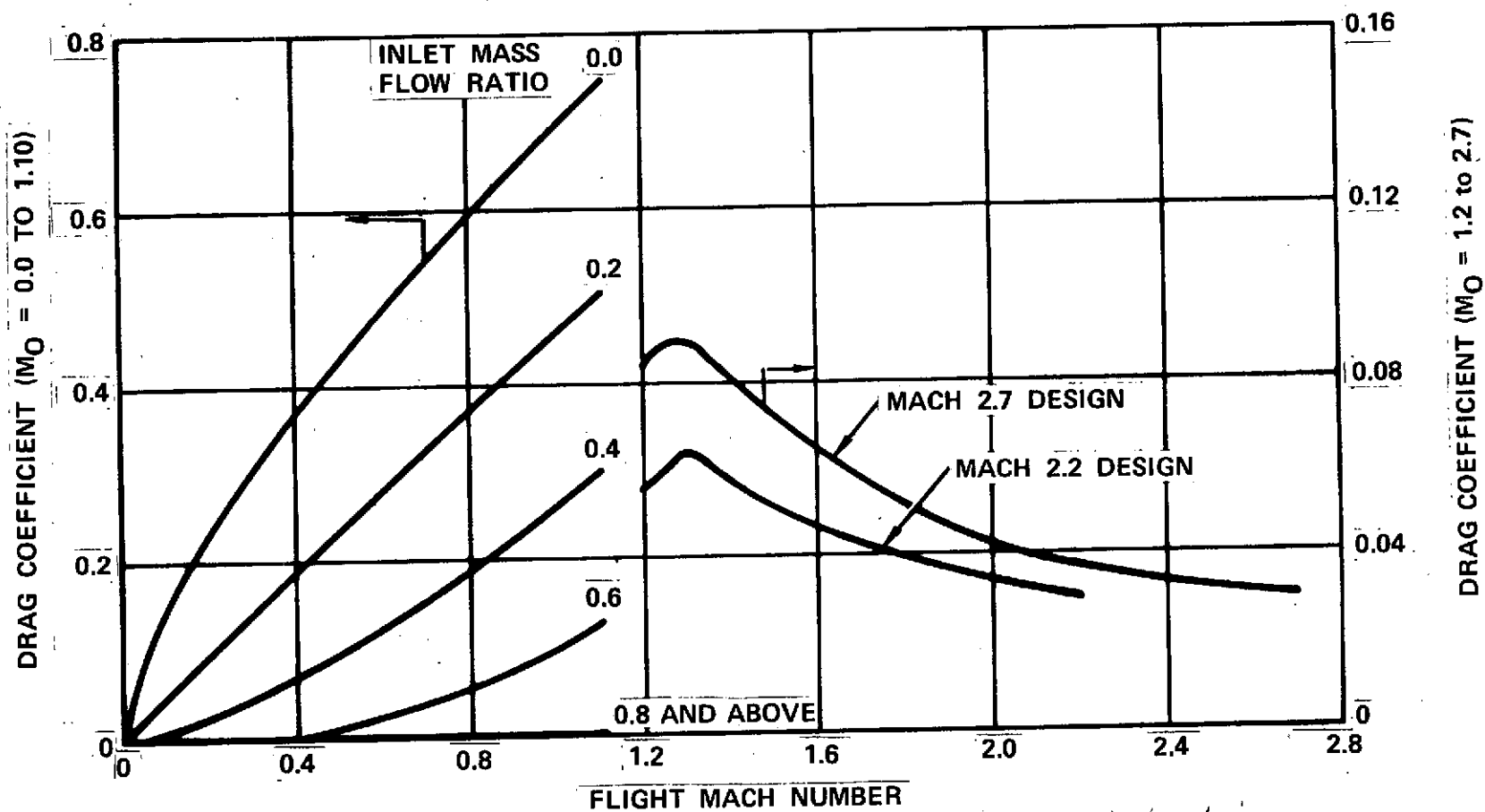


Figure 17. Spillage and Drag Coefficients

was assumed that the propulsion system would be sufficiently responsive so that in normal operation the inlet bypass doors would be closed, and that they would be opened only intermittently to prevent the shock from moving upstream and that downstream shock movements would be trimmed with engine speed changes. Figure 18 presents the nozzle velocity coefficient. These data are based on the P&WA, FAA-SST blow-in-door nozzle data. The performance also accounts for approximately one pound per second compressor discharge air bleed and 129 kw (173 horsepower) extraction.

All data were calculated using Keenan and Kayes' hydrocarbon combustion tables in conjunction with a lower heating value of 119,430 kJ per kg (51,590 BTU per pound) to represent LH_2 /air combustion products. These assumptions will not materially affect the findings of this parametric engine and aircraft study. Further studies should include the cycle effects of the products of hydrogen combustion, and a hydrogen-to-engine and aircraft heat balance that determines the effect of adding energy to the hydrogen fuel on the effective heating value of LH_2 .

3.1.3.1 Mach 2.7 Turbofan

3.1.3.1.1 Cycle Selection - A parametric study was made to select the best fan pressure ratio, over all pressure ratio, and turbine inlet temperatures for a Mach 2.7 duct burning turbofan using a liquid metal to H_2 heat exchanger. Figure 19 presents the results of this study. These data show that the performance of a Mach 2.7 cruise turbofan is relatively insensitive to turbine temperature; that a fan pressure ratio of 3 is nearly optimum and that there is little gain above an overall pressure ratio of 25. Therefore, when combined with the fuel consumption characteristics shown for subsonic operation, the cycle parameters listed in Table 7 were selected for the Mach 2.7 duct augmented turbofan. The maximum duct burning temperature of 1927°C (3500°F) was selected to provide an adequate Mach 2.7 end-of-climb thrust margin.

3.1.3.1.2 Performance Characteristics - Installed flight performance characteristics of the Mach 2.7 turbofan are shown by Figures 20, 21, 22, 23, 24 and 25, for the engine size based on Table 4. It should be noted that all the data are for a standard atmosphere except the takeoff data which is for an

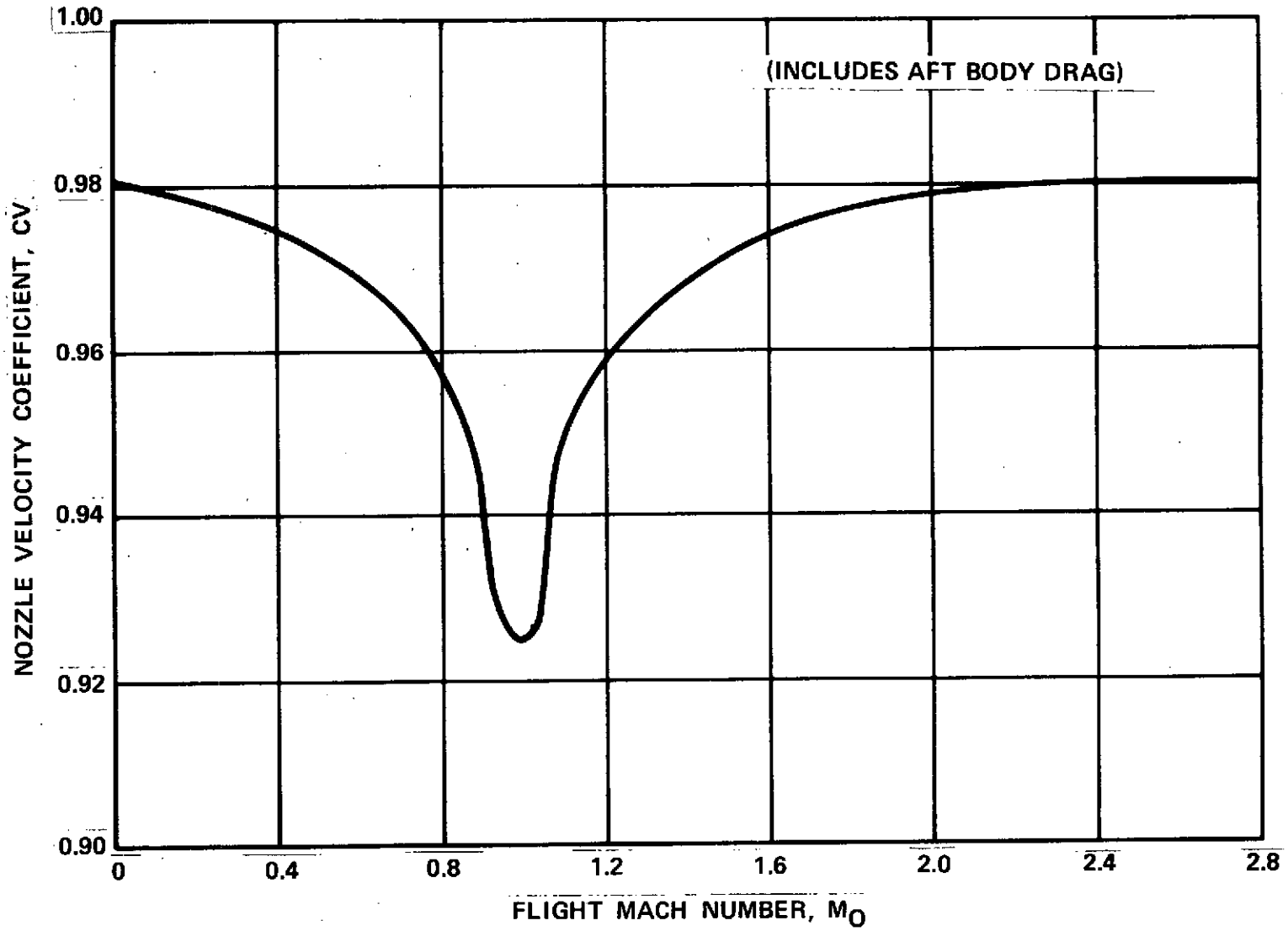
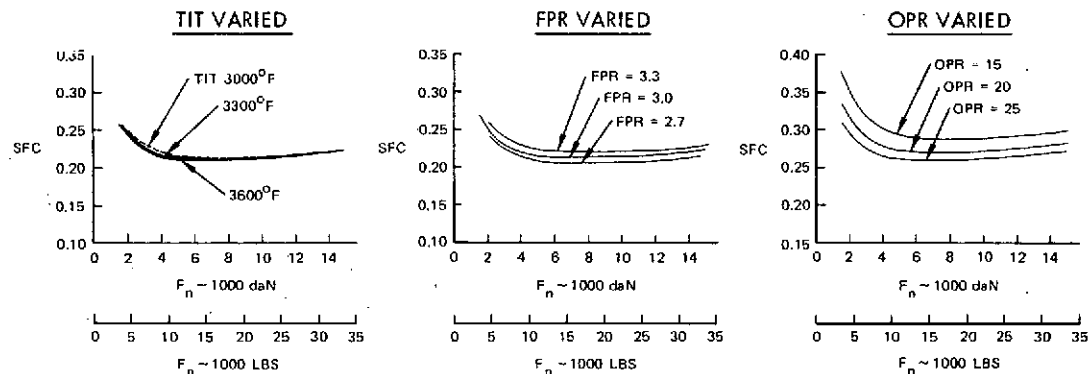


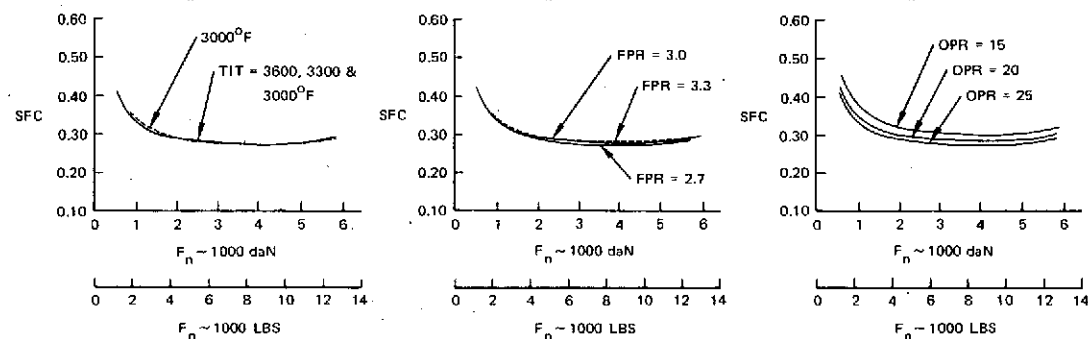
Figure 18. Nozzle Velocity Coefficients

FLIGHT
CONDITION

$M = 0.4$
 $h = 1,524 \text{ M (5,000 FT.)}$



$M = 0.9$
 $h = 11,019 \text{ M (36,150 FT.)}$



$M = 2.7$
 $h = 19,812 \text{ M (65,000 FT.)}$

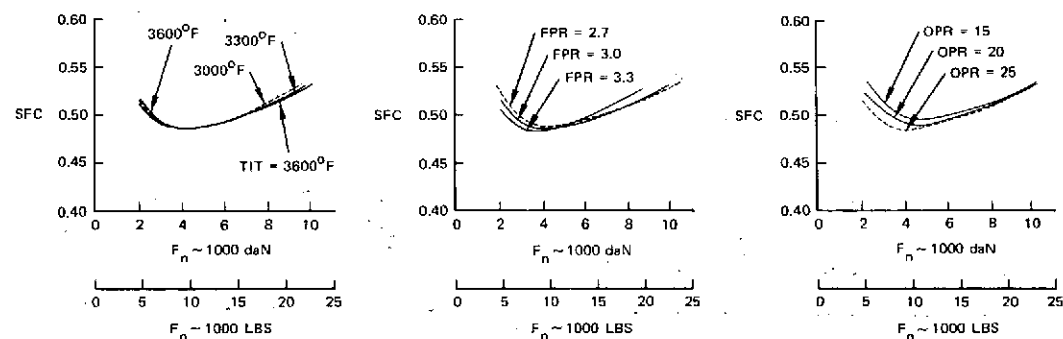


Figure 19. D-B Turbofan Engine Cycle Selection

NOISE LIMITED TAKEOFF POWER (AUGMENTED)

1214

AST MACH 2.7 DUCT-BURNING TURBOFAN LH2TF-1 STD+15C

U.S. STANDARD ATMOSPHERE 1962

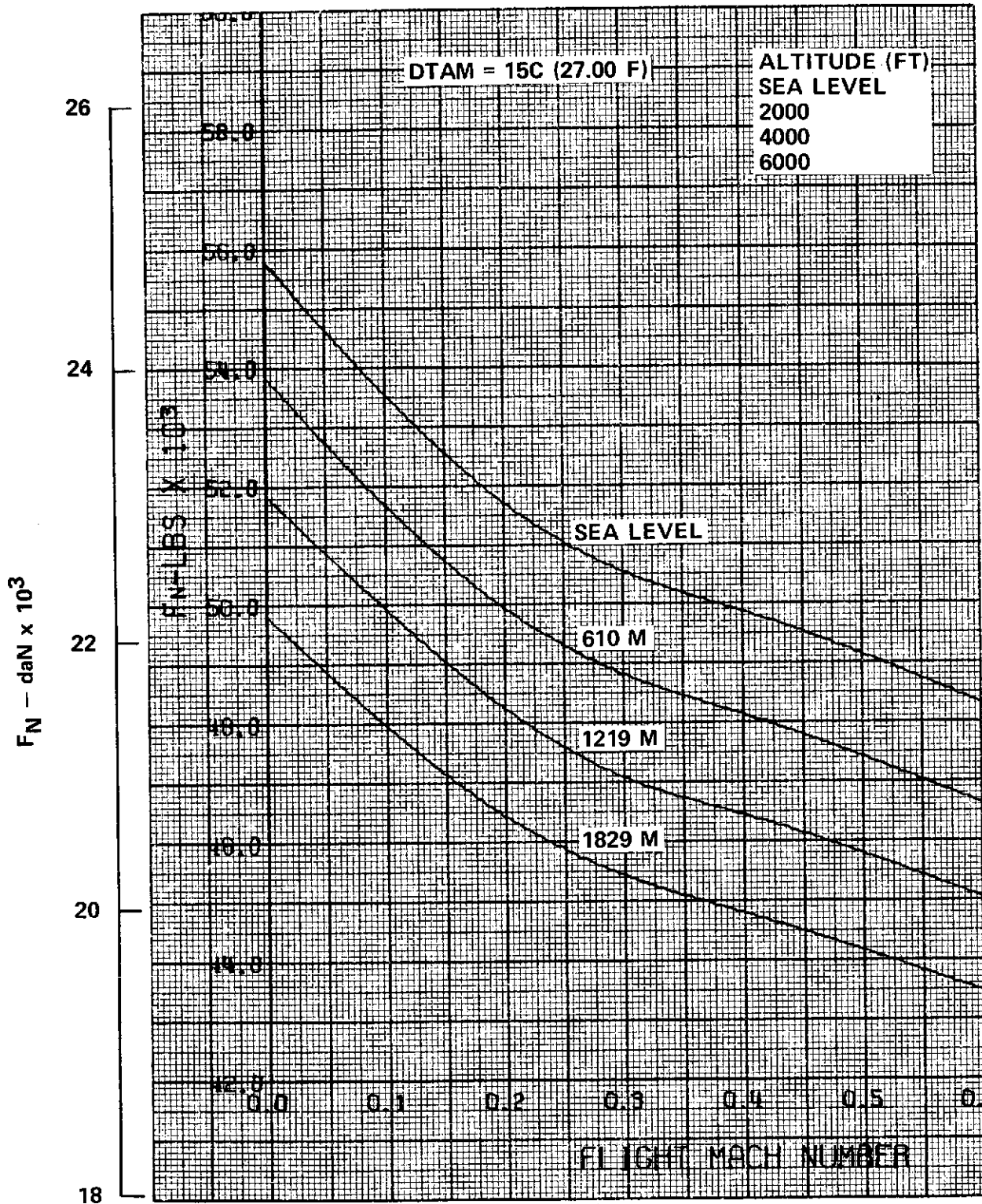


Figure 20. Installed Flight Performance (Thrust)

AUGMENTED MAX CLIMB
1201
AST MACH 2.7 DUCT-BURNING TURBOFAN LH2-1
U.S. STANDARD ATMOSPHERE 1962

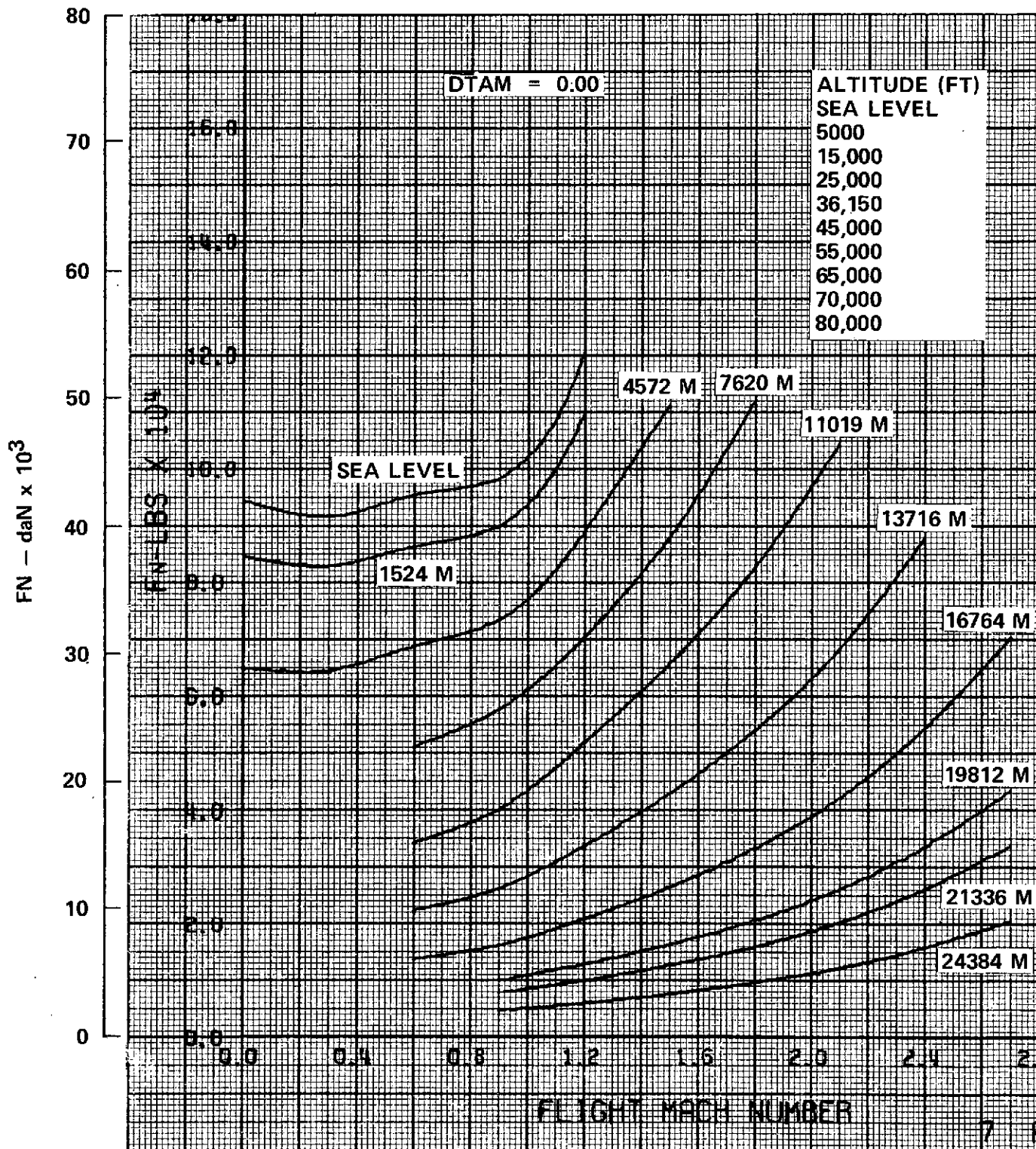


Figure 21. Installed Flight Performance (Thrust)

AUGMENTED MAX CLIMB
1201
AST MACH 2.7 DUCT-BURNING TURBOFAN LH2-1
U.S. STANDARD ATMOSPHERE 1962

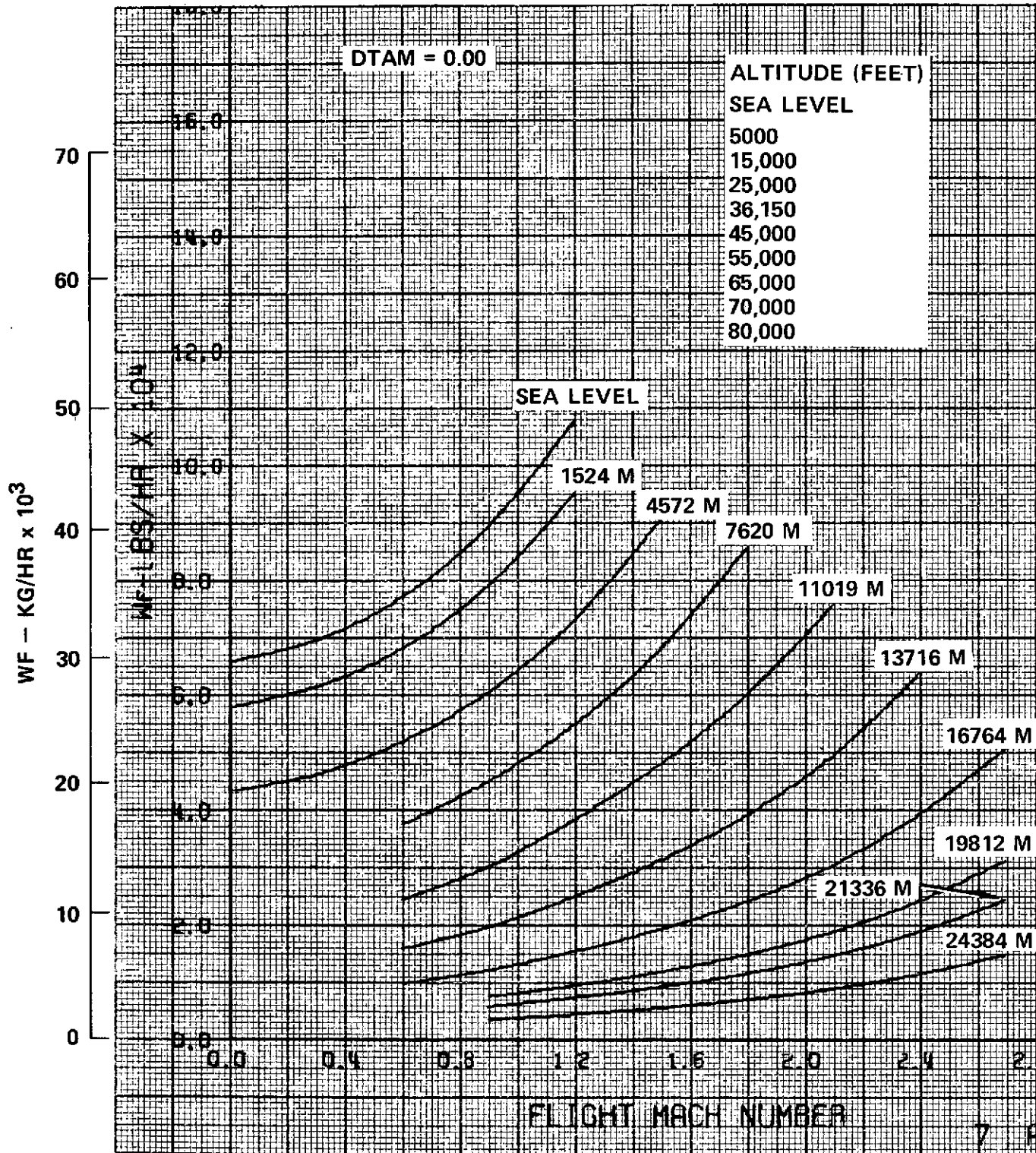


Figure 22. Installed Flight Performance (Fuel Consumption)

NON-AUGMENTED PART POWER
-1101
AST MACH 2.7 DUCT-BURNING TURBOFAN LH2-1
U.S. STANDARD ATMOSPHERE 1962

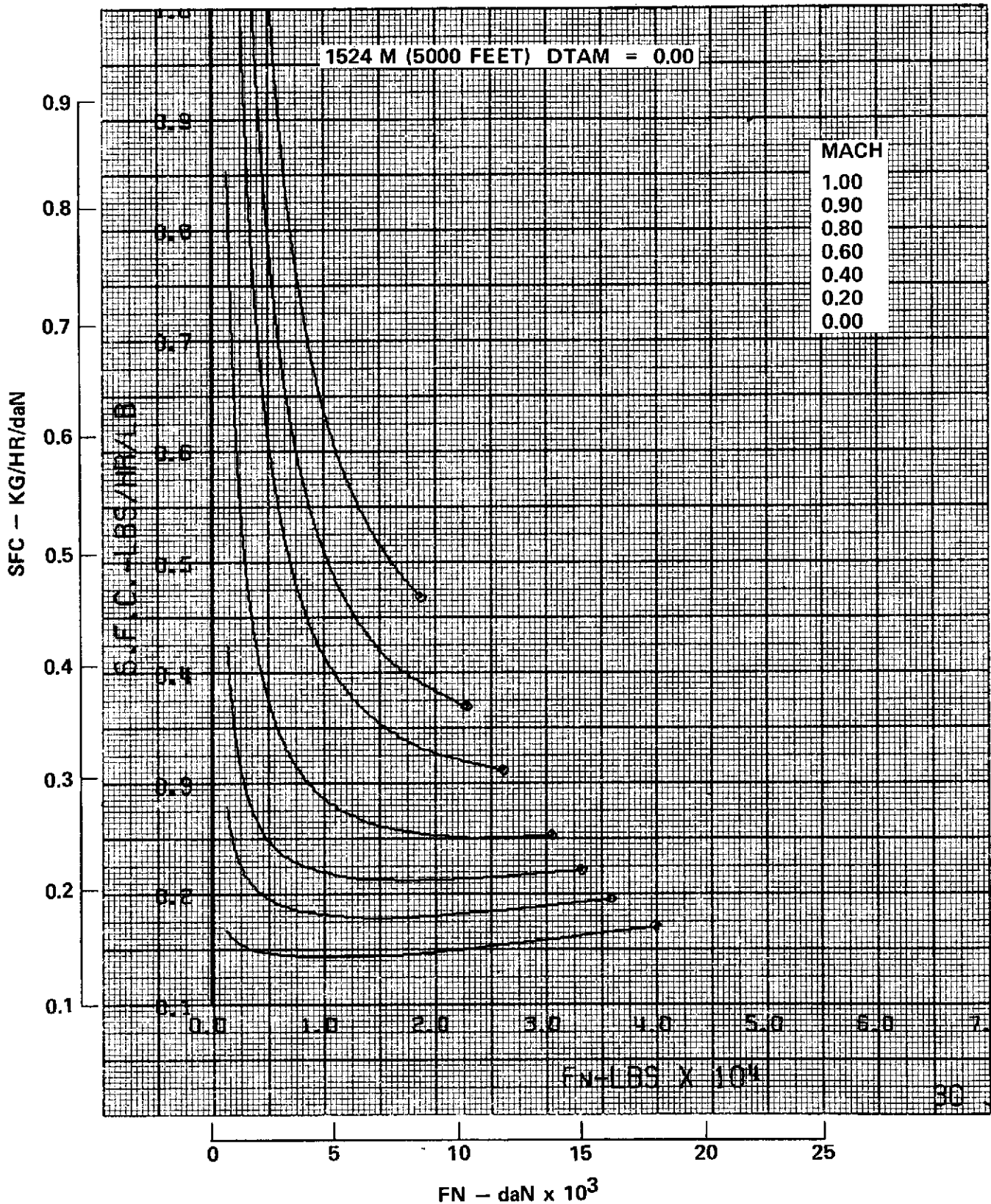


Figure 23. Installed Flight Performance (SFC)

NON-AUGMENTED PART POWER

-1101

AST MACH 2.7 DUCT-BURNING TURBOFAN LH2-1
U.S. STANDARD ATMOSPHERE 1962

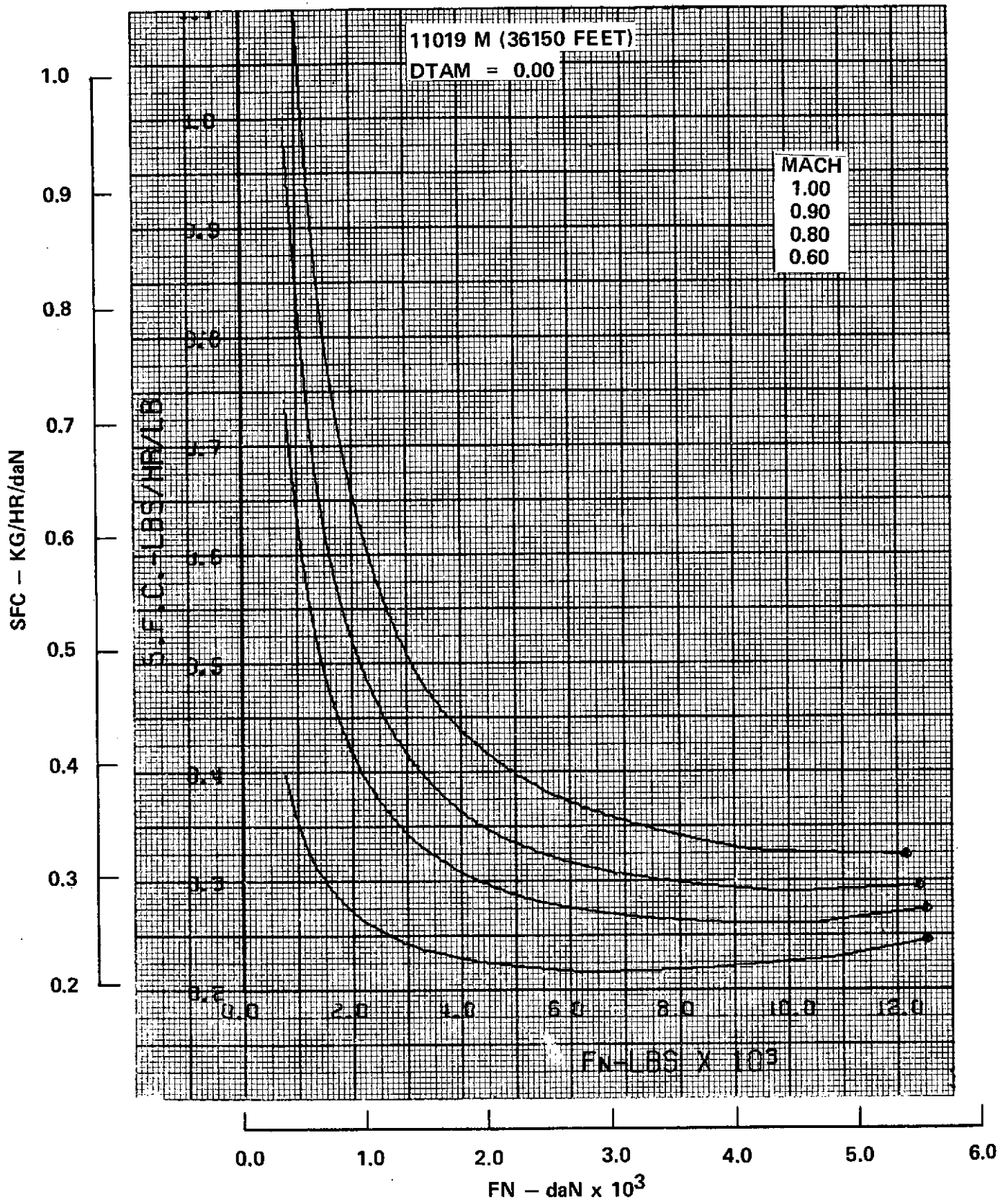


Figure 24. Installed Flight Performance (SFC)

AUGMENTED PART POWER
-1201
AST MACH 2.7 DUCT-BURNING TURBOFAN LH2-1

U.S. STANDARD ATMOSPHERE 1962

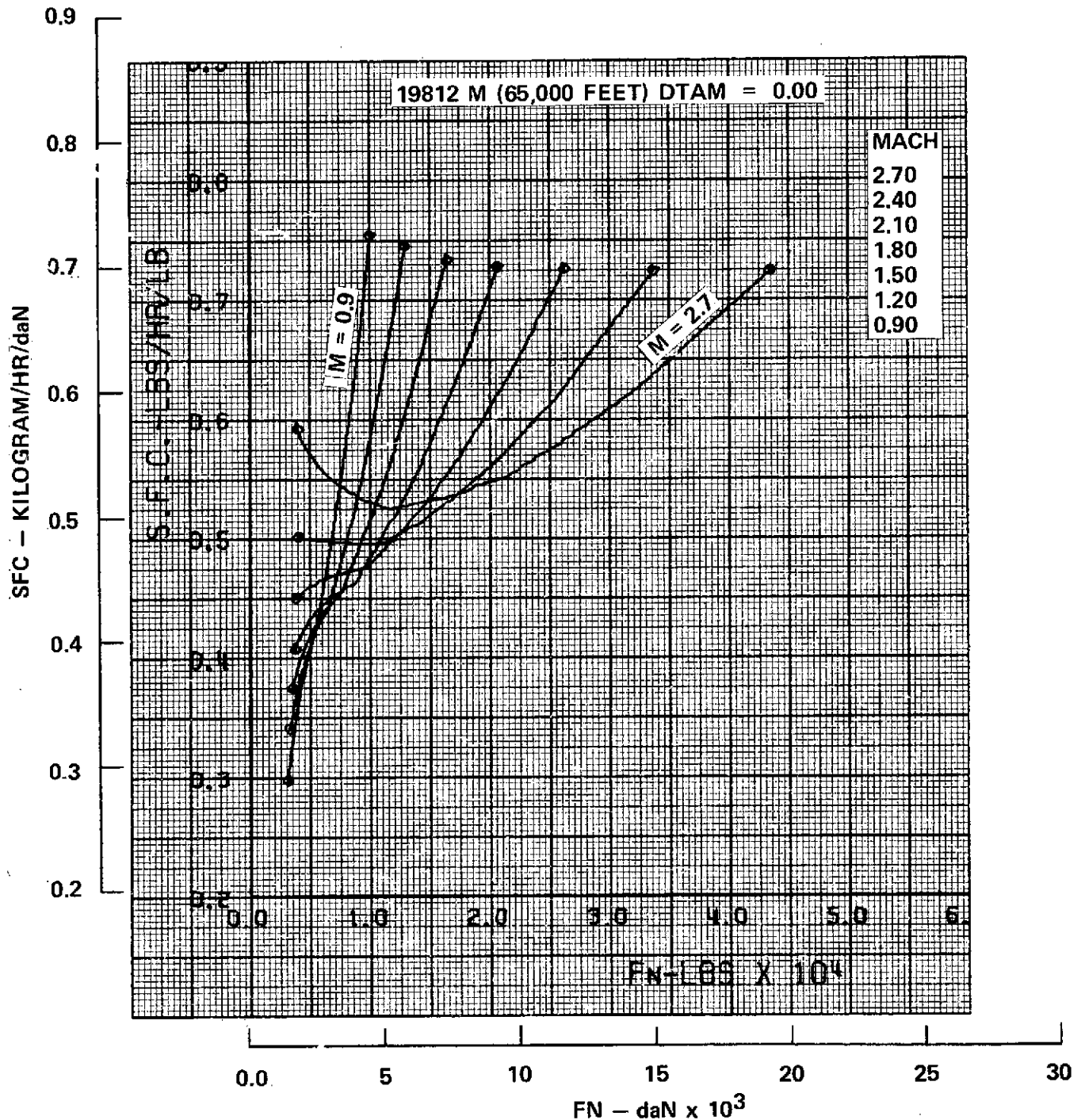


Figure 25. Installed Flight Performance (SFC)

ISA +15°C (27°F) day. Figure 20 is shown as an example of the many duct temperature-limited engine operation schedules which were evaluated at take-off conditions to meet FAR Part 36 minus 5 EPN dB noise constraints.

3.1.3.1.3 Physical Characteristics - The internal flowpath of the Phase I and Phase II Mach 2.7 duct burning turbofans is shown by Figure 26. This sketch shows Phase II engine dimensions and presents the engine lines used for installation configuration purposes. These dimensional characteristics are based on inlet, fan, compressor, combustor, turbine, and exhaust component configurations, and gas velocities commonly used by engine manufacturers. Nacelle configuration, dimensions and scaling data for the Phase I engine are shown in Figure 27.

3.1.3.1.4 Noise Considerations - The scope of the parametric study did not provide for a completely integrated acoustic-propulsion system design. However, as shown by Figure 26 the fan stages are spaced to reduce the blade passage noise while the blow-in-door nozzle provides tertiary air for sound suppression. The engine size was selected to meet aircraft liftoff thrust requirements, and to also satisfy the low noise limit, by restricting duct burning temperature to 849°C (1560°F) during takeoff. The cycle turbine energy is split so that the noise of the gas generator exhaust is lower than the FAR Part 36 minus 5 EPNdB noise goals and therefore a noise suppressor is only required for the fan exhaust. Figures 28a, b and c show the P&WA noise data that were used for preliminary estimations of sound suppressed noise at the point of aircraft liftoff. These P&WA data were used to establish the following noise limited engine characteristics: thrust size, takeoff power setting, installation configuration, and weight estimates. These curves were also used for the initial sizing of the Mach 2.7 and Mach 2.2 turbojet engines at the point of liftoff. Subsequent to the initial engine sizing effort, Lockheed developed the suppression curve labeled "Lockheed Assumed Locus of Optimum Designs" shown superimposed on P&WA suppression data by Figure 29. These estimates are based on a conglomeration of available data from tests and analyses of several suppressor configurations which indicate suppression requirements at a particular jet velocity would be best satisfied by a suppressor designed for that velocity. A locus of such point designs would have

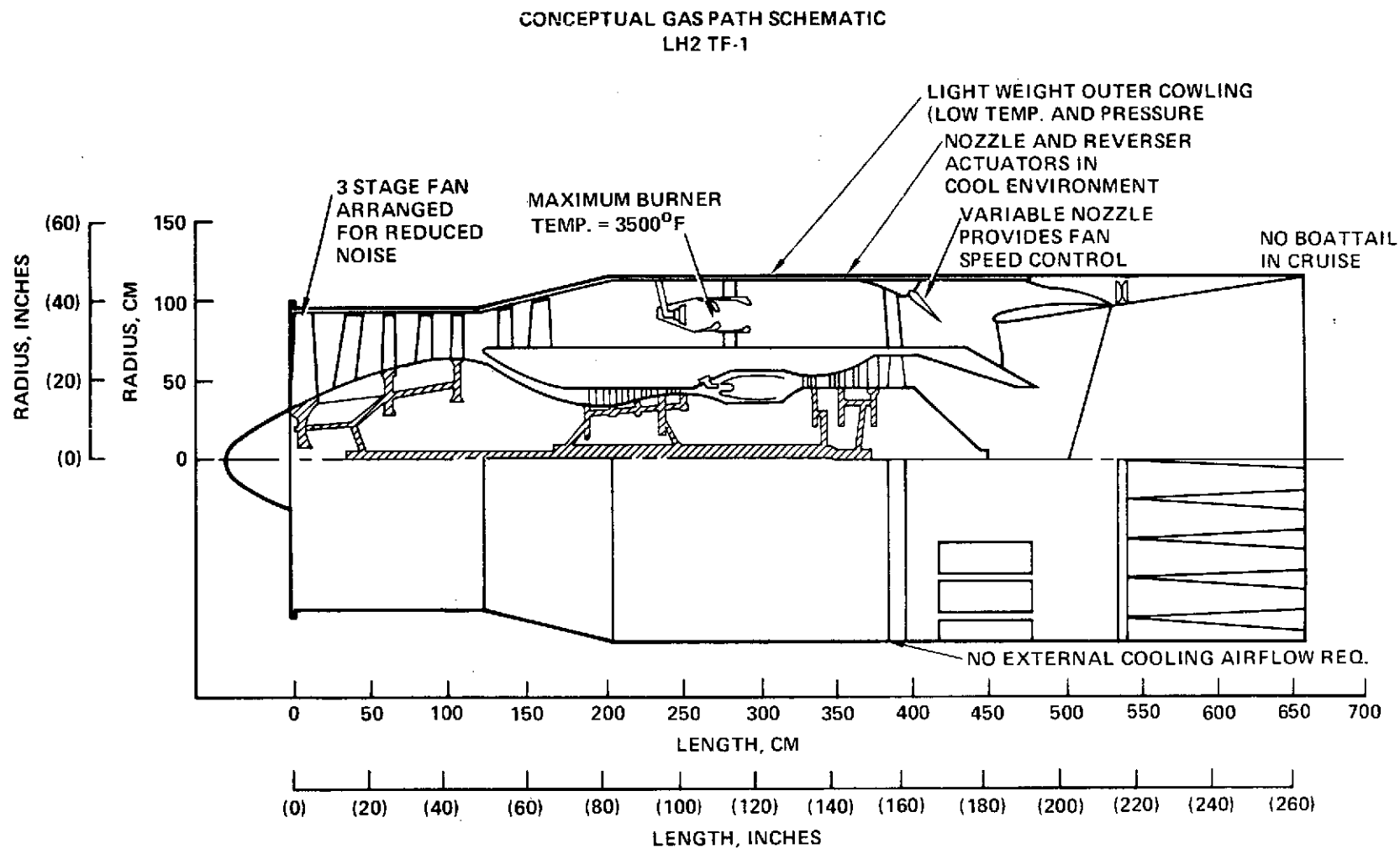


Figure 26. Duct Burning Turbofan Schematic

PARAMETER	REFERENCE VALUE	
$FN_{SLS} \text{ MAX}^\dagger$	45120 daN	(100860 LB)
$FN \text{ L.O.}$	25320 daN	(56500 LB)
A_C	3.01 M ²	(32.4 FT ²)
D_{COMP}	2.014 M	(79.3 IN.)
D_{MAX}	2.515 M	(99.0 IN.)
D_{NOZ}	2.515 M	(99.0 IN.)
L_{ENG}	6.756 M	(266.0 IN.)
L_{INLET}	5.131 M	(202.0 IN.)
WEIGHT*	5260 KG	(11600 LB)

† D/B TEMP = 3960°R

* INCLUDES REVERSER AND SUPPRESSOR

$$DIAM = DIAM_{REF} \left(\frac{FN_{SLS}}{FN_{SLS_{REF}}} \right)^{0.5}$$

$$L_{ENG} = L_{ENG \text{ REF}} \left(\frac{FN_{SLS}}{FN_{SLS_{REF}}} \right)^{0.35}$$

$$L_{INLET} = 2.56 \times D_{COMP}$$

$$WEIGHT = WEIGHT_{REF} \left(\frac{FN_{SLS}}{FN_{SLS_{REF}}} \right)$$

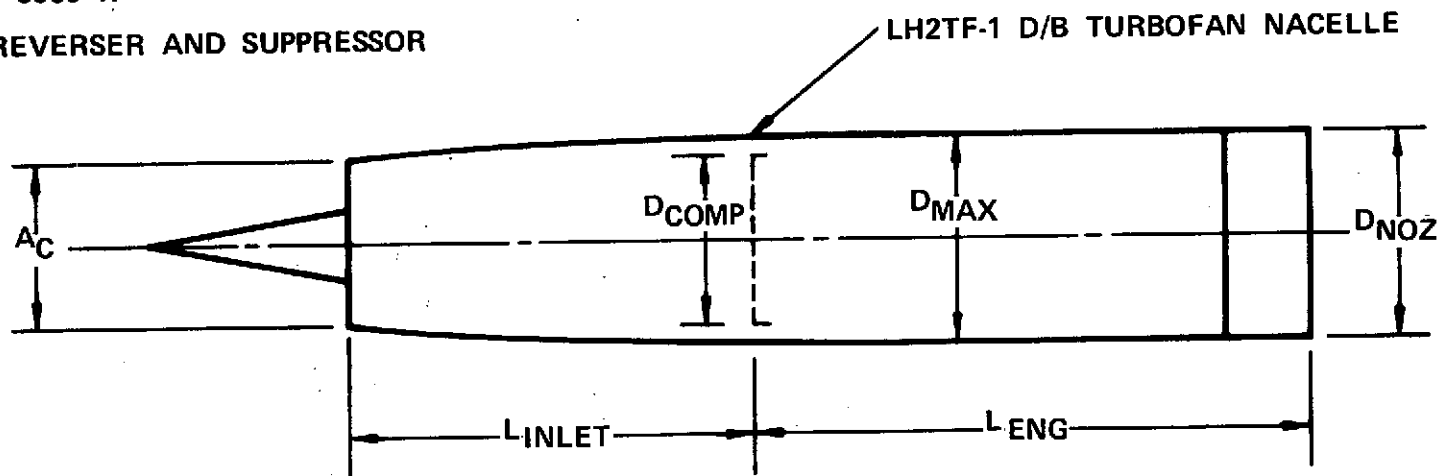


Figure 27. Dry Turbojet LH2TJ-2 Nacelle Dimensions and Scaling Data

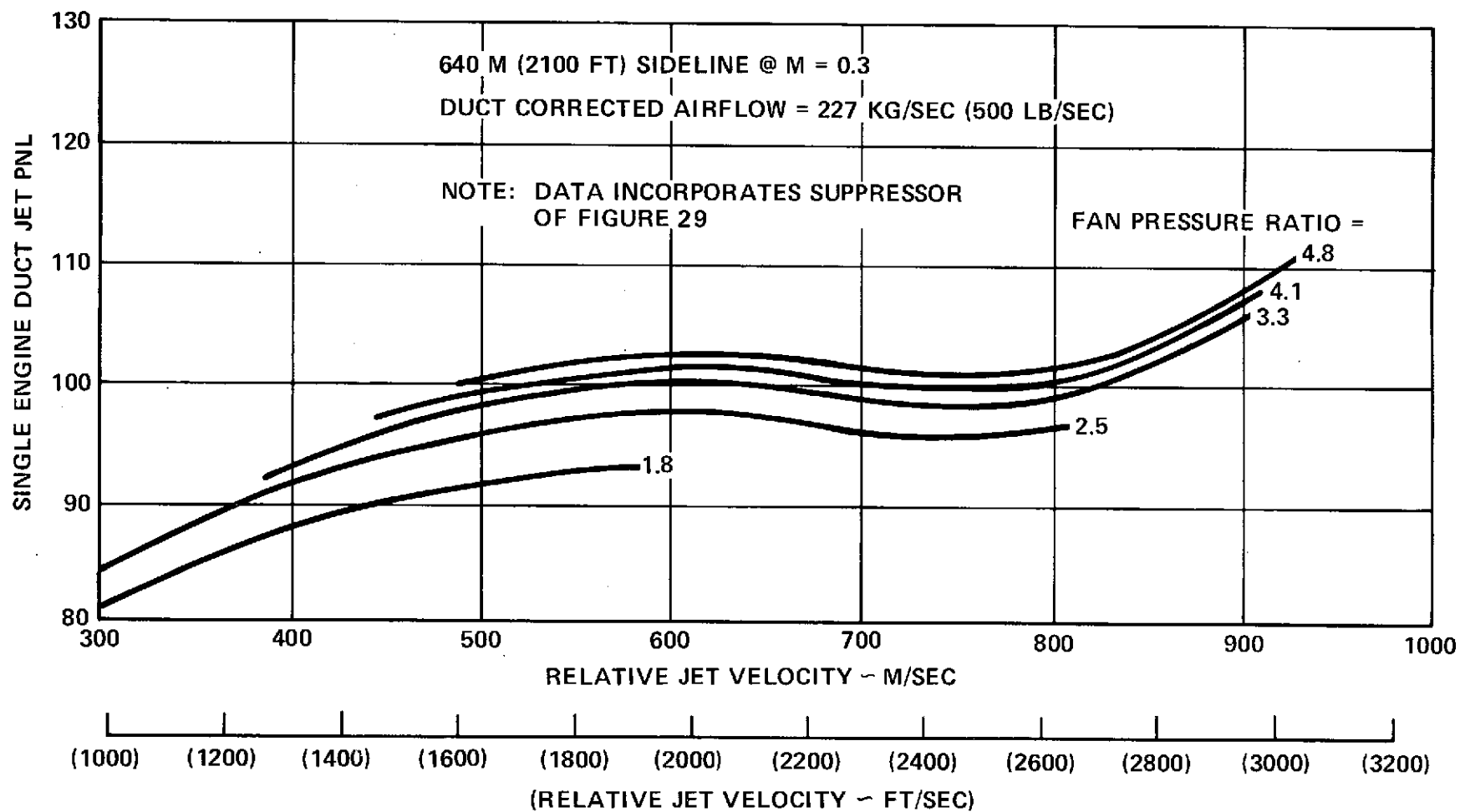


Figure 28a. Sideline Suppressed Duct Jet Noise (Augmented)

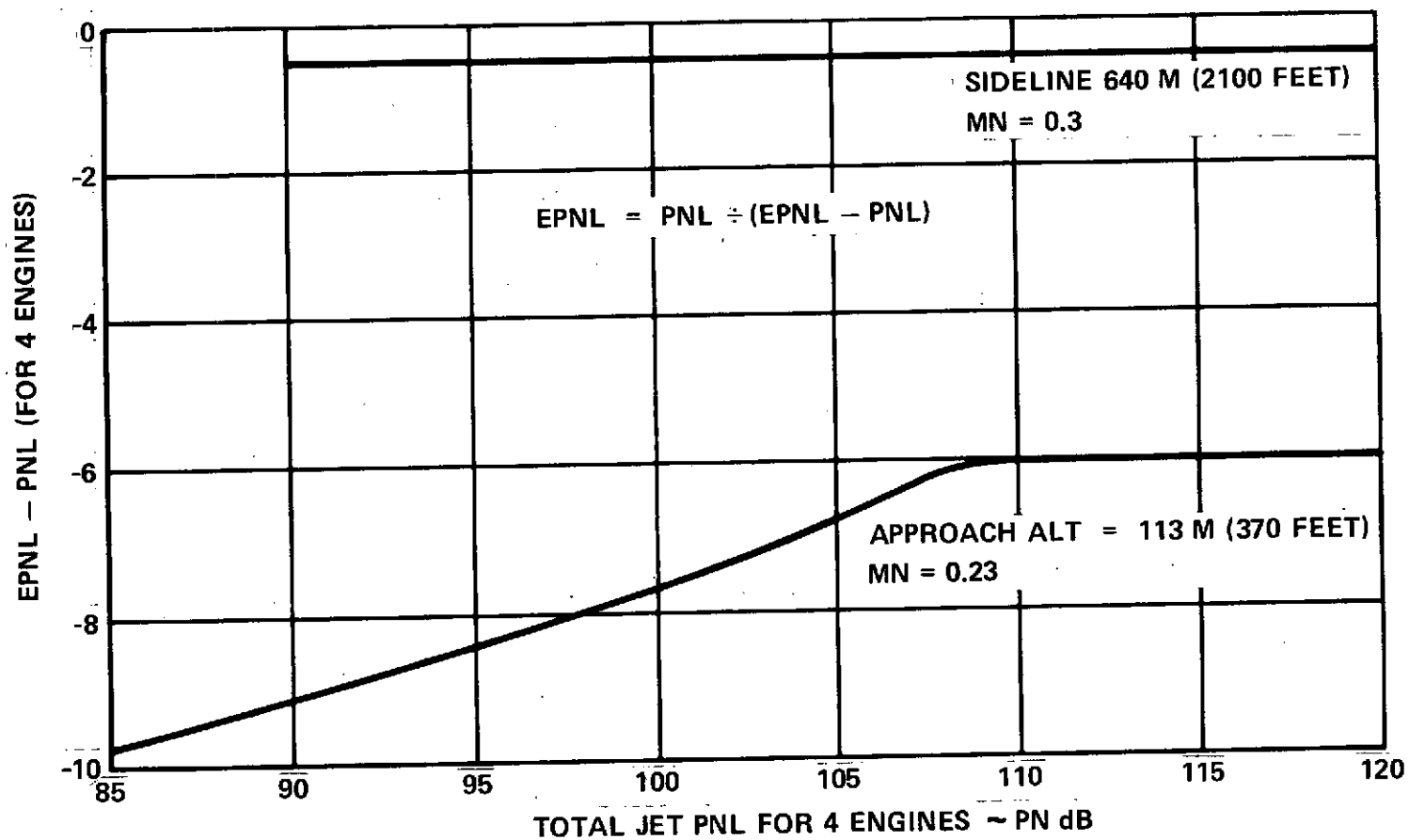


Figure 28b. Jet Noise Conversion to EPNL

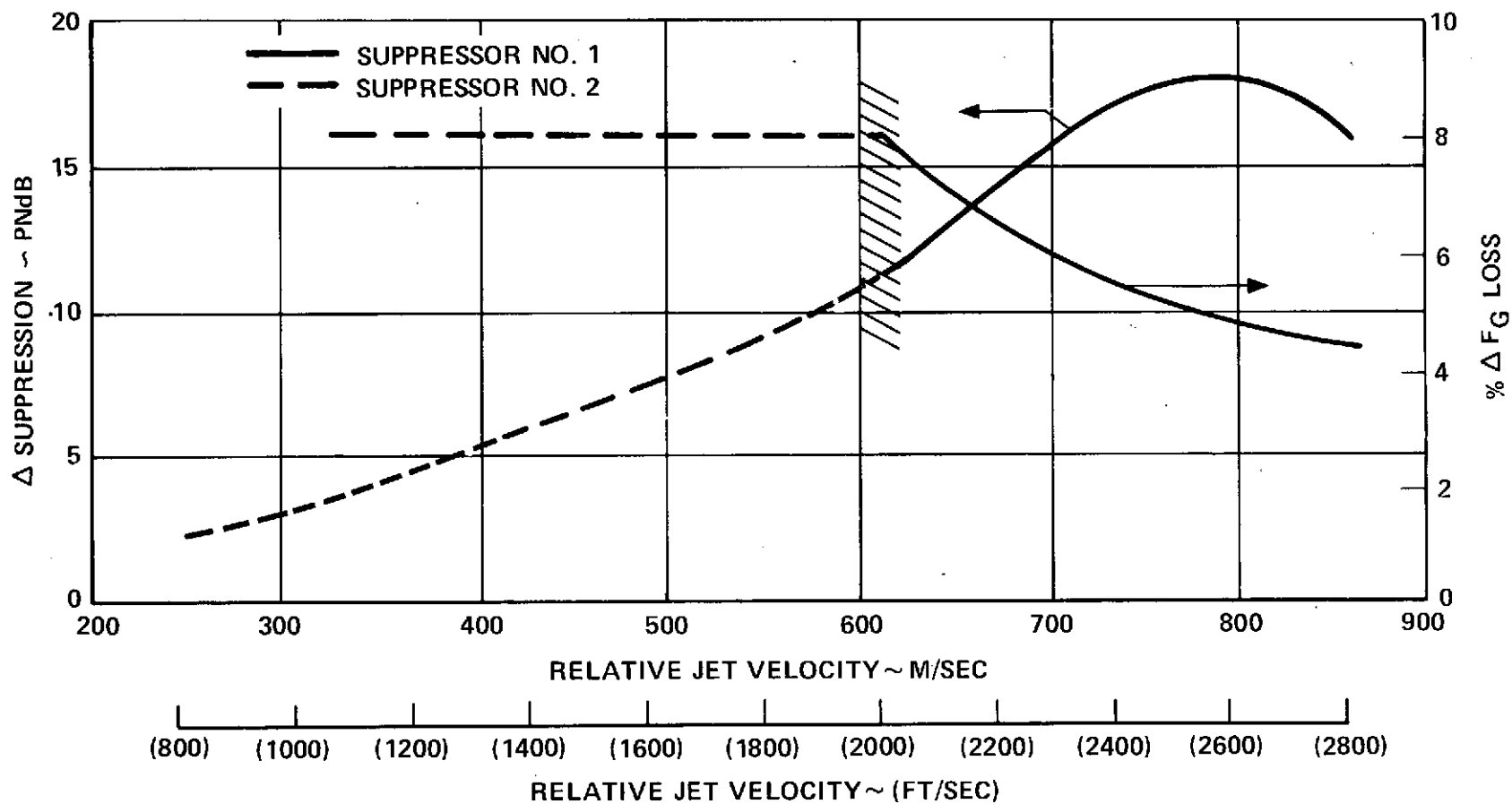


Figure 28c. Jet Noise Suppressor Performance

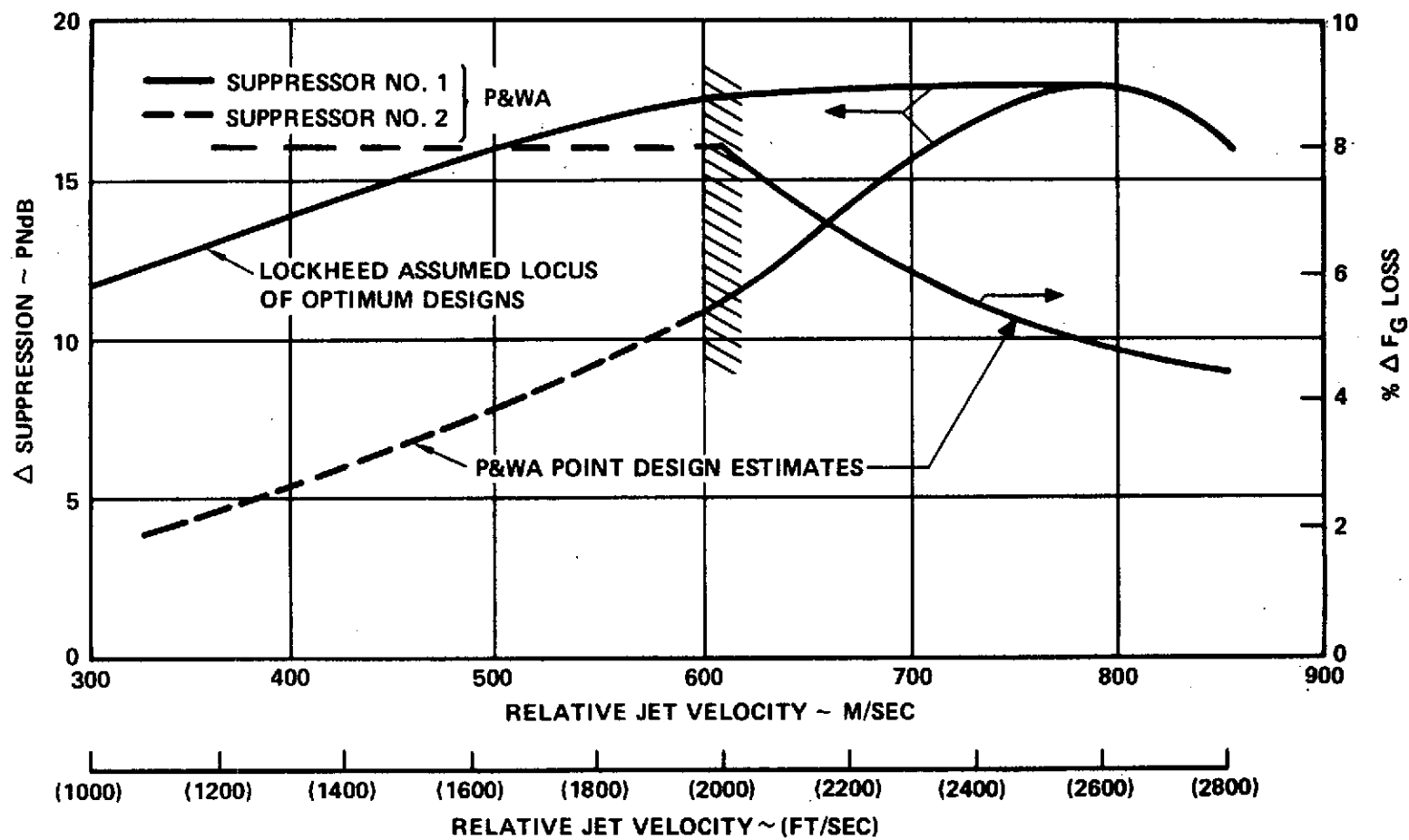


Figure 29. AST Jet Noise Suppressor Performance

higher suppression capability in the lower velocity region than suppressor #2 shown by P&WA. These Lockheed assumed noise suppression characteristics were used for engine sizing in the Phase I and Phase II ASSET parametric aircraft analyses.

3.1.3.2 Mach 2.7 Turbojet

3.1.3.2.1 Cycle Selection - Turbojet engines are power limited at the high altitude Mach 2.7 end of climb and thus require the highest possible turbine inlet temperature. To reduce the engine size for climb and cruise a turbine temperature of 1982°C (3600°F) was chosen as the practical maximum for all parametric cycle and installed engine performance calculations. Because the Mach 2.7 turbojet was assumed to be a single spool, variable stator engine, a limiting compression ratio of 25 was selected as a practical maximum. A study was then made to determine the effects of cycle compression ratio on the turbojet's performance. Figure 30 presents results of this study. As shown, there is significant loss in performance with compression ratios less than 25. Therefore, a turbine temperature of 1982°C (3600°F) and a compression ratio of 25 were selected which, when combined with the component performance characteristics shown in Table 7, provided performance for the Mach 2.7 LH_2 fueled turbojet for the parametric analyses.

3.1.3.2.2 Performance Characteristics - Selected installed flight performance data for the Mach 2.7 turbojet are shown in Figures 31, 32, 33, 34, 35 and 36. Again, as in the case of the duct temperatures for the turbofan, several turbine inlet temperatures were investigated for the turbojet to find the condition that would satisfy the noise specification at takeoff. The plot of Figure 31 is for $\text{TIT} = 1200^{\circ}\text{K}$ (2160°R).

As shown by comparison of Figures 36 and 25, the turbojet has better supersonic cruise specific fuel consumption than the duct augmented turbofan. A direct comparison of the SFC differential is shown by the SFC vs thrust/pound of airflow presentation of Figure 37.

3.1.3.2.3 Physical Characteristics - The internal flow path of the Mach 2.7 turbojet is shown in Figure 38. This sketch shows that the conceptual turbojet generally conforms to common engine industry design practices. As shown, the

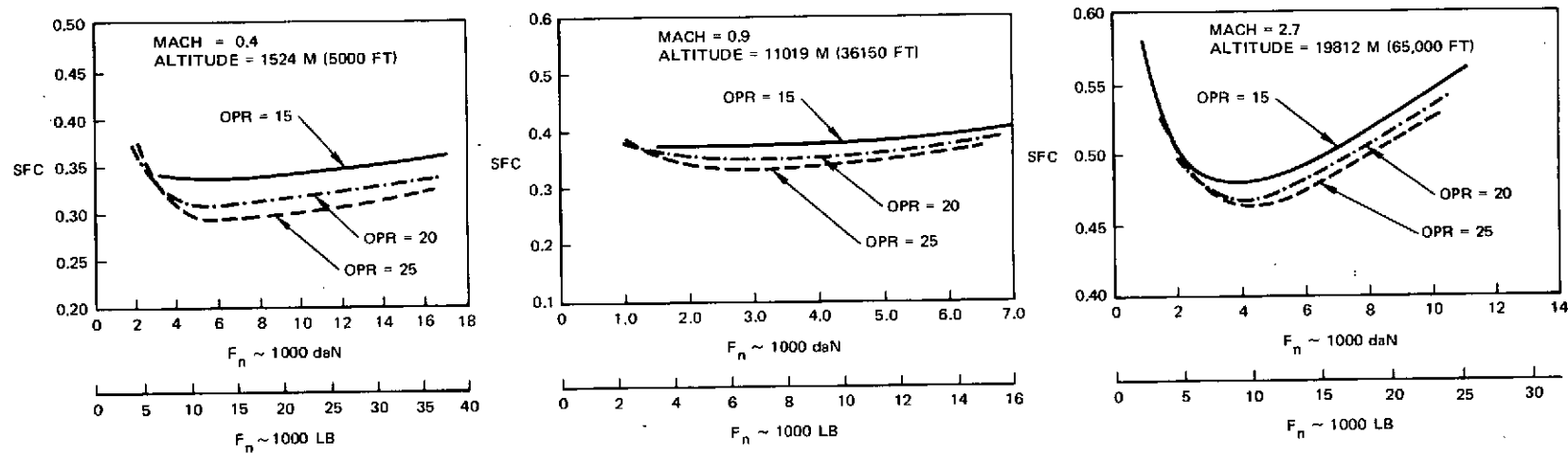


Figure 30. Turbojet Engine Cycle Selection - OPR Varied

TABLE 7
LIQUID HYDROGEN TURBOJET AND TURBOFAN CYCLE CHARACTERISTICS
(SLS, UNINSTALLED)

PHASE I

Engine Designation Engine Type Design Cruise Mach	LH2TF-1 DB TF 2.7	LH2TJ-1 DRY TJ 2.7	LH2TJ-2 DRY TJ 2.2
Max Thrust daN (lb)	45,100 (100,660)	33,900 (76,100)	42,300 (95,100)
Specific Fuel Consumption kg/hr (lb/hr)	0.696 (0.683)	0.414 (0.406)	0.414 (0.406)
Corrected Airflow - $\omega\sqrt{\theta/\delta}$ kg/sec (lb/sec)	464 (1024)	250 (551)	312 (689)
Bypass Ratio	4.4	--	--
Fan Pressure Ratio	3.0	--	--
Fan Adiabatic Efficiency	0.866	--	--
Compressor Pressure Ratio	8.33	25.0	25.0
Compressor Adiabatic Efficiency	0.871	0.835	0.835
Overall Pressure Ratio	25.0	25.0	25.0
Nozzle Velocity Coefficient (Duct)	0.981	--	--
Nozzle Velocity Coefficient (Primary)	0.981	0.981	0.981
Max Turbine Inlet Temp °C (°F)	1649 (3000)	1982 (3600)	1982 (3600)
Max Duct Burning Temp °C (°F)	1927 (3500)	--	--
Fuel Heating Value kD/kg (BTU/lb)	119,430 (51,590)	199,430 (51,590)	119,430 (51,590)
Peak Fan Polytropic Efficiency	0.900	--	--
Peak Compressor Polytropic Efficiency	0.915	0.915	0.915
HP Turbine Adiabatic Efficiency	0.920	0.920	0.920
LP Turbine Adiabatic Efficiency	0.910	--	--
Primary Burner Efficiency	1.000	1.000	1.000
Duct Burner Efficiency	0.916	--	--
Primary Burner Pressure Loss Ratio	0.060	0.060	0.060
Duct Burner Pressure Loss Ratio	0.071	--	--
Primary Nozzle Pressure Loss Ratio	0.005	0.005	0.005
Thrust to Engine WT Ratio daN/kg (lb/lb)	8.6 (8.7)	7.8 (7.9)	7.8 (7.9)

NOISE LIMITED TAKEOFF POWER

AST MACH 2.7 DRY TURBOJET LH2TJ-1 STD + 15C T/O

U.S. STANDARD ATMOSPHERE 1962

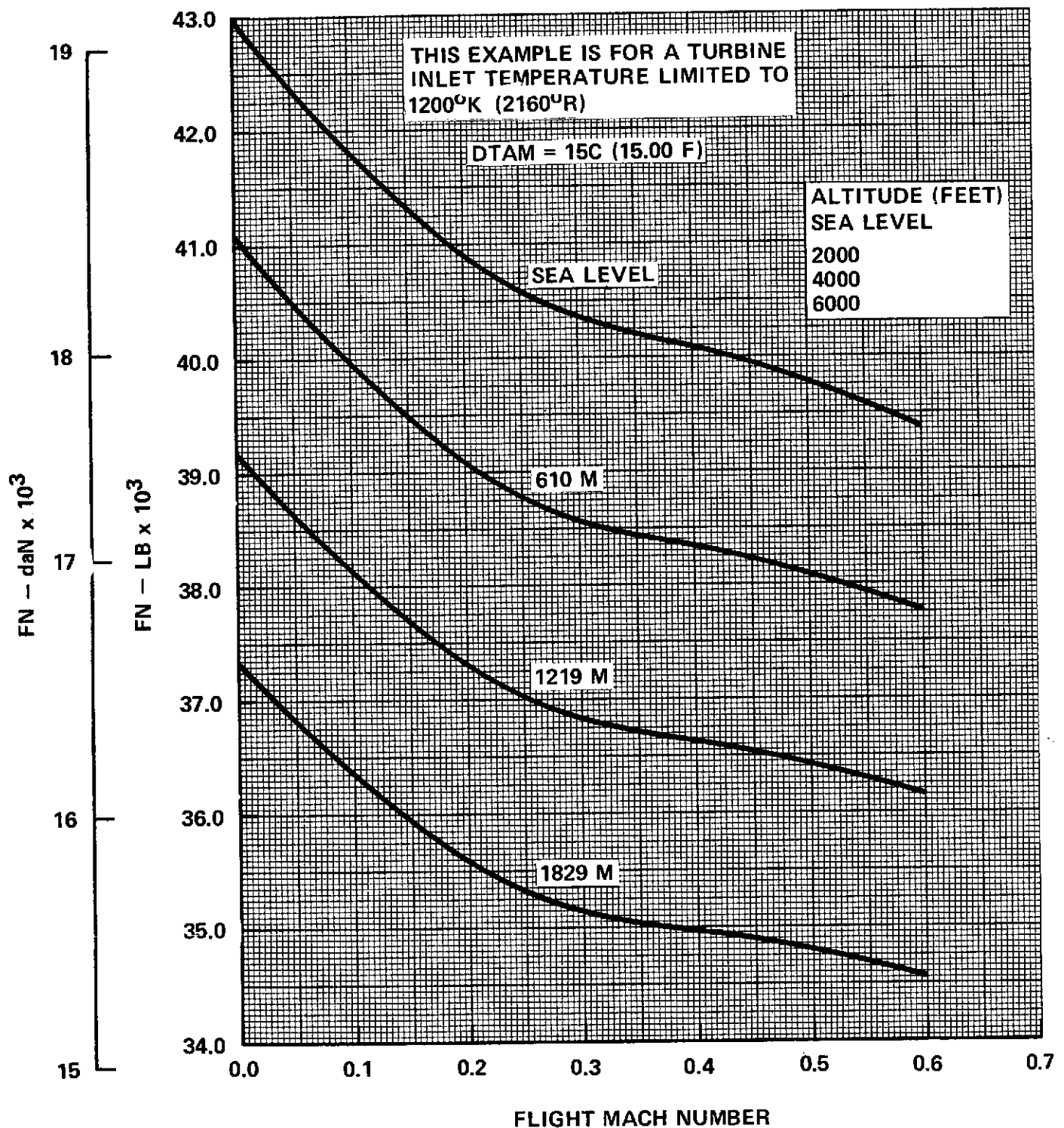


Figure 31. Installed Flight Performance - Thrust

MAX CLIMB POWER

AST MACH 2.7 DRY TURBOJET LH2TJ-1

U.S. STANDARD ATMOSPHERE 1962

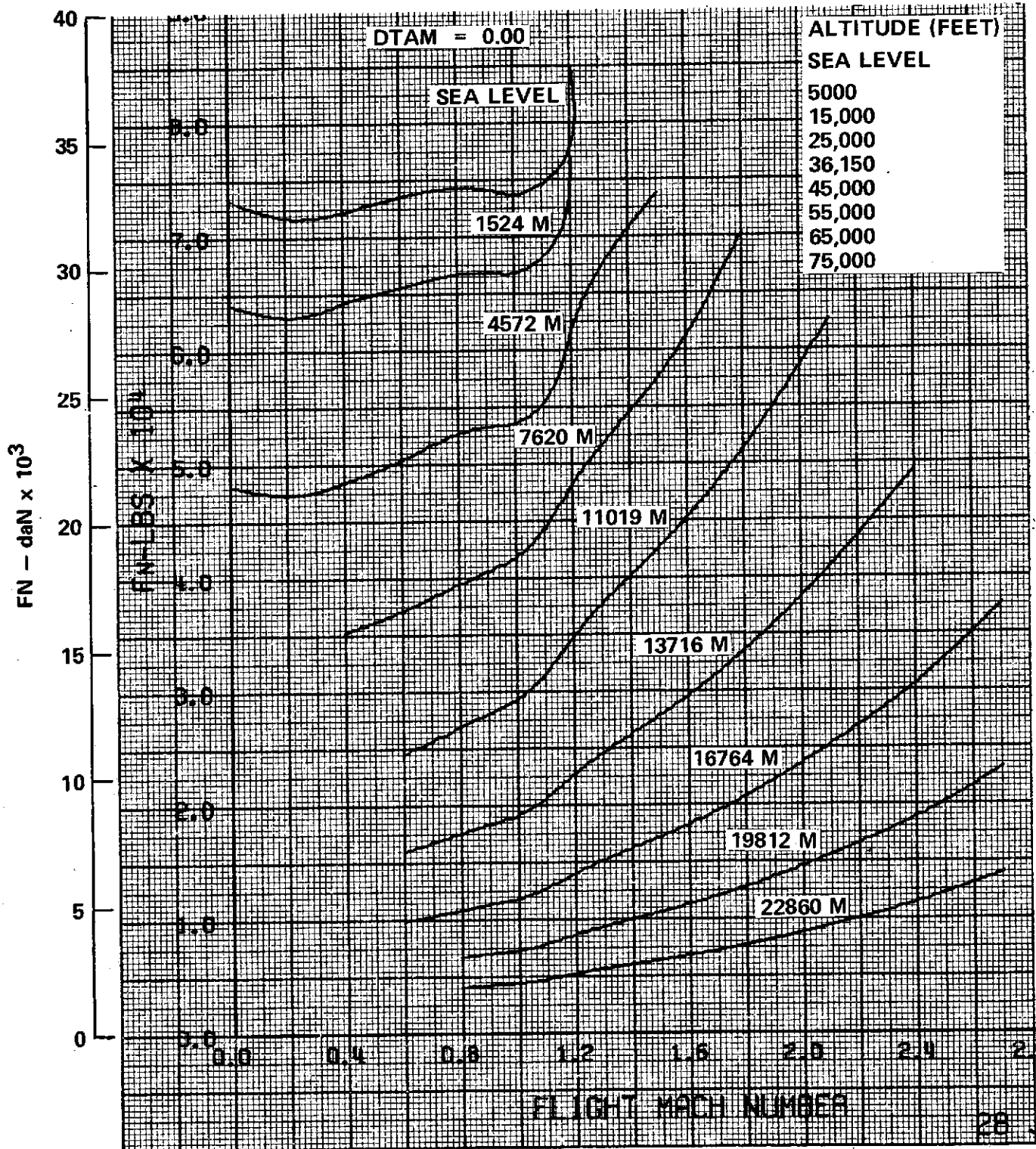


Figure 32. Installed Flight Performance - Thrust

MAX CLIMB POWER
AST MACH 2.7 DRY TURBOJET LH2TJ -1
U.S. STANDARD ATMOSPHERE 1962

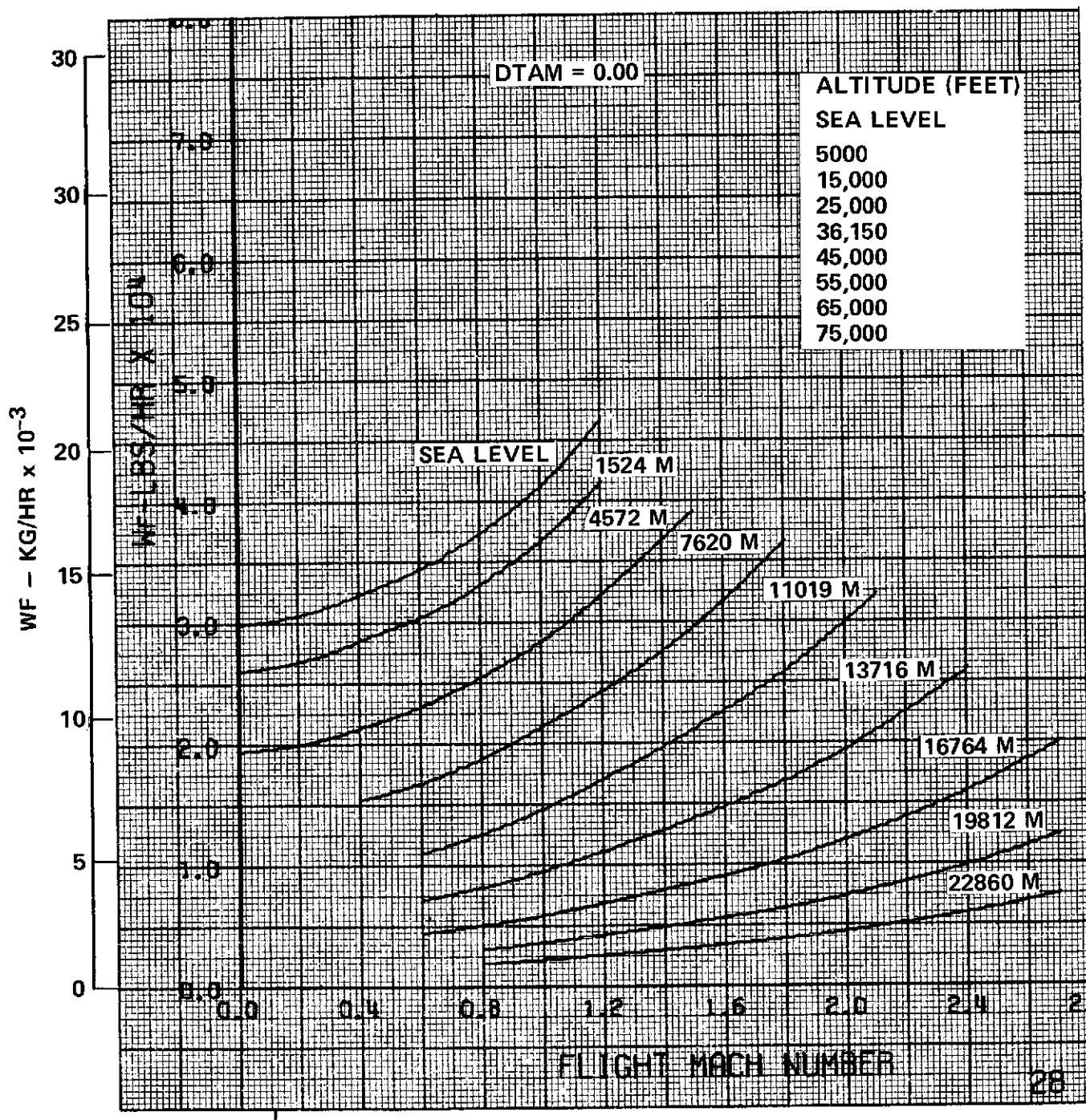


Figure 33. Installed Flight Performance - Fuel Consumption

PART POWER

AST MACH 2.7 DRY TURBOJET LH2TJ-1

U.S. STANDARD ATMOSPHERE 1962

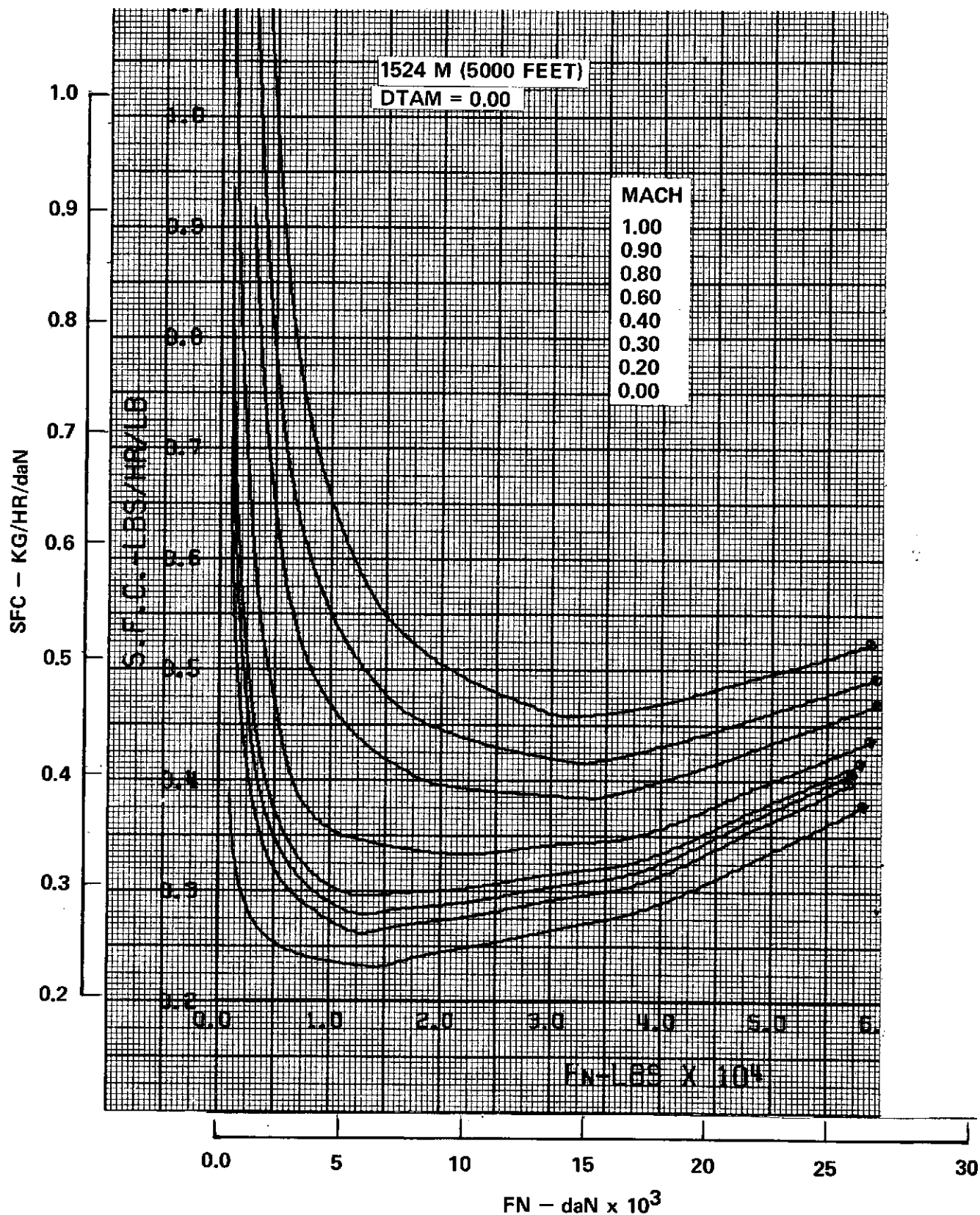


Figure 34. Installed Flight Performance - SFC



PART POWER
AST MACH 2.7 DRY TURBOJET LH2TJ-1
U.S. STANDARD ATMOSPHERE 1962

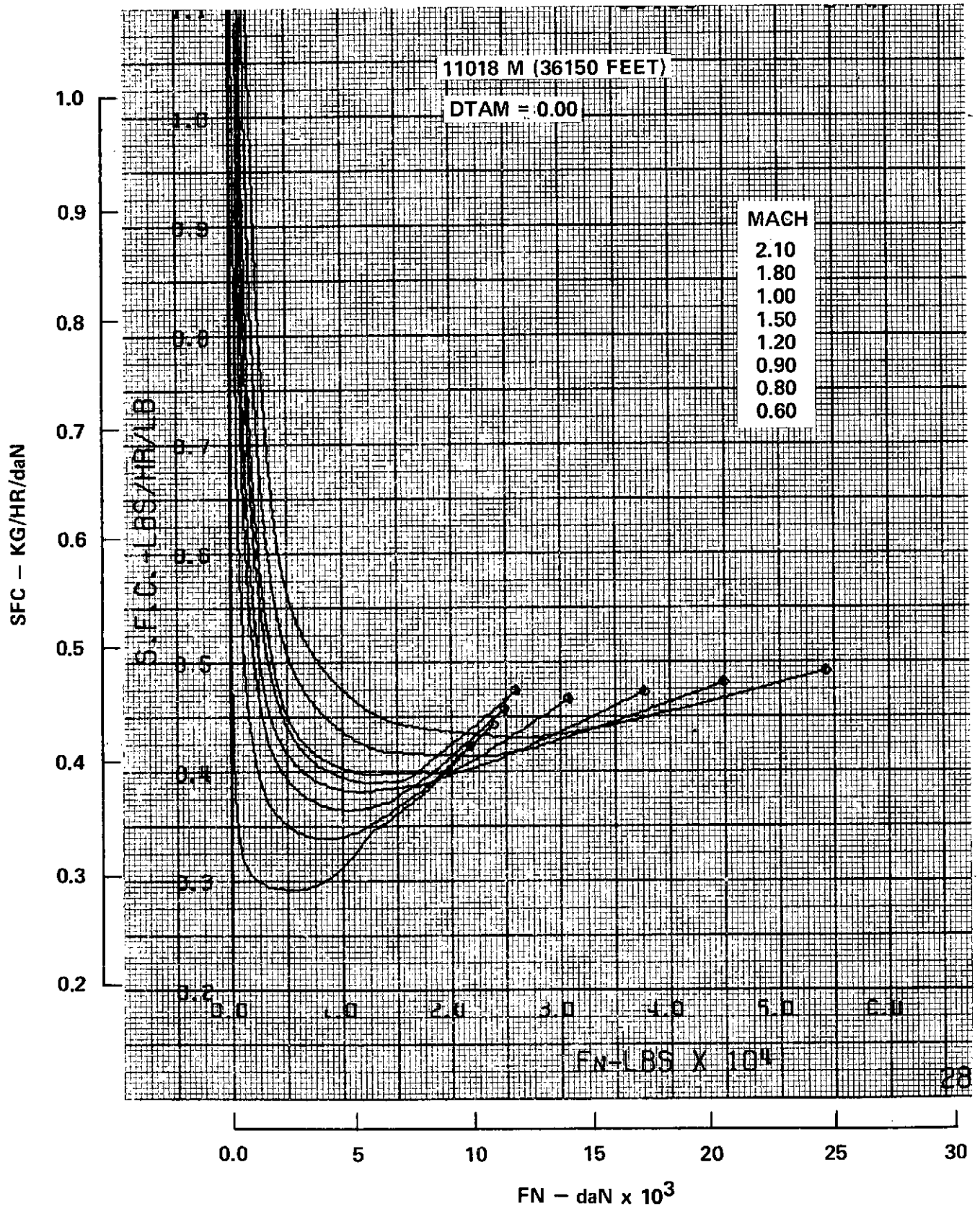


Figure 35. Installed Flight Performance - SFC

PART POWER

AST MACH 2.7 DRY TURBOJET LH2TJ-1

U.S. STANDARD ATMOSPHERE 1962

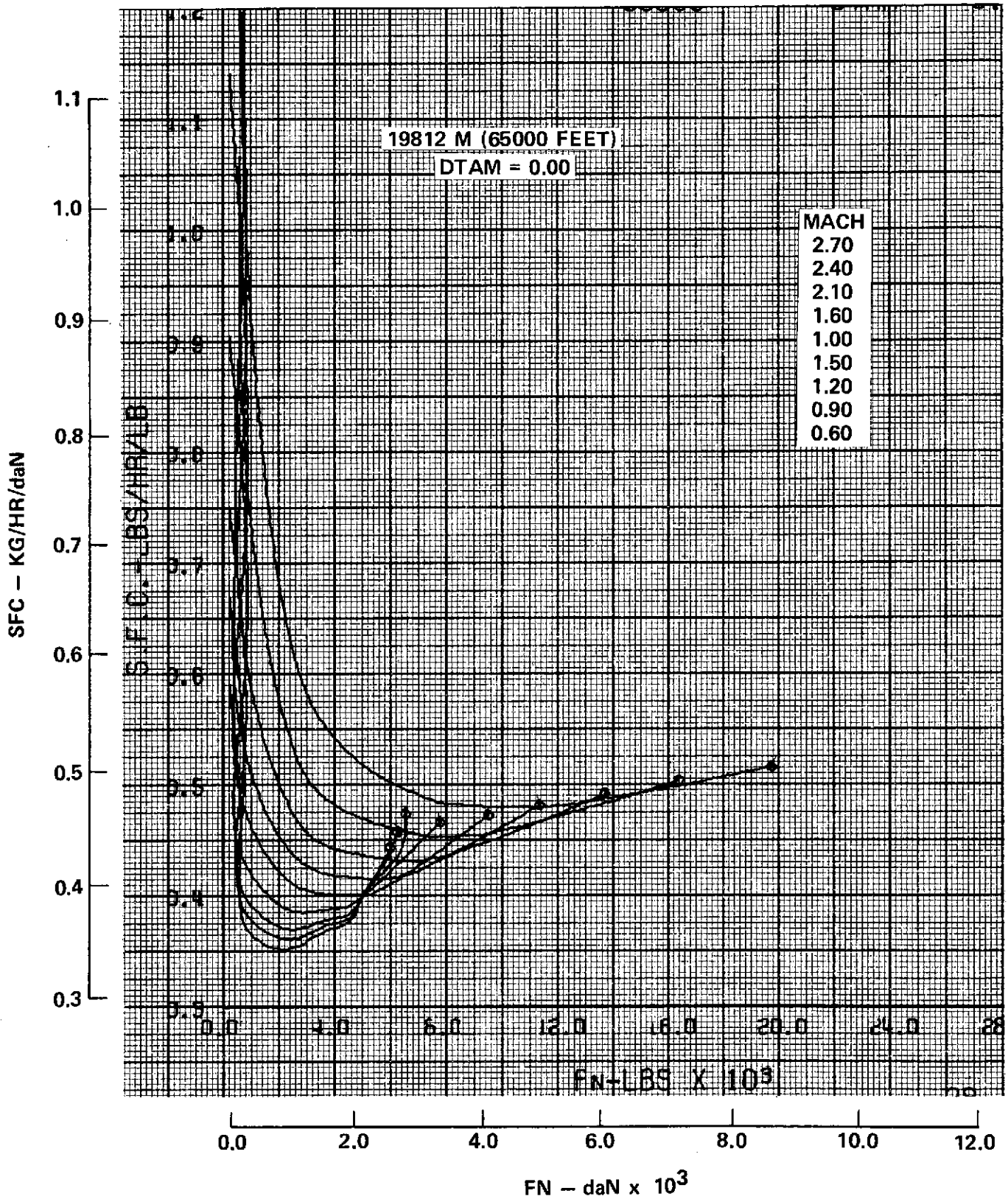


Figure 36. Installed Flight Performance - SFC

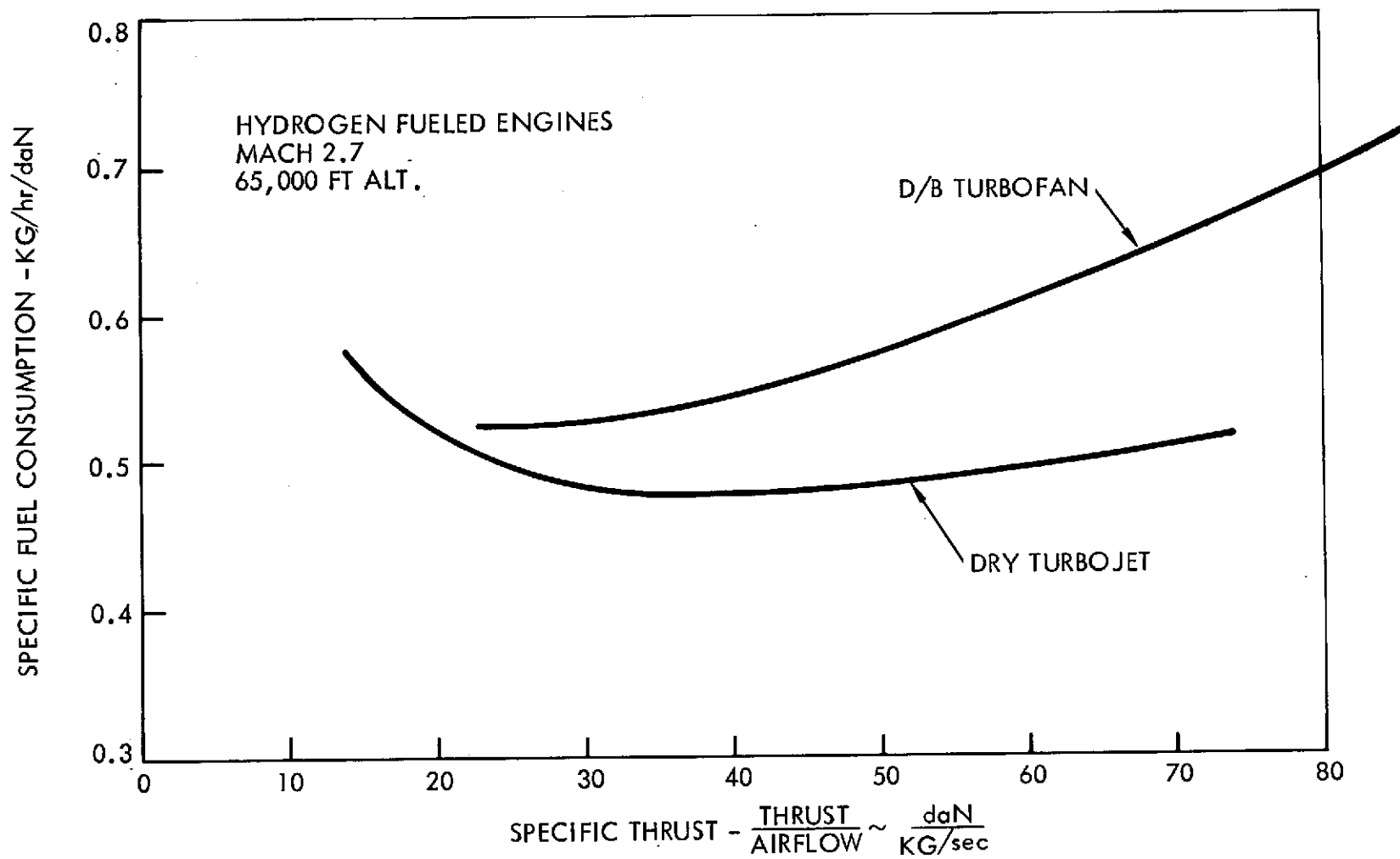
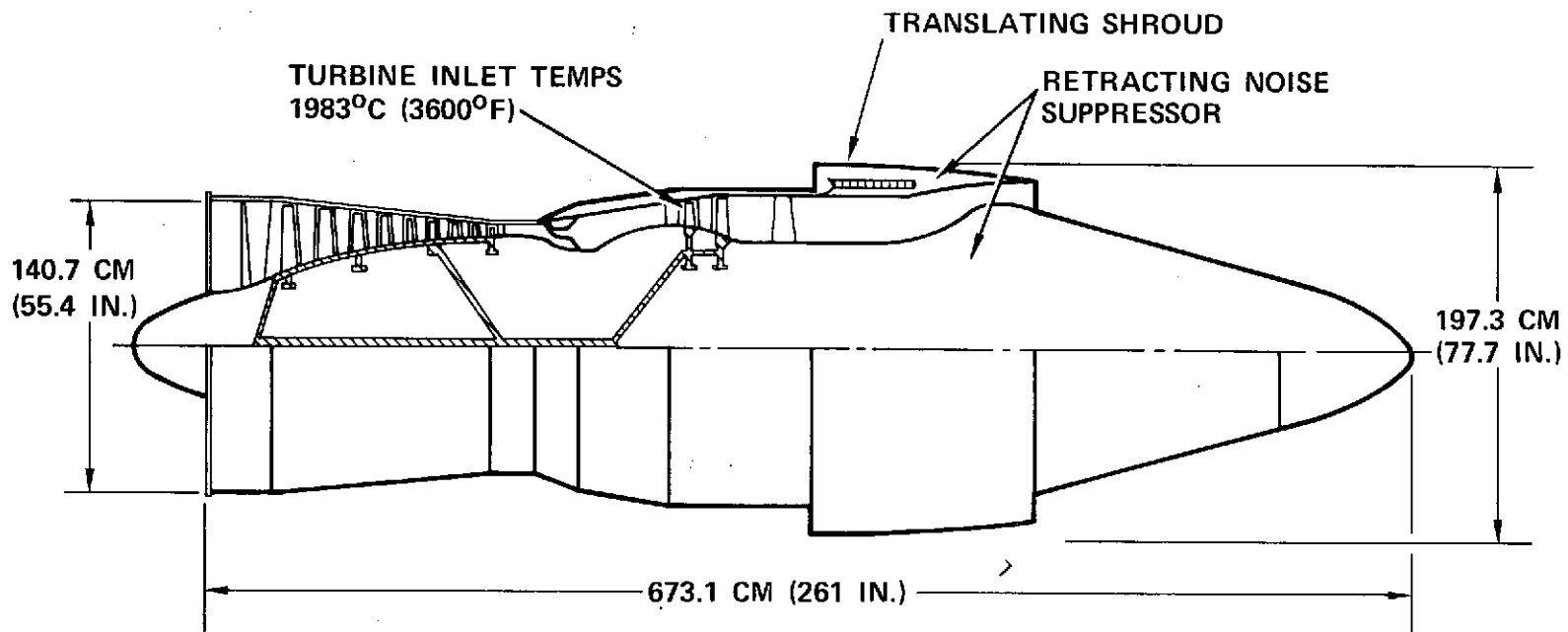


Figure 37. Turbojet vs. Turbofan Performance Comparison

THRUST = 33,850 daN
(76,100 LB)



NOTE: NOT TO SCALE

Figure 38. Hydrogen Fueled Dry Turbojet LH2TJ-1 (Mach 2.7)

PARAMETER		REFERENCE VALUE	
FN _{SLS} MAX	daN (LB)	33850	(76100)
FN L.O.	daN (LB)	11250	(25300)
A _C	M ² (FT ²)	1.579	(17.0)
L _{COMP}	CM (IN.)	140.7	(55.4)
D _{MAX}	CM (IN.)	197.4	(77.7)
D _{NOZ}	CM (IN.)	189.5	(74.6)
L _{ENG}	CM (IN.)	673.1	(265)
L _{INLET}	CM (IN.)	360.7	(142)
WEIGHT *	KG (LB)	4375	(9645)

*INCLUDES REVERSER AND SUPPRESSOR

$$DIAM = DIAM_{REF} \left(\frac{FN_{SLS}}{FN_{SLS(REF)}} \right)^{0.5}$$

$$L_{ENG} = L_{ENG_{REF}} \left(\frac{FN_{SLS}}{FN_{SLS_{REF}}} \right)^{0.35}$$

$$L_{INLET} = 2.56 \times D_{COMP}$$

$$WEIGHT = WEIGHT_{REF} \left(\frac{FN_{SLS}}{FN_{SLS_{REF}}} \right)$$

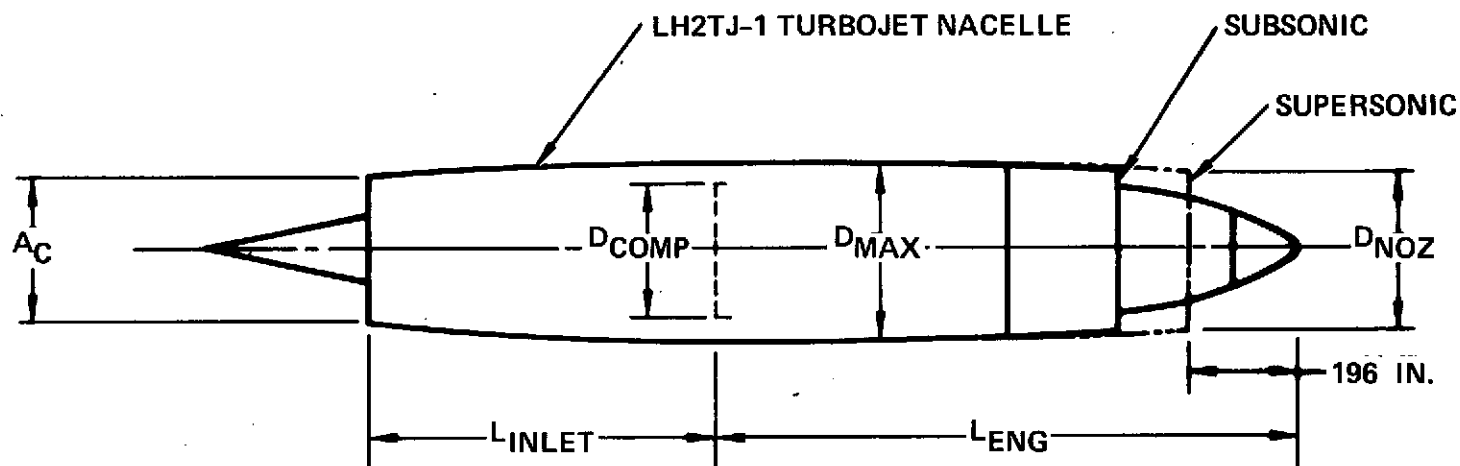


Figure 39. Mach 2.7 Hydrogen Fueled Dry Turbojet Nacelle Dimensions and Scaling Data

dry turbojet engine was configured with a translating shroud plug nozzle, with provision for the thrust reverser mechanisms and provisions for a retracting sound suppressor in the plug. Nacelle configuration, dimensions and scaling data are shown by Figure 39.

3.1.3.2.4 Noise Considerations - The Mach 2.7 turbojet has a very high jet velocity at the maximum 1982°C (3600°F) turbine inlet temperature. Thus, considerable throttle cut back to reduce jet velocity is required to meet FAR Part 36 minus 5 EPNdB noise levels during takeoff. Figure 31 presents an example of the reduced noise power setting required. Because jet noise is a function of jet velocity to the eighth power and thrust is the product of airflow multiplied by jet velocity, the turbojet engine control was designed so as to maintain 100 percent engine speed and airflow when the engine was throttled back for noise consideration. This minimizes the engine size required to meet noise requirements.

3.1.3.3 Mach 2.2 Turbojet

3.1.3.3.1 Cycle Selection - Because of single spool engine pressure limitations and maximum turbine temperature limitations, the Mach 2.2 turbojet was assumed to have nearly the same cycle as the Mach 2.7 turbojet. This is shown by Table 7.

3.1.3.3.2 Performance Characteristics - Selected installed flight performance characteristics for the Mach 2.2 turbojet are shown by Figures 40, 41, 42, 43, 44, and 45.

3.1.3.3.3 Physical Characteristics - The internal flow path and engine outline of the Mach 2.2 turbojet are shown by Figure 46. These are very similar to those shown for the Mach 2.7 turbojet in Figure 38, except that the relative nozzle diameter is lower because at Mach 2.2 the nozzle expansion ratio required for efficient thrust conversion is much less than it is for Mach 2.7. The nacelle configuration dimensions and scaling data are shown by Figure 47.

3.1.3.3.4 Noise Considerations - The noise considerations for the Mach 2.2 turbojet are similar to those of the Mach 2.7 turbojet, however, the design of the thrust reverser and sound suppressor will be more difficult in the relatively smaller nozzle.

NOISE LIMITED TAKE OFF PWR
AST MACH 2.2 DRY TURBOJET LH2TJ-1 STD + 27F T/O
U.S. STANDARD ATMOSPHERE 1962

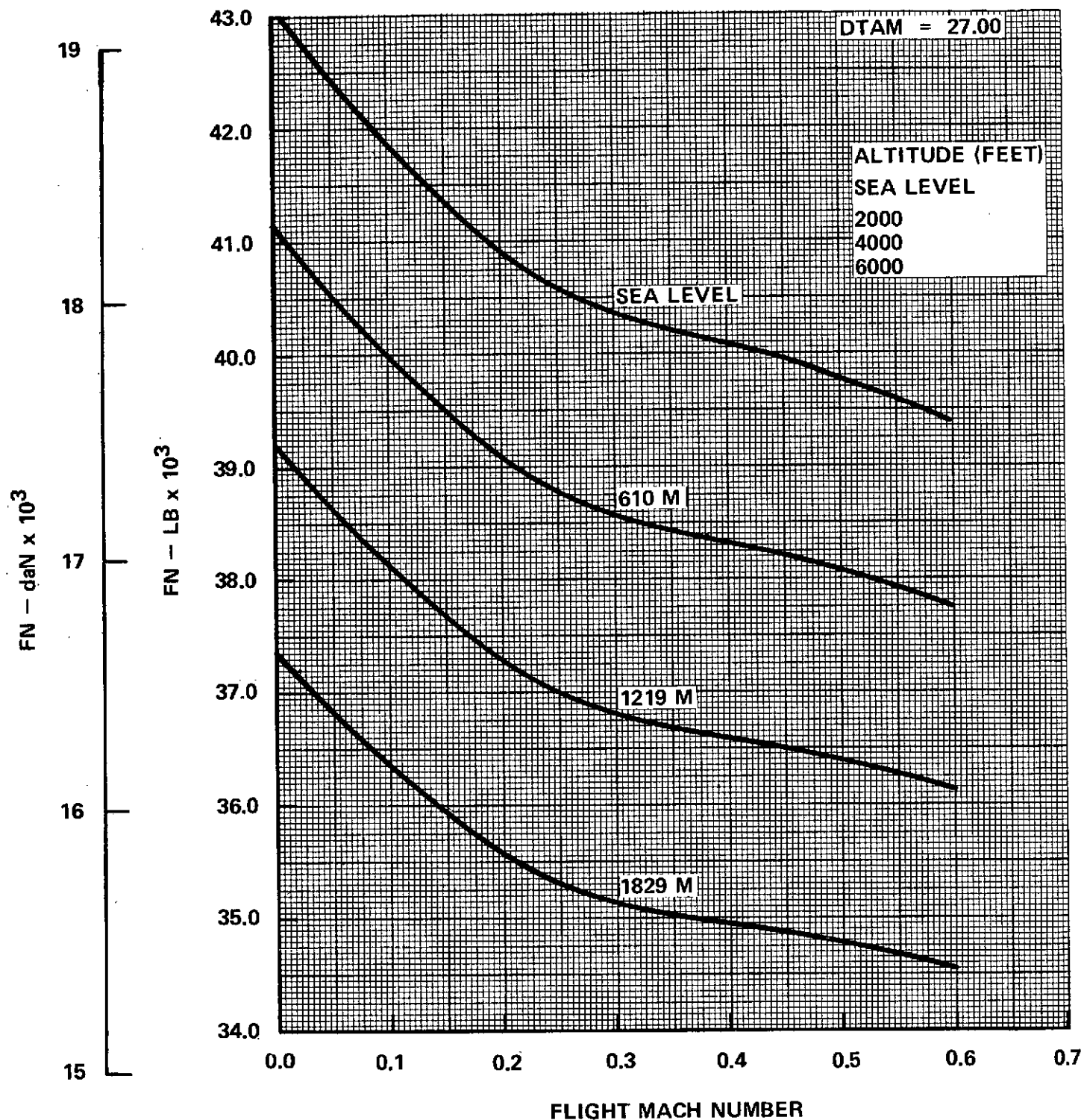


Figure 40. Installed Flight Performance - Thrust

MAX CLIMB POWER
MACH 2.2 DRY TURBOJET LH2TJ-2
U.S. STANDARD ATMOSPHERE 1962

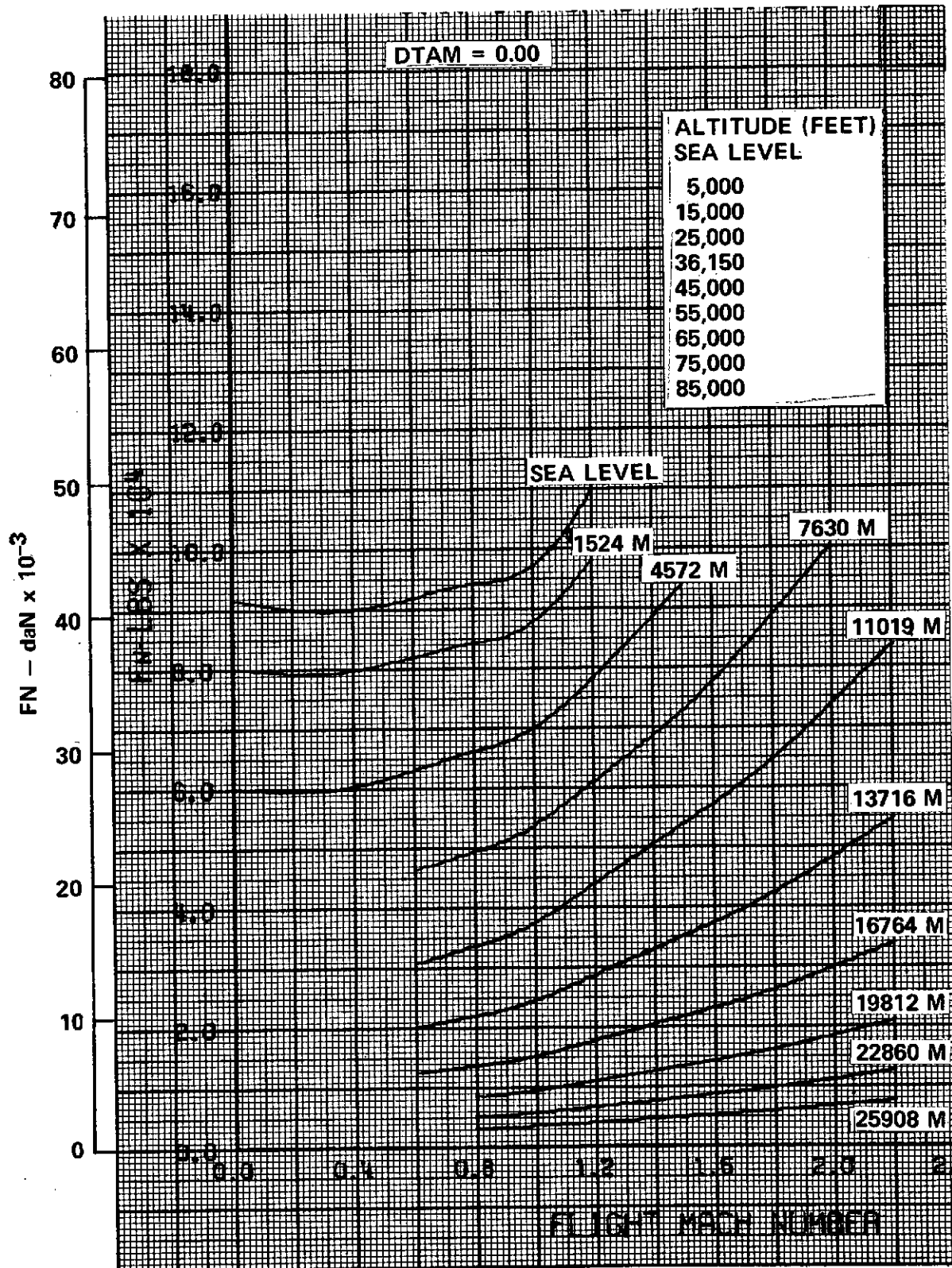


Figure 41. Installed Flight Performance - Thrust

MAX CLIMB POWER
MACH 2.2 DRY TURBOJET LH2TJ-2
U.S. STANDARD ATMOSPHERE 1962

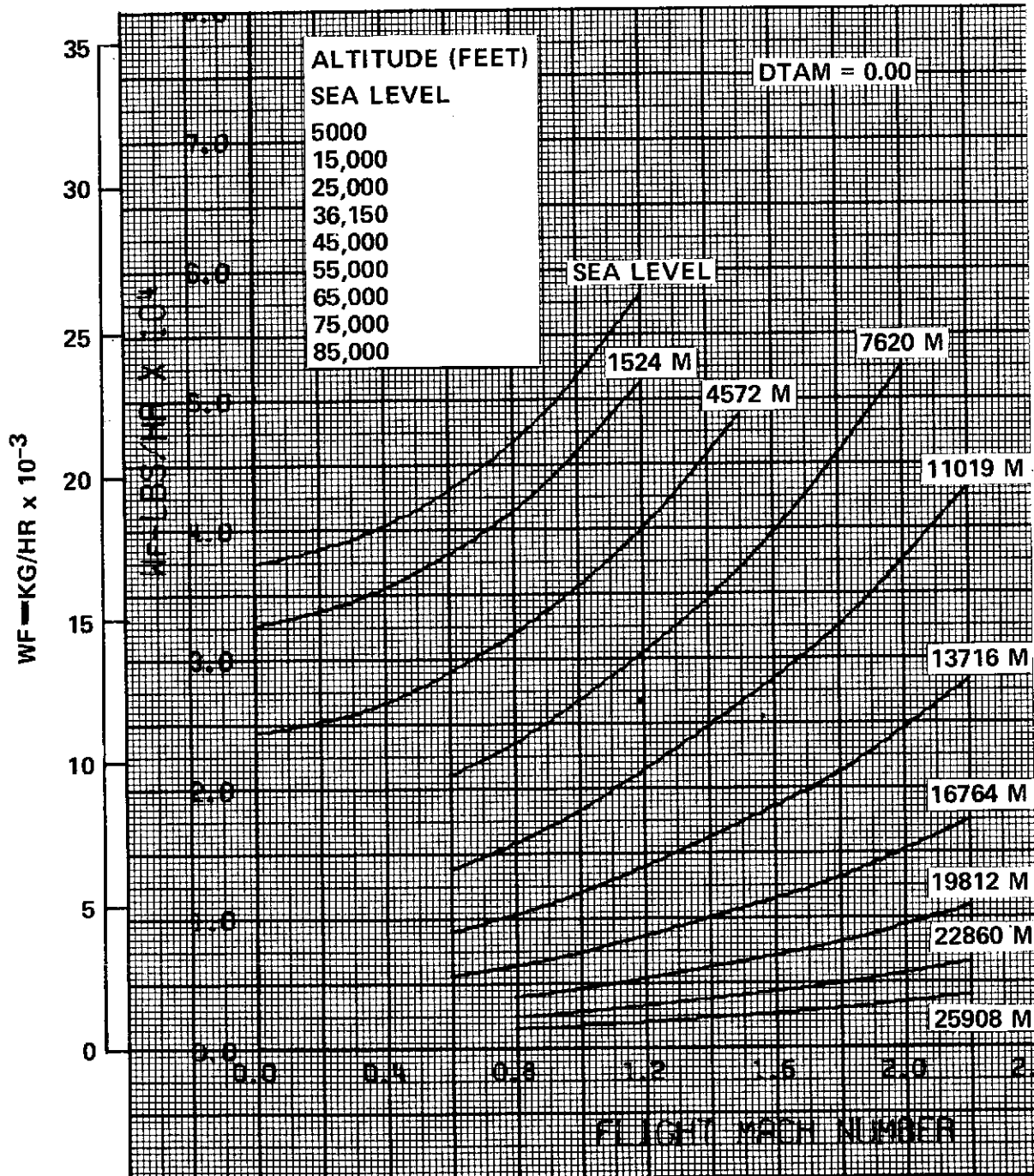
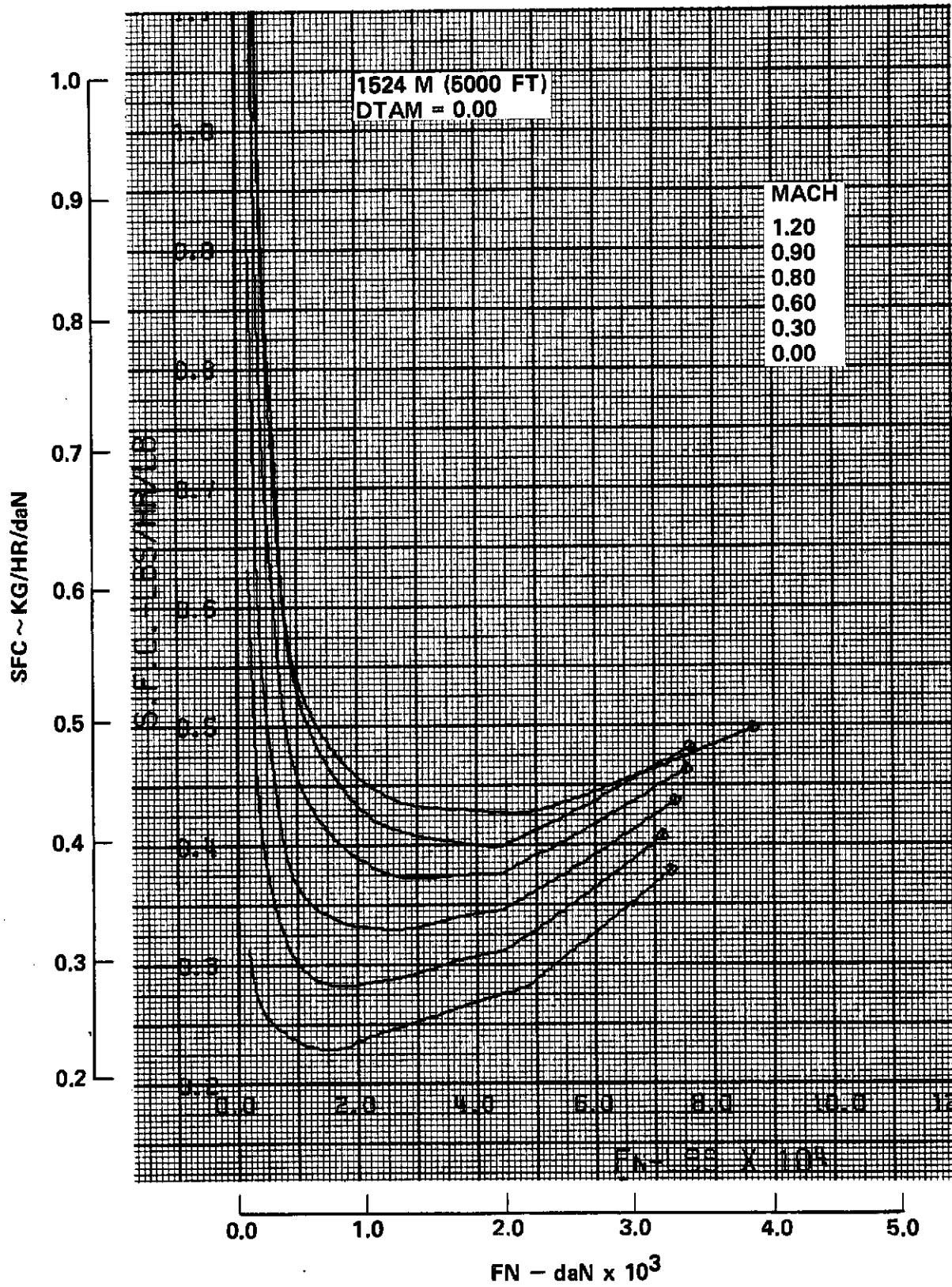


Figure 42. Installed Flight Performance - Fuel Consumption

PART POWER

MACH 2.2 DRY TURBO JET LH2TJ-2

U.S. STANDARD ATMOSPHERE 1962



PART POWER
MACH 2.2 DRY TURBOJET LH2TJ-2
U.S. STANDARD ATMOSPHERE 1962

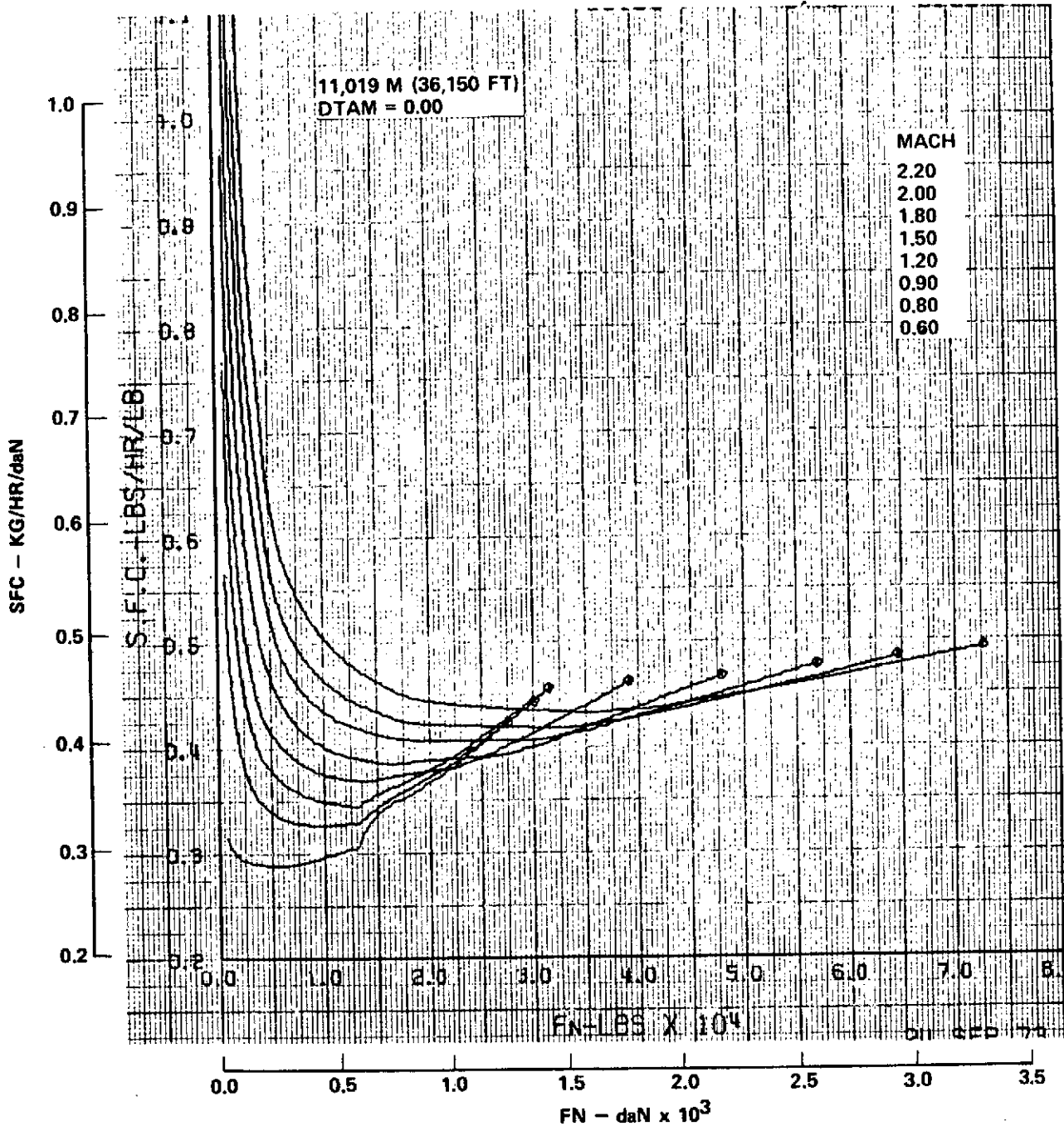


Figure 44. Installed Flight Performance - SFC

PART POWER

MACH 2.2 DRY TURBOJET LH2TJ-2

U.S. STANDARD ATMOSPHERE 1962

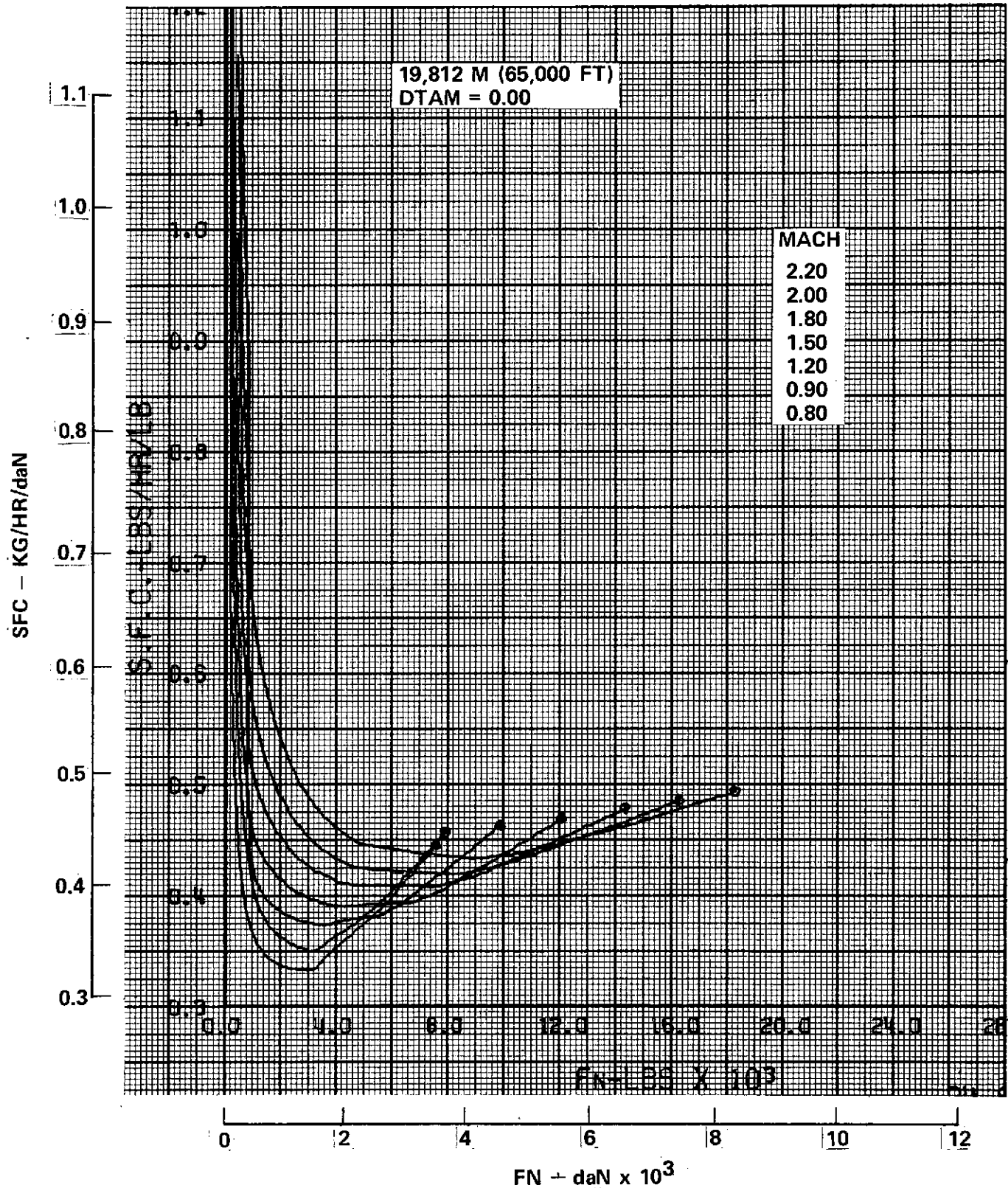


Figure 45. Installed Flight Performance - SFC

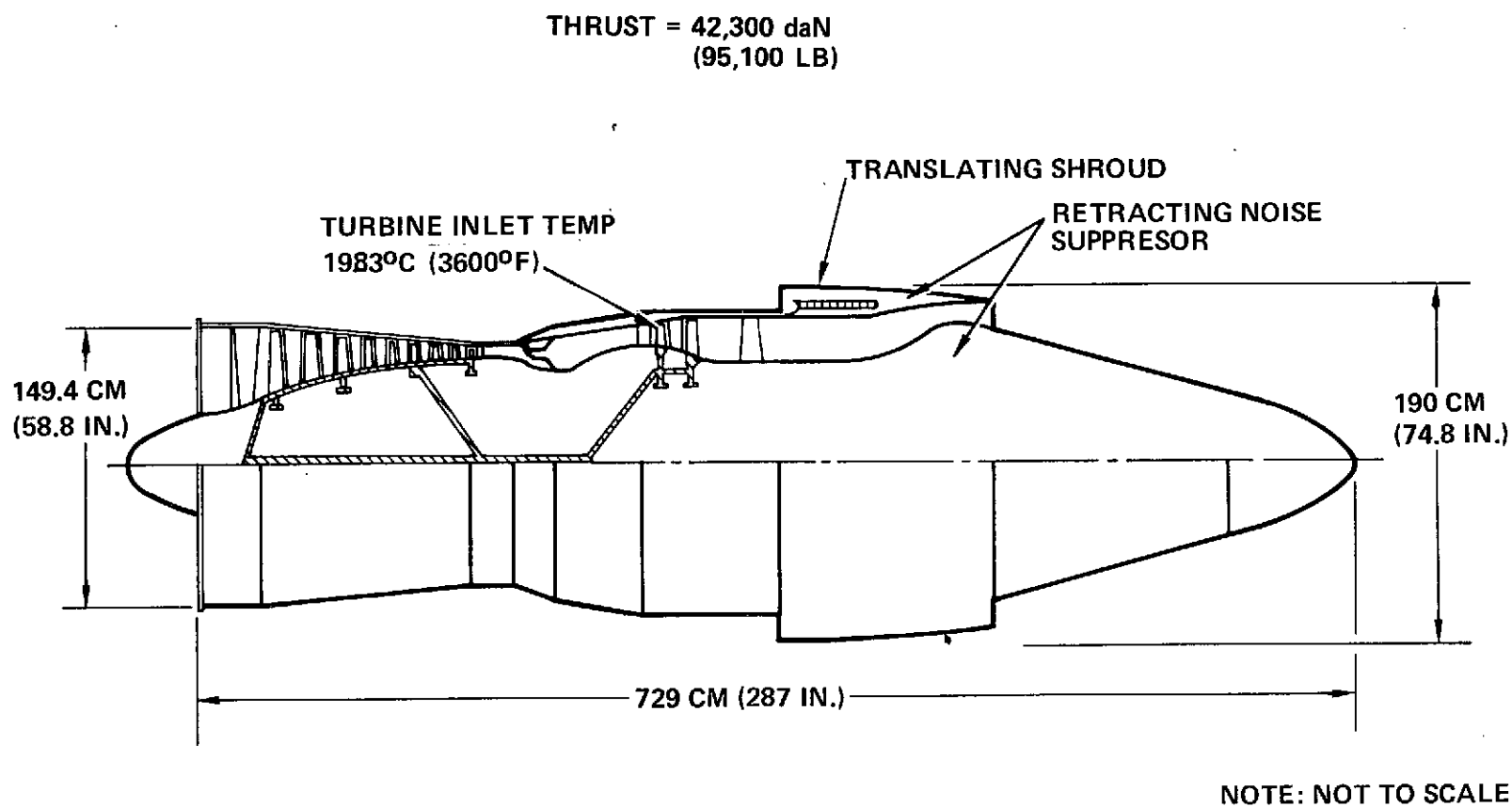


Figure 46. Hydrogen Fueled Dry Turbojet LH2TF-2 (Mach 2.2)

PARAMETER		REFERENCE VALUE	
FN_{SLS} MAX	daN (LB)	42314 (95125)	①
FN_{LO}	daN (LB)	22285 (50100)	②
A_C	M^2 (FT ²)	1.632 (17.57)	
D_{COMP}	CM (IN.)	149.5 (58.84)	
D_{MAX}	CM (IN.)	190.0 (74.84)	
D_{NOZ}	CM (IN.)	181.4 (71.4)	
L_{ENG}	CM (IN.)	727.7 (286.5)	
L_{INLET}	CM (IN.)	381.0 (150.)	
WEIGHT	KG (LB)	5466 (12050)	③

NOTES: ① UNINSTALLED

② INSTALLED, MACH 0.3 SEA LEVEL

③ INCLUDES REVERSER AND SUPPRESSOR

$$DIA = DIA_{REF} \left(\frac{FN_{SLS}}{FN_{SLS(REF)}} \right)^{0.5}$$

$$L_{ENG} = L_{ENG_{REF}} \left(\frac{FN_{SLS}}{FN_{SLS_{REF}}} \right)^{0.35}$$

$$L_{INLET} = 2.56 \times D_{COMP}$$

$$WEIGHT = WEIGHT_{REF} \left(\frac{FN_{SLS}}{FN_{SLS_{REF}}} \right)$$

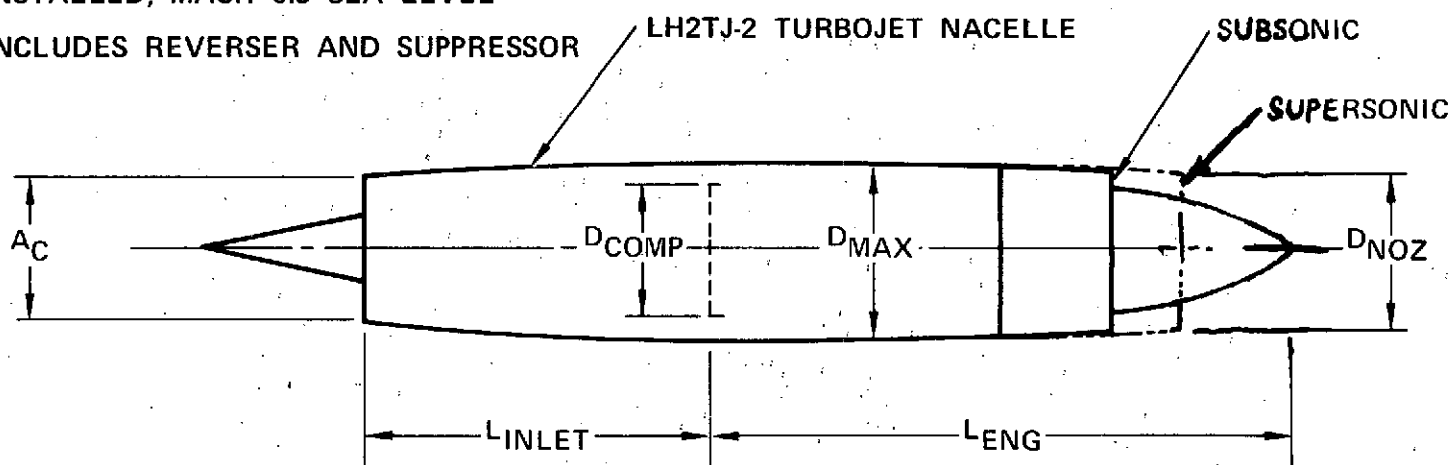


Figure 47. Mach 2.2 Hydrogen Fueled Dry Turbojet LH2TJ-2 Nacelle Dimensions and Scaling Data

3.1.4 Material Selection

3.1.4.1 Requirements

The major structural materials considered for near-term supersonic transport aircraft were titanium alloys with some portions of the structure being made of boron/graphite/Kevlar or other high strength filamentary composites. For the "far-term" airplane (i.e., 1985 era technology), it was considered that approximately 40 percent of the aircraft structure (including the wing surfaces) would be made from filamentary composites.

The introduction of liquid hydrogen (LH_2) as a fuel, requires that the materials used for fuel tanks be capable of:

- Remaining ductile at LH_2 cryogenic temperatures of minus 253°C (423°F).
- Resistant to embrittlement by absorption or reaction with either liquid or gaseous hydrogen.

Furthermore, if the weight saving advantages of integral type fuel tanks are to be realized, the tank walls will have to exhibit the structural characteristics of typical aircraft structural materials; namely, high strength-weight ratios, good fatigue characteristics, corrosion and stress corrosion resistance, and high fracture toughness.

3.1.4.2 Candidate Materials

The known susceptibility of titanium alloys to hydrogen embrittlement (NASA-CR-2163, dtd March 1973) prevents their consideration for use as LH_2 fuel tank walls. Even the question of using titanium alloys as aircraft structure, with nonintegral LH_2 fuel tank of a compatible material, is suspect in view of the high diffusivity of hydrogen gases. The high risk of titanium alloy embrittlement from hydrogen diffusing through fuel tank wall discontinuities would require the addition of protective barrier films, plus sensitive H_2 sniffers to insure the structural integrity of the airplane.

The materials that have exhibited compatibility with both cryogenic temperature and hydrogen environments are the high strength aluminum alloys, the austenitic stainless steels, and filamentary composites, primarily fiberglass.

Figure 48 shows a comparison of some new and current high strength aluminum alloys at room temperature. The resistance to flaw growth of 2219-T851 at room temperature is among the highest of the aluminum alloys being studied. Interestingly, testing at cryogenic temperatures has not indicated any embrittlement of 2219-T851 as reported in the "Damage Tolerant Resistant Handbook", MCIC-HB-01, Metals & Ceramics Information Center and Air Force Materials Laboratory, as revised September 1973.

Comparing the austenitic stainless steels (i.e., Type 304) with the aluminum alloys at room and cryogenic temperatures does not indicate any advantage for the austenitic stainless steels.

In view of its weldability, formability, stress corrosion resistance and high fracture toughness, plus resistance to flaw growth, 2219 aluminum alloy was selected for the fuel tanks.

Composite Materials - Filamentary composites used for missile LH₂ tanks are primarily fiberglass-epoxy resin. AFML-TDR-64-280 (revised 1970) Cryogenic Materials Data Handbook documents room temperature and cryogenic properties for a number of fiberglass-epoxy resin combinations.

Cryogenic testing of new fibers, such as boron, graphite and Kevlar -49, either with epoxy resin or metal matrix resins, has been extremely limited. Table 8 compares some typical properties of the fiberglass-epoxy, boron-epoxy and boron-aluminum composites at room and/or cryogenic temperatures. Test data on graphite-epoxy resin composites at cryogenic temperatures could not be found.

The advantages of graphite and boron fibers, when compared to fiberglass, are higher modulus and compressive strengths. These higher properties may be utilized in integral tanks which also serve as structural airplane components. However, a great deal more data must be developed prior to selecting these materials for either an integral (LH₂) tank and airplane structure, or even for a nonintegral LH₂ tank carrying only pressure tank loads. Primarily, it must be proven that the filament-matrix combination would be compatible with the LH₂ plus service environments and loads for long time cyclic exposure,



C-2

78

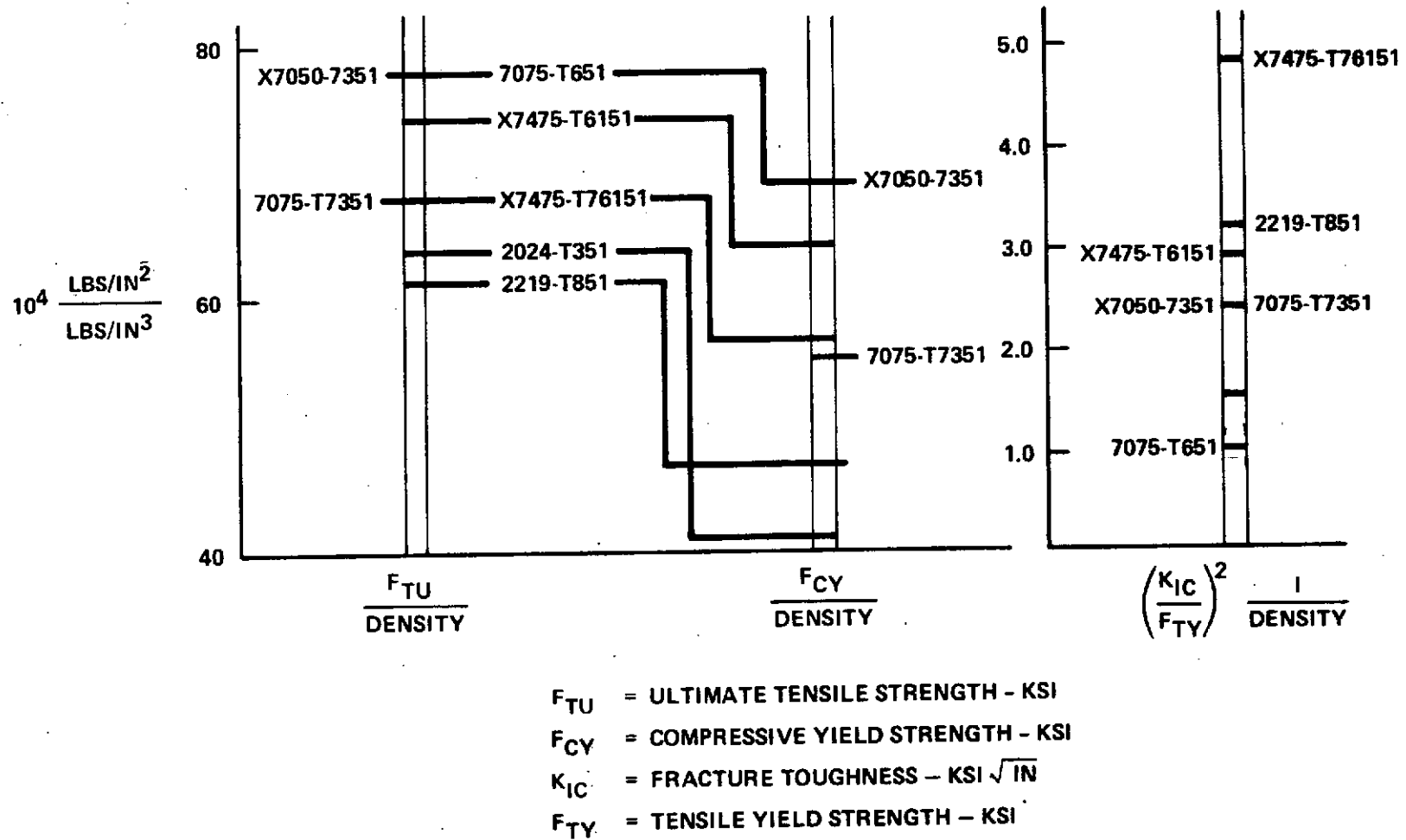


Figure 48. Candidate Aluminum Alloys Comparison



TABLE 8
COMPOSITE MATERIAL PROPERTIES

Material	Fiber Vol.	Density lb/in. ³	Test Temp. °C	F _{tu} * KSI	E _t * MSI	F _{cu} * KSI	E _c * MSI	IZOD Un-notch FT-LB	Notch FT-LB	Notch Depth/Radius
Boron/Epoxy Fiber B4	0.50	0.0725	21	188	30	362	32	46.3	22.8	0.104 - 0.010
AVCO 5505/4 Matrix 2387 0° Fiber Flat Coupon			-253	204	33	542	31	39.5	27.0	0.098 - 0.010
Fiberglass/ Epoxy	18% resin	0.0721	21	280	8.3	155				
S/901 Roving 0° Fiber E-787 Laminate Coupon			-253	300	9.4	238				
									146	$\frac{\text{Notch}}{\text{Un-notch}}$ ratio 0.68
Boron/Alum. Fiber 5.6 Mill	0.48	0.095	21	216	31.1	283	37.3			
Matrix - AL 6061-F 0° Fiber Flat Coup.			-196	218	30.4	271	38.5		109	0.5

*Unidirectional

TABLE 8
COMPOSITE MATERIAL PROPERTIES (Cont'd)

Material	Fiber Vol.	Density lb/in. ³	Test Temp. °C	F _{tu} * KSI	E _t * MSI	F _{cu} * KSI	E _c * MSI	IZOD UN-notch FT-LB	Notch FT-LB	Notch Depth/Radius
<u>Boron/Polyimide</u> Boron (4 mil filament tape)- Polyimide(P-13N) Fiber	50	0.072	21 -55 260	180 170 135	32 30.5 28	175 - 150	30 - 30.5			
<u>Graphite/Polyimide</u> Modmar II (Graphite)- Skybond 703 Polyimide 0° Fiber	58-62	0.056	21 260	213 169.1	23.7 23	178.3 63.88	21.9 22.5			

*Unidirectional

both under load and cycling between loads and temperatures. This is particularly necessary for resin matrix composites where permeability of hydrogen gas would be high and a barrier material would be required.

Barrier Materials

Design Considerations - There are basically two design applications:

- (a) Cryogenic insulation applied to the inside of the tank structure.
- (b) Filament wound/resin LH₂ storage tanks.

In either design, the choice of barrier film materials is limited by the expected service temperatures to be encountered by the film. These temperatures could range from -423°F to +470°F, depending on the location chosen for the application of the film. Resistance to LH₂, gaseous H₂ or both, could be a requirement for the film material, also depending on its location.

Internal Cryogenic Insulation

For this application the use of a barrier film would be necessary to prevent the gaseous H₂ from permeating through the insulation, thus reducing the effectiveness of the cryogenic insulation. The task of providing a continuous film inside the tank appears extremely difficult. Achieving gas-tight bonded joints or heat sealed seams in view of the available film widths and the geometry of the structure requiring isolation will not be easy. Table 9 lists the candidate film materials which should be evaluated, along with some of their essential properties. Aluminum foil is another candidate barrier material which should be considered.

Filament Wound/Resin Storage Tank

For this design concept, the barrier film material can be located in three different places to perform the function of preventing LH₂ or H₂ gas from escaping from the storage tanks. If placed internally, the barrier film need not be compatible with the resin system; however, it must be serviceable at -423°F. When placed on the exterior of tank or under a restraining layer of fiber/resin winding, the film must be fairly compatible in adhesion to the resin system. Service life at -423°F and resistance to LH₂ and gaseous H₂ permeability are essential requirements.

TABLE 9
PHYSICAL PROPERTIES OF FILMS

Barrier Film	Spec. Gravity	H ₂ Permeability (100 in. ²)(24 hrs)(mil)23.5°C	Temp. Limit Service Life	Remarks
Polyester (Mylar)	1.39	600 cc (1 atm)	-100°F to 300°F	Could possibly be used at lower temp where no flex life required.
Polyvinyl fluoride (Tedler)	1.57	950 cc (1 atm)	-100°F to 300°F	Could possibly be used at lower temp where no flex life required.
Polyvinyl Chloride (Saran)	1.68	450 cc	-65°F to 200°F	Could possibly be used at lower temp where no flex life required.
Teflon (FED)	2.15	2340 cc (1 atm)	-425°F to 400°F	
Polyimide (Kapton)	1.42	250 cc	-425°F to 470°F	
Fluorohalocarbon (Aclar)	2.1	1500 cc (1 atm)	-100°F to 300°F	Could possibly be used at lower temp where no flex life required.

External Heat Shield Structure

The selection of graphite and/or Kevlar -49 polyimide composites for use as a heat shield is based on data from in-house programs at Lockheed. It has been shown that Graphite/Kevlar -49/epoxy composites have about three times the foreign object impact resistance of graphite-epoxy systems. The aging characteristics of polyimide systems under load and temperature are being evaluated.

3.1.5 Weight Parameters

3.1.5.1 Basis for Weight Estimates - Phase I

Weight equations to represent the subject LH_2 AST were developed using the Jet A-1 fueled AST aircraft of the NASA-Langley Systems Study (Reference 1) and the Arrow-Wing Structures Study (Reference 4) as the starting point. The equations relate the component weights to aircraft geometry, materials selection, and loading parameters.

The Jet A-1 AST weight equations were modified to apply to the hydrogen-fueled transport in the following manner:

Wing - Increased 11.2 percent for fewer ribs and spars due to internal wing tanks and support.

Fuselage - Floor weight increased 300 percent to 9.37 kg/m^2 (1.92 lb/ft^2) for pressure deck and tank support structure.

Fuel System - Weight increased 20 percent for venting, pressurization and refueling systems.

Unusable Fuel - Increased from 0.9 to 2 percent of total LH_2 weight.

Tankage - Tank and thermal protection system weight is unique to the LH_2 fueled aircraft; therefore, it is expressed as a fraction of the hydrogen weight:

Tanks	.146	} kg/kg of LH_2
Thermal Protection	<u>.11 to .13</u>	
Total	.256 to .276	

Boil-off - Included in thermal protection system weight.

The weight estimating equations were further modified to reflect advanced technology in such fields as composite materials and structural concepts. This was accomplished by applying a matrix of materials distribution for each major vehicle element with an associated weight reduction factor. The weight of components and systems associated with the use of liquid hydrogen was influenced by Lockheed's experience on the following programs:

CL400 - A Mach 2.5 hydrogen-fueled interceptor aircraft, 1956 - 1958,
LR 12296. (Reference 17).

Manned Hypersonic Cruise Vehicle - structural concepts and tankage comparisons, 1966 - 1968 (F33615-67-C1088). (Reference 18).

Airbreathing Launch Vehicles with Cruise Capability - Volume IV of study report explores structural and weight aspects of these vehicles. (NAS 2-4084, CR 73197) This study pointed out that maximum payload and minimum vehicle cost is obtained with integral in lieu of non-integral hydrogen tankage. (Reference 19).

Lockheed Independent Development - a series of investigations involving both design studies and hardware testing of LH_2 fueled aircraft and related components from 1962 - 1968.

From the above data, and related prototype and production programs, parametric equations were derived using a least squares multiple regression mathematical approach. In conjunction with analytical methods, this approach obtains selected parameters that correlate best with historical data. The resulting weight equations were used in the ASSET Program to get a direct comparison between a Jet A-1 AST and the LH_2 AST.

3.1.5.2 Fuel Volume Available

During Phase I, it was planned to carry hydrogen in both the fuselage and wing. To facilitate evaluation of total fuel volume available, body and wing capacity curves were developed which showed the effect of varying body radius, wing thickness and area. Table 10 is a summary of the fuel volume estimated to be available.

TABLE 10. VEHICLE LH₂ CAPACITY ESTIMATE

Body Radius		t/c (%)	Wing Area		LH ₂ Weight (@ .0676 gm/cm ³)					
					Wing to BL = R _B		Body		Total	
m	(in.)		m ²	1000 ft. ²	kg.	(lb.)	kg.	(lb.)	kg.	(lb.)
1.60	63.1	3	743.	8	1,769	3,900	19,504	43,000	21,273	46,900
1.98	77.9	3			1,043	2,300	39,780	87,700	40,823	90,000
2.24	88.2	3			590	1,300	54,430	120,000	55,020	121,300
1.60	63.1	5			10,478	23,100	19,504	43,000	29,982	66,100
1.98	77.9	5			8,981	19,800	39,780	87,700	48,761	107,500
2.24	88.2	5			8,029	17,700	54,430	120,000	62,459	137,700
1.60	63.1	7			19,005	41,900	19,504	43,000	38,509	84,900
1.98	77.9	7			16,737	36,900	39,780	87,700	56,517	124,600
2.24	88.2	7	743.	8	15,286	33,700	54,430	120,000	69,716	153,700
1.60	63.1	3	1022.	11	5,670	12,500	19,504	43,000	25,174	55,500
1.98	77.9	3			4,536	10,000	39,780	87,700	44,316	97,700
2.24	88.2	3			3,674	8,100	54,430	120,000	58,104	128,100
1.60	63.1	5			21,772	48,000	19,504	43,000	41,276	91,000
1.98	77.9	5			19,414	42,800	39,780	87,700	59,194	130,500
2.24	88.2	5			17,962	39,600	54,430	120,000	72,392	159,600
1.60	63.1	7			35,743	78,800	19,504	43,000	55,247	121,800
1.98	77.9	7			32,250	71,100	39,780	87,700	72,030	158,800
2.24	88.2	7	1022.	11	30,118	66,400	54,430	120,000	84,543	186,400
1.60	63.1	3	1301.	14	12,020	26,500	19,504	43,000	31,524	69,500
1.98	77.9	3			10,569	23,300	39,780	87,700	50,349	111,000
2.24	88.2	3			9,616	21,200	54,430	120,000	64,046	141,200
1.60	63.1	5			35,380	78,000	19,504	43,000	54,884	121,000
1.98	77.9	5			32,432	71,500	39,780	87,700	72,212	159,200
2.24	88.2	5			30,436	67,100	54,430	120,000	84,866	187,100
1.60	63.1	7			56,427	124,400	19,504	43,000	75,931	167,400
1.98	77.9	7			51,981	114,600	39,780	87,700	91,761	202,300
2.24	88.2	7	1301.	14	49,033	108,100	54,430	120,000	103,463	228,100

3.1.6 Cost Parameters

The cost estimates applicable to the liquid hydrogen AST are:

- Development
- Investment
- Operation
 - DOC
 - IOC
- Return on Investment

The estimate for the above categories of cost are produced by a series of subroutines within the ASSET Program, plus use of a separate computer program for the final ROI calculation. The computer programs are described in Appendix A. The bases for deriving the input parameters and factors to these various models are discussed in the following paragraphs.

3.1.6.1 Development

The following list of input factors are used in the development cost model (see Appendix A) for the evaluation methodology for the LH₂ AST.

Maximum Mach number (XMMAX)	2.7
Tooling material rate (TMR)	1.73
Number of aircraft in the development program (XNYO)	4
Complexity factor for engineering (XKE)	.8
Complexity factor for tooling (XKT)	.88
Complexity factor for flight test (XKFT)	.37
Number of test articles for structural tests (XNSTA)	1.0
Number of test articles for fatigue tests (XNFTA)	1.0
Number of test articles for systems test (XMTSF)	.30
Engineering test material rate (ETSMR)	0
Flight Material Rate (EFTMR)	0
Value of constant for engine development (CEDCF)	21.3 x 10 ⁶
Development production rate for development (DR)	3 or 6
Development cost factor for avionics (DAV)	0
Airframe spares factor for development (AFSF)	.15
Engine spares factor for development (EDSF)	.50

Avionics spares factor for development (AVSF)	.30
Special support factor for development (DSSEF)	.02
Technical data cost factor for development (DATAF)	.005
Profit factor for development (DPROF)	.15
Operator trainer cost factor for development (DOT)	0
Maintenance trainer cost factor for development (DMT)	0

The estimates for design engineering flight test, and tooling are primarily dependent upon the aircraft performance characteristics, and the aircraft size as denoted by weight and the complexity of the configuration. The remainder of the estimates are either direct inputs or simple algebraic expressions developed from historical data. In the subject study the development equations are being applied to a vehicle that has size and performance characteristics that fall outside of the range of characteristics from which the equations were developed; therefore, the equations were validated by comparison to other estimates and reported costs for the Concorde.

Lockheed has developed a parametric approach to assist in validation of cost quotes. The parametric approach uses a multiple regression technique to arrive at selected parameters that correlate best with historical data. The Lockheed historical data bank encompasses 14 prototype programs and 17 production programs. The selected independent variables are manufacturer's empty weight (MEW), design speed, duration of the flight test program in months, quantity of prototypes to be built, and an overall program index relating to state-of-the-art.

The Lockheed parametric approach was applied to the liquid hydrogen AST and the results compared to the results obtained from the parametric equations in the ASSET Program. The results from the Lockheed parametric approach were used to modify the ASSET equations. Appropriate modifications are reflected in the input listing shown above. As noted in the listing, the complexity factors for engineering, tooling and flight test of the LH₂ AST are less than unity although they are greater than corresponding factors used for the Jet A-1 AST. Both factors are less than unity in recognition that the basic equations reflect excessively high values. These inputs and the

development model described in Appendix A form the basis for the development cost estimate for the LH₂ AST.

3.1.6.2 Investment

The investment cost for the LH₂ AST includes the production cost for the aircraft, the spares, production tooling, special support equipment, and technical data. Operator and maintenance trainers are not included at this time. The number of trainers is determined through a complete analysis of total airline requirements and policy as to centralized or decentralized training concepts. The study of trainer requirements is beyond the scope of this study and thus costs are not included. The premises and factors used for calculating the investment cost are shown in Table A-1, included in Appendix A. The definition of the factors is included in the investment cost model description.

Cost Estimating Data - The input labor hours per kg (pound) and material dollars per kg (pound) are based on an aircraft with an empty weight of 102,965 kg (227,000 pound) (1967 SST). An analysis of historical aircraft manufacturing costs indicated that as aircraft empty weight increased, the cost per pound decreases. The cost per pound increase or decrease approximates a straight line on log-log graph paper, similar to a cost quantity plot except that dollars are plotted against weight. For the AST study, it is assumed that typical slopes for supersonic aircraft with a high percentage of materials other than aluminum are 99 percent for material and 96 percent for labor. Straight line logarithmic cumulative average learning curves are used for adjustment of the baseline input values at 100 units. The baseline input values are adjusted for quantities of 300 and 600 aircraft with learning curve slopes of 80 and 90 percent for labor and material respectively.

The labor hours and material dollar inputs as listed on Table A-1 in Appendix A are based on the Lockheed SST effort and are updated to reflect the material composition in the AST Systems Study (Reference 1) and the detailed value engineering effort performed on the AST structural analysis study (Reference 4). The engine cost estimate is based on the quantity of engines required for the aircraft produced plus 30% spares.

Engines for 300 aircraft = $4 \times 300 \times 1.3 = 1560$

Engines for 600 aircraft = $4 \times 600 \times 1.3 = 3120$

The learning curve slope for engines is 90%. The avionics are considered as off-the-shelf purchase at \$500,000 regardless of quantity.

3.1.6.3 Operations

The direct operating costs (DOC) are determined from a modified ATA method. This method is described in Appendix A. The basic input factors used for calculation of the DOC are included here.

Flight Crew

Supersonic bonus (SSB)	\$15/hour
International flight bonus	\$20/hour
Inflation rate for crew	7% per year

Fuel & Oil

Jet A-1 4.34 cents per kg (1.97 cents per pound)
LH₂ (basic) .22 cents/kg (.10 cents/lb) up to .661 cents/kg
(.30 cents/lb) for sensitivity analysis
Oil \$2.083 per kg (\$.945 per pound)

Insurance

Premium rate of 2.5 percent

Depreciation

Write off period	14 years
Residual value	0

Spares Ratio

Airframe	15 percent
Engine	30 percent
Avionics	30 percent

Maintenance

Maintenance labor inflation rate	5 percent
Maintenance burden factor	1.9

The indirect operating costs (IOC) are determined by a method also described in Appendix A. The indirect expense factors evaluated in the following table are those experienced by the international carriers. See Appendix A for definitions.

XKSE = 0.6	XKPH = 12.0
XKOE = 2.87	XKCH = 96.0
XKCO = 58.0	XKOP = .0061
XKAT = 27.0	XKOC = .0065
XKFB = 0.58	XKGA = .064

3.1.6.4 Return on Investment (ROI)

The ROI as calculated by the ASSET Program for screening purposes is in the form:

$$ROI = \frac{(TOTREV - TOTEXP)}{TOTINV/2}$$

where

TOTREV = total revenue
TOTEXP = total expense (DOC + IOC)
TOTINV = total cost for aircraft including amortized R & D plus spares and tooling

Another form of ROI calculation has been devised to include more of the economic factors generally included in an ROI calculation. The model description for this ROI calculation is included in Appendix A. The ROI is dependent upon the aircraft performance and cost, the passenger demand, range, and the interest rate. The factors used in the calculation of the economic ROI are:

Gate Time (GT), hours	.25
Block Time (TB), hours	obtained from ASSET
Block Fuel (FB), lbs	obtained from ASSET
Flyaway Cost for the Airplane (CFA), dollars	obtained from ASSET
Passenger Size (XNPASS)	234
Stage Length Flown (RANGE), kilometers (n.mi.)	7783 (4200)
Load Factor (LF)	.55
Utilization (U), hours/year	3,600

Number of years of depreciation (YRDP), years	14
Airframe spares factor (AFSF)	.10
Engine spares factor (ENSF)	.30
Special support spares factor (SSE)	.05
Zero range fare cost (REV 1), dollars	9
Fare cost as a function of range (REV 2), \$/km (\$/n.mi.)	.0919 (.0496)
Debt to equity ratio (DBTR)	60/40
Interest rate on borrowed money (IR)	.08
Tax rate (TXRATE)	.48
Average amount of cargo (AVCARG), kg (lbs)	907.2 (2,000)
Revenue rate for cargo (REV 3), \$/kg.km. (\$/ton n.mi)	504.0 (.30)
Number of aircraft delivered per quarter (DSQ)	.38
Number of aircraft available for operations from the total number purchased (AVAIL)	.90

The revenue is based on a fare level that is approximately 20% above the current coach fare between Los Angeles and Honolulu. The LH₂ AST fare is calculated on the basis of a 10/90 ratio for first class-to-coach with a 30% increase in the first class fare and an additional 15% charge for all passengers for the supersonic surcharge.

The fleet size and the number of trips flown by each aircraft is a function of the passenger demand and the aircraft size and performance. The passenger demand is taken from the forecast demand for the Los Angeles to Honolulu route as indicated in the Phase II AST study (Market Analysis) contract NAS-1-11940 (Reference 1). The estimated passenger demand for this route is 1,806,750 passengers per year.

3.2 PARAMETRIC VEHICLE STUDY

The focal point for the technology data generated as described in the previous sections is the ASSET (Advanced System Synthesis and Evaluation Technique) synthesis model. This model is designed to size, weigh, perform, and cost large numbers of aircraft design options parametrically. The synthesis cycle required to size the vehicle for given payload/mission requirements is accomplished within ASSET by integrating data describing vehicle geometry, aerodynamics, propulsion, structures/materials/weights, and cost. A schematic presentation of the inputs and outputs involved in the synthesis cycle is shown on Figure 49. The key elements and the flow of information through ASSET are depicted on Figure 50.

The three major subprograms in ASSET are sizing, performance, and costing. The Sizing subprogram sizes each parametric aircraft to the design mission. The design characteristics and component weights of the sized aircraft are then transferred to (1) the Costing subprogram, which computes aircraft cost on the basis of component weights and materials, engine cycle and size, avionics packages, production and operational schedules, and input cost factors, and (2) the Performance subprogram which computes acceleration, maximum speed, ceiling, landing and takeoff distances, and other performance parameters. The ASSET program output consists of a group weight statement; vehicle geometry description; mission profile summary; a summary of the vehicle's performance evaluation; RDT&E, production, and operational cost breakdowns for each candidate vehicle; and summaries of these data for the matrices of candidate aircraft. Plots of these weight, cost, size and performance parametric data can be automatically plotted on 35 mm microfilm from which hard copies are made.

The range of vehicle mission and configuration parameters investigated is shown in Table 1. All parameters were not investigated for all vehicles but were limited by the results of previous runs. For example, a t/c of 7% was not included in the Mach 2.2 airplane as data from the Mach 2.7 cases had shown it to have an excessive drag penalty.

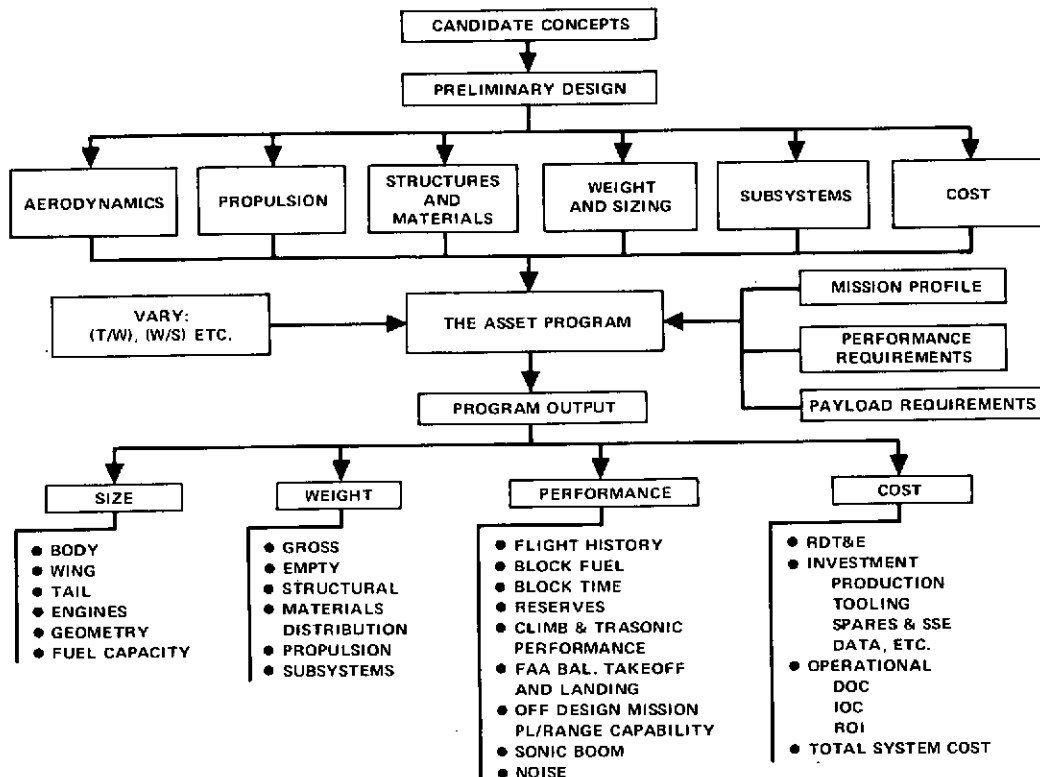


Figure 49. ASSET Synthesis Cycle

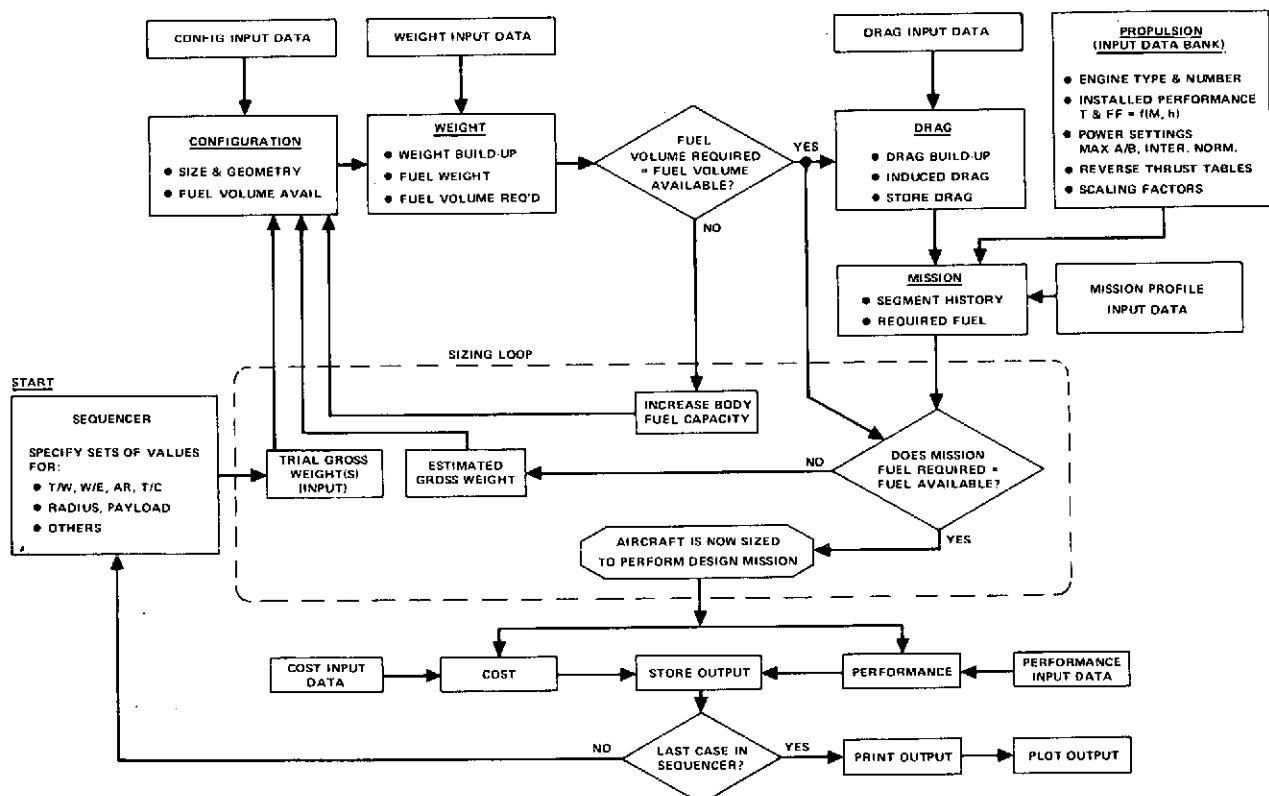


Figure 50. ASSET Program Schematic

The final data from the ASSET runs is presented in both tabulated and autoplotting carpet format. Figure 51a is an example of an automatically plotted carpet plot, complete with three sample constraint lines. From a series of working level autoplot presentations the final vehicle characteristics desired such as gross weight, cost, range, etc. can be selected and displayed in a conventional manner as shown in Figure 51b.

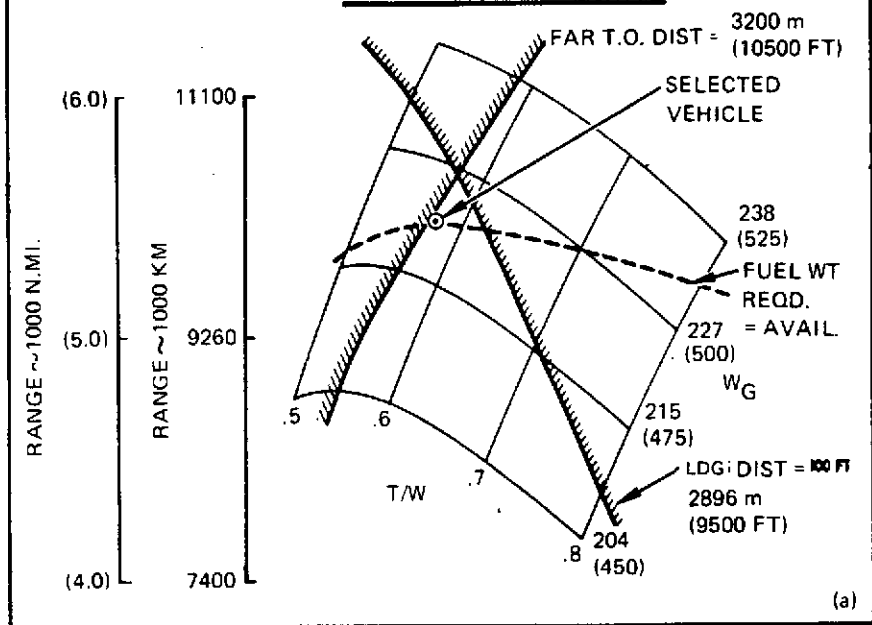
Included in the schematic of Figure 50 is a capability to calculate jet noise, recently incorporated in the ASSET program. The calculation method is based on Aerospace Information Report No. 876. When parametric variations are made to thrust, wing loading and any other performance and/or aircraft characteristics, different takeoff flight profiles are effected which results in a change in the noise footprint. The inputs required are:

- (1) Engine exhaust characteristics such as; velocity, density and area for each exhaust stream, i.e., core engine or fan duct.
- (2) The engine exhaust noise directivity profile.
- (3) The number of microphones and their location relative to the point of brake release.
- (4) Exhaust noise suppressor effectiveness.
- (5) Aircraft characteristics.

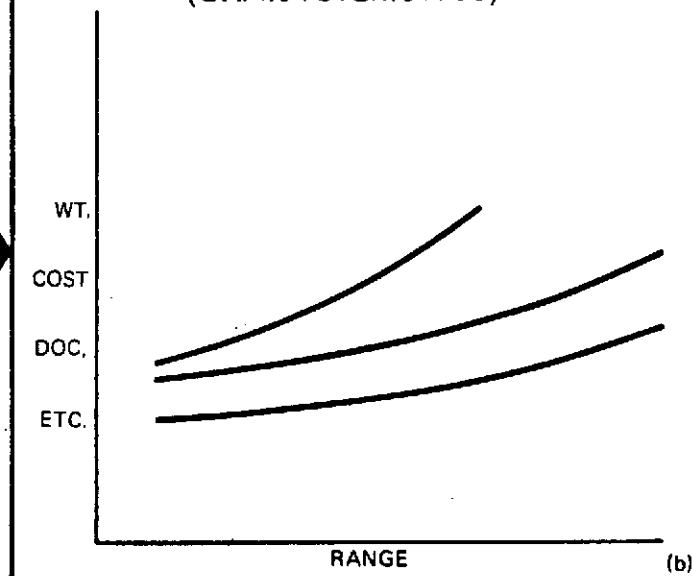
During takeoff both the flyover 6.48 km ((3.5 n.mi.) from brake release) and peak sideline 0.648 km ((0.35 n.mi.) from runway centerline) noise levels are computed, the greater of which is the critical noise level. At each microphone location noise calculations are made at half second intervals to build up a noise history for use in computing the duration correction factor. This correction factor is added to the tone corrected perceived noise level and results in the effective perceived noise level (EPNL) which is the noise evaluation quantity. This method of predicting noise generated, is applicable to both conventional turbojet and turbofan engines. The noise calculation described does not include fan, compressor, machinery, combustion or aerodynamic noise.

ASSET
PROGRAM

SAMPLE AUTO PLOT



SELECTED VEHICLES
(CHARACTERISTICS)



3.3 RESULTS OF PHASE I PARAMETRIC STUDY

3.3.1 Design Trends

The results and design trends of the Phase I Parametric Study are presented in this section. All vehicles represented in the curves which follow meet all the constraints of takeoff and landing distances and the noise limitations, and were picked from ASSET computer results on the basis of minimum weight.

Geometric Parameters. - Figure 52 shows the effect of wing thickness ratio (t/c), wing area (S_W), and wing loading (W/S) on gross weight for aircraft designed for a range of 8,704 km (4,700 n.mi.), selected as a typical example. The range of t/c 's and wing areas considered produce vehicle cross sections which vary from a discrete wing-body ($t/c = 3$, $S_W = 743.2 \text{ m}^2$ (8,000 ft^2) to a modified lifting-body ($t/c = 7$, $S_W = 1,765 \text{ m}^2$ (19,000 ft^2) as indicated by the sketches on the figure. The trend of the curves illustrates the tradeoff between drag and structural weight. Increasing wing area, relative to the fuselage size, causes the L/D to increase and fuel required to decrease. However, these advantages are more than offset by increasing wing weight.

This effect is also shown in Figure 53 in which weight fractions, cruise L/D and wing loading (W/S) are plotted vs. wing size for a t/c of 3%. The increase in cruise L/D causes a slight reduction in fuel fraction which is more than offset by the wing weight resulting in a net decrease in the weight fraction available for payload and equipment. This in turn requires an increasing gross weight to carry the fixed payload.

A further effect of increasing wing size (low W/S) is that as the cruise wing loading is lowered, higher altitudes (lower ' q ') are required to achieve L/D_{max} . These higher altitudes require larger engines and the net result is a compromise limiting the actual cruise L/D compared to the maximum attainable as shown in the figure.

Figure 54a, which is derived by cross plotting data from Figure 52, shows the effect of wing thickness on gross weight indicating about the same gross weight for t/c 's from 3 to 4% but a rapid rise due to the drag increase beyond 5%. Figure 54b illustrates that in general, due to the low quantity

- RANGE = 8704 KM
(4700 N. MI.)
- M = 2.7
- TURBOFAN ENGINE

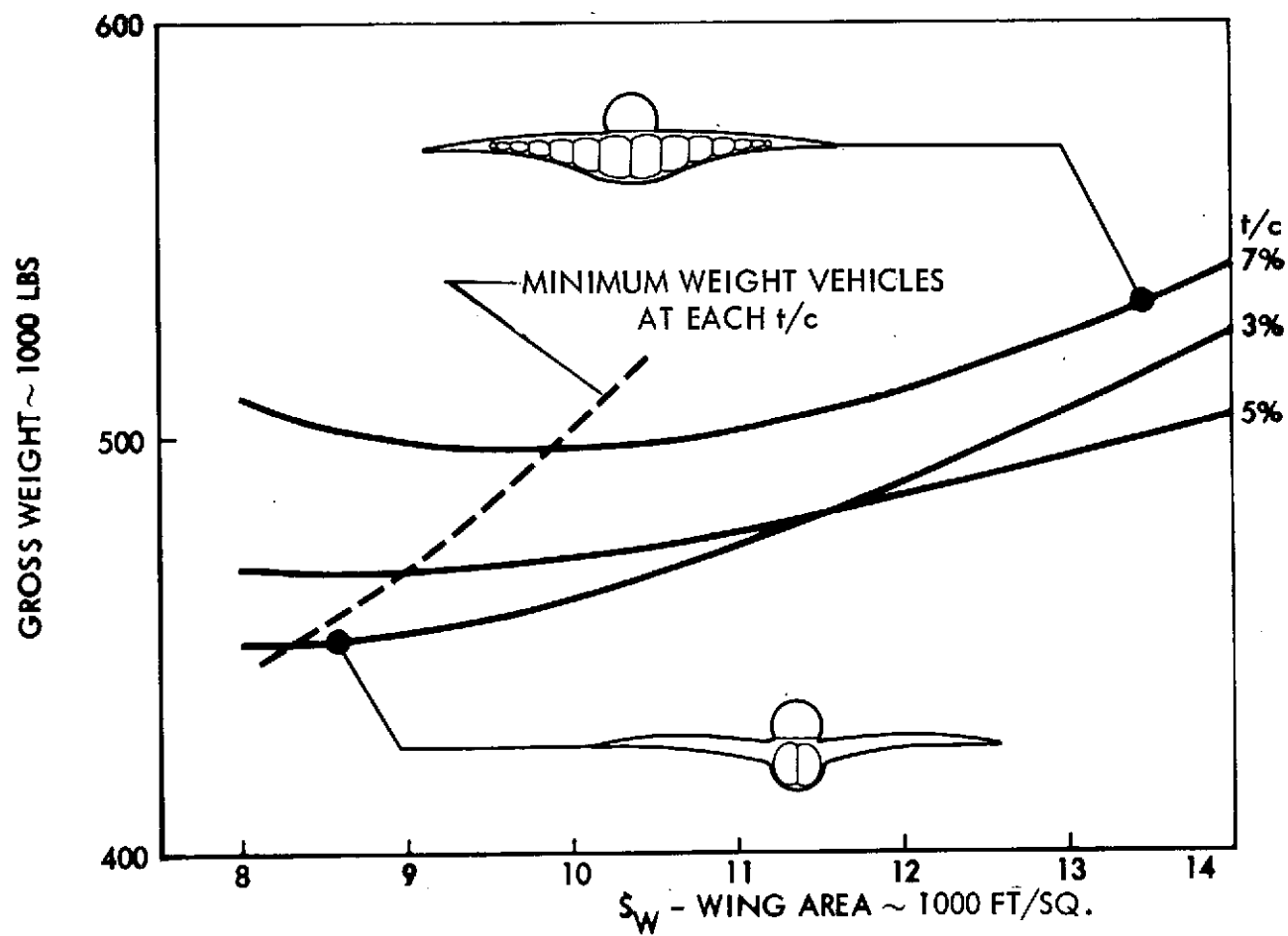


Figure 52. Wing Area and t/c vs. Gross Weight (Constant Range)

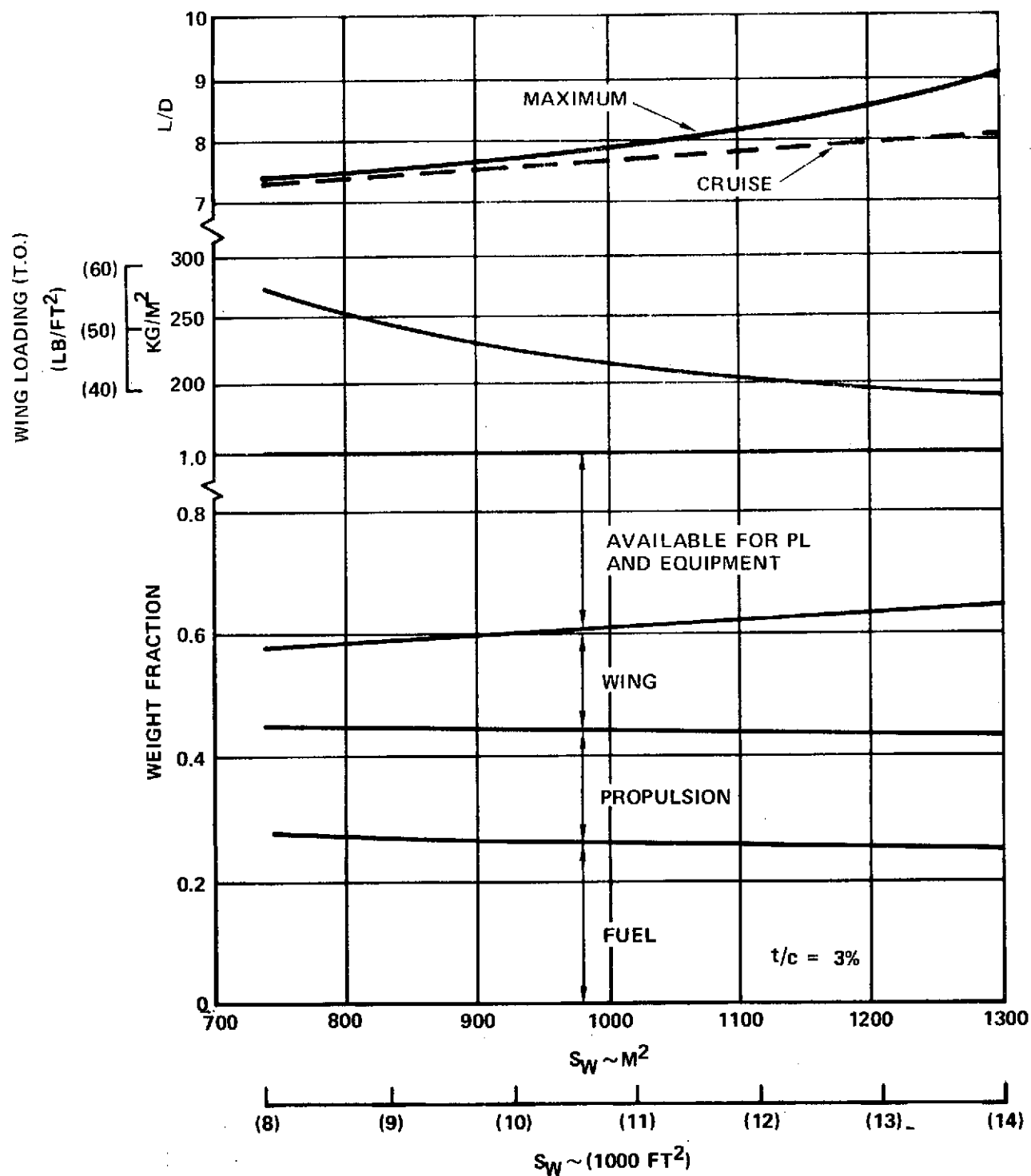


Figure 53. Weight Fractions and Cruise L/D vs. Wing Area

- TURBOFAN ENGINE
- 8704 Km
(4700 NM) RANGE

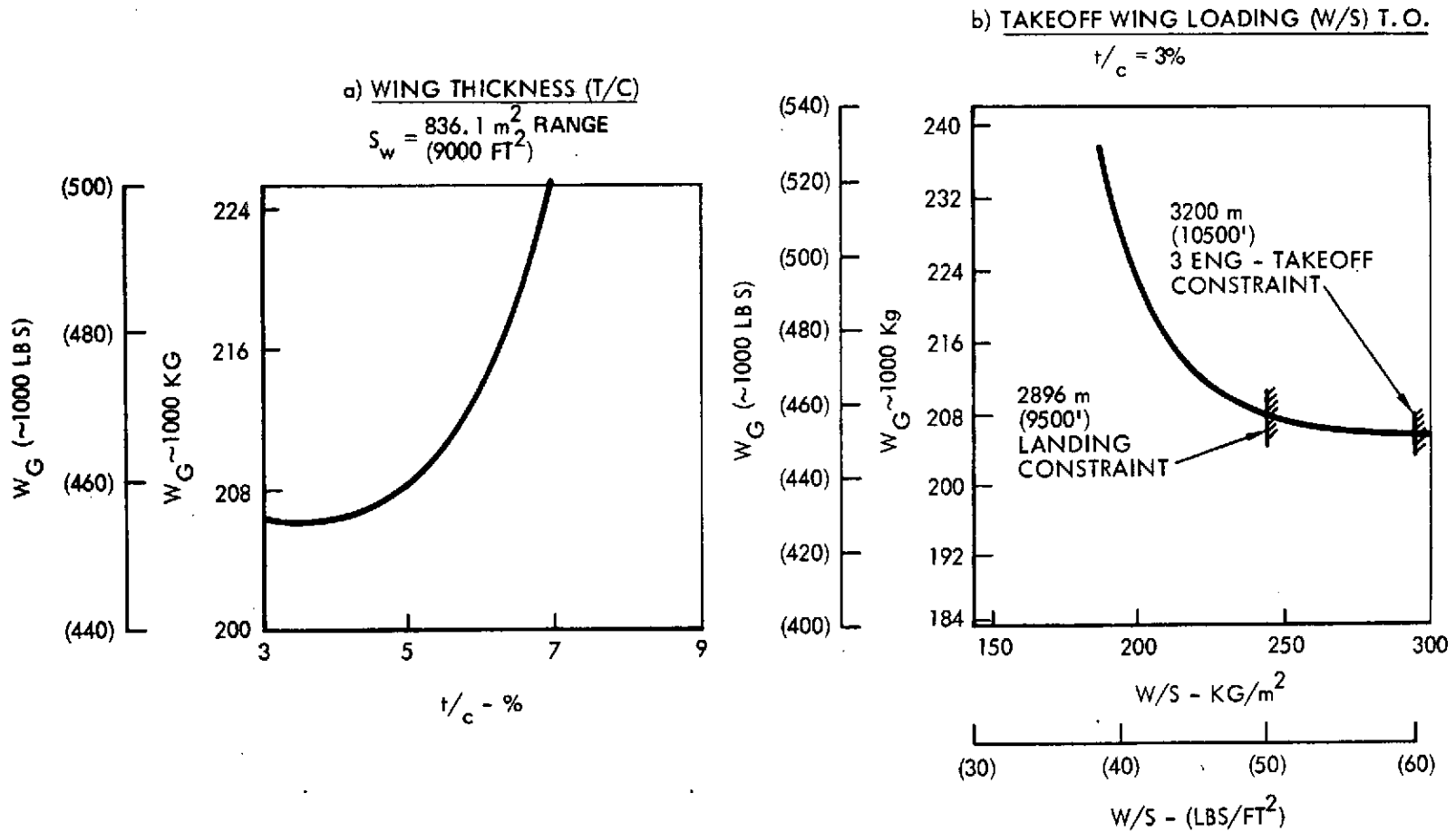


Figure 54. Effect of t/c and W/S on Gross Weight

of fuel burnoff of hydrogen AST's, the wing is sized by landing field length and not the takeoff condition.

Engine Selection. - One of the primary considerations in the choice of engines is the ability to meet the Phase I ground rule of FAR 36 minus 5 EPNdB with regard to airport and community noise. The propulsion section (3.1.3) has described the assumptions made with regard to relative jet exhaust velocity and noise suppressor effectiveness for both turbojet and turbofan engines. The net effect for both engines is to limit the relative exhaust velocities to the range of 549-579 m/sec (1,800 - 1,900 fps). With this jet velocity fixed the second consideration is to meet the 3200 m (10,500 ft) engine-out takeoff distance which required a thrust/weight of approximately 0.3 at lift off. The relative jet velocity required to meet the noise constraint is achieved by power cut-back. In the case of the turbojet this limits thrust for takeoff to about 39 percent (61 percent cutback) of maximum while the turbofan can use 56 percent (44 percent cutback). The net result is that the uninstalled thrust/weight (T/W) for the turbojet is 0.8 compared to only 0.58 for the turbofan to meet both the noise and takeoff distance constraints. The high installed thrust/weight required of the turbojet is partially offset by a lower SFC during supersonic cruise (see Section 3.1.3). This is illustrated in Figure 55 which shows the turbojet superior to the turbofan at ranges exceeding 9,260 km (5,000 n.mi.).

A further consideration, while not explicit in the study ground rules, is the ability to accomplish off-design missions in which either initial or final cruise legs are flown subsonically to avoid sonic booms in populated areas. Figure 56 shows a comparison of vehicles powered with turbofan and turbojet engines which reflects the lower specific fuel consumption (SFC) = 0.296 kg/hr/daN (0.29 lb/hr/lb) of the turbofan compared to the turbojet SFC = .377 kg/hr/daN (0.37 lb/hr/lb) during the subsonic cruise. It should be emphasized that the turbojet cycle characteristics were not optimized for this consideration and that were a subsonic leg actually a design requirement the range deterioration could possibly be reduced. In any event, the turbofan engine cycle is inherently more flexible with regard to choice of performance and noise characteristics than the turbojet.

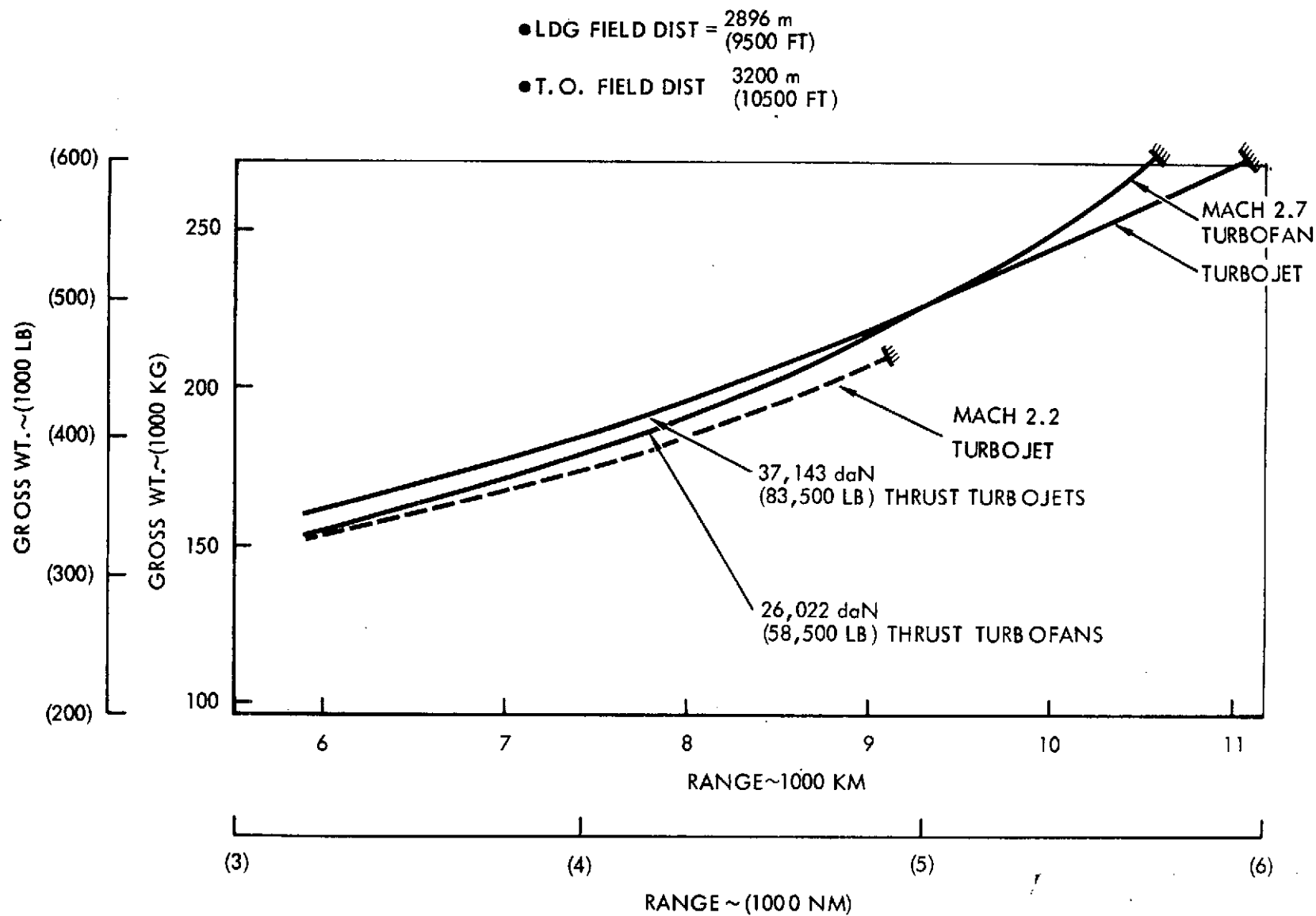
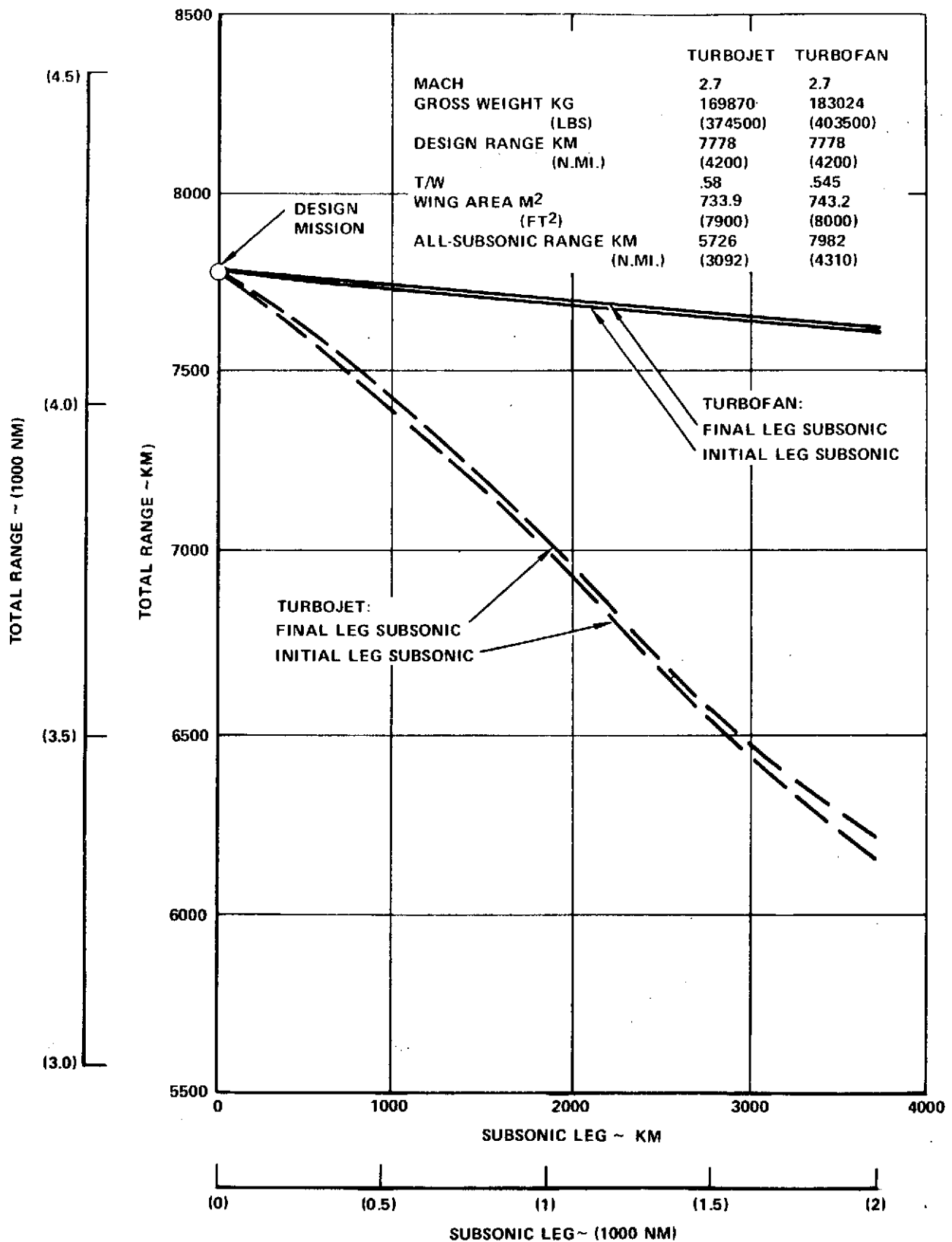


Figure 55. Vehicle Range - Weight and Engine Comparison



COMPARISON OF OFF-MISSION PERFORMANCE - TJ VS TF

Figure 56. • Comparison of Off-Mission Performance - Turbojet vs Turbofan

Cruise Speed Comparison. - Figure 55 is a summary plot showing a comparison of range vs. gross weight of a series of vehicles powered by turbojets and turbofans, each designed to cruise at Mach 2.7, in addition to a similar curve for vehicles designed to cruise at Mach 2.2 and powered by turbojets. While Mach 2.2 turbofan engines were not run, it is not expected that the results would be any different than indicated by the Mach 2.7 vehicle comparison. As previously stated, all vehicles chosen meet all the constraints of takeoff, landing, and noise and were picked on a minimum weight basis. The Mach 2.2 vehicles exhibit slightly lower gross weights all the way up to the maximum range investigated 8,890 km (~4,800 n.mi.).

3.3.2 Cost Trends

The Direct Operating Costs (DOC) for the vehicles shown in Figure 55 are presented in Figure 57. It should be remembered that this is not a plot of given airplane flying different ranges but rather, different point designs flying at various design ranges. Consequently, the longer the range, the larger and heavier the vehicle with an attendant increase in DOC. These DOC's are based on an arbitrary fuel cost of 22¢/kg (10¢/lb) for the liquid hydrogen fuel.

Table 11 is presented to illustrate a typical production cost comparison for an LH₂ fueled AST, compared with a Jet A-1 fueled AST. The \$/kg (\$/lb) cost factors indicated have been increased for the hydrogen vehicle by an estimated complexity factor, where appropriate. In both cases the range and payload are the same.

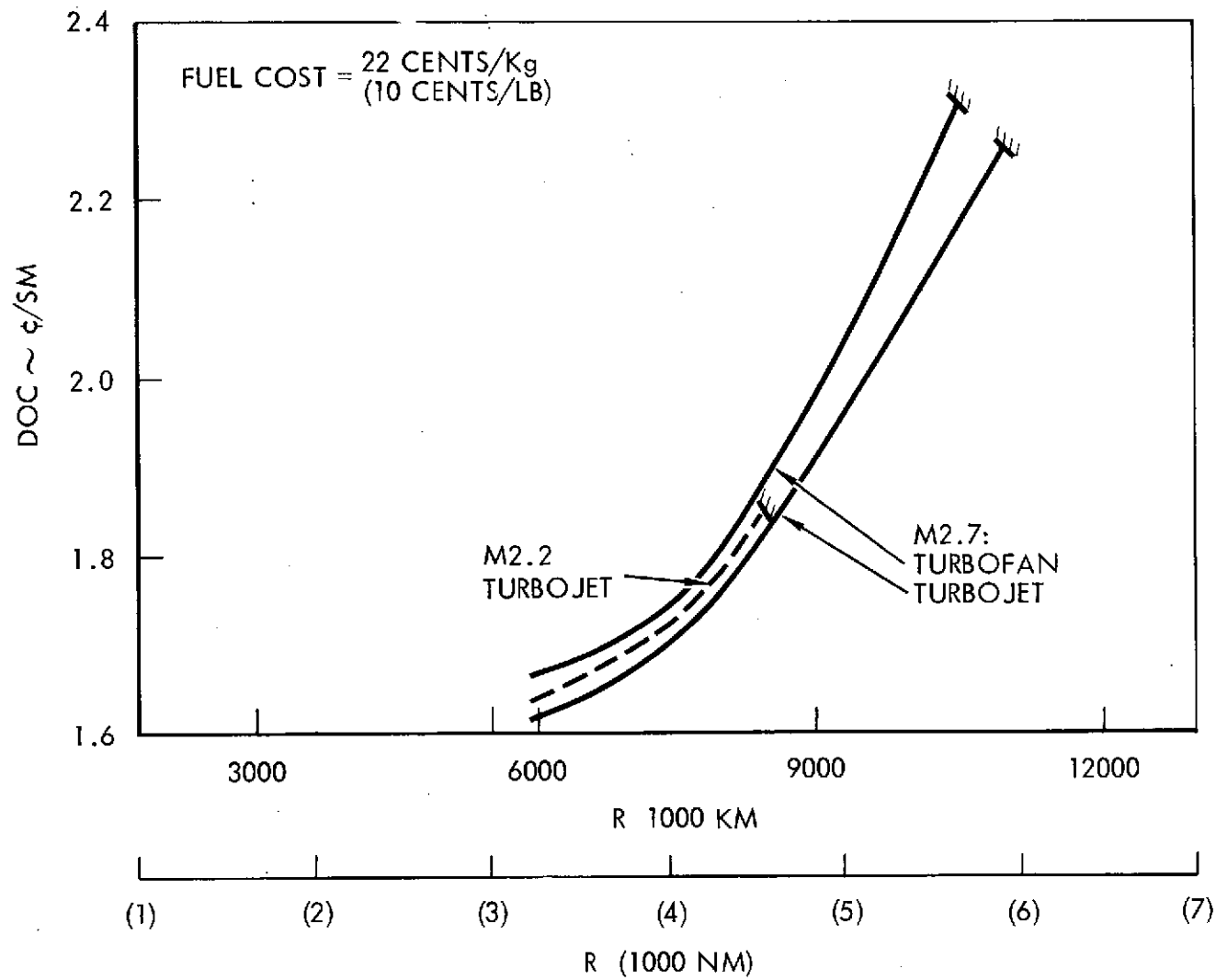


Figure 57. DOC Cost Comparison

TABLE 11. PHASE I PRODUCTION COST COMPARISON
(Jet A-1 vs. LH₂ Fueled AST)

BASIS:

- No R&D Amortization
- 300 Aircraft
- 1972 Dollars Using 1980-85 Technology

	7,778 km (4,200 n.mi.)/2.7/TF			7,778 km (4,200 n.mi.)/2.7/TJ		
	Jet A-1 Fuel			LH ₂ Fuel		
	Weight~ kg (lbs)	Dollars	\$/kg (\$/lb)	Weight~ kg (lbs)	Dollars	\$/kg (\$/lb)
Wing	43,551 (96,013)	13,670,000	313 (142)	23,479 (51,763)	8,998,000	384 (174)
Fuselage	17,056 (37,602)	5,247,000	309 (140)	19,121 (42,154)	6,906,000	362 (164)
Fuel System and Tank	2,400 (5,291)	832,000	346 (157)	12,100* (26,675*)	1,660,000	137 (62)
Other	47,106 (103,851)	38,320,000	814 (369)	30,220 (66,624)	27,088,000	897 (407)
Engine	20,615 (45,448)	7,684,000	373 (169)	11,733 (25,868)	7,604,000	648 (294)
Avionics	863 (1,903)	500,000	5,798 (2,630)	863 (1,903)	500,000	5,798 (2,630)
	131,590 (290,108)	66,253,000		97,516 (214,987)	52,756,000	

*Includes LH₂ Tankage

3.3.3 General Conclusions

As a result of the parametric design study of Phase I, the following general conclusions were reached concerning liquid hydrogen fueled supersonic transport aircraft:

- Configurations with relatively thin wings and large fuselages (to contain the fuel) provide superior performance.
- LH₂ Fueled AST aircraft are capable of ranges in excess of 11,112 km (6,000 n.mi.) with reasonable gross weights.
- Low mission fuel burn-off dictates wing loading (W/S) of approximately 195 kg/m² (40 lbs/ft²) to meet landing field length of 2,896 m (9,500 ft).
- Low take-off wing loading 220 - 224 kg/m² (45 - 50 lb/ft²) means aircraft reach L/D max at low q's (high altitude) requiring high thrust/weight
- High thrust/weight results in satisfactory engine-out takeoff field length performance even with power cut back required by noise constraint.
- Turbofan engines are most promising for shorter ranges... Turbojet engines are most promising for long range, all-supersonic mission.
- Use of turbojets requires very large engines, deeply throttled at takeoff, to meet noise constraints.

3.3.4 Candidate Vehicle Selection

The completion of the Phase I parametric studies required the selection of the four most promising vehicles as candidates for the Phase II configuration refinement study. In cooperation with NASA, it was decided the four vehicles selected should reflect two range capabilities: 7,778 km (4,200 n.mi.), which represents transatlantic capability; and 10,186 km (5,500 n.mi.), representing transpacific capability, each with adequate subsonic cruise range either before or after supersonic cruise. It was also decided the selected vehicles should be designed for Mach 2.7 cruise, except that one vehicle should be designed for Mach 2.2 cruise and 7,778 km (4,200 n.mi.) range, to provide a specific comparison. Finally, although the turbojet engine was demonstrated to be more economical at long range cruise (Figure 55), it was felt that aircraft with both types of engines should be compared at the shorter range. As a result, the following requirements were established for the four aircraft designs which were to be compared leading to the ultimate selection of one design for detailed study in Phase II.

<u>Cruise Speed</u>	<u>Range</u>	<u>Engine Type</u>
M 2.7	7,778 km (4,200 n.mi.)	Turbofan
M 2.7	7,778 km (4,200 n.mi.)	Turbojet
M 2.7	10,186 km (5,500 n.mi.)	Turbojet
M 2.2	7,778 km (4,200 n.mi.)	Turbojet

Table 12 presents the characteristics of the four vehicles which were picked from the parametric data generated in Phase I to define the most attractive candidate aircraft to satisfy the stated requirements. There are several interesting items to note in comparing some of the values listed in the table. For example, the wing area of the Mach 2.2 aircraft is shown to be significantly smaller than that of the Mach 2.7 aircraft of equivalent range and engine type. The aircraft have wing loadings of 286.5 kg/m^2 (58.6 lb/ft^2) and 227.0 kg/m^2 (46.5 lb/ft^2), respectively. This is due to the higher aspect ratio ($AR = 2$) of the Mach 2.2 airplane compared to only 1.62 for the Mach 2.7. The wing is sized by airport performance requirements in both cases so the higher available lift coefficient (0.69) for the Mach 2.2 airplane, compared

TABLE 12. CHARACTERISTICS OF SELECTED VEHICLES FROM PHASE I

Vehicle Configuration No.		1	2	3	4
General	Mach	2.7	2.7	2.7	2.2
	Range - km (n.mi.)	7,778 (4,200)	7,778 (4,200)	10,186 (5,500)	7,778 (4,200)
	Engine Type	Turbofan	Turbojet	Turbojet	Turbojet
	T/W	.58	.80	.80	.80
	Wing Area - m^2 (ft^2)	743.2 (8,000)	836.1 (9,000)	1,035.8 (11,150)	630.3 (6,785)
	W/S - kg/m^2 (lbs/ ft^2)	246 (50.4)	227 (46.5)	242 (49.6)	286 (58.6)
	t/c - %	3	3	3	3
	Aspect Ratio	1.62	1.62	1.62	2
Weights	Gross Wt. kg (lb)	183,024 (403,500)	189,737 (418,300)	250,835 (553,000)	180,392 (397,700)
	Fuel Wt. ~ kg (lb)	45,813 (101,000)	42,774 (94,300)	67,721 (149,300)	43,318 (95,500)
	Zero Fuel Wt.-kg (lb)	137,211 (302,500)	146,863 (324,000)	183,114 (403,700)	137,075 (302,200)
	Payload kg (lb)	28,032 (61,800)	28,032 (61,800)	28,032 (61,800)	28,032 (61,800)
	OEW - kg (lb)	109,179 (240,700)	118,931 (262,200)	155,082 (341,900)	109,043 (240,400)
	PL/ W_G	.153	.148	.112	.155
	WH ₂ / W_G	.25	.228	.27	.24
Performance	FAR T.O. Dist. ~ m (ft)	3,200 (10,500)	2,730 (8,970)	2,865 (9,400)	2,730 (8,950)
	FAR Ldg. Dist. ~ m (ft)	2,860 (9,382)	2,866 (9,404)	2,890 (9,483)	2,896 (9,500)
	Average Alt. - Cruise m (ft)	20,733 (68,000)	21,495 (70,500)	21,495 (70,500)	18,900 (62,000)
	Average L/D - Cruise	7.38	7.71	7.69	7.72
	Average SFC - Cruise kg/hr/daN (lbs/hr/lb)	.581 (.57)	.502 (.493)	.500 (.491)	.456 (.447)
	SFC - Subsonic Cruise kg/hr/daN (lbs/hr/lb)	.300 (.294)	.378 (.371)	.378 (.371)	.357 (.350)
	SFC - Subsonic Loiter kg/hr/daN (lbs/hr/lb)	.220 (.216)	.359 (.352)	.367 (.36)	.359 (.352)
Cost	DOC - ϕ /SM	1.79	1.70	2.02	1.74
	*Basic Price $\$ \times 10^6$	58.3	61.1	78	55.7

*300 Aircraft Production Base



to 0.48 for the lower aspect ratio wing of the Mach 2.7 design, allows a reduction in wing size and correspondingly higher wing loading.

The Mach 2.2 vehicle shows a slightly lower gross weight than the Mach 2.7 but almost equal fuel consumption. The DOC of the Mach 2.2 is slightly higher than the 2.7 in spite of its lower cost. This is due to its higher crew, insurance, and depreciation cost per seat mile which results from the lower productivity of the slower Mach 2.2 vehicle. (888 flights per year vs 1039 for the Mach 2.7).

A third interesting point to consider in Table 12 is the comparison between aircraft #1 and #2, the turbofan vs. the turbojet powered Mach 2.7 vehicles. The turbofan airplane has a higher SFC in cruise and requires 3,039 kg (6,700 lbs) more fuel, but its gross and empty weights are significantly less than those of the turbojet aircraft. Explanations for this also involve several factors. First, the SFC of the duct-burning turbofan in both subsonic cruise and loiter is much lower than the counterpart turbojet, partially offsetting its higher supersonic cruise SFC. Therefore, less fuel is needed to meet the reserve requirement. Second, the turbofan need not be throttled as deeply at takeoff to meet the noise limitation so smaller, lighter engines can be used. Thirdly, because the accumulation of such factors results in a lower landing weight, the wing area required to meet the landing distance requirements is smaller, leading to additional weight saving, finally resulting in the values of OEW, ZFW, and G.W. shown in the table.

4.0 PHASE II: POINT DESIGN VEHICLE STUDY

The purpose of Phase II was to establish design, performance, and cost characteristics of a selected configuration of liquid hydrogen fueled supersonic transport aircraft at a greater level of detail than was possible in Phase I. The design study focused on definition of structural concepts for both the aircraft in general and the LH_2 tanks in particular. In addition, a feasible thermal protection system for the cryogenic tankage was defined. The objective was to provide confidence in the aircraft performance, weight, and cost data, and additional guidance for directing further development.

The following sections describe the point design vehicle and explain how the final configuration was evolved. Its performance, cost, structural design, and thermal protection system are described. The viability of the concept of using LH_2 as the fuel for an advanced design of supersonic transport aircraft is then discussed by comparing it to an equivalent design of Jet A-1 fueled aircraft and by outlining major technology development required for its fruition. Finally, recommendations are made for follow-on studies and development.

4.1 VEHICLE DESCRIPTION

During the Phase I part of the study it became evident that the real measure of worth of a hydrogen fueled AST transport aircraft would only be apparent by comparing it to an equivalent Jet A-1 fueled design. Accordingly, the contractor was directed to focus design attention in Phase II on an aircraft which would have the same mission performance and be designed to the same state-of-the-art and ground rules as a Jet A-1 fueled vehicle which was concurrently being studied by Lockheed for NASA - Langley Research Center under contract NAS 1-12288 (Reference 4). In this section, the design requirements that were selected to provide compatibility with the reference Jet A-1 airplane are described, the basis for evolving the characteristics of the "point design" LH_2 AST airplane are explained, the selected airplane configuration is described, and weight and balance data are provided.

4.1.1 Design Requirements

As described, an overriding objective in Phase II was to provide a one-for-one basis for comparing a conventionally fueled (Jet A-1) AST with one fueled with liquid hydrogen. Conveniently, a design of Jet A-1 AST being studied by Lockheed for NASA-Langley Research Center under Contract 1-12288 (Reference 4) matched the cruise speed and range of one of the LH₂ AST designs selected at the end of Phase I as a preferred configuration (Configuration Number 1 in Table 12). Accordingly, it was decided to use the following mission requirements, taken from the Arrow - Wing Structures Study of Reference 4, as a basis for design of the Phase II Point-Design LH₂ AST aircraft.

Cruise speed	Mach 2.7
Range	4200 n.mi.
Payload (234 passengers)	49,000 lb

To assure equivalency in design and evaluation between the Jet A-1 and LH₂ aircraft being evolved in the two separate NASA studies, several changes from the basic premises used in Phase I of the subject study were made for Phase II. For example, a more conservative definition of materials and technology state-of-the-art was assumed for the Jet A-1 aircraft than had been used for the LH₂ studies in Phase I. The Langley study of Jet A-1 aircraft was based on what was labeled 1981 technology, defined characteristically as use of titanium skin and structure, reinforced with layup of boron-polyimide composite. By contrast, in Phase I of the subject study, 1985 technology was defined as use of from 60 to 90 percent advanced composite materials in the empennage, fuselage, and wing structures. In addition, the Langley study used more relaxed noise standards, viz., FAR Part 36, contrasted with FAR Part 36 minus 5 EPNdB for the subject study in Phase I.

Table 13 lists the changes in the Basic Premises which were made to accommodate the objective of providing for a direct comparison with a conventionally fueled hydrocarbon AST design. The point design airplane of Phase II was designed to these revised Basic Premises.

TABLE 13
CHANGES IN BASIC GUIDELINES FOR PHASE II
(Refer to Table 2)

	<u>Phase I</u>	<u>Phase II</u>
Materials and Technology	1985	1981 *
State-of-the-Art		
* technology level defined per agreement for contract NAS 1-12288		
Noise	FAR 36 minus 5	FAR 36
Cost	1972 dollars	1973 dollars
Payload	61,800 lb. (300 passengers)	49,000 lb. (234 passengers)

4.1.2 Design Evolution

Payload/Fuel/Structural Arrangements


At the end of the Phase I parametric study several conclusions regarding the fuel containment assumptions of Phase I (fuel in lower fuselage and inboard wing) became apparent:

- The wing carry-through structure was severely compromised by the lower fuselage tanks.
- The small volume of fuel carried in the optimum wing thickness (3-4 percent) was not worth the 11 percent penalty in wing weight incurred.
- The underfloor location of the fuselage tanks required a 9.37 kg/m^2 (1.22 lb/ft^2) penalty in the floor pressure deck and tank support structure and was not desirable from the standpoint of either passenger-fuel proximity or relative locations.

As a consequence, at the start of Phase II alternate arrangements and concepts were studied. These concepts, shown in Figure 58, were qualitatively rated against the following criteria:

- Passenger-fuel separation distance
- Passenger-fuel relative locations

LEGEND:

H₂ = HYDROGEN TANK  = WING STRUCTURE
C = CARGO E = EQUIPMENT

ARRANGEMENT NO. =

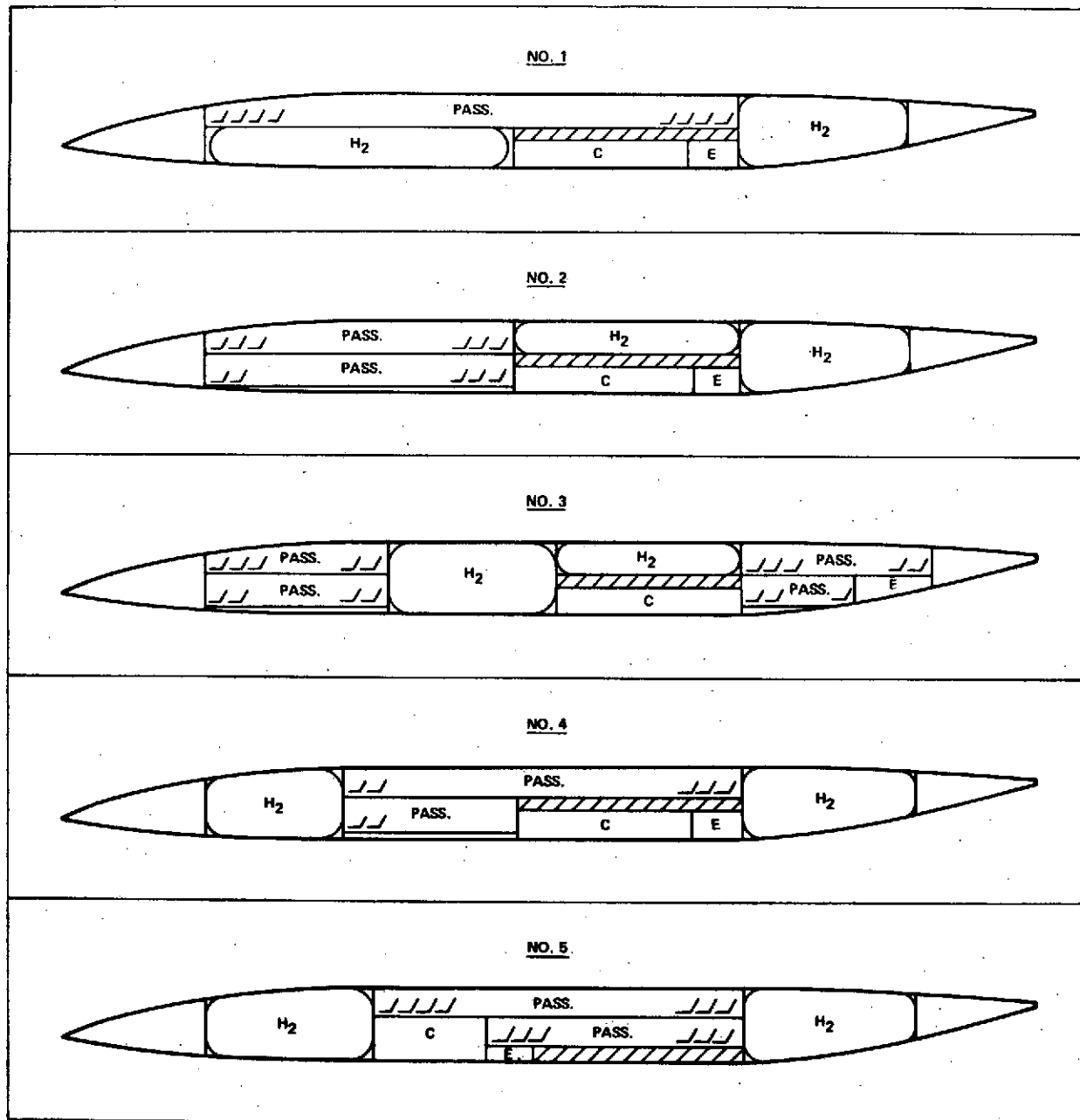


Figure 58. Candidate Payload/Tank/Structural Arrangements

- Structural feasibility
- c.g. control
- Passenger seating and accessibility
- Volume utilization
- Option to make tank integral (load-carrying) or non-integral.

The following brief comments are made as to the suitability of each arrangement:

No. 1: Adequate separation not achieved

Relative arrangement poor

Non-integral (no option). A leak in the forward tank could result in gaseous hydrogen flowing around (possibly into) the passenger compartment.

Forward tank must be non-integral (no option)

Structurally feasible

No. 2: Maximum separation

Forward tank must be non-integral

Structurally feasible

c.g. travel impossible

No. 3: Separation adequate

Mid-tank must be non-integral

Structurally feasible

Aft passenger seating not efficient

No. 4: Separation adequate

Tank option available

Structurally feasible

Passenger loading and emergency exits below wing not acceptable.

No. 5: Separation adequate

Tank option available

Structural feasibility the best

Passenger seating and loading OK

Volume utilization best

Arrangement number 5 was chosen on the basis of the above arguments.

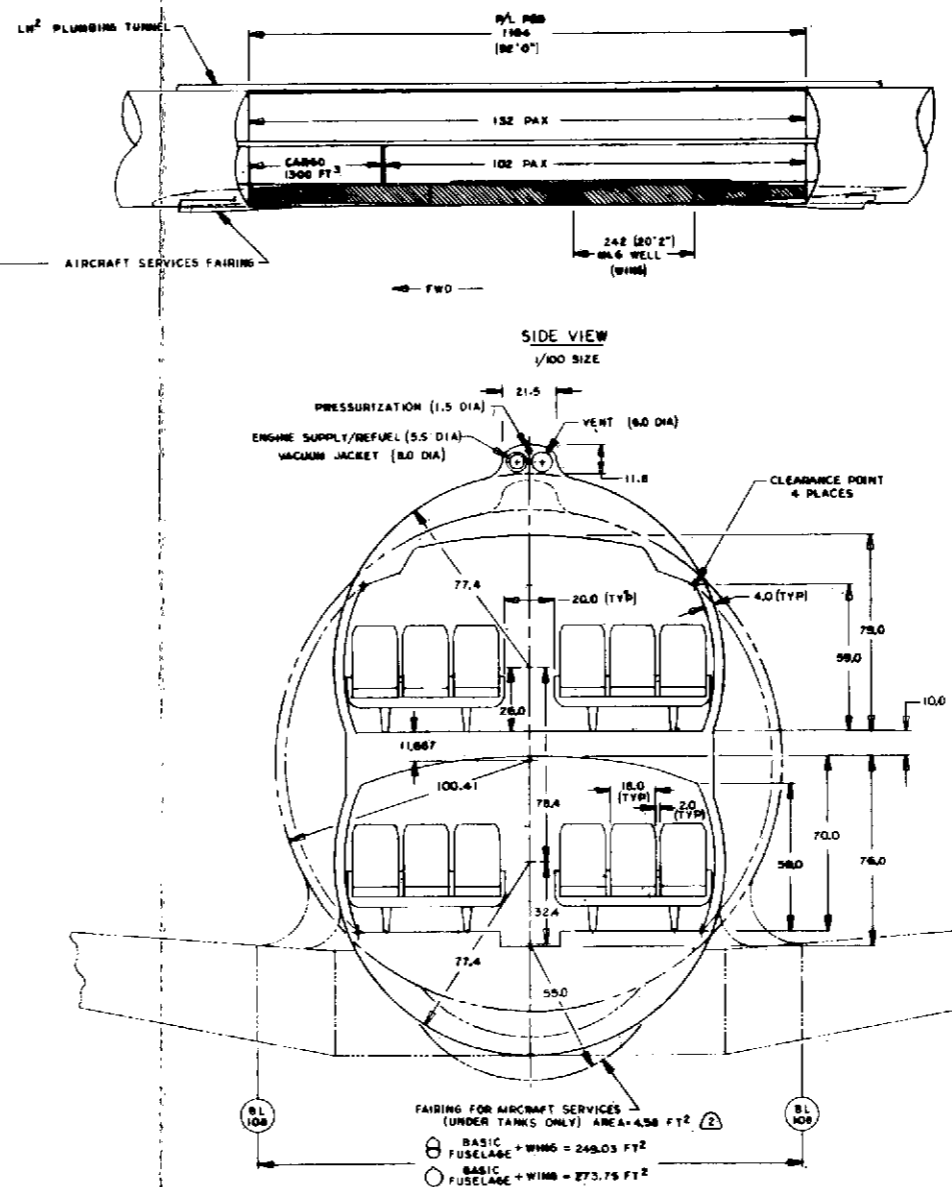
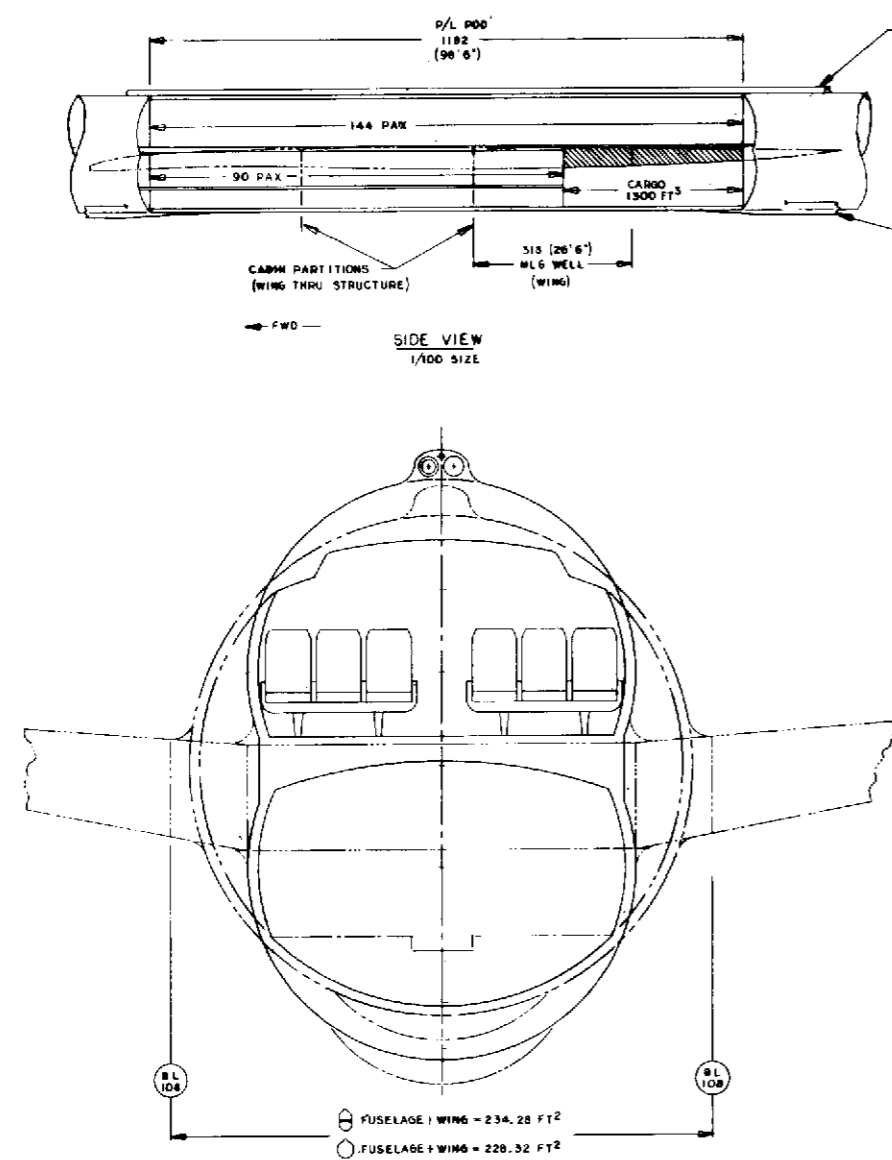
Establishment of the basic arrangement allowed consideration of the most efficient seating arrangement. The trade-off involved was the fuselage cross-section area (number of seats abreast) vs the fuselage total length including crew compartment, tanks and tail cone. Consideration was given to 4, 5, 6, and 7 abreast (on each deck), with 6 abreast being selected as the best compromise between weight, ground rotation requirements, and fuselage wave drag (as influenced by the fineness ratio).

A third design trade-off concerned the choice between a round fuselage vs. a double-lobe, and mid-wing vs low-wing. Figure 59 is a sample layout showing some of the areas and volumes involved in the comparison. The design selected was the double-lobe, low-wing arrangement which gives the best combination of frontal area and compartment length.

Tankage/Thermal Protection System (TPS)

In accordance with the emphasis of the Phase II study, further consideration was given to the tankage and thermal protection system concepts. The minimum criteria for a fuel containment system operating in an air transport environment were assumed to be as follows:

- The use of helium as a purge or pressurant gas is not feasible from the standpoints of logistics, availability, and cost.
- Systems using expendable insulation (such as CO₂ frost) are not practical due to the turn-around time required.
- Safety at least equal to hydrocarbon fuel systems with regard to leakage, fail-safe provisions, and crash loads must be assured.



② AREA NOT INCLUDED IN BASIC FUSELAGE AREA
 1. BASIC FUSELAGE AREA: \ominus = 214.00 FT²
 \bigcirc = 221.71 FT²
NOTE

LOCKHEED	
CL1701-6	CL1701-6-4

Figure 59. Passenger Compartment Arrangements

- Tankage design life = 50,000 hours. Thermal protection system same objective with reasonable maintenance.
- Fail-safe tank structure based on same design consideration as pressurized cabins.
- All components accessible for inspection and repair with minimum manhours.

The candidate possibilities consist of combinations of non-integral and integral tankage, together with both internal and external insulation. Non-integral tankage is required to take only thermal stress, pressurization and fuel dynamic loads, and is supported by the vehicle basic structure. On the other hand, since integral tankage is the vehicle structure (becomes an "integral" part of the basic structure) in addition to the above loads, it must be capable of withstanding all the usual fuselage axial, bending, and shear stresses resulting from the normal aircraft loading conditions. In addition, it requires an interconnect system to transfer loads from the adjacent hot fuselage structure to the tank with a minimum or acceptable heat leak.

Figure 60 is a sketch of the non-integral tank concept with external insulation. The detail shown is a section of the upper forward fuselage tank. Also shown is the tank mounting schematic. To inspect or repair the basic vehicle structure or the insulation, the vehicle must be separated and the tank removed by sliding it out on the removal rail. To prevent cryo-pumping, the insulation must be closed cell as shown or be enclosed in a vapor barrier.

Figure 61 illustrates two integral tank concepts, one for 1981 technology and the other a later, or postulated "198X" technology, dependent on the development items listed in the notes.

To permit a comparison of the various concepts, preliminary estimates were made of the installed fuel weight fractions (kg/kg of LH_2) and are shown in Table 14 together with comments on the component accessibility and technology required. The 198X is included only as an example of the potential gains that might be possible with advanced technology.

Preceding page blank

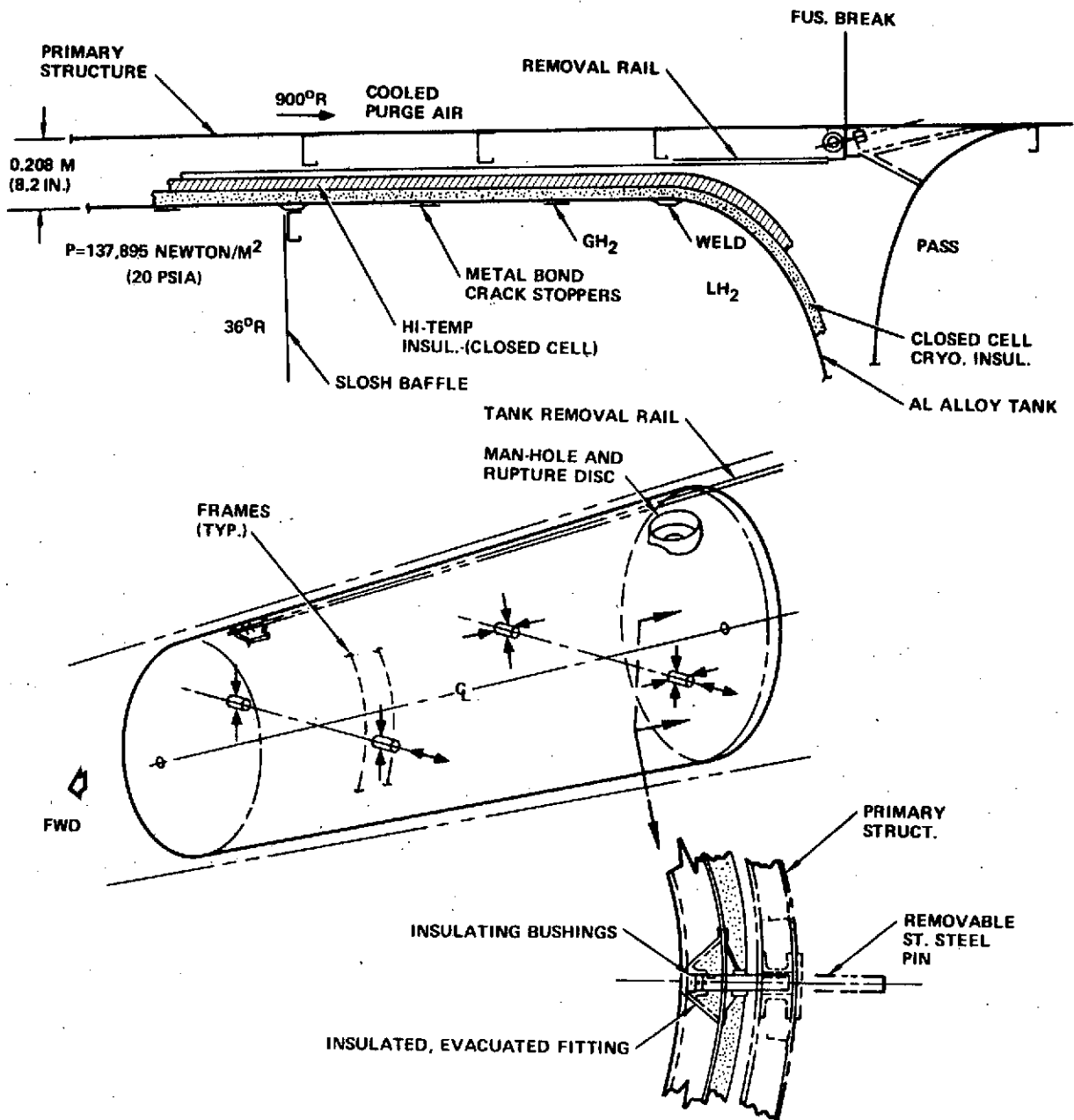


Figure 60. 1975 Technology - Non-Integral Tank Concept

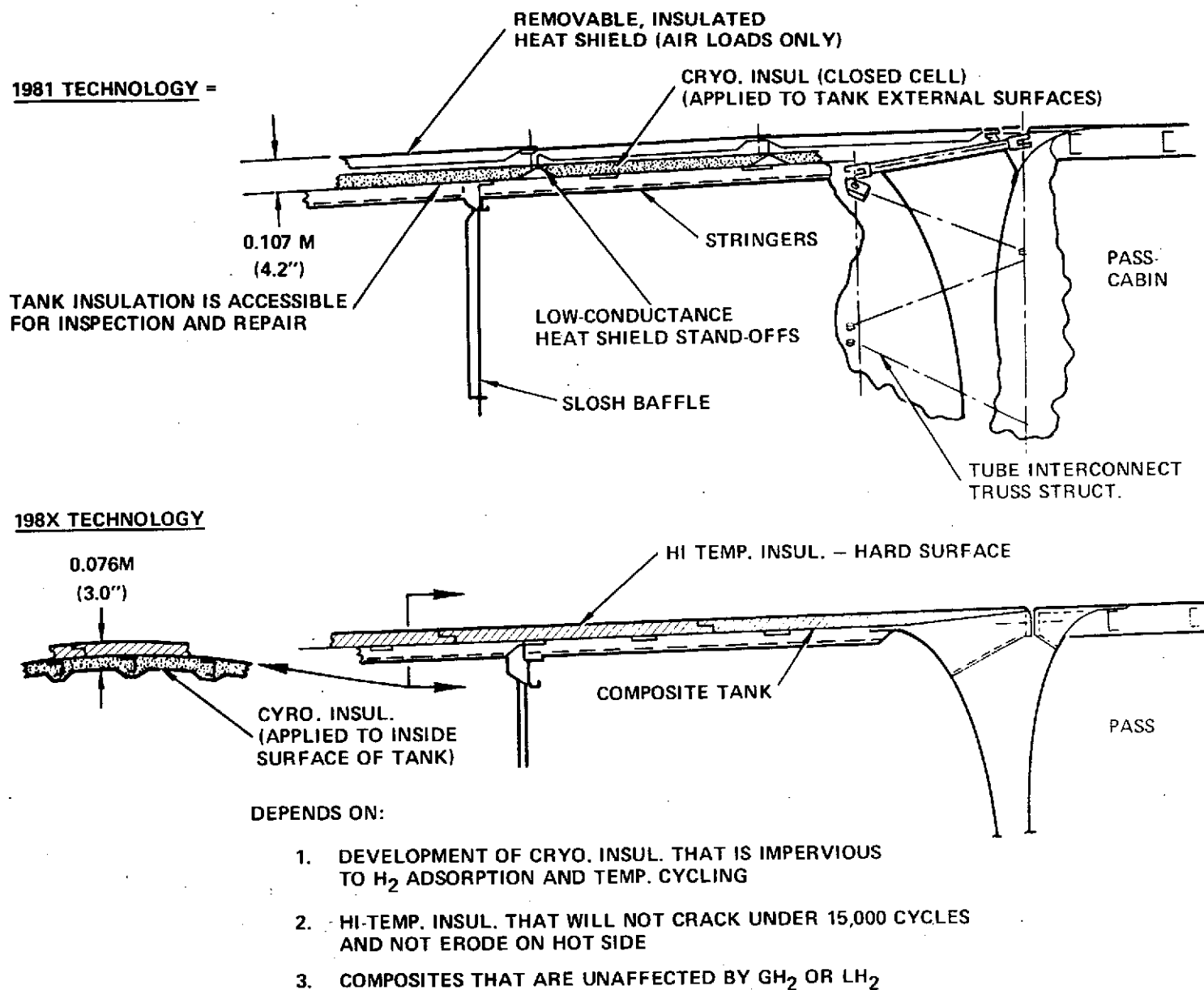


Figure 61. Integral Tank Concepts

TABLE 14
TANKAGE/THERMAL PROTECTION CONCEPT COMPARISON

Tank Design	Concept		
	Non-Integral	Integral	
Technology Level	1975	1981	198X
Fuel Wt Fraction: (kg/kg of LH ₂)			
Tank	0.146	0.17	0.135
TPS	0.11	0.11	0.125
Heat Shield	0	0.06	0
Fuselage Struct	<u>0.152</u>	<u>0</u>	<u>0</u>
Total	0.408	0.340	0.260
Volumetric Efficiency	0.855	0.927	0.936
Est TOGW* ~ kg	158,757	151,408	149,503
(1b)	<u>(350,000)</u>	<u>(333,800)</u>	<u>(329,600)</u>
Mission Fuel ~ kg	32,885	31,842	30,935
(1b)	(72,500)	(70,200)	(68,200)
Inspection/Repair	Remove Tank	Remove Heat Shield	Remove Heat Shield

*Does not include volume effects on drag.

Consideration of this and the thermodynamic preliminary analysis resulted in the choice of the integral, 1981 technology concept as the baseline for Phase II - and allowed a more detailed analysis which is reported in sections 4.4 and 4.5.

Heat Shield Design

The integral tank concept selected for Phase II requires the use of an outer cover or heat shield with the following design requirements:

- Must be readily removable for inspection of the insulation and for repair of the tank.

- Compatible with the vehicle exterior thermal and acoustic environment
- Mounting scheme - must accommodate tank shrinkage and heat shield expansion.
- Must be flutter free with differential air loads up to approximately 1 psig.
- Shall preferably have low heat transfer characteristics to allow a possible reduction in the tank insulation thickness.
- The heat shield standoffs or supports shall have a low conductance to minimize heat leak to the tank.
- Must be compatible with gaseous hydrogen (leakage)

Various schemes used in past Lockheed studies were reviewed for applicability but while the concepts were suitable they were mostly for hypersonic vehicles so the materials were costly and weights excessive. Using the above requirements and background, the concept described in paragraph 4.4.2.2 (see Fig. 113, Structural Arrangement - sht 2) was chosen. The outer panels are of honeycomb construction consisting of a fiberglass/polyimide core with graphite/kevlar polyimide faces, selected for strength/weight, thermal compatibility, low heat conductance, and low cost.

The 0.019m (3/4 in.) thick panels are approximately 1.524m x 1.524m (60 in. x 60 in.), constrained at the edges but free to expand. A center support is used as a fixed support and also locates the panel. Silicone rubber seals are provided at all panel joints as back-up to the edge retainer strips. The retainer strips are held by shoulder bolts to prevent excessive clamping pressure. The circumferential edges of the panels rest against KEL-F combination insulator-wear strips. The panels are supported by circumferential heat shield stand-offs of low conductance reinforced fiberglass rings held by aluminum clips weld-bonded to the tank wall. Slip joints are provided where required between the support clips. Removal of any panel is possible without disturbing an adjacent panel.

4.1.3 Vehicle Description

General Arrangement

The general arrangement of the liquid hydrogen fueled (LH_2) AST Phase II Point Design Vehicle is presented in Figure 62.

For comparison, the Jet A-1 fueled M2.7 Arrow Wing Configuration developed by Lockheed under NASA contract NAS 1-12288 (Reference 4), which is used as a baseline for comparison in the present study, is shown in Figure 63. Comparison of the two configurations shows that the LH_2 fueled aircraft has a considerably smaller wing. However, its fuselage is both longer and has increased cross sectional area.

The arrow wing of the CL1701-7-1 Phase II Point Design (Figure 62) is scaled down from the CL1606-4 Jet A-1 AST (Figure 63) arrow wing to reflect the lower aircraft weight of the LH_2 fueled airplane. In sizing the wing a wing loading of approximately 200.2 kg/m^2 (41 lbs/sq ft) at the design landing weight is used for both aircraft to provide equivalent landing performance. The thin, flexible, highly swept and cambered wing is continuous under the fuselage except at the forward apex of the wing.

Flight control and high lift devices for the CL1701-7-1, as shown in Figure 62, are similar to those for the CL1606-4-1 aircraft in Figure 63. Pitch control is obtained from an all-moving horizontal stabilizer with a geared elevator while yaw control is provided by a fuselage-mounted all-moving vertical tail with a geared rudder. A fixed vertical fin is located on each side of the wing. The outer wing includes ailerons for roll control at low speeds and Krueger leading edge flaps for use at subsonic and transonic speeds. Plain spoilers next to the fuselage are used for deceleration on the ground. The Fowler inboard trailing edge flaps increase lift at low speeds while flaperons function, dependent on speed, as either high lift or roll control devices.

Wing-mounted main landing gears retract forward into the wing just outboard of the fuselage. Four duct burning turbofan engines, each with 204,650 newtons (46,000 pounds) of uninstalled thrust, are mounted in underwing pods having axisymmetric inlets and thrust reversers near the wing trailing edge.

④ EXPOSED AREA
③ DATA RELATIVE TO ZRP
2. LINEAR DIMS. IN METERS (INCHES)
ANGLES IN RADIANS (DEGREES)
1. DIMS IN SI (ENGLISH) UNITS
NOTE -

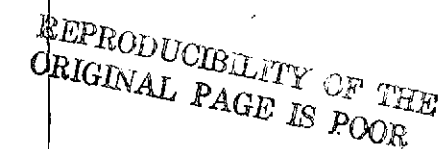


POWER PLANT- DUCT BURNING TURBOFAN
UNINSTALLED THRUST- 204,648 NEWTONS (46,007 LBS) SLS
TA XI MASS - 166,946 KILOGRAMS (368,054 LBS)



FOLDOUT FRAME

REPRODUCIBILITY OF THE
ORIGINAL PAGE IS POOR



FOLDOUR FRANK

POWER PLANT - DUCT BURNING TURBOFAN
UNINSTALLED THRUST- 397,964 NEWTONS, (89,466 LBS) SLS
TAXI MASS - 340,000 KILOGRAMS (750,000 LBS)

	WING (5)	HORIZ. TAIL (4)	FUS. VERT. TAIL (5)	WING VERT. TAIL (EACH) (5)
AREA - M ² (FT ²)	1014.69 (10,923)	73.868 (795)	30.190 (325.4)	21.65 (233)
ASPECT RATIO	1.607	1.707	0.517	0.495
TAPER RATIO	0.1135	0.225	0.230	0.136
SPAN - M (IN)	40.386 (1590)	11.217 (441.6)	3.941 (155.55)	3.277 (1290)
ROOT CHORD - M (IN)	55.766 (2195.5)	10.739 (422.8)	12.426 (489.22)	11.643 (458.4)
TIP CHORD - M (IN)	6.330 (249.192)	2.416 (95.1)	2.858 (112.521)	1.585 (62.4)
MAC - M (IN)	34.317 (1351.067)	7.455 (293.5)	8.640 (340.174)	7.889 (310.6)
L.E. SWEEP	1.292 (74°)	1.058 (60.64°)	-1.190 (68.2°)	1.281 (73.42°)
RADIANS (DEGREES)	1.236 (70.84°)			
	1.047 (60.00°)			
DIHEDRAL, RELATIVE TO Z PLANE		-1.745 (-40°)		

1. DIMENSIONS IN SI (ENGLISH) UNITS
NOTE:

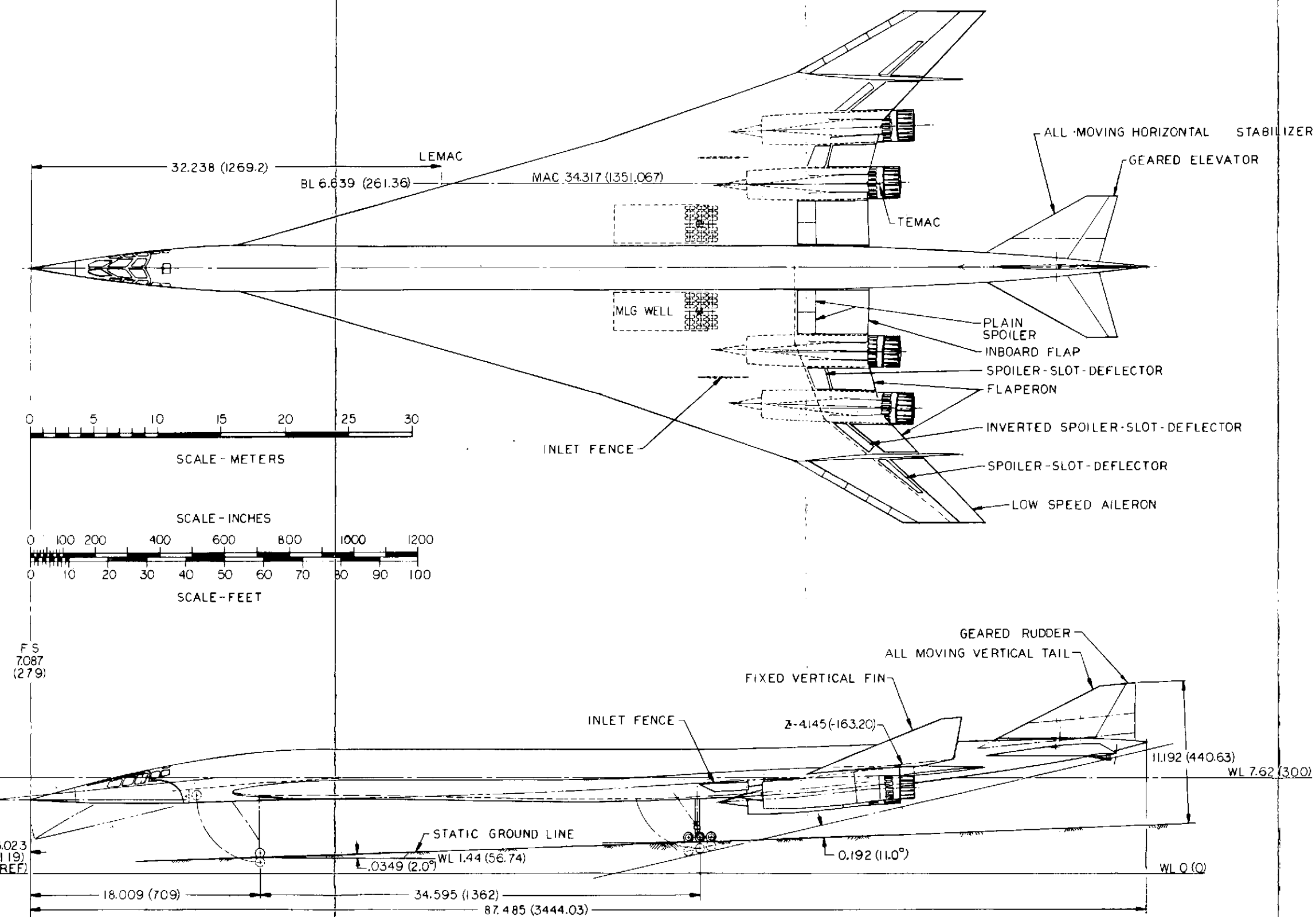
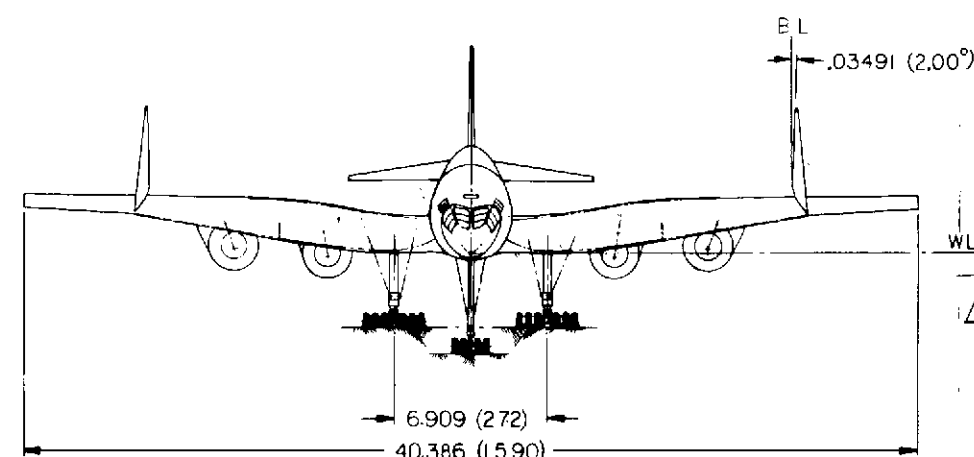


Figure 63. General Arrangement - Jey A-1 AST

[illegible]

Preceding page blank

PRECEDING PAGE BLANK NOT FILMED

REPRODUCIBILITY OF THE
ORIGINAL PAGE IS POOR.

FOLDOUT FRONT *140*

The fuselage of the CL1701-7 aircraft has a deep, double lobe cross section. Its length requires the aft end to be swept up slightly to obtain the scrape angle adequate for the desired takeoff and landing performance. The static ground angle, scrape angle, and wing incidence shown for the CL1701-7 in Figure 62 are identical to the corresponding values for the CL1606-4 in Figure 63.

A convenient tabular summary comparing major dimensional, weight and other data for the CL1701-7 and the Jet A-1 fueled CL1606-4 is given in Section 5.1.

Inboard Profile

The interior arrangement of the Phase II Point Design, as shown in Figure 64, illustrates the passenger seating arrangement and the location of the liquid hydrogen fuel tanks.

The large portion of fuselage volume devoted to LH_2 stowage is readily apparent. In contrast to the Jet A-1 fueled CL1606-4 aircraft of Figure 63, no fuel is carried in the wing of the Phase II Point Design. Instead, all LH_2 fuel is stowed in four large fuselage tanks arranged so that two are forward, and two are aft, of a central payload section. Balance and c.g. management are facilitated by the location of fuel both forward and aft of the aircraft c.g. Use of fuselage stowage for fuel also provides an efficient ratio of tank volume to tank surface area and minimizes the fuel plumbing and tank insulation required. In addition, the integral tank structure also serves as the fuselage primary structure. Both the forward and aft fuel tank sections are shown, in Figure 64, as being divided into two separate tanks by means of a vertical divider. This divider is not a pressure bulkhead since provision is made for pressure equalization between the two compartments of each tank. It simply serves to provide fuel to each engine from a separate compartment.

With the payload in close proximity to the aircraft c.g., minimum c.g. movement results when the passenger and/or cargo load is varied. Passengers are seated six abreast on both levels of a double deck arrangement. This not only provides spacious accommodations but also minimizes the length of the payload section. Figure 65 shows the interior arrangement and passenger seating of the CL1606-4 Jet A-1 fueled aircraft.

Preceding page blank

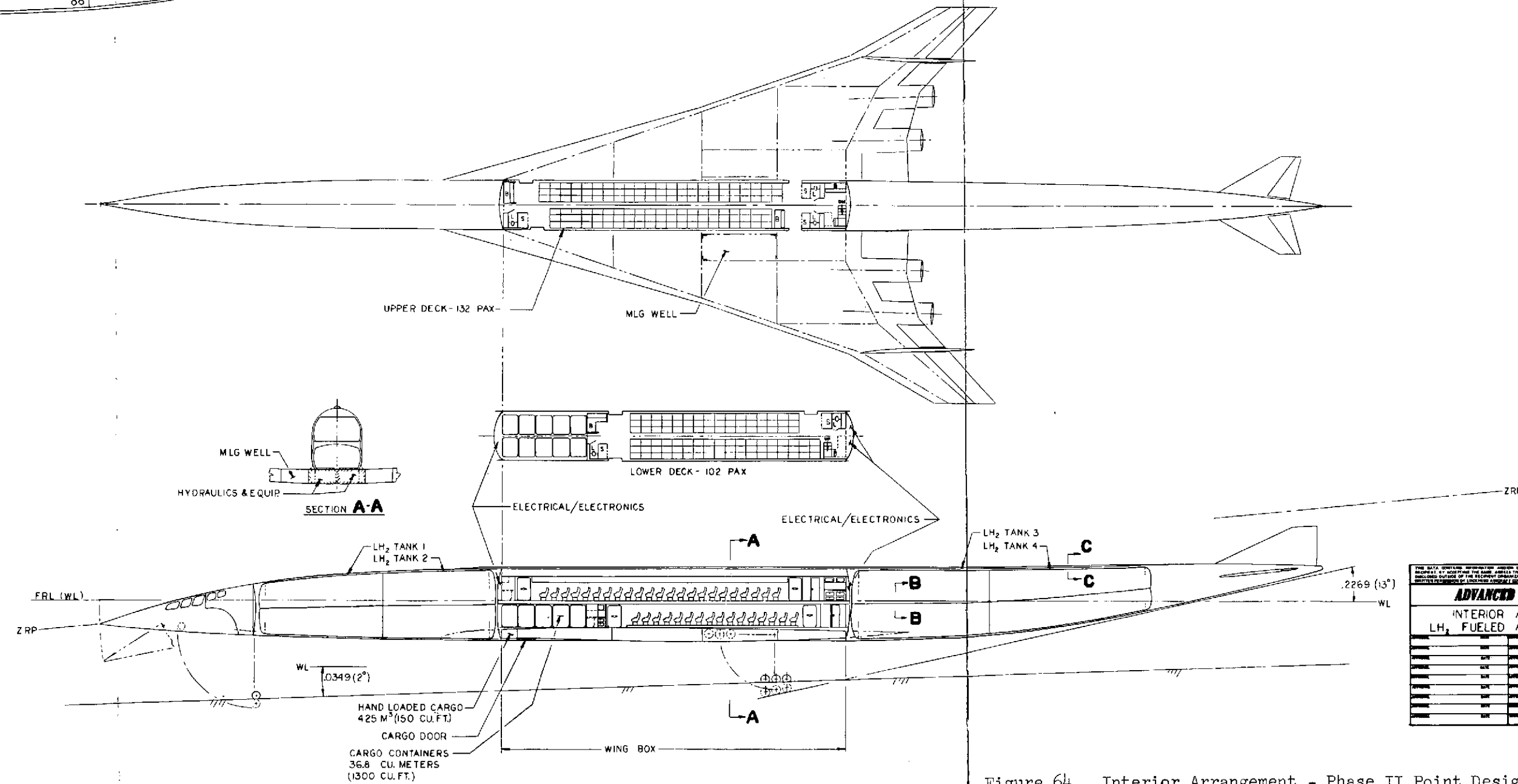
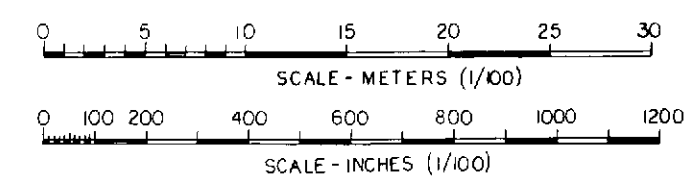
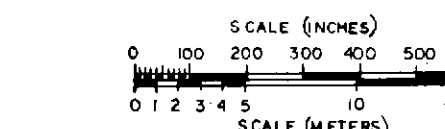
[illegible]

Figure 64. Interior Arrangement - Phase II Point Design Aircraft



<p>THIS PAGE CONTAINS INFORMATION OF A CONFIDENTIAL NATURE. IT IS THE PROPERTY OF LOCKHEED MISSILES & SPACE COMPANY, INC. IT IS TO BE CONTAINED AND CONTROLLED BY THE ADDRESSEE OF THIS MESSAGE. IT IS NOT TO BE REPRODUCED, COPIED, OR DISCLOSED TO OTHERS WITHOUT THE WRITTEN PERMISSION OF THE LOCKHEED MISSILES & SPACE COMPANY.</p>		<p>LOCKHEED MISSILE NO. CL1606-4</p>	
<p>ADVANCED DESIGN</p>		<p>LOCKHEED - CALIFORNIA</p>	
<p>INTERIOR ARRANGEMENT -</p>		<p>ROCKAWAY, CALIF.</p>	
<p>ARROW WING CONFIGURATION - TASK II</p>		<p>CODE 0011 IN TASK</p>	
<p>1. TITLE</p>	<p>2. DATE</p>	<p>3. PROJECT</p>	<p>4. DRAWING</p>
<p>5. REVISION</p>	<p>6. DATE</p>	<p>7. PROJECT</p>	<p>8. DRAWING</p>
<p>9. REVISION</p>	<p>10. DATE</p>	<p>11. PROJECT</p>	<p>12. DRAWING</p>
<p>13. REVISION</p>	<p>14. DATE</p>	<p>15. PROJECT</p>	<p>16. DRAWING</p>
<p>17. REVISION</p>	<p>18. DATE</p>	<p>19. PROJECT</p>	<p>20. DRAWING</p>
<p>21. REVISION</p>	<p>22. DATE</p>	<p>23. PROJECT</p>	<p>24. DRAWING</p>
<p>25. REVISION</p>	<p>26. DATE</p>	<p>27. PROJECT</p>	<p>28. DRAWING</p>
<p>29. REVISION</p>	<p>30. DATE</p>	<p>31. PROJECT</p>	<p>32. DRAWING</p>
<p>33. REVISION</p>	<p>34. DATE</p>	<p>35. PROJECT</p>	<p>36. DRAWING</p>
<p>37. REVISION</p>	<p>38. DATE</p>	<p>39. PROJECT</p>	<p>40. DRAWING</p>
<p>41. REVISION</p>	<p>42. DATE</p>	<p>43. PROJECT</p>	<p>44. DRAWING</p>
<p>45. REVISION</p>	<p>46. DATE</p>	<p>47. PROJECT</p>	<p>48. DRAWING</p>
<p>49. REVISION</p>	<p>50. DATE</p>	<p>51. PROJECT</p>	<p>52. DRAWING</p>
<p>53. REVISION</p>	<p>54. DATE</p>	<p>55. PROJECT</p>	<p>56. DRAWING</p>
<p>57. REVISION</p>	<p>58. DATE</p>	<p>59. PROJECT</p>	<p>60. DRAWING</p>
<p>61. REVISION</p>	<p>62. DATE</p>	<p>63. PROJECT</p>	<p>64. DRAWING</p>
<p>65. REVISION</p>	<p>66. DATE</p>	<p>67. PROJECT</p>	<p>68. DRAWING</p>
<p>69. REVISION</p>	<p>70. DATE</p>	<p>71. PROJECT</p>	<p>72. DRAWING</p>
<p>73. REVISION</p>	<p>74. DATE</p>	<p>75. PROJECT</p>	<p>76. DRAWING</p>
<p>77. REVISION</p>	<p>78. DATE</p>	<p>79. PROJECT</p>	<p>80. DRAWING</p>
<p>81. REVISION</p>	<p>82. DATE</p>	<p>83. PROJECT</p>	<p>84. DRAWING</p>
<p>85. REVISION</p>	<p>86. DATE</p>	<p>87. PROJECT</p>	<p>88. DRAWING</p>
<p>89. REVISION</p>	<p>90. DATE</p>	<p>91. PROJECT</p>	<p>92. DRAWING</p>
<p>93. REVISION</p>	<p>94. DATE</p>	<p>95. PROJECT</p>	<p>96. DRAWING</p>
<p>97. REVISION</p>	<p>98. DATE</p>	<p>99. PROJECT</p>	<p>100. DRAWING</p>
<p>101. REVISION</p>	<p>102. DATE</p>	<p>103. PROJECT</p>	<p>104. DRAWING</p>
<p>105. REVISION</p>	<p>106. DATE</p>	<p>107. PROJECT</p>	<p>108. DRAWING</p>
<p>109. REVISION</p>	<p>110. DATE</p>	<p>111. PROJECT</p>	<p>112. DRAWING</p>
<p>113. REVISION</p>	<p>114. DATE</p>	<p>115. PROJECT</p>	<p>116. DRAWING</p>
<p>117. REVISION</p>	<p>118. DATE</p>	<p>119. PROJECT</p>	<p>120. DRAWING</p>
<p>121. REVISION</p>	<p>122. DATE</p>	<p>123. PROJECT</p>	<p>124. DRAWING</p>
<p>125. REVISION</p>	<p>126. DATE</p>	<p>127. PROJECT</p>	<p>128. DRAWING</p>
<p>129. REVISION</p>	<p>130. DATE</p>	<p>131. PROJECT</p>	<p>132. DRAWING</p>
<p>133. REVISION</p>	<p>134. DATE</p>	<p>135. PROJECT</p>	<p>136. DRAWING</p>
<p>137. REVISION</p>	<p>138. DATE</p>	<p>139. PROJECT</p>	<p>140. DRAWING</p>
<p>141. REVISION</p>	<p>142. DATE</p>	<p>143. PROJECT</p>	<p>144. DRAWING</p>
<p>145. REVISION</p>	<p>146. DATE</p>	<p>147. PROJECT</p>	<p>148. DRAWING</p>
<p>149. REVISION</p>	<p>150. DATE</p>	<p>151. PROJECT</p>	<p>152. DRAWING</p>
<p>153. REVISION</p>	<p>154. DATE</p>	<p>155. PROJECT</p>	<p>156. DRAWING</p>
<p>157. REVISION</p>	<p>158. DATE</p>	<p>159. PROJECT</p>	<p>160. DRAWING</p>
<p>161. REVISION</p>	<p>162. DATE</p>	<p>163. PROJECT</p>	<p>164. DRAWING</p>
<p>165. REVISION</p>	<p>166. DATE</p>	<p>167. PROJECT</p>	<p>168. DRAWING</p>
<p>169. REVISION</p>	<p>170. DATE</p>	<p>171. PROJECT</p>	<p>172. DRAWING</p>
<p>173. REVISION</p>	<p>174. DATE</p>	<p>175. PROJECT</p>	<p>176. DRAWING</p>
<p>177. REVISION</p>	<p>178. DATE</p>	<p>179. PROJECT</p>	<p>180. DRAWING</p>
<p>181. REVISION</p>	<p>182. DATE</p>	<p>183. PROJECT</p>	<p>184. DRAWING</p>
<p>185. REVISION</p>	<p>186. DATE</p>	<p>187. PROJECT</p>	<p>188. DRAWING</p>
<p>189. REVISION</p>	<p>190. DATE</p>	<p>191. PROJECT</p>	<p>192. DRAWING</p>

Figure 65. Interior Arrangement - Jet A-1 AST



~~PRECEDING PAGE BLANK NOT FILMED~~

FOLDOUT FRAMES

FOLDOUT FRAM

•

Cargo is stowed at the forward end of the lower deck so that the cutout for container installation/removal results in cutting only the relatively lightly loaded spar caps at the wing apex. Some of the electrical/electronic equipment is carried in the domed cavities in the pressure bulkheads at each end of the cabin in both decks to provide both good accessibility and a controlled environment. The space below the floor and between the MLG wells is used for aircraft equipment and service centers. Components large enough to require cutting spar caps to obtain sufficient space can be accommodated with relatively low penalty since the spar cap loads are not high in this area.

Throughout the length of the payload section, fuel supply and vent lines are contained in a dorsal fairing above the fuselage so that any fuel vapors accidentally released will tend to rise away from the aircraft and minimize damage possibilities. Pressure bulkheads domed in opposite directions are shown in Figure 64 at the fuel tank/cabin interface joints. As described in a subsequent section, a truss type interstage structure provides the connection. In an alternate design which also should be considered, the end bulkheads would be domed in a nested, rather than opposed, manner. This approach would result in a shortened fuselage.

Landing Gear Installation

Figure 66 depicts the main landing gear (MLG) design used in the Phase II Point Design aircraft. As shown, the MLG is wing mounted and retracts forward into a well entirely within the wing. The preliminary study in Figure 66 indicates that the MLG can be stowed within the existing wing contour if a small local bump in the upper surface is provided above the joint between the upper and lower scissors. It is felt that further design and development should permit the elimination of this small bump and thereby avoid complexity in the upper surface structure as well as a small potential increase in drag.

The MLG design is very nearly identical to that used in the CL1606-4 aircraft of Figure 63. The major difference is that 12 wheels per strut are used instead of the special 18 wheel per strut MLG designed for the Jet A-1 CL1606-4. The 18 wheel per strut design in the CL1606-4 was necessary to avoid wing

Preceding page blank

thickening or bumps in the wing upper surface of the CL1606-4. In the Phase II Point Design, the greatly reduced aircraft weight permits the use of a more conventional 12 wheel per strut arrangement.

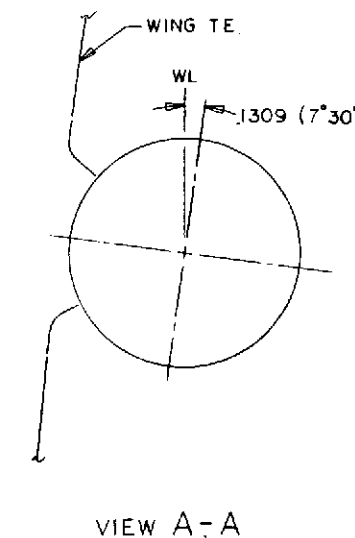
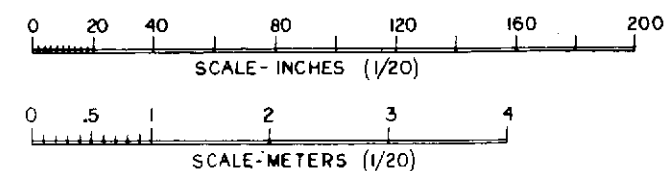
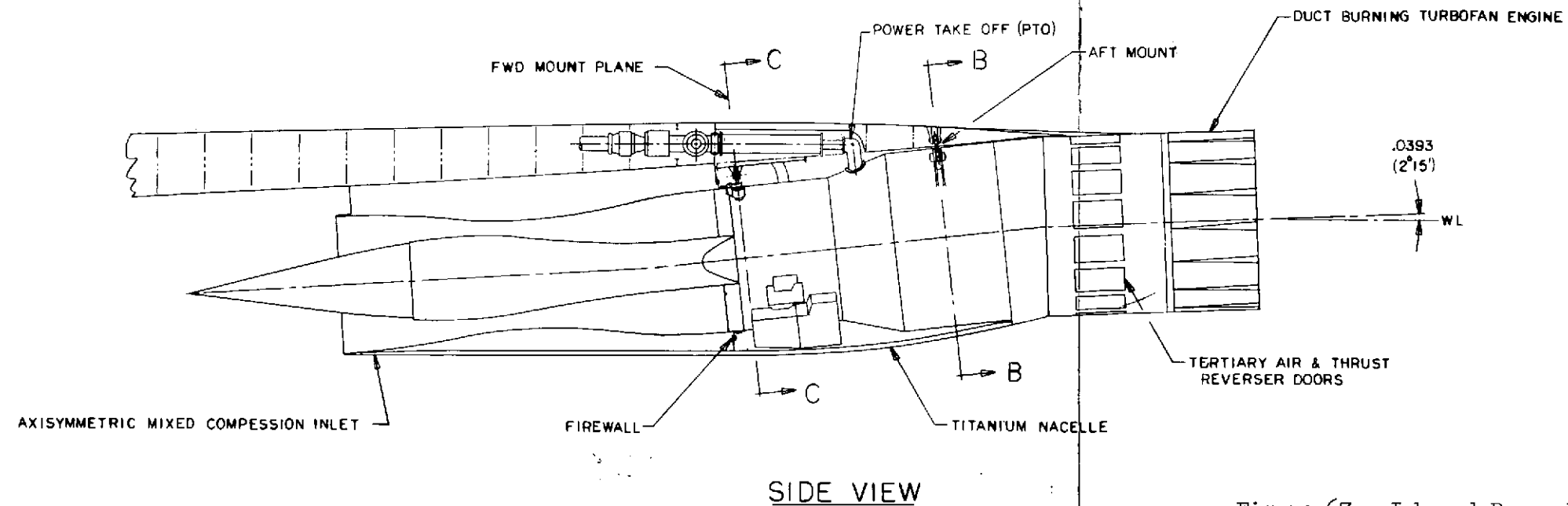
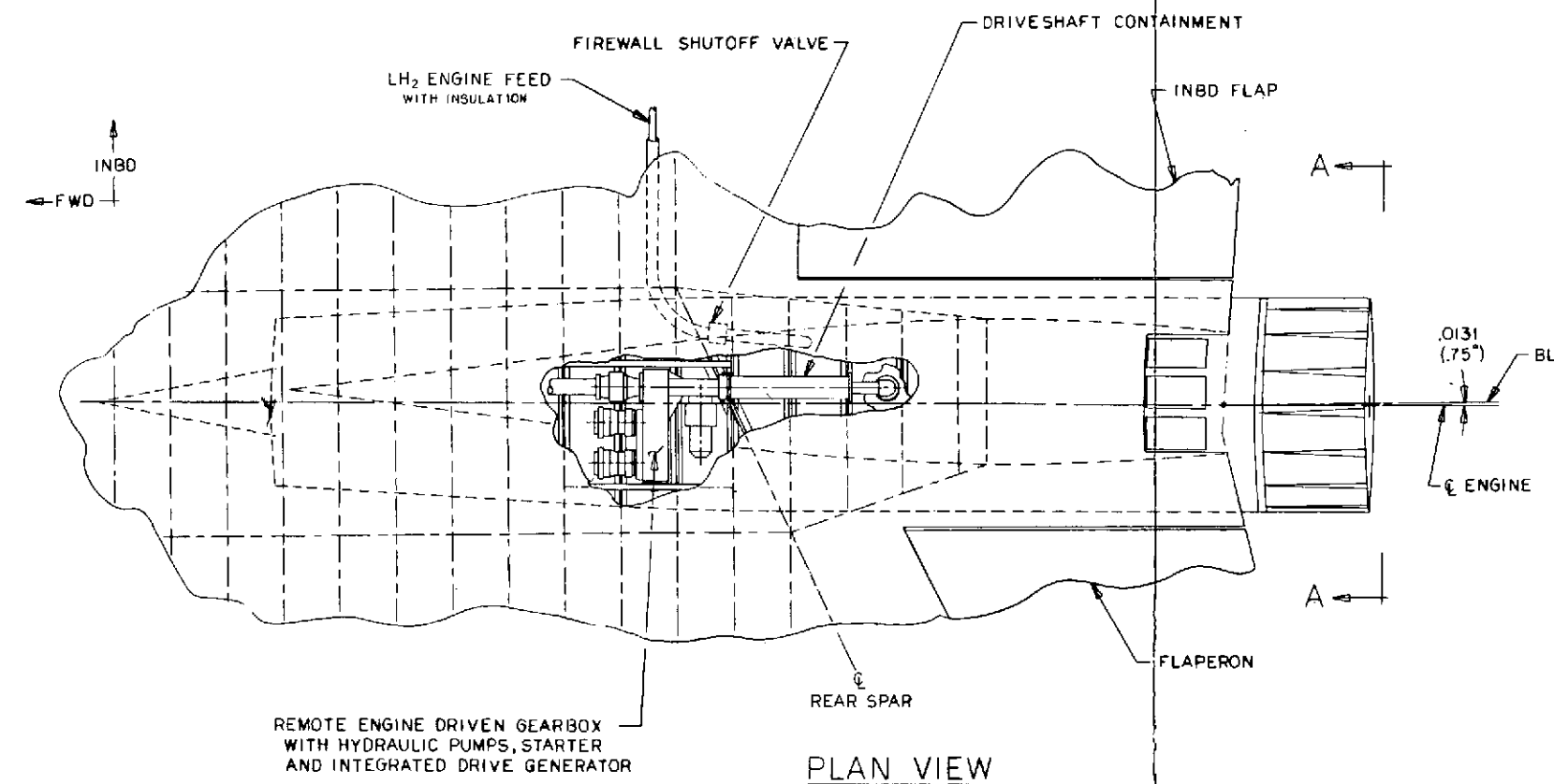
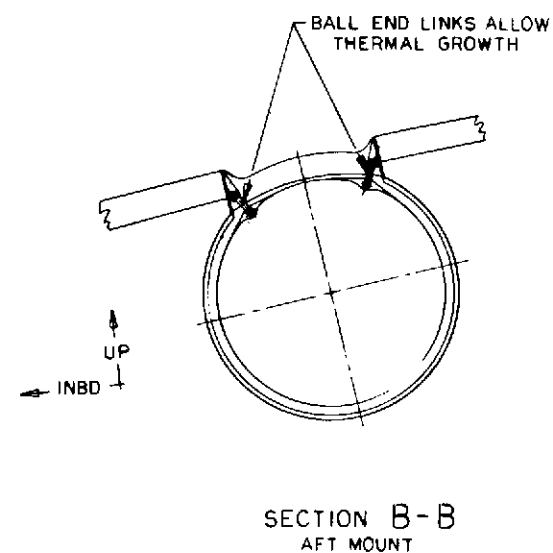
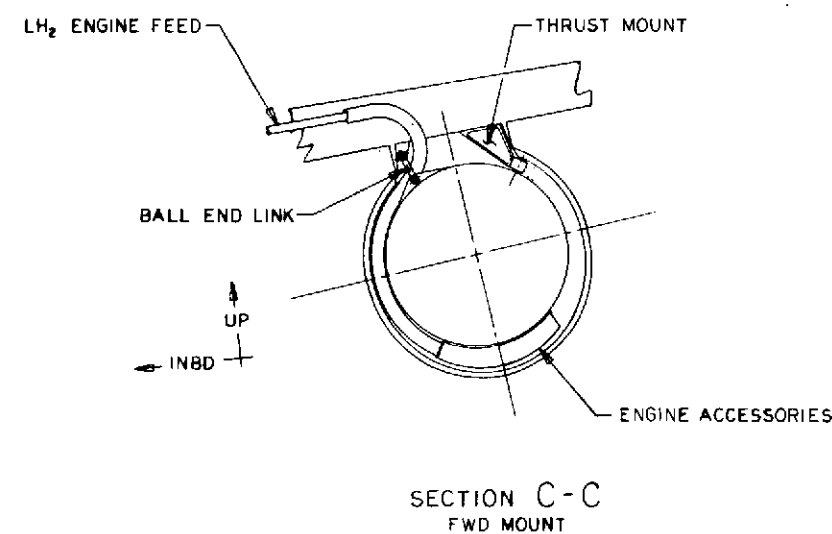
The nose landing gear (NLG) of the Phase II Point Design is mounted slightly forward of the forward LH₂ tank and retracts forward to provide a free-fall extension capability. As shown in the interior arrangement of Figure 64, the weather vision nose must be configured so that its operation is compatible with the movement of the NLG.

An evaluation of tip-over potential should be made during any further design development. It is possible that such an investigation may show the need to move the MLG farther outboard. Tip-over considerations may be expected to be more severe in the Phase II Point Design, in relation to the Jet A-1 fueled CL1606-4, because the aircraft's vertical c.g. tends to be higher above the ground.

In the Jet A-1 fueled CL1606-4, a design objective is the stowage of the maximum portion of fuel in the thermally protected wing center section to make the maximum use of the fuel as a heat sink. This is one of the factors tending to favor a forward retracting MLG in the CL1606-4. In the Phase II Point Design, the MLG design is not so constrained (since no fuel is carried in the wing) and other MLG designs, such as inboard retracting types, could be considered. After review of a variety of MLG designs, however, the forward retracting MLG shown in Figure 66 has been selected as a good representative arrangement.

Propulsion Installation

The inboard engine installation for the CL1701-7 Phase II Point Design, Figure 67, closely follows the corresponding design for the Jet A-1 fueled CL1606-4. Each engine is installed in an underwing pod and uses an axisymmetric mixed compression inlet. Thrust reverser doors are located near the trailing edge. Each pod is located at the same percentage of the wing span as in the CL1606-4 aircraft. In the fore and aft direction, the pods are shown approximately in the same relative position as in the CL1606-4. Since the longitudinal position of the engines relates to wave drag, wing flutter



ADVANCED DESIGN		DESIGN NO. CL1701-7
POWER PLANT INSTAL-		
INBOARD-LH ₂ FUELED AST-POINT DESIGN		
DATE	1-15-74	LOCKHEED - CALIFORNIA CO.
BY	CL1701-7-4	BURBANK, CALIFORNIA
CHECKED		CODE IDENT. 00000
APPROVED		
DATE	1-20-74	LOCKHEED AIRCRAFT CORPORATION
BY		CL1701-7-4
CHECKED		1 OF 1

Figure 67. Inboard Power Plant Installation -
LH₂ Fueled AST

Preceding page blank

PRECEDING PAGE BLANK NOT FILMED

FOLDOUT FRAME 1



FOLDOUT FRAME 2

FOLDOUT FRAME 3

and other considerations, the final longitudinal location of the engines should reflect an evaluation of these factors before determination of the most desirable position. Such an evaluation has been performed for the CL1606-4 aircraft.

A duct burning turbofan engine configured by Calac and providing 204,650 newtons (46,000 pounds) of SLS uninstalled thrust is located in each pod. A four point mounting system is shown, with one point designed to withstand thrust and drag loads. Appropriate damage tolerance capabilities are incorporated in the system, particularly at the thrust/drag mount.

Hydraulic pumps and other aircraft system components are shown mounted on a remote engine driven gearbox installed in the wing box. Also located in that area but not shown on the drawing would be the heat exchanger to convert LH_2 to gaseous form before introduction into the combustion process (see Figure 83). It is anticipated that access to some of these components can be obtained through the rear beam. For others, access doors through the wing surfaces are required. In further design development, additional evaluation is recommended on the feasibility of installing most, or all, of the components in the space behind the rear spar. The very limited space available makes this objective difficult to achieve. Nevertheless, the improved access and reduced structural penalty potentially achievable justify further efforts in this area. Installation of system components in the wing, rather than the engine pod, is based on the desire to minimize the size of the engine pod.

4.1.3.1 Aerodynamic Characteristics

The aerodynamic characteristics for the Phase II "Point Design Vehicle" Figure 62, were developed primarily from the parametric data presented in Section 3.1.2. The pertinent data are collected and presented here for convenience, Figures 68 through 73. Certain of the data, particularly the ground effect increments, have been updated. These changes reflect the results of detailed analyses of AST wind tunnel test data in ground effect. While these changes are relatively significant as compared to the earlier data, they are not expected to have a significant effect on overall mission performance. This is reasonable since airport performance did not impose stringent demands on aircraft sizing in the earlier studies.

Preceding page blank

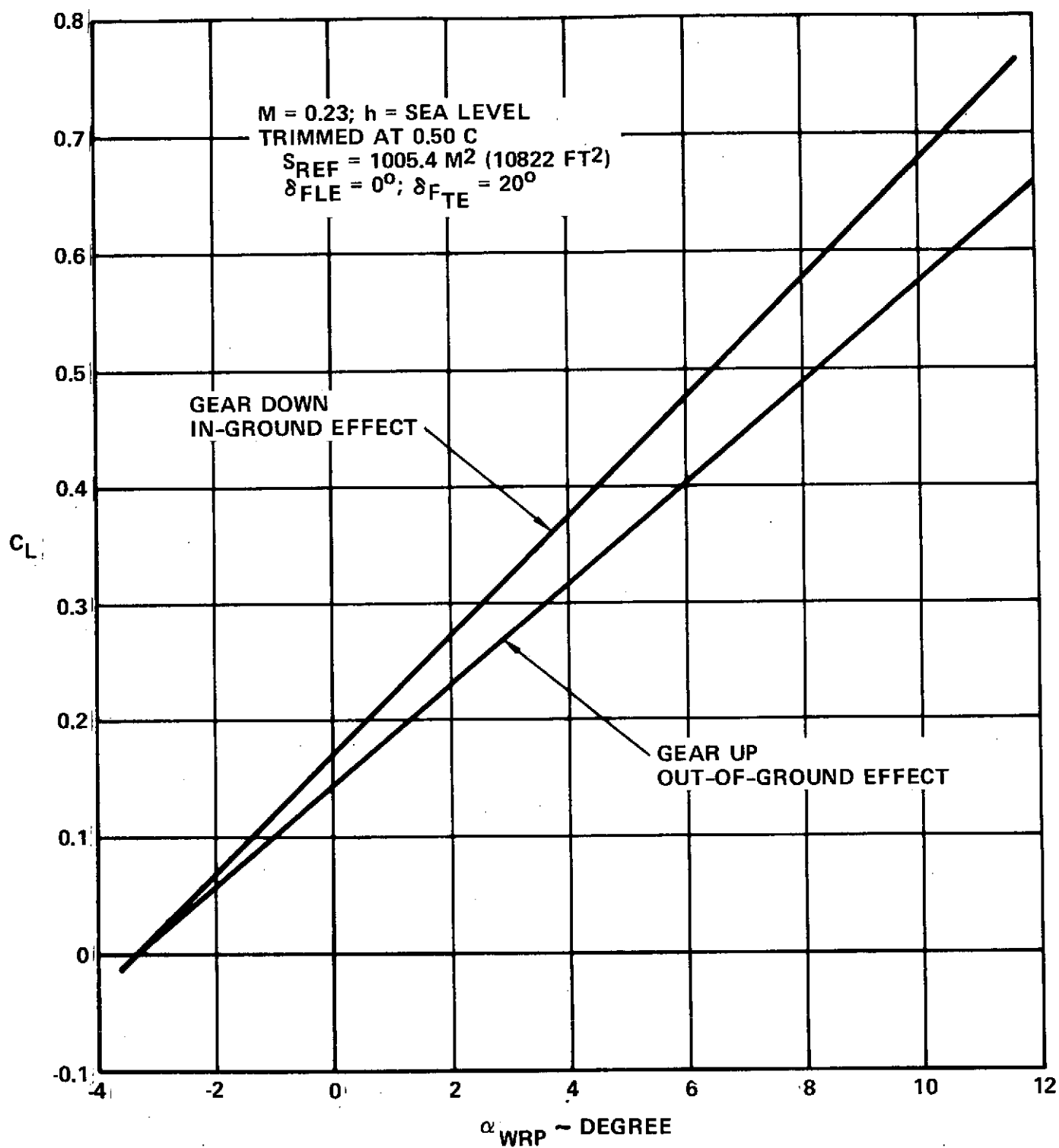


Figure 68. Low Speed Lift Characteristics

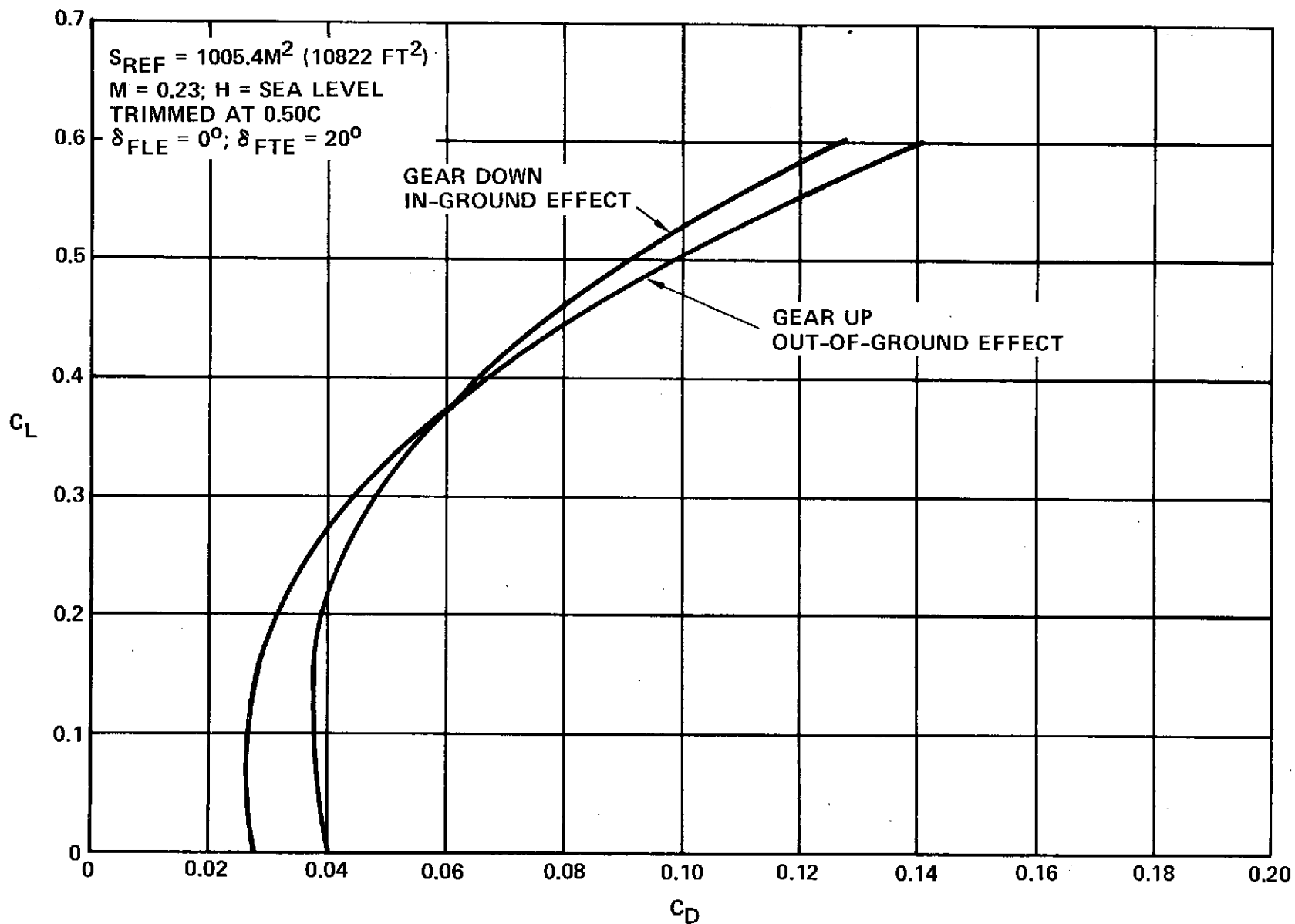


Figure 69. Low Speed Drag Polars

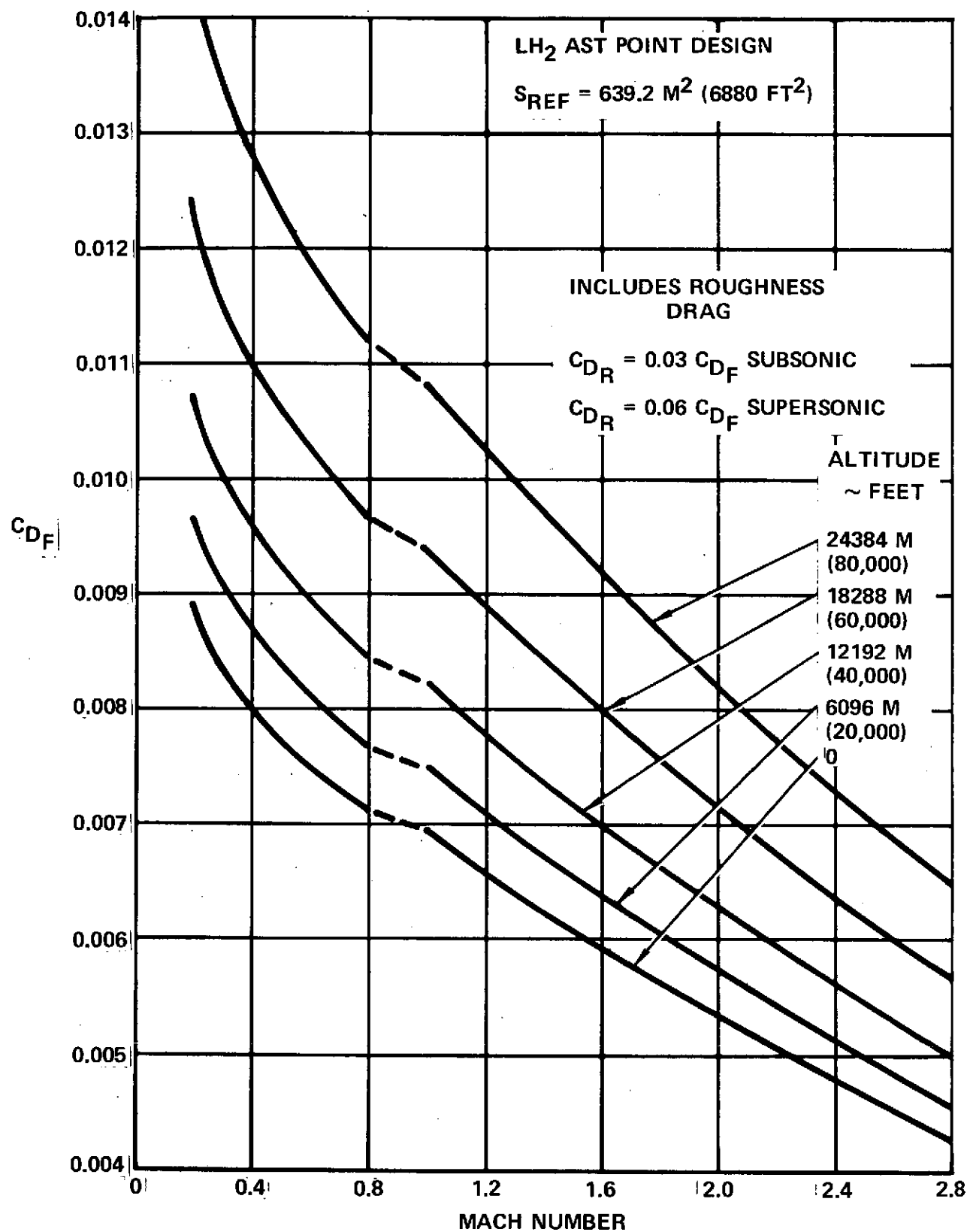


Figure 70. Skin Friction Drag

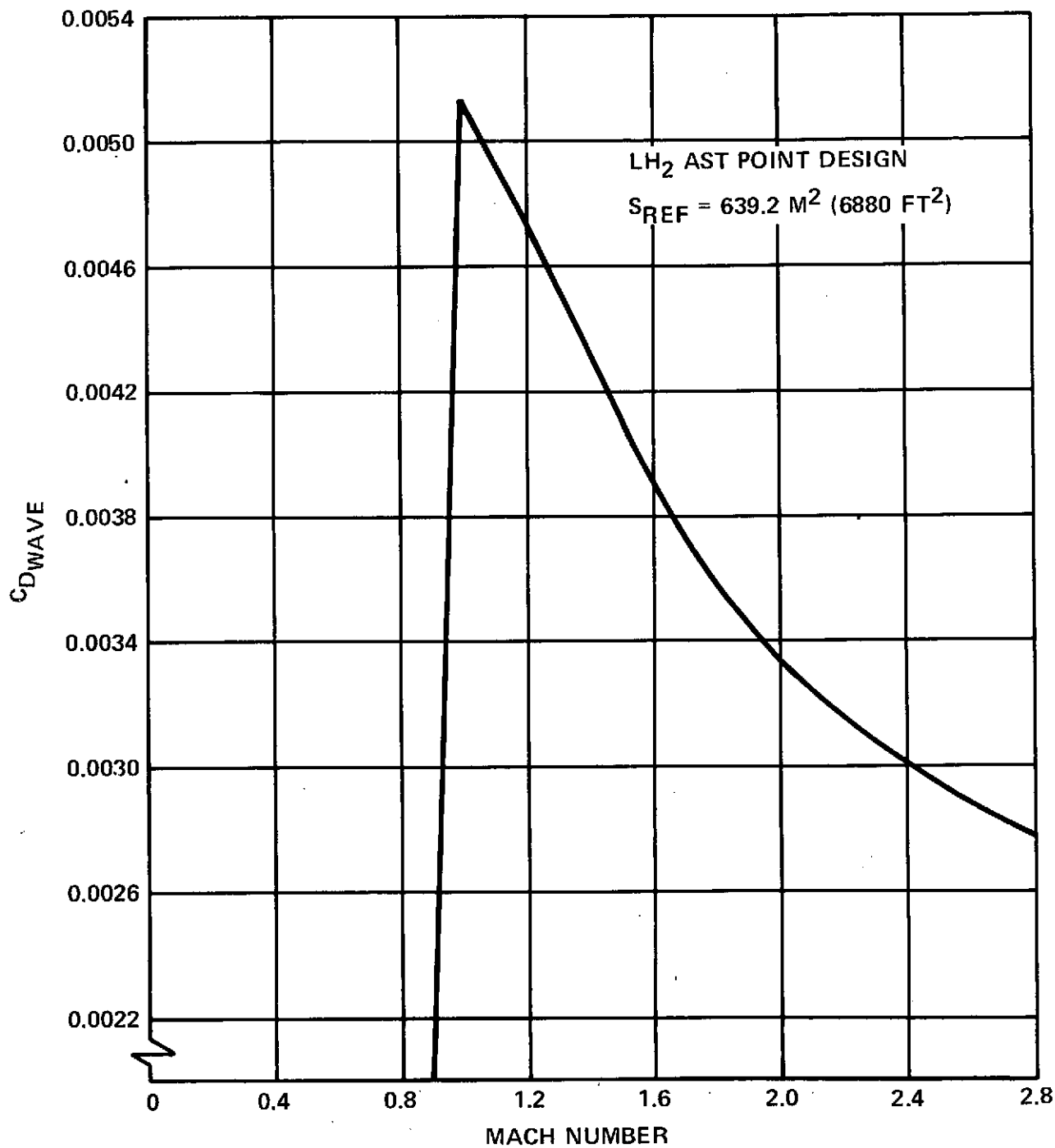


Figure 71. Wave Drag

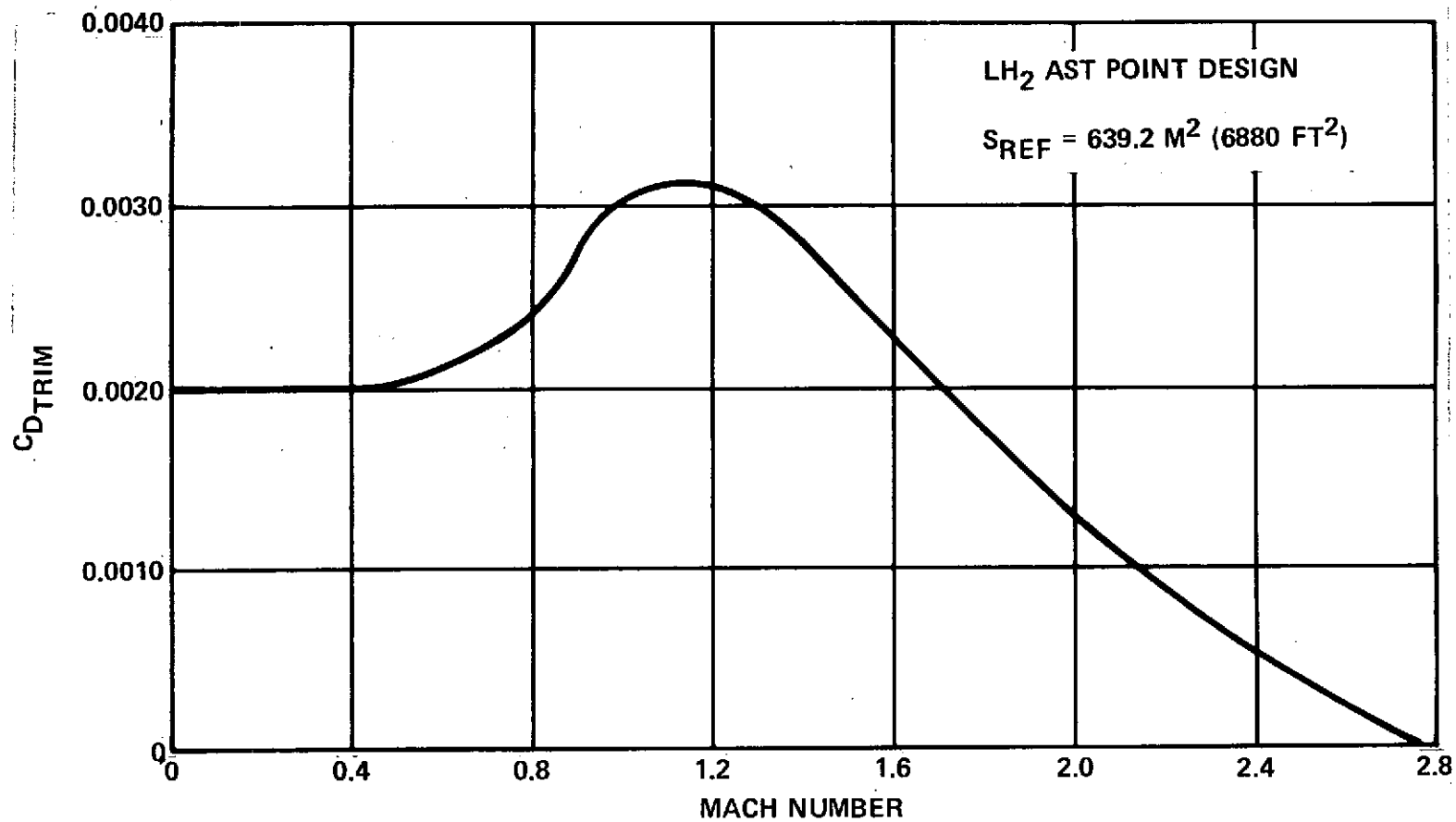


Figure 72. Trim Drag

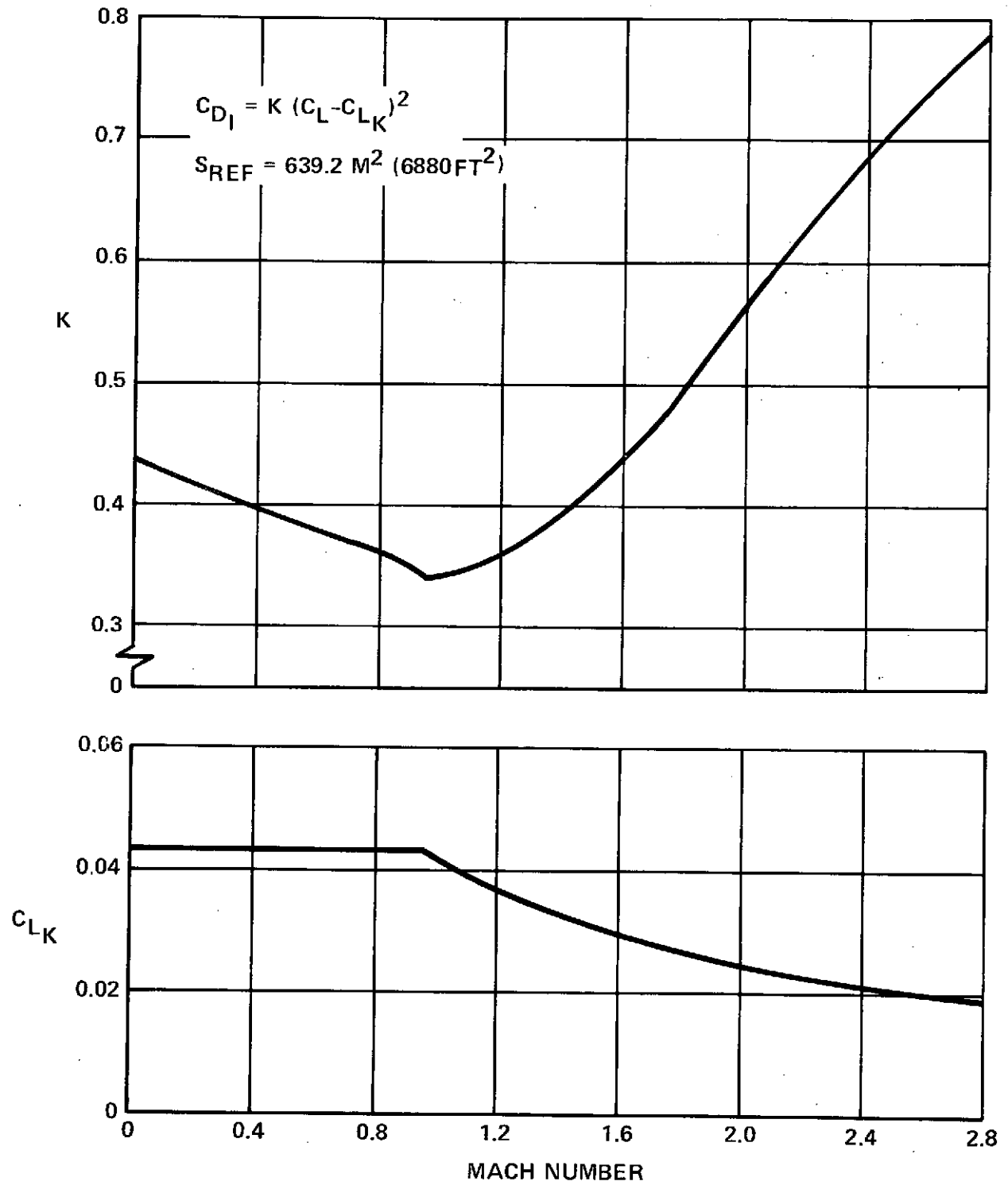


Figure 73. Drag Due-to-Lift Parameters

The wing camber drag increment (Figure 74) is essentially a computer programming device to permit the calculation of zero-lift drag and minimum drag coefficients for the development of high speed lift-drag polar. The increment was calculated from wind tunnel test data.

4.1.3.2 Propulsion System Description

At the start of the Phase II effort it was suspected from inspection of the Phase I mission profiles that the use of the maximum duct burning temperature of 2200°K (3960°R) during climb (Mach 0.99 to start-of-cruise at 2.7) provided thrust levels with the turbofan engines in excess of that required for maximum range efficiency (km/kg). Accordingly, a series of ASSET runs were made limiting this temperature during climb. The vehicle gross weight, wing loading, take-off distance and other constraints were held constant. The resulting effect on total range vs the maximum duct burning temperature is shown in Figure 75. As a result of the trend shown, a more modest temperature of 1367°K (2460°R) was selected for the Phase II study. The engine weight was then reduced approximately 5 percent to reflect this 833°K (1500°R) reduction in maximum operating duct temperature.

Cycle characteristics for the duct burning turbofan engine used for the point design aircraft in Phase II are shown by Table 15, a schematic of the engine flow path is shown by Figure 26, and general nacelle dimensions, weights, thrust size, and scaling data are shown by Figure 76. Figures 77, 78, 79, 80, 81 and 82 show the engine's installed performance.

The selected blow-in-door exhaust nozzle system provides for excellent high speed aft engine body drag and aerodynamic aircraft integration when used in conjunction with a turbofan. The blow-in-door nozzle, by virtue of its tertiary airflow induced through the blow-in-doors at low flight speeds and its aerodynamically actuated secondary nozzle trailing edges, also produces relatively good subsonic and transonic nozzle performance. Further, the tertiary flow mixes with the high velocity exhaust gases and acts as a sound suppressor during takeoff. It is estimated that this could reduce takeoff noise as much as 5 EPNdB.

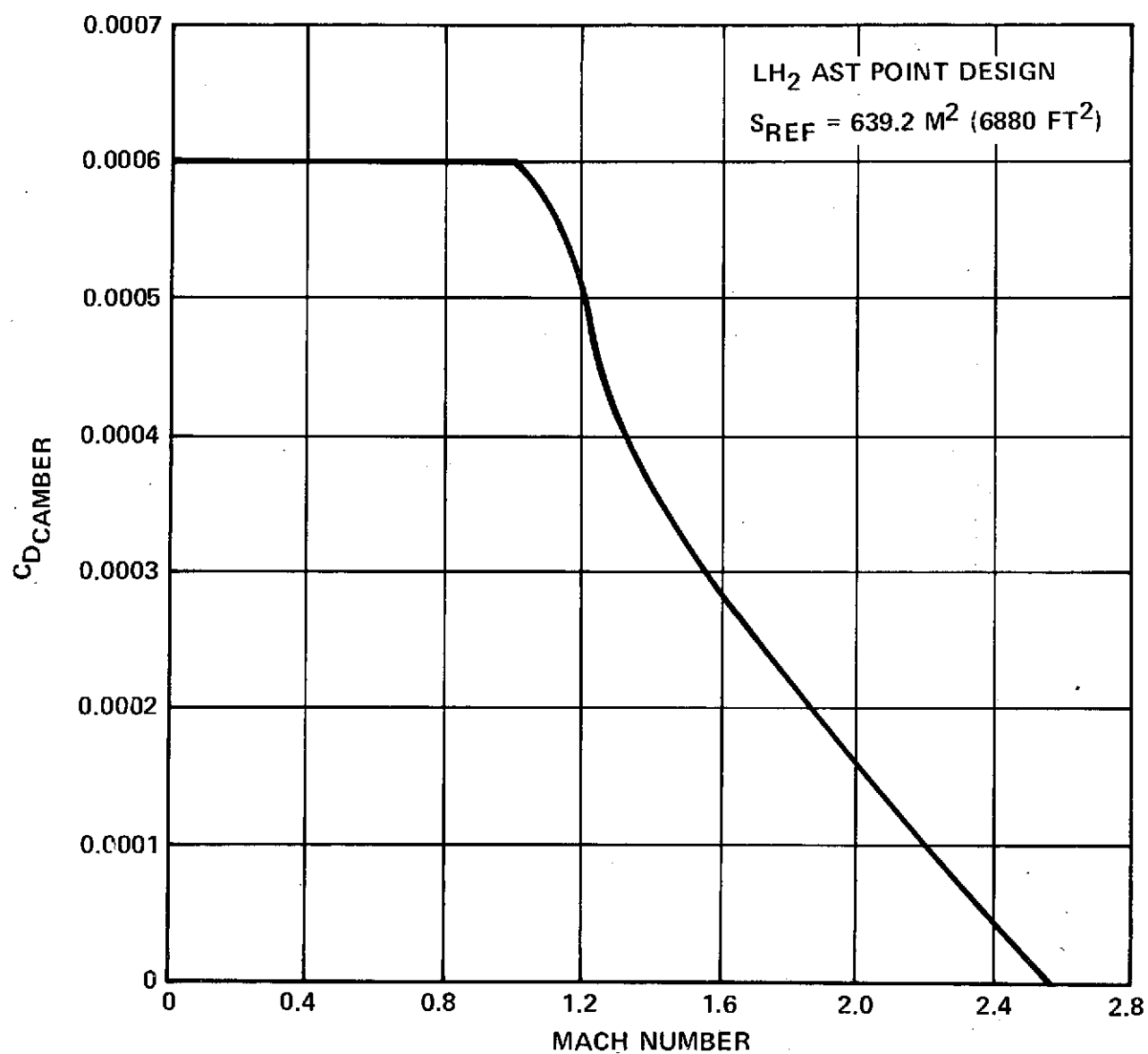


Figure 74. Wing Camber Drag

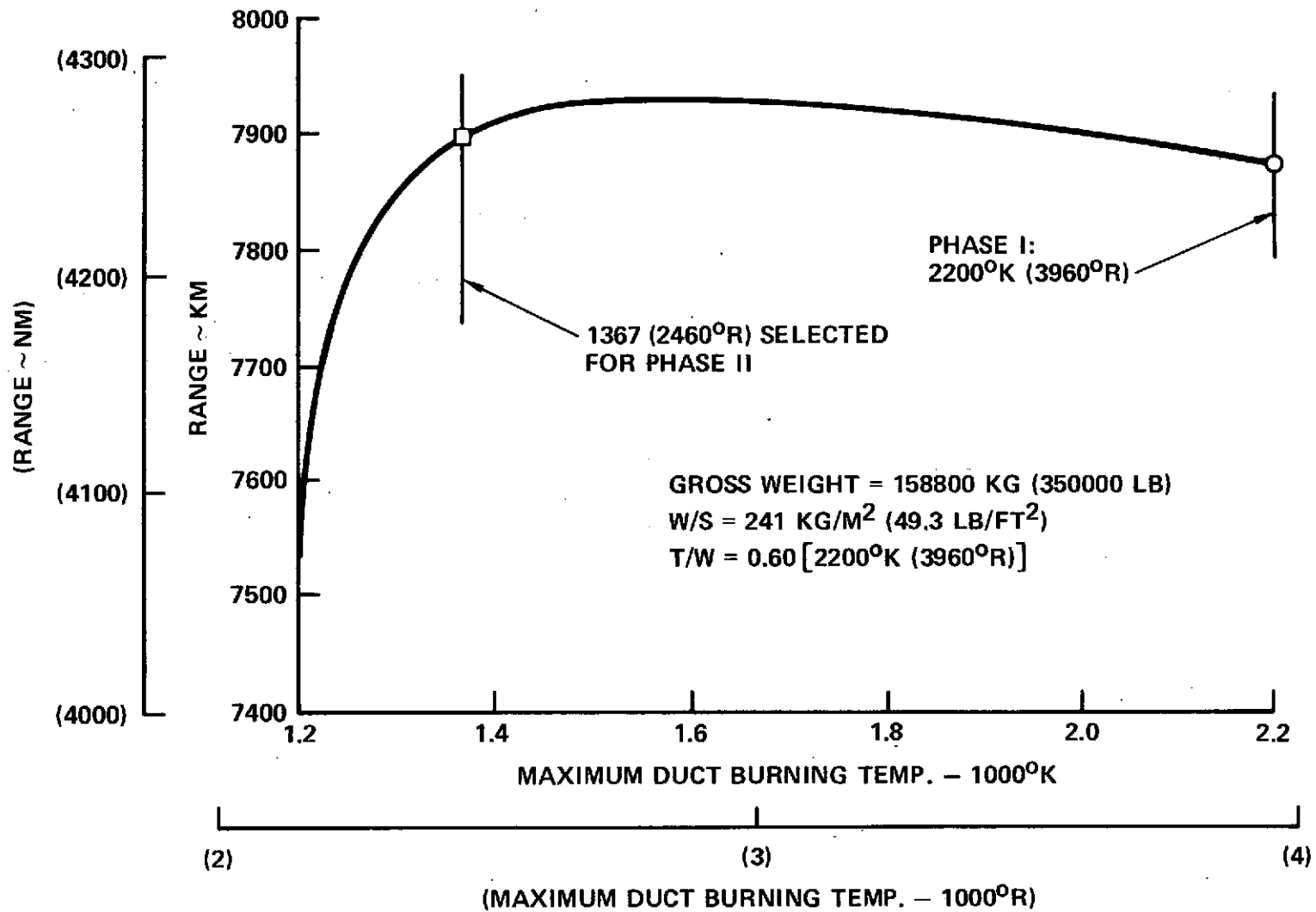


Figure 75. Range vs Duct Burning Temperature

TABLE 15
LIQUID HYDROGEN DUCT BURNING TURBOFAN CYCLE CHARACTERISTICS
(SLS, UNINSTALLED)

- PHASE II POINT DESIGN -

Engine Designation Engine Type Design Cruise Mach	LH2TF-1 DB TF 2.7
Max Thrust	36160 daN (81300 lb)
Specific Fuel Consumption	0.458 kg/hr/daN (0.449 lb/hr/lb)
Corrected Airflow - $\omega\sqrt{\theta/\delta}$	465 kg/sec (1025 lb/sec)
Bypass Ratio	4.4
Fan Pressure Ratio	3.0
Fan Adiabatic Efficient	0.866
Compressor Pressure Ratio	8.33
Compressor Adiabatic Efficiency	0.871
Overall Pressure Ratio	25.0
Nozzle Velocity Coefficient (Duct)	0.981
Nozzle Velocity Coefficient (Primary)	0.981
Max Turbine Inlet Temp °F	1922°K (3460°F)
Max Duct Burning Temp °F	1367°K (2460°R)
Fuel Heating Value	119430 kJ/kg (51590 BTU/lb)
Peak Fan Polytropic Efficiency	0.900
Peak Compressor Polytropic Efficiency	0.915
HP Turbine Adiabatic Efficiency	0.920
LP Turbine Adiabatic Efficiency	0.910
Primary Burner Efficiency	1.000
Duct Bruner Efficiency	0.916
Primary Burner Pressure Loss Ratio	0.060
Duct Burner Pressure Loss Ratio	0.071
Primary Nozzle Pressure Loss Ratio	0.005
Thrust to Engine wt Ratio	7.3 daN/kg 714 lb/lb

—PHASE II POINT DESIGN—

PARAMETER	REFERENCE VALUE	
FN_{SLS} , MAX +daN(LB)†	36452	(81330)
AC, M ² (FT ²)	3.010	(32.4)
D _{COMP} , CM (IN)	201.4	(79.3)
D _{MAX} , CM (IN)	235.0	(92.5)
D _{NO2} , CM (IN)	235.0	(92.5)
L _{ENG} , CM (IN)	660.4	(260.0)
L _{INLET} , CM (IN)	513.1	(202.0)
WEIGHT, KG, (LB) *	4990	(11,000)

$$DIAM = DIAM_{REF} \left(\frac{FN_{SLS}}{FN_{SLS_{REF}}} \right)^{0.5}$$

$$L_{ENG} = L_{ENG_{REF}} \left(\frac{FN_{SLS}}{FN_{SLS_{REF}}} \right)^{0.35}$$

$$L_{INLET} = 2.56 \times D_{COMP}$$

$$WEIGHT = WEIGHT_{REF} \left(\frac{FN_{SLS}}{FN_{SLS_{REF}}} \right)$$

† D/B TEMP DESIGN = 1367°K (2460°R)

* INCLUDES REVERSER AND SUPPRESSOR

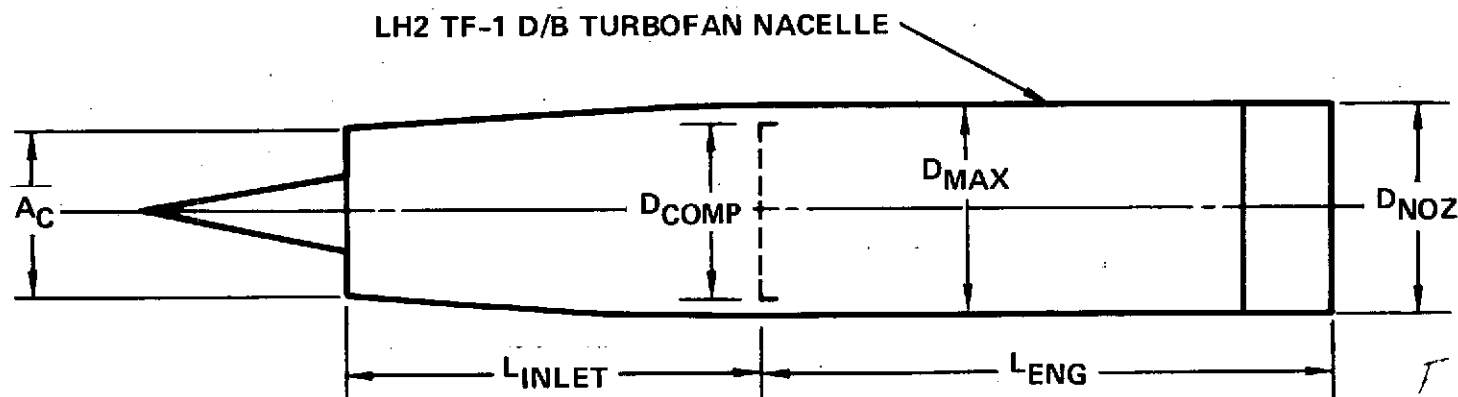


Figure 76. Mach 2.7 Hydrogen Fueled Duct Burning Turbofan Nacelle Dimensions and Scaling Data

AST MACH 2.7 DUCT-BURNING TURBOFAN LH2TF-1 STD + 15C
 U.S. STANDARD ATMOSPHERE 1962
 DTAM = 15C (27.00F)

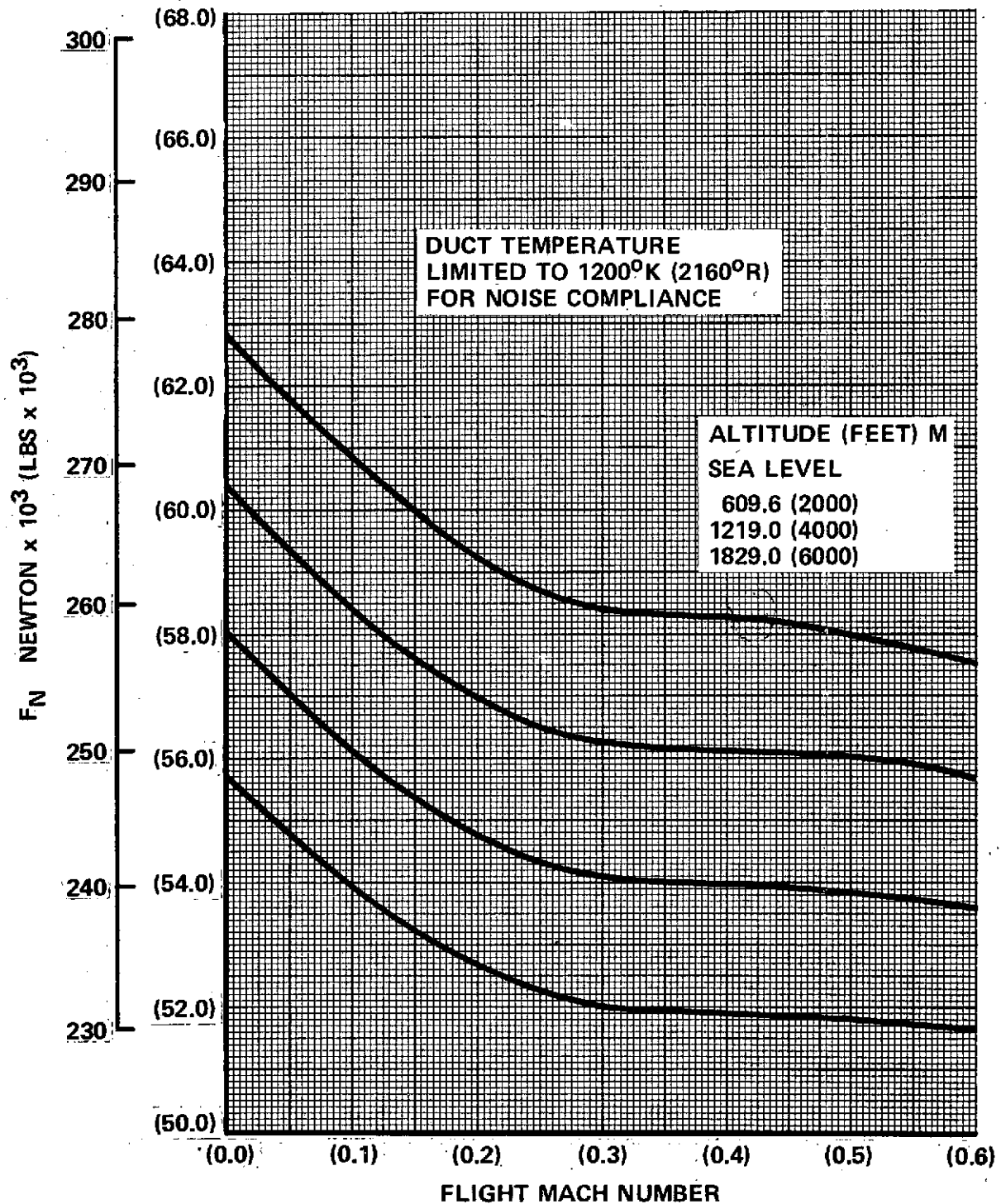


Figure 77. Installed Flight Performance - Noise Limited Takeoff Power (Augmented)

AUGMENTED MAX CLIMB
AST MACH 2.7 DUCT-BURNING TURBOFAN LH2-1
U.S. STANDARD ATMOSPHERE 1962
DTAM = 0.00

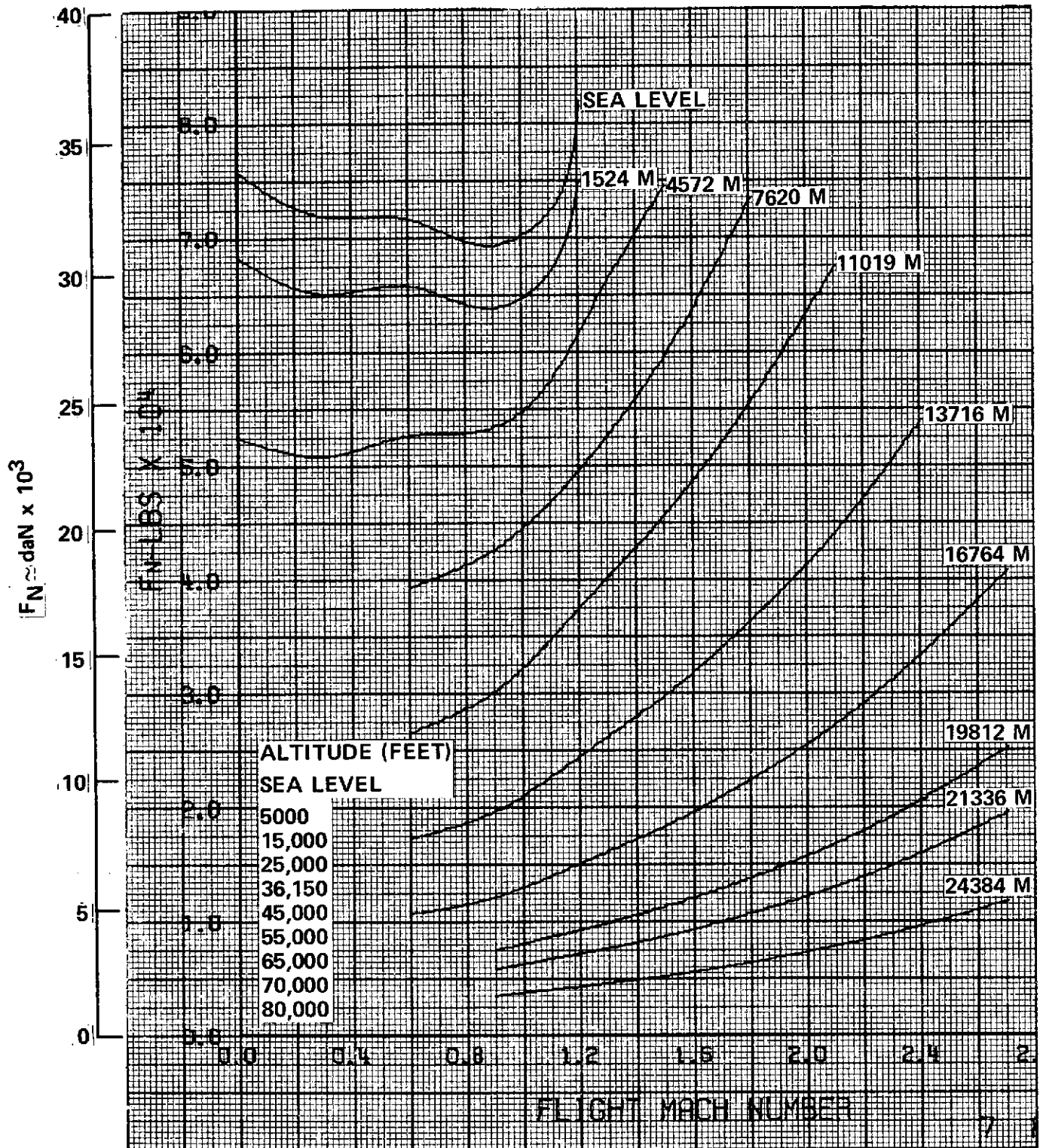


Figure 78. Installed Flight Performance - Augmented Max Climb

REPRODUCIBILITY OF THE
ORIGINAL PAGE IS POOR

AUGMENTED MAX CLIMB
AST MACH 2.7 DUCT-BURNING TURBOFAN LH2-1
U.S. STANDARD ATMOSPHERE 1962
DTAM = 0.00

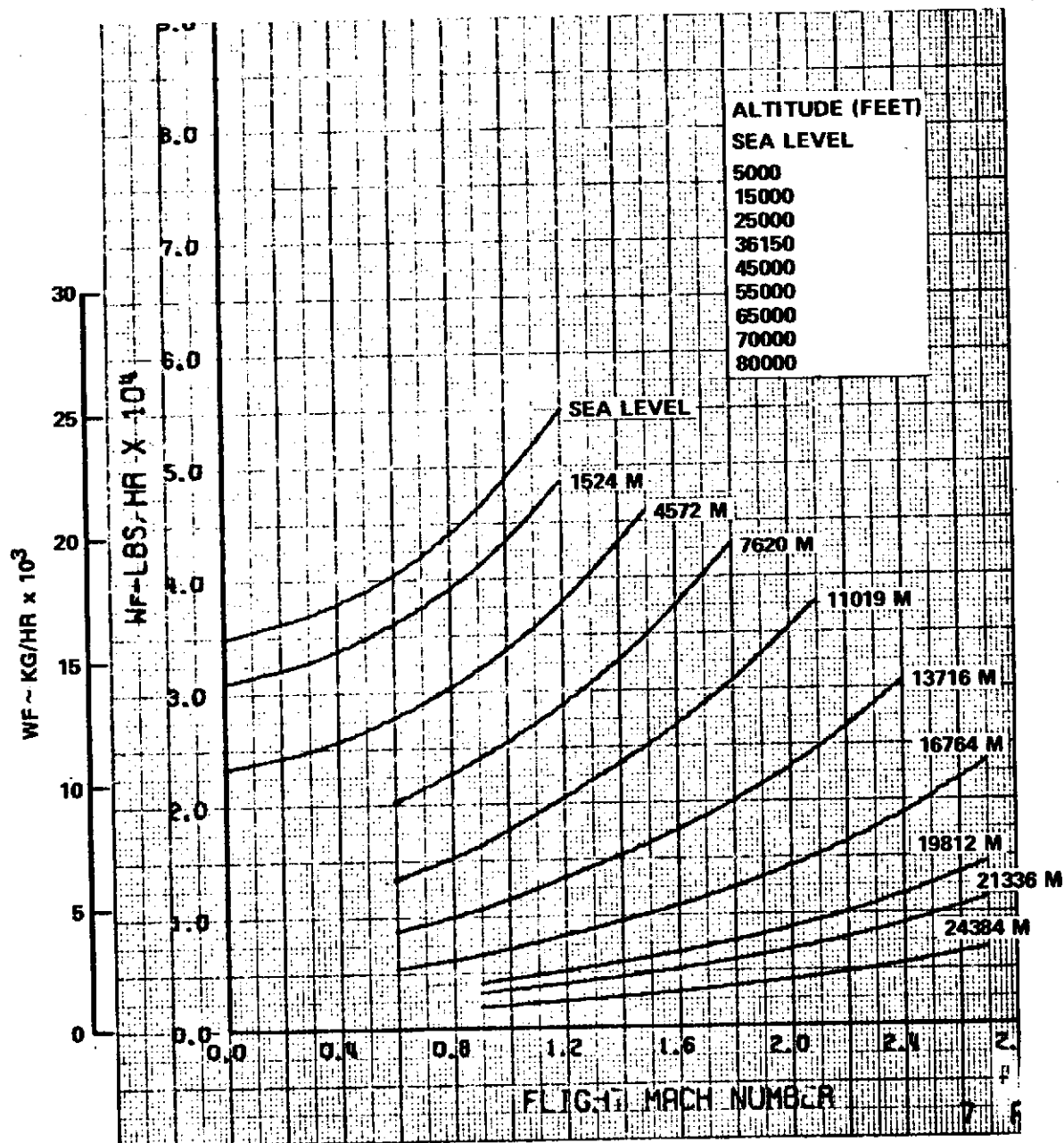


Figure 79. Installed Flight Performance - Augmented Max Climb

NON-AUGMENTED PART POWER
 AST MACH 2.7 DUCT-BURNING TURBOFAN LH2-1
 U.S. STANDARD ATMOSPHERE 1962
 1524 M (5000 FT)

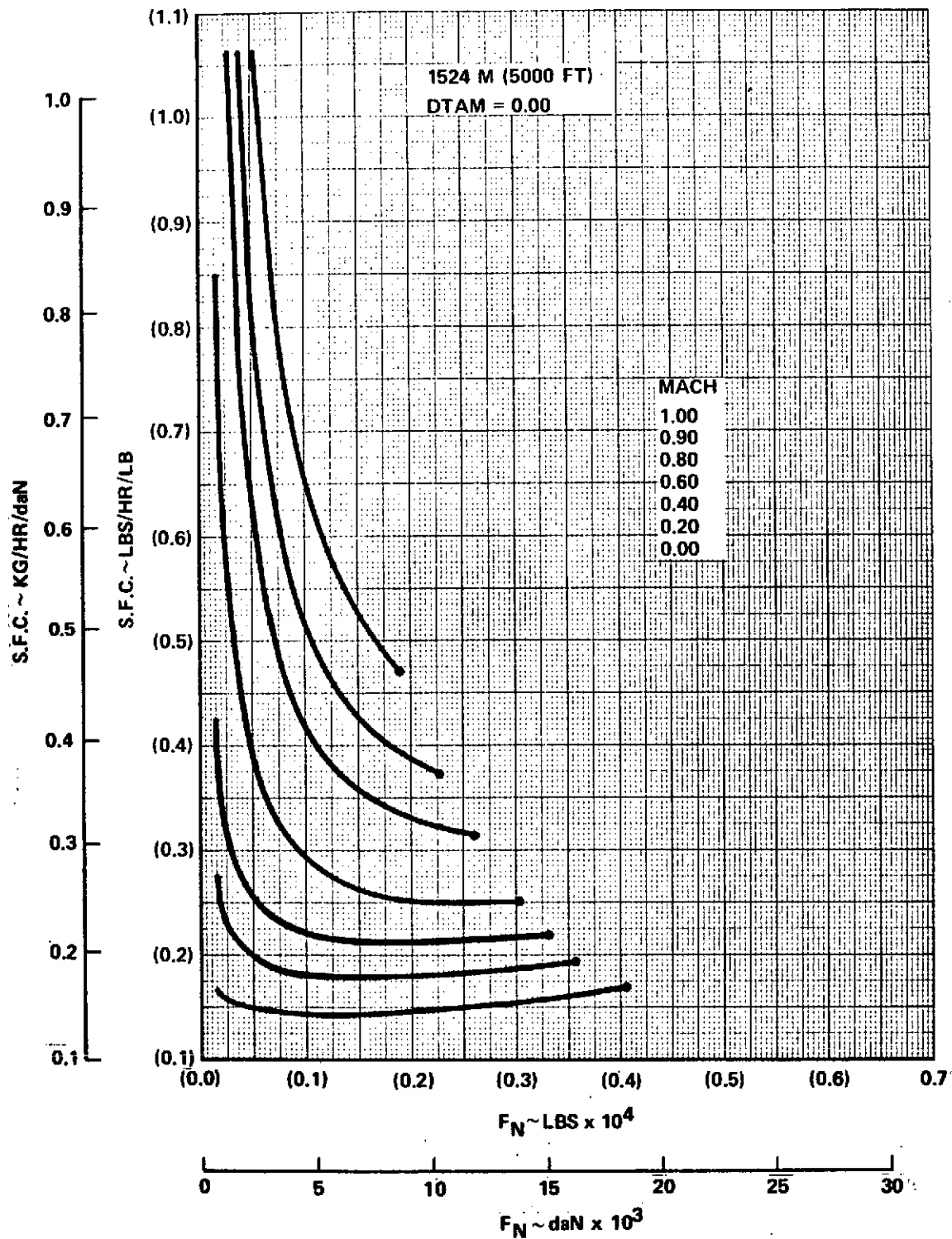


Figure 80. Installed Flight Performance - Non-Augmented Part Power.

NON-AUGMENTED PART POWER
 AST MACH 2.7 DUCT-BURNING TURBOFAN LH2-1
 U.S. STANDARD ATMOSPHERE 1962
 11019 M (36150 FT)

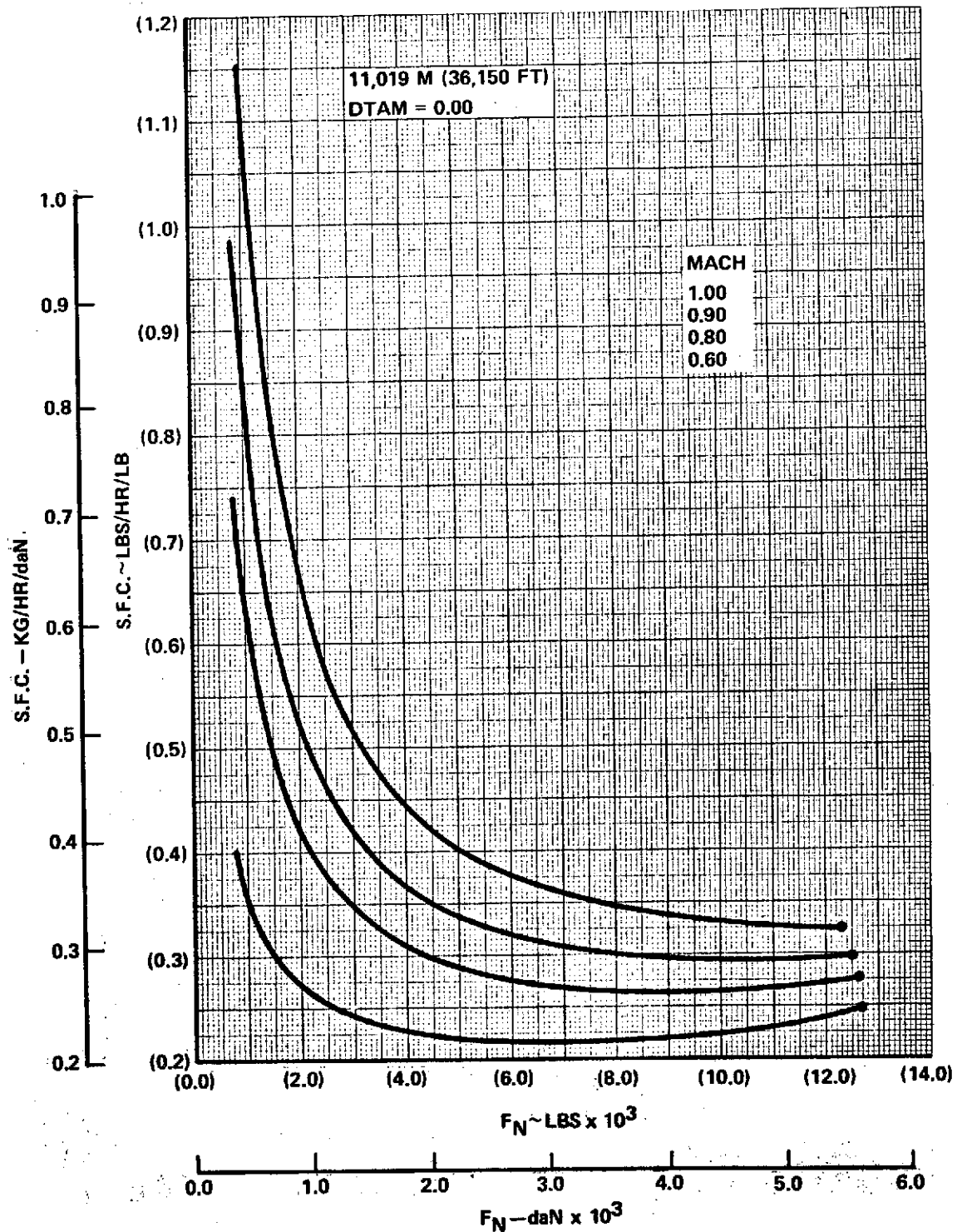


Figure 81. Installed Flight Performance - Non-Augmented Part Power

AUGMENTED PART POWER
 AST MACH 2.7 DUCT-BURNING TURBOFAN LH2-1
 U.S. STANDARD ATMOSPHERE 1962
 19812 M (65,000 FT) DTAM = 0.0

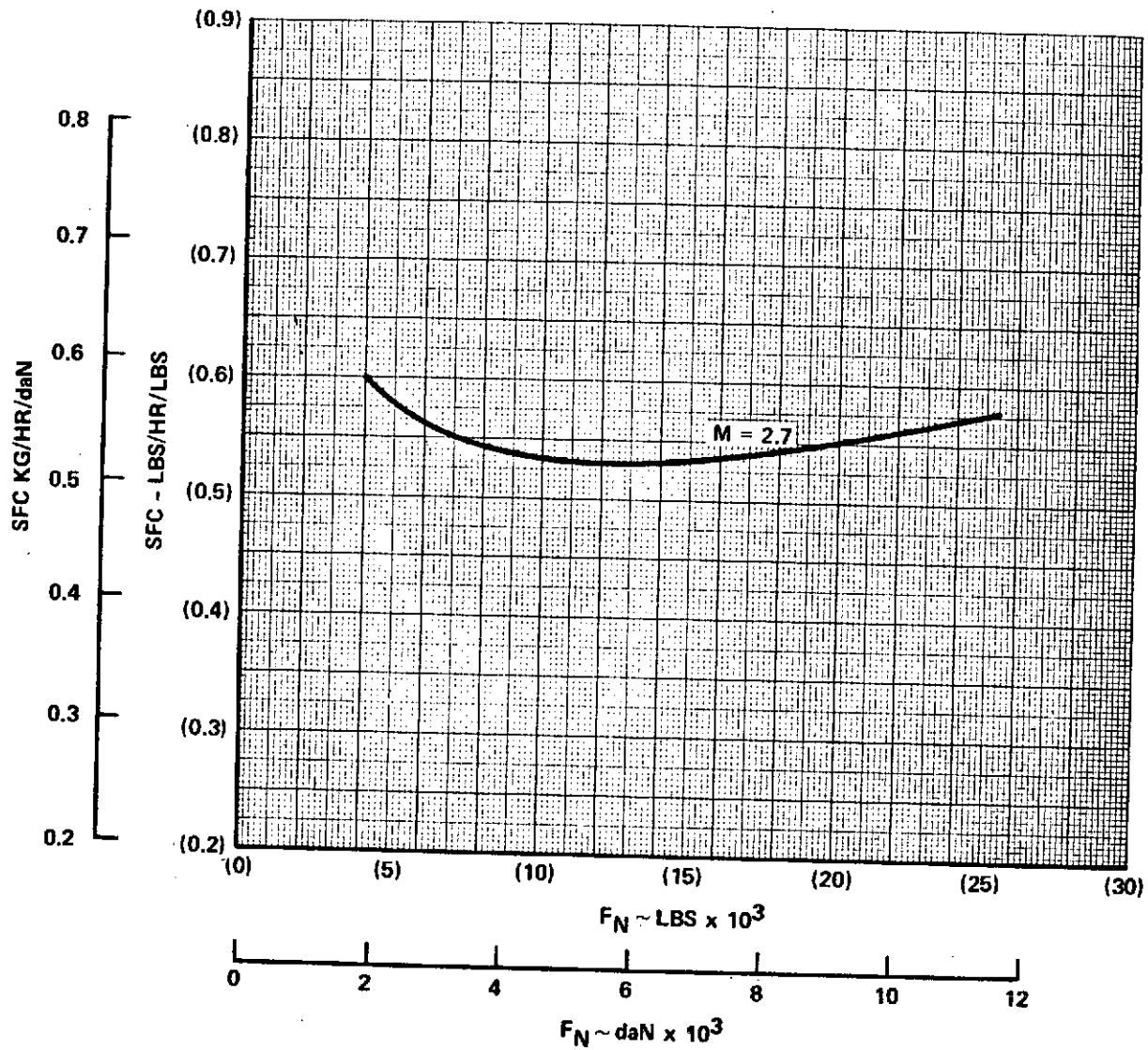


Figure 82. Installed Flight Performance - Augmented Part Power

The inlet is an adaptation of the Boeing 2707 SST air intake (References 9 and 10) and is shown in Figure 67. The design is a mixed-compression axisymmetric intake, incorporating a translating centerbody and four movable cowl panels (throat doors), eight butterfly-type secondary air valves, four overboard bypass doors, and eight aerodynamically operated vortex valves. The vortex valves are located in the cowl at the intake throat and are used for increasing normal shock stability in the started mode.

During supersonic cruise (Mach 2.7), the centerbody is fully retracted. In this condition the conical shock from the centerbody tip is located close to the cowl lip. The centerbody translates forward to increase the throat area for off-design operation. During transonic and subsonic flight, it is extended to its maximum translation of 1.25 times the cowl lip radius. The throat doors move between parallel beam walls while rotating about hinge lines near the cowl lip. Position of the throat doors is a scheduled function of the centerbody position.

The overboard bypass doors are activated when large amounts of air must be removed from the intake. On the normal climb and acceleration placard the bypass doors are closed. The doors open to a maximum of 31.5° from the closed position. At this opening the aft facing discharge area is equal to 45 percent of the lip area.

The vortex valves are fluidic devices containing no moving parts. The valves automatically react to small airflow disturbances in the intake, maintaining high intake performance during these disturbances.

In determining the size of the intake, it was essential to avoid overboard bypass airflow during cruise to minimize drag. The cowl lip area was sized to match the standard-day engine cruise power demand. For maximum power demand on a standard or cold day, the engine rpm is trimmed to avoid excessive supercritical intake operation. On a hot day with the engine operating at design rpm, the excess intake airflow supply is discharged through the secondary nozzle via the secondary air system. The overall system is matched such that essentially no overboard bypass airflow is needed during normal climb and cruise intake operation.

4.1.3.3 Fuel System Description

The fuel system (Figure 83) consists of four pressurized and insulated tanks arranged in tandem pairs in the forward and aft fuselage sections, insulated feed lines to each of four turbofan engines and one auxiliary power unit, heat exchangers to transfer airframe and engine heat loads to the cryogenic fuel, fuel quantity gauging equipment, refueling, defueling and jettison subsystems.

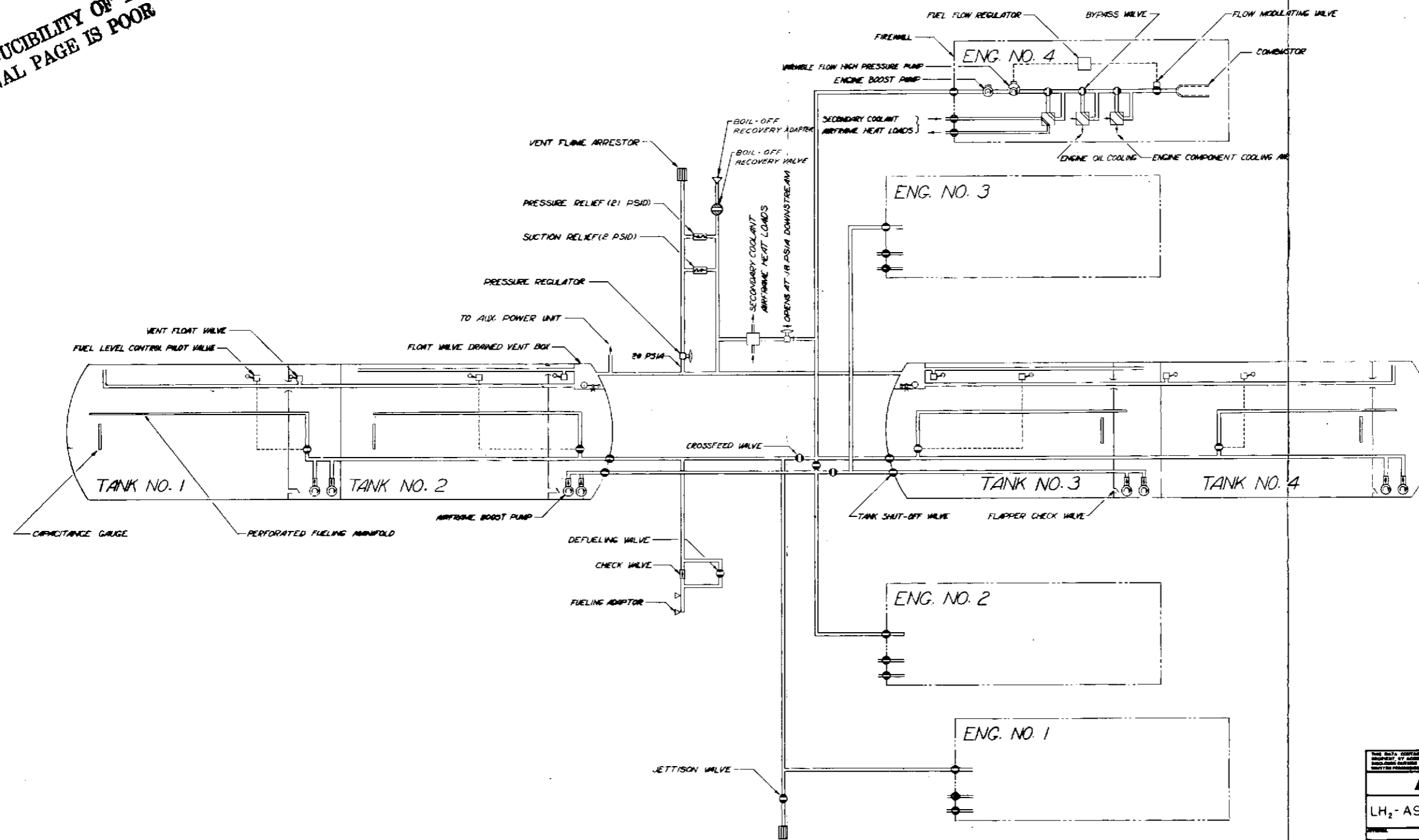
Tank Vent and Pressurization - To prevent pump cavitation and reduce fuel flashing losses, the fuel tanks are maintained at a pressure of 138,000 newton/m² (20 psia) by an absolute pressure regulator located between the common vent line for all fuel tanks and a flame arrestor which permits overboard discharge of gaseous boil-off without the hazard of flame propagation back to the fuel tanks. If the tank pressure drops below 124,000 newton/m² (18 psia) because of exceptionally high engine fuel demand, a secondary absolute pressure regulator located in the No. 4 engine feed lines opens allowing a small amount of fuel to be vaporized by heat from the airframe heat loads before it is conveyed to the tanks through the normal vent system.

In the event tank pressure exceeds 145,000 newton/m² (21 psi) above free stream ambient, a pressure relief valve opens to bleed off the excess pressure through the vent line flame arrestor. If, for any reason, the tank pressure falls below ambient outside pressure, suction relief is provided at 14,000 newton/m² (2 psi) below ambient to prevent catastrophic collapse of the tanks. This condition could only exist if all of the fuel had been exhausted during a descent.

A boil-off recovery adaptor and valve are provided to minimize boil-off losses on the ground. This system permits the operator to return gaseous boil-off to ground storage facilities for reliquification.

Vent openings are located in the forward and aft ends of each tank. Float-operated vent valves in the opening nearest the vent box prevent fuel from flowing by gravity into the vent box. Liquid fuel which collects in the vent box is drained into the adjacent fuel tank through a float-operated drain valve.

REPRODUCIBILITY OF THE
ORIGINAL PAGE IS POOR



ADVANCED DESIGN		DESIGN NO. CL 1701-7
LH ₂ -AST FUEL SYSTEM SCHEMATIC		
1-21-74	1-17-74	LOCKHEED - CALIFORNIA CO. TULSA, CALIFORNIA CODE IDENT NO. 10000
1-21-74	1-17-74	CL1701-7.5
1-21-74	1-17-74	1 OF 1

Figure 83. Fuel System Schematic

FOLDOUT **2**

Propulsion Engine Feed System - Each fuel tank is normally connected to its identically numbered engine. However, a system of cross-feed valves permits any one tank to supply fuel to any engine if required or, by properly sequencing the operations of the cross-feed and refueling valves, permits transfer of fuel from one tank to another.

Two boost pumps are located in a surge box in each tank to ensure fuel availability and to prevent fuel starvation during aircraft maneuvering at low fuel levels. The boost pumps are designed to pump boiling hydrogen and to supply it to the main engine pumps in a subcooled state by means of vacuum-jacketed feed lines. All airframe and engine heat loads, with the exception of the tank pressurization heat loads, are added downstream of the high-pressure engine pumps.

APU Feed System - The auxiliary power unit is operated on gaseous hydrogen, thereby minimizing boil-off losses during the considerable periods of APU operation while on the ground. APU feed is available from the common tank vent line. If insufficient boil-off is released from the tanks, due to the presence of super-cooled hydrogen just subsequent to refueling, operation of the No. 4 tank-mounted boost pump will maintain gas flow through the secondary coolant heat exchanger at $124,000 \text{ newton/m}^2$ (18 psia) to the APU.

Refueling and Defueling System - All tanks are refueled through a pair of pressure fueling adaptors located at the bottom of the fuselage. Part of the refueling manifold is common with the engine feed lines. Inside the tank, the fueling manifold is perforated along its entire length to distribute the liquid hydrogen uniformly over all of the tank walls, thus minimizing the tank wall thermal stresses. A dual fuel level control pilot valve in each tank shuts off the tank fueling valve when the respective tank has reached its full level. Integral with the float valve is a solenoid valve which permits manual or preset shut-off of the valve at any tank level.

Prior to refueling tanks that have contained air, the fueling system must be purged by an inert medium (e.g., gaseous nitrogen) to remove all oxygen, followed by gaseous hydrogen to remove all inerting gas. The purge system will utilize the boil-off recovery adaptor and valve to discharge the purge gases around the pressure relief valve and overboard.

Defueling may be accomplished through the defueling valve to the fueling adaptors by operating the boost pumps with open cross-feed valves. The tanks may be defueled individually or simultaneously.

Fuel Jettison System - A jettisoning system is provided to permit dumping the fuel from any or all tanks in flight. This system operates similarly to the defueling system except that fuel is routed to a dump mast through a jettison valve and flame arrestor.

Fuel Quantity Indicating System - Capacitance gauges are used to measure fuel volumes. The units are calibrated to indicate fuel quantity in pounds at the fuel management panel.

Fuel System Design Considerations - As a design objective, fuel system components such as pumps and valves should be designed for quick removal and field replacement in a manner commensurate with present commercial operation. System failure provisions should also provide for back-up of critical dispatch items as in current practice.

The broad aspects of flight safety require consideration and development of fuel system components and arrangement in terms of malfunction and leak detection, isolation, inerting and/or purging and fire containment. Safety criteria and acceptable design practices must be established in relation to and based on current practice realizing the unique properties of a cryogenic fuel with the ignition energy and temperature levels of hydrogen.

4.1.4 Mass Properties

4.1.4.1 Weight Statement

The Phase II point design vehicle reflects the latest selected concepts for wing and fuselage structure as derived from the Arrow-Wing Structure Study (NAS1-12288) (Reference 4) and as determined by analysis performed during this study. The following changes were made in the bases used for calculating weights from that used in Phase I:

Wing - Removed 11.2 percent penalty for LH_2 tanks in wing. All fuel is now in integral fuselage tanks.

Fuselage - Removed 9.37 kg/m^2 (1.92 psf) penalty for passenger cabin pressure deck over fuel tanks.

Tanks (Fuel System) - The Phase II design study reported in Sections 4.4.2 and 4.5.3, resulted in the following installed weight fractions for the tank plus support, thermal protection system and heat shield:

Tank and supports	=	0.196	} kg/kg LH_2
Insulation	=	0.060	
Heat Shield	=	0.080	

Engines - Revised thrust/weight ratio due to decreased maximum duct temperature

ECS - 8 percent lighter than JP-fueled AST due to availability of LH_2 fuel as a heat sink.

Auxiliary Gear - Allowance for customer options and manufacturing tolerance = 898 kg (1,980 pounds)

Unusable Fuel - Increased to .030 Kg/Kg LH_2 (including boil-off) as a result of analysis reported in Section 4.5.3. This is part of Standard Items in the Weight Statement shown in Table 16.

The vehicle is presently configured with approximately equal distribution of hydrogen fuel between the forward and aft tanks. Each tank has a volume of 339.8 cubic meters (11,400 cubic feet). With a usable fuel weight per tank of 21,763 kg (47,980 pounds) and a density of 67.28 kg/m^3 (4.43 pounds per cubic foot), there is an excess volume of 16.28 cubic meters (600 cubic feet) per tank. This provides a 2 percent expansion space (ullage) and 3 percent extra fuel for boil-off allowance.

Table 16 is a group weight statement compiled for the point design airplane. For typical weight fractions, see the Weight Statement page of the ASSET computer printout reproduced in Appendix B.

TABLE 16
WEIGHT STATEMENT

CL 1701-7 LH2-AST D-B TURBOFAN ENGINES						
	t/c	AR	W/S (lb/ft ²)	T/W (lb/lb)	Weight (Pounds)	Kilograms
	<u>3.00</u>	<u>1.62</u>	<u>53.5</u>	<u>0.500</u>		
Take-Off Weight					(368,054)	166,946
Fuel Available					95,960	43,527
Zero Fuel Weight					(272,094)	123,419
Payload					49,000	22,226
Operating Weight					(223,094)	101,193
Operating Items					5,358	2,430
Standard Items					4,678	2,122
Empty Weight					(213,058)	96,641
Wing					47,205	21,412
Tail					6,914	3,136
Body					44,646	20,251
Landing Gear					17,201	7,802
Surface Controls					4,620	2,096
Nacelle and Engine Section					2,734	1,240
Propulsion					(57,996)	26,307
Engines					24,890	11,290
Thrust Reversal					0	
Air Induction System					9,854	4,470
Fuel System					21,927	9,946
Engine Controls and Starter					1,324	601
Instruments					1,092	495
Hydraulics					2,797	1,269
Electrical					4,593	2,083
Avionics					1,900	862
Furnishings and Equipment					11,500	5,216
Environmental Control System					7,800	3,574
Auxiliary Gear					1,980	898

4.1.4.2 Material Utilization

The utilization and distribution of materials for the major structural components of the LH_2 AST point design airplane is shown in Table 17. Material usage in the wing, empennage, and those portions of the fuselage not affected by the presence of the liquid hydrogen fuel is based on latest data from the Arrow-Wing Structure Study (Reference 4), modified to fit the requirements of the point design airplane. The structural requirements which are peculiar to the subject LH_2 study airplane are described in Section 4.4.2. This work served as a basis for the appropriate weights listed in Table 17.

4.1.4.3 Vehicle Balance and Moment of Inertia

Figure 84 presents the vehicle center of gravity travel and moment of inertia variations with changes in fuel and payload weight.

TABLE 17
MATERIALS UTILIZATION ~ kg (lb)

Component	Material					Total
	Alum.	Titan.	Steel	Compos.	Other	
Wing	985 (2,171)	18,329 (40,408)	428 (944)	1,328 (2,927)	342 (755)	21,412 (47,205)
Tail	141 (311)	2,914 (6,423)	31 (69)	0	50 (111)	3,136 (6,914)
Fuselage	6,601 (14,554)	10,409 (22,948)	365 (804)	506 (1,116)	2,370 (5,224)	20,251 (44,646)
Landing Gear	8 (17)	1,950 (4,300)	2,996 (6,605)	0	2,848 (6,279)	7,802 (17,201)
Nacelles	24 (52)	184 (406)	412 (909)	0 0	0 0	620 (1,367)
Air Induction	206 (453)	3,960 (8,731)	45 (99)	0 0	259 (571)	4,470 (9,854)
Surface Contr	503 (1,109)	94 (208)	440 (970)	31 (69)	1,027 (2,264)	2,095 (4,620)
Totals	8,468 (18,667)	37,840 (83,424)	4,717 (10,400)	1,865 (4,112)	6,896 (15,204)	59,786 (131,807)

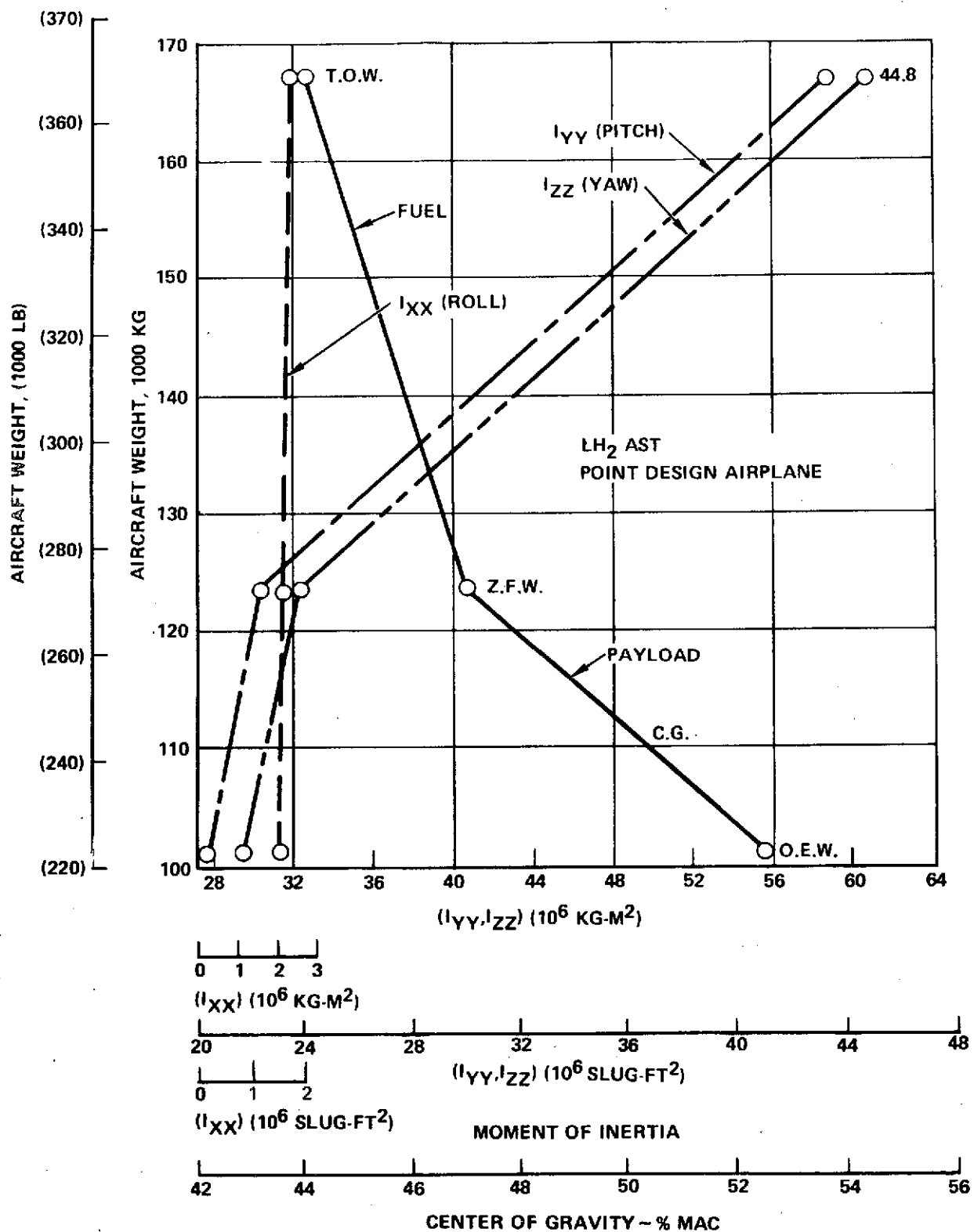


Figure 84. Mass Properties vs. Aircraft Gross Weight

4.2 VEHICLE PERFORMANCE

Previous sections have described the size, shape, and general arrangement of the Phase II point design airplane. This section describes its basic design and performance characteristics, starting with a brief explanation of the process by which the choice of design relationships was narrowed to the point where further optimization produced negligible benefits, resulting in selection of the specified design. A number of design sensitivities are explored to establish the effect minor changes in the vehicle might have on its performance, and finally, a summary of the environmental characteristics of the aircraft is presented.

4.2.1 Design and Performance Characteristics

Because of the significant changes in the design requirements for the Phase II airplane, as described in Section 4.1.1, compared to those used in Phase I, the first task of Phase II was to do a basic resizing. Once this was done, alternate passenger/fuel tank arrangements could be considered, structural concepts studied, and thermal protection systems explored as discussed in Section 4.1.2, to develop preferred designs and determine realistic weights. Finally, the characteristics of the Phase II point design vehicle were determined using the ASSET program on the basis of updated propulsion, aerodynamic, weight, and cost inputs, and in accordance with the changed premises listed in Table 18. The principal trade-off involved was that of determining the combination of wing loading (W/S) and thrust/weight (T/W) at which the three constraints of the 2,896 m (9,500 ft) landing field length, and the FAR 36 sideline noise and flyover noise would be balanced. As described in Section 3, the constraint of the 3,200 m (10,500 ft) engine-out takeoff field length is not critical if the other 3 constraints are met. Figure 85 illustrates the relation between noise, field length, W/S, and T/W for LH₂ AST's using the duct burning turbofan engine defined for Phase II.

The final point design vehicle selected was that vehicle which met the above criteria with minimum weight as indicated on the figure. Characteristics of this vehicle are summarized in Table 18. Copies of sheets from the actual

TABLE 18. POINT DESIGN VEHICLE CHARACTERISTICS

Performance:

Take-off Weight	166,946 kg (368,054 lbs)
Range	7,778 km (4,200 n.mi.)
Payload	22,226 kg (49,000 lbs)
Wing Loading	261.2 kg/m ² (53.5 lb/ft ²)
Thrust/Weight (SLS, Uninstalled)	0.50
Thrust/Eng. (SLS, Uninstalled)	204,618 newton (46,000 lbs)
Wing Area	639.2 m ² (6,880 ft ²)
Fuselage Length	100 m (328 ft)
FAR T.O. Field Length	2,179 m (7,150 ft)
FAR Ldg. Field Length	2,894 m (9,496 ft)
Landing Approach Speed	80.3 m/sec (156 keas)
Average Cruise L/D	6.99
Average Cruise SFC	0.572 kg/hr/daN (0.561 lbs/hr/lb)
Average Cruise Altitude	20,574 m (67,500 ft)
Mission Fuel	36,940 kg (81,440 lbs)
Mission Time	3.45 hrs

Weights:

Structures	55,937 kg (123,320 lbs)
Propulsion*	26,306 kg (57,996 lbs)
Equipment and Furnishings**	9,689 kg (21,360 lbs)
Empty Weight	<u>96,641 kg (213,058 lbs)</u>
Standard + Operating Items	4,552 kg (10,036 lbs)
Operating Empty Weight (OEW)	<u>101,193 kg (223,094 lbs)</u>
Payload	22,226 kg (49,000 lbs)
Zero Fuel Weight (ZFW)	<u>123,419 kg (272,094 lbs)</u>
Fuel - Total	43,209 kg (95,960 lbs)
Take-off Gross Weight	<u>166,946 kg (368,054 lbs)</u>

*Includes tanks, thermal protection system and fuel system

**Includes 898 Kg (1980 lb.) for Customer options

computer printouts which contain a greater level of detail are included as Appendix B.

4.2.2 Sensitivity Analysis

The point design vehicle was perturbed on the basis of range, inert weight, SFC, subsonic cruise leg, payload, noise, drag, and landing field length to determine its sensitivity to each of these factors. Figures 85 thru 95 show the results of these excursions, together with approximate sensitivity factors where appropriate.

Figure 86 examines the growth of the point design aircraft if the design mission range were increased. To accommodate the increased fuel required the fuselage was allowed to grow in length up to a maximum of 114.3 m (374 ft) at 10,000 km (5,400 n.mi.). In each case the vehicle is resized and the constraints of landing field length and noise held constant. Since the landing wing loading is held constant to meet the landing distance, the takeoff wing loading can be increased slightly as more mission fuel is consumed. FAR 36 allows increasing takeoff and flyover noise as gross weight is increased which results in a slightly higher allowable jet velocity. The result is that the turbofan engine power cut-back can be reduced. More usable thrust allows a slight decrease in the installed thrust-to-weight as shown. This increases the takeoff field length but it remains well within the 3,200 m (10,500 ft) constraint. The result of this study shows that the design range of a hydrogen vehicle can be greatly extended with only a reasonable increase in gross weight (a 22.8 percent increase for a 2,222 km (1,200 n.mi.) range increment.)

Figures 87 and 88 illustrate the effect of a change in empty weight as would be the case if equipment or structural weight were to increase or decrease from the original target weight. Two different situations are examined in this study:

In Figure 87, the assumption is that the vehicle design has not been frozen and the option exists to resize the vehicle to accomplish the original mission. This might be the case if, for example, the target wing weight were exceeded by 10,000 lbs at the original design gross weight. This causes a

subsequent increase in fuel, propulsion, structure, etc. and finally a further increase in the wing itself to maintain the vehicle performance. The sensitivity or growth factor shown is about 2.65 pounds of gross weight per pound of original empty weight change.

Figure 88 assumes that the design gross weight has been frozen and that the fuel available must be adjusted to reflect the change in empty weight. The result is a change of about .04 n.mi. per pound of empty weight change.

Figure 89 shows the effect of a uniform change in engine specific fuel consumption (SFC) on total range. The vehicle is not resized but flies at different ranges as the fuel consumption is varied. This is a significant sensitivity and allows an increase of 54 n.mi. with each 1 percent decrease in SFC.

As in Phase I, the penalty in total range that results from having to fly initial or final legs at subsonic speeds over populated areas, is shown in Figure 90. The decay in total range amounts to only about .1 of a n.mi. per n.mi. of subsonic leg. It is of interest that if the whole mission were flown subsonically the range would only decay 40 n.mi. although it would be a long, expensive trip. The inability to continue the mission at supersonic speeds, e.g. loss of an engine, would mean that the original destination could probably be held if the distance to the designated alternate is short enough to be within the total fuel capacity limit including legal reserves at the alternate.

Figure 91 is simply the change in range as the payload is off-loaded. The increase is about .073 km/kg (.018 n.mi. per lb) of payload. Of interest here is that as designed, the point design vehicle is fuel volume limited and no additional fuel can be added as the payload is reduced as is the case for most conventional hydrocarbon fueled aircraft. In the real world, the advisability of carrying extra tankage to increase flexibility would be a matter of route structure and economics. The method of construction of the vehicle would allow enlargement of the tanks by a simple fuselage plug within the limits of aircraft strength and the wing area selected.

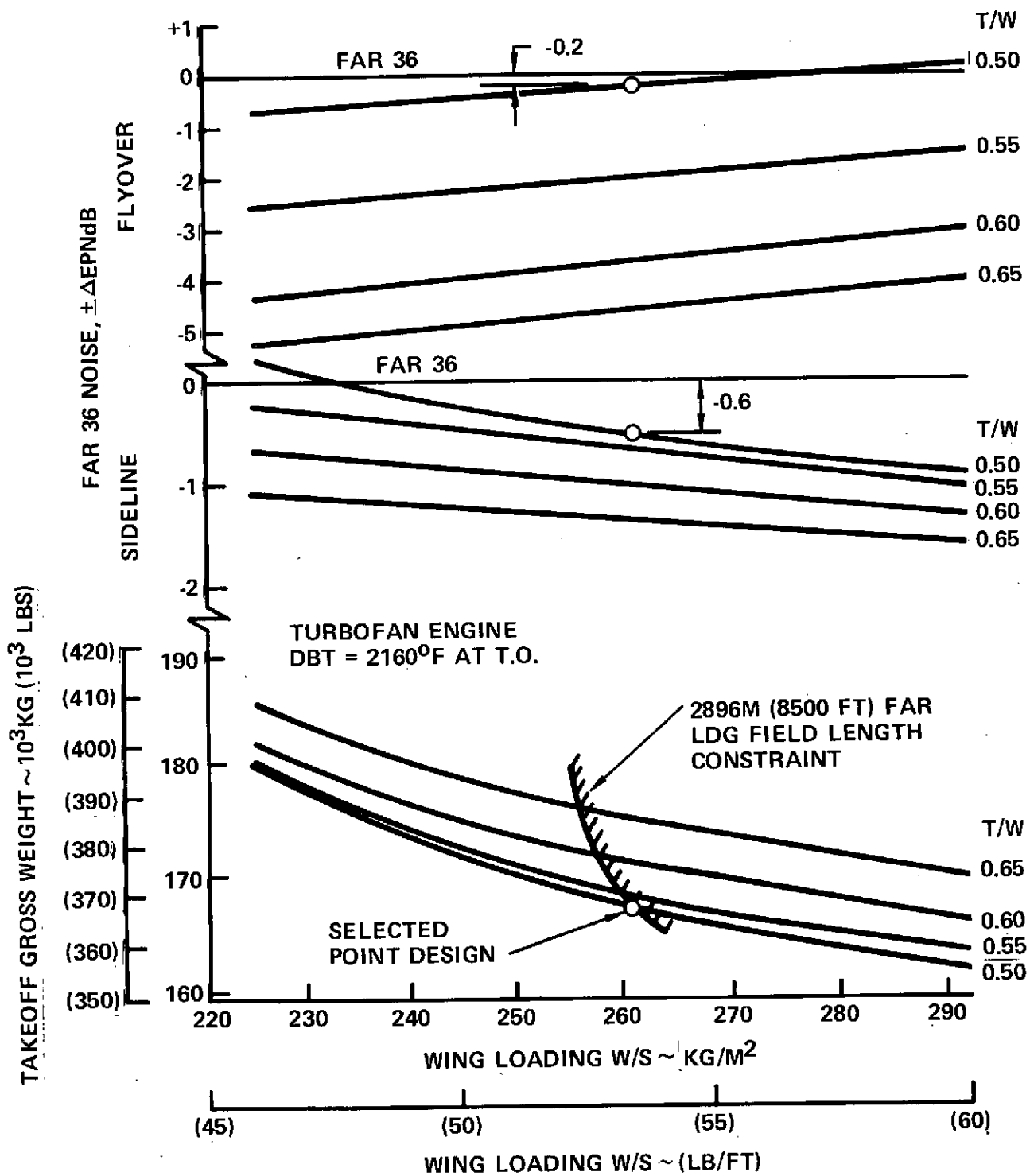


Figure 85. Noise and Gross Weight vs. T/W and W/S

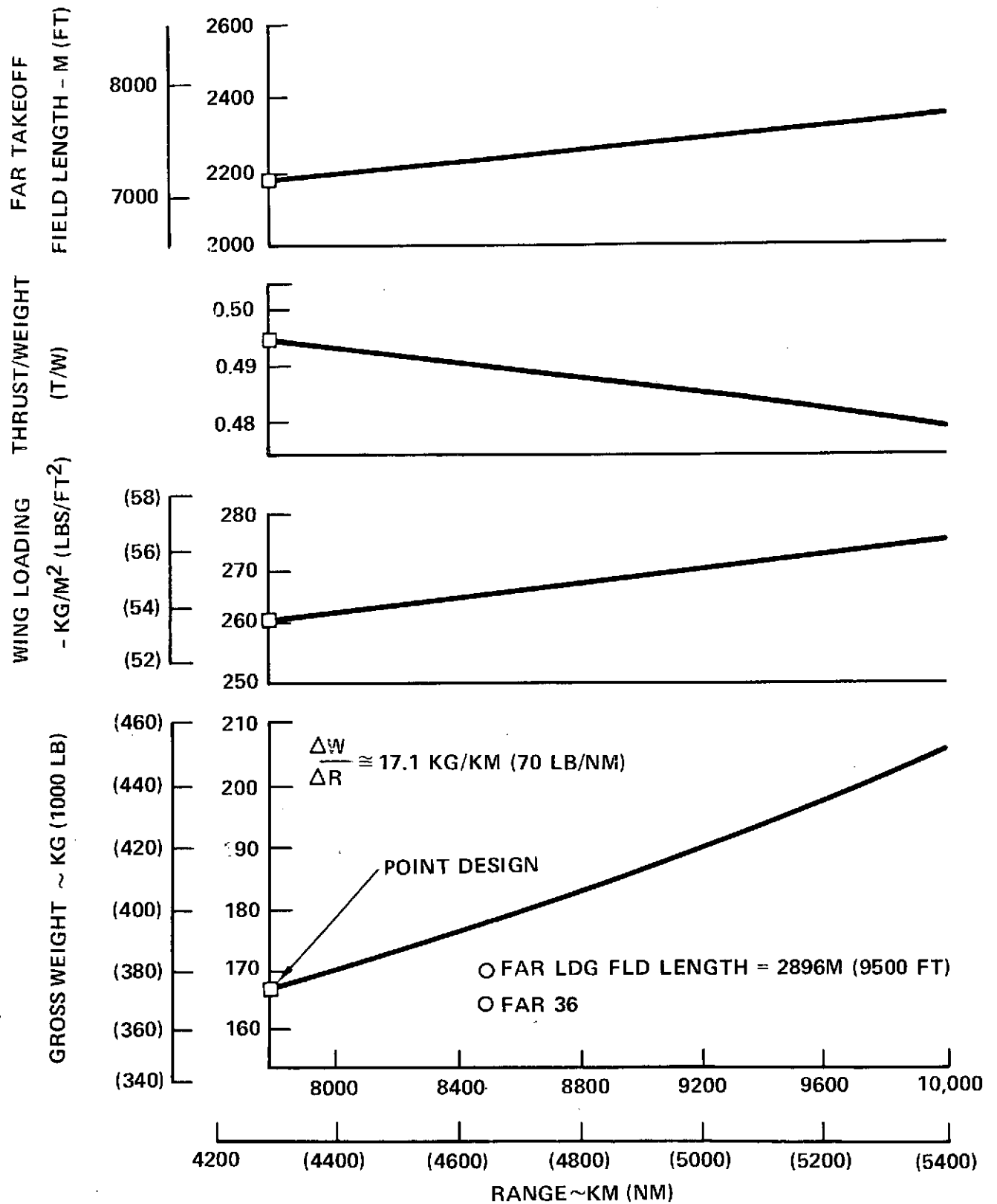


Figure 86. Gross Weight, W/S, T/W, and T.O. Field Length vs Range

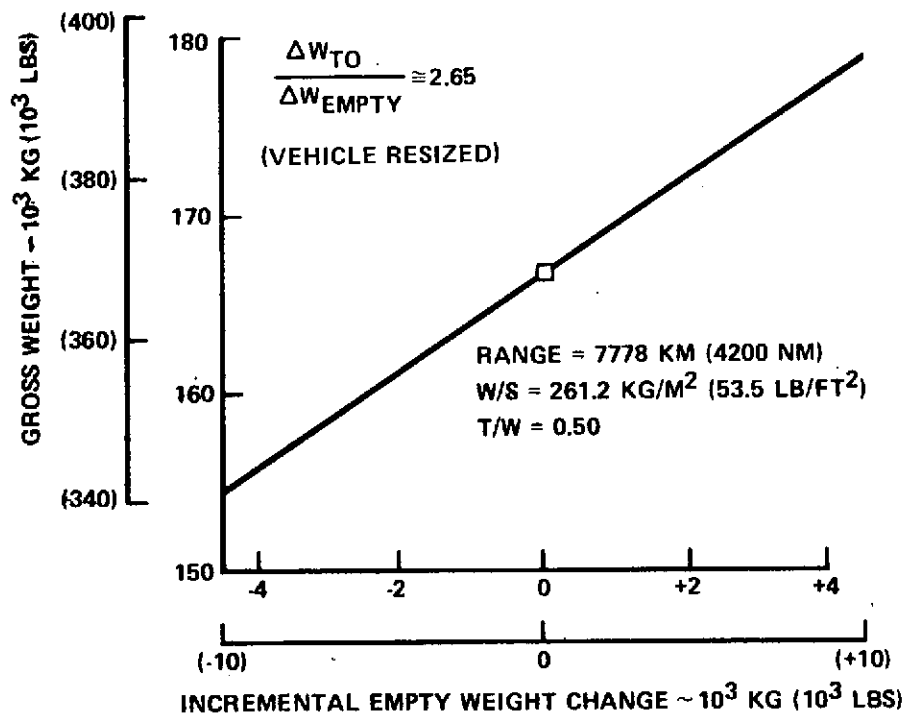


Figure 87. Empty Weight Change vs. Gross Weight (Constant Range)

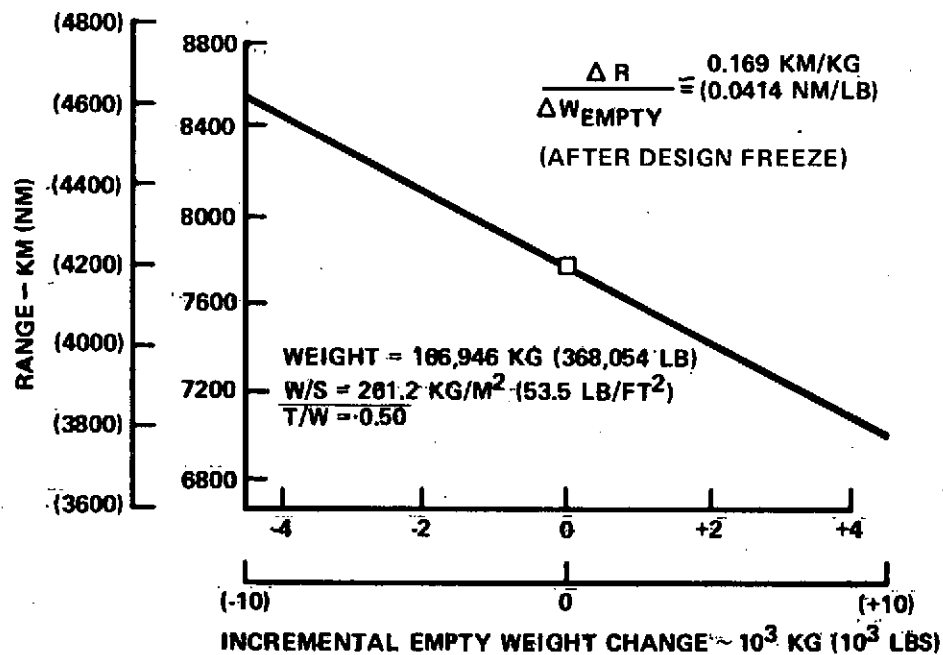


Figure 88. Empty Weight Change vs. Range (Constant Gross Weight)

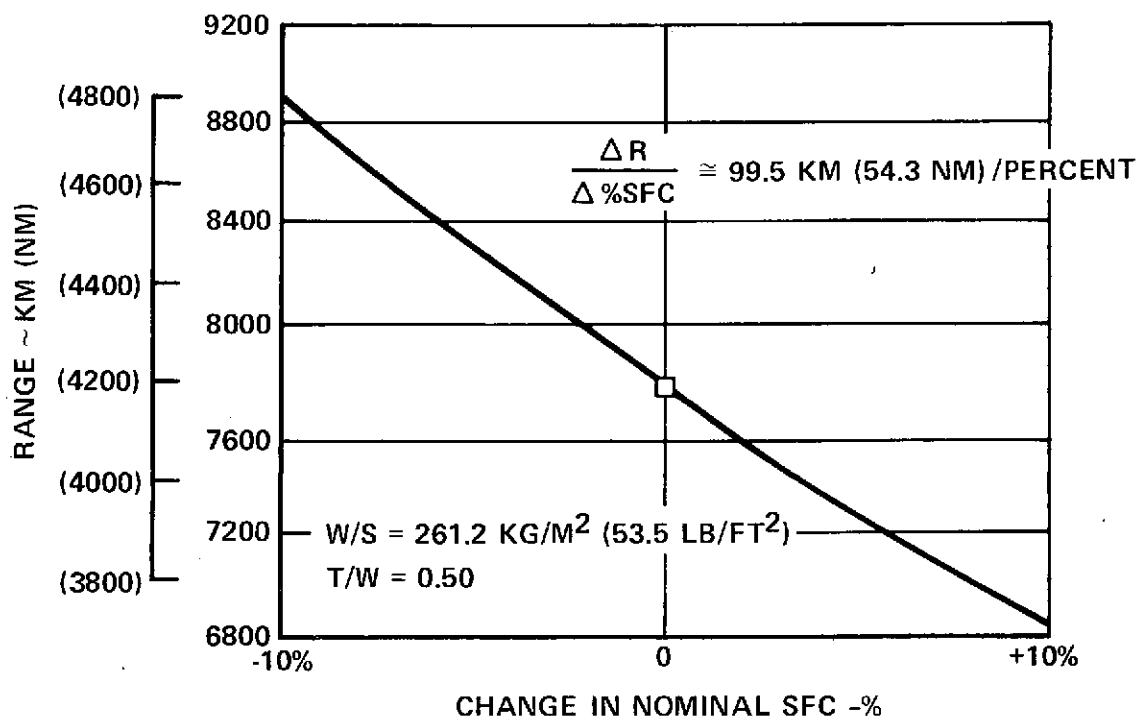


Figure 89. Specific Fuel Consumption vs. Range

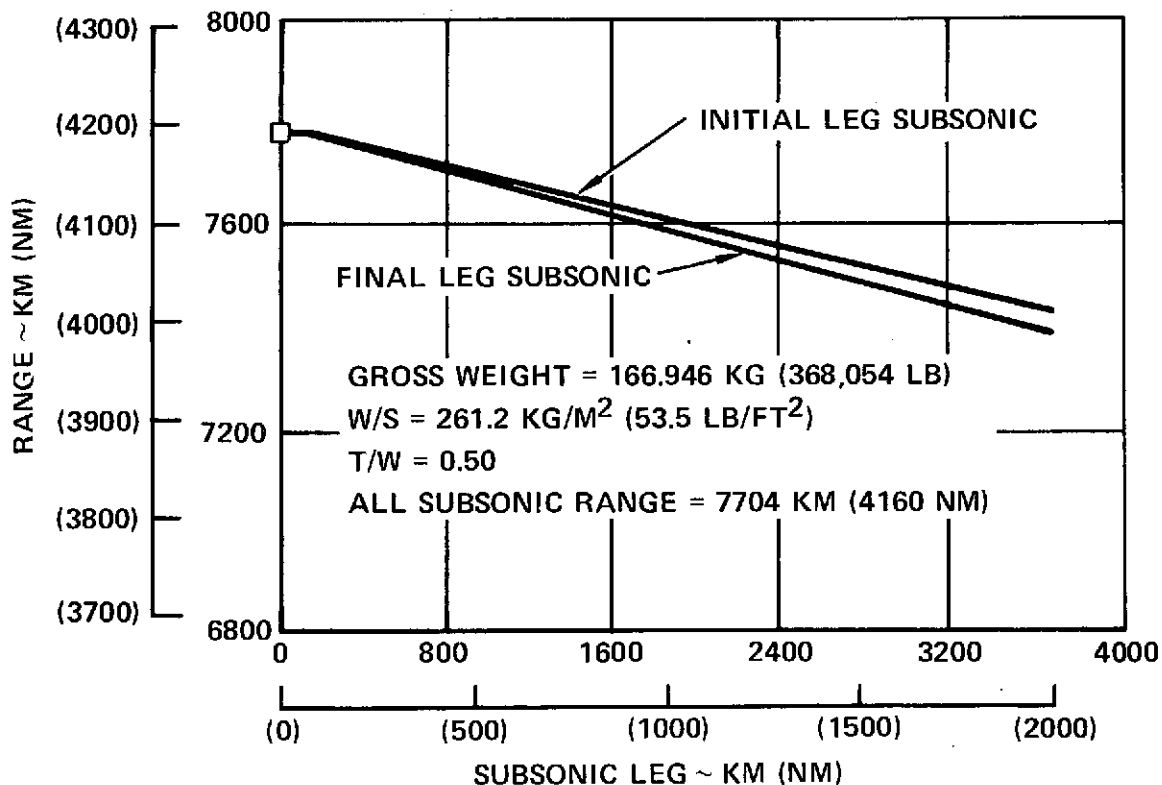


Figure 90. Effect of Subsonic Cruise Leg on Total Range

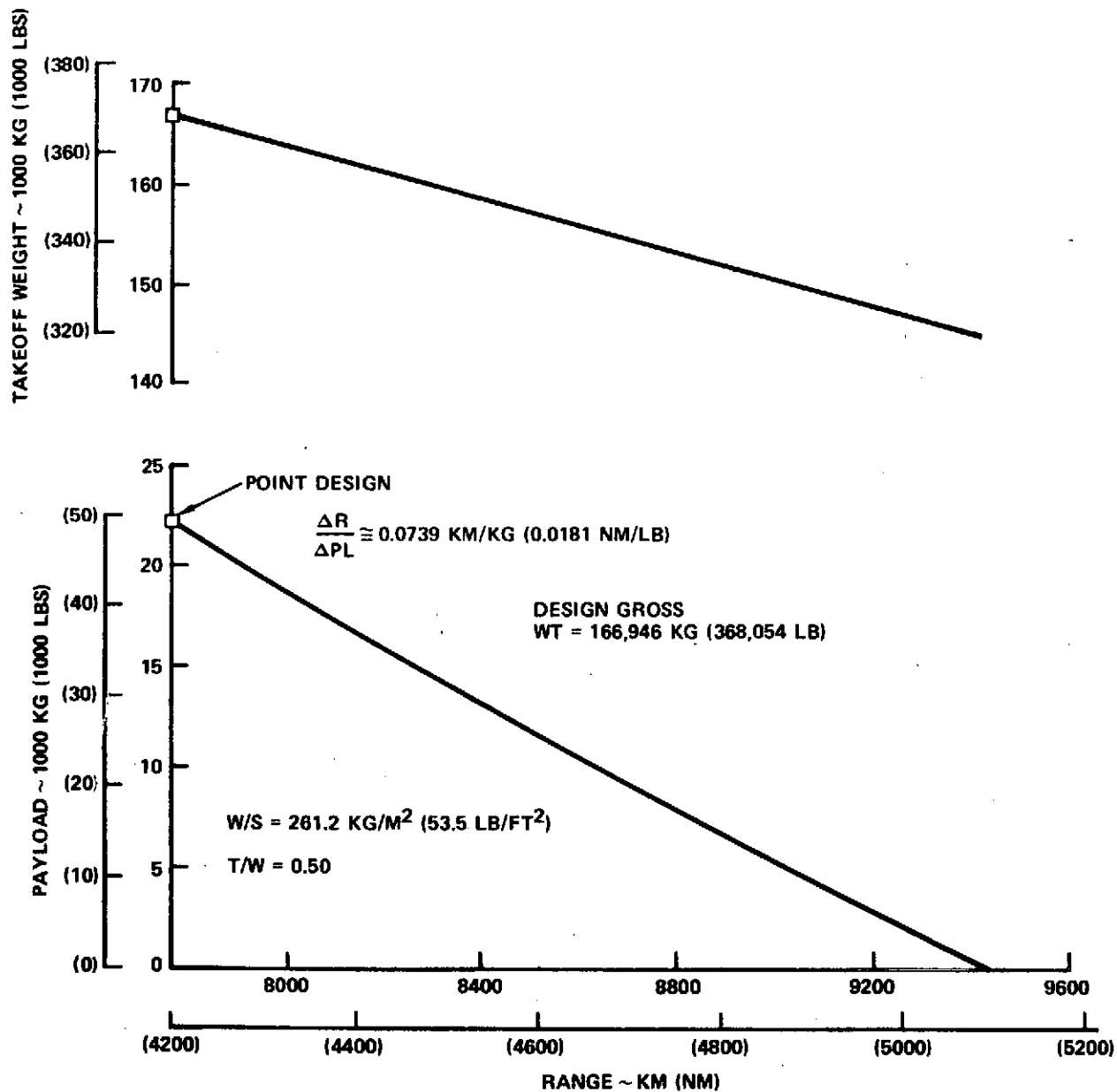


Figure 91. Payload vs. Range (Point Design)

If the engine noise constraint were to be tightened (made more restrictive), the point design gross weight would increase about 3,000 lbs for each EPNdB reduction. This is shown in Figure 92 which also indicates the increase in thrust-to-weight required as the allowable jet velocity is reduced. The wing loading is decreased to allow a higher climb-out flight path angle, thereby increasing altitude at the critical flyover point 6.48 km (3.5 n.mi.) from brake release. The increasing slope of the curve should also be noted as the maximum noise reduction investigated (5 EPNdB) is approached.

Of equal importance to engine specific fuel consumption is the drag level. Figure 93 shows a change of about 100 km (54 n.mi.) for each drag count. The analysis assumed that the change in nominal drag was applied uniformly to the zero-lift drag at all Mach numbers.

Figure 94 shows a gross weight increase of about 8.62 kg (19 lb) per .3048 m (1 ft) reduction in FAR landing field distance. In each case the wing area has been increased (lower W/S) in order to reduce the landing approach speed as the field length is shortened.

In Figure 95, the effect of a reduction from the selected noise limited take-off duct burning temperature of 2160°R is shown for the point design airplane. As the power is reduced, the takeoff distance increases, maximum sideline noise decreases and flyover noise increases. The increase of flyover noise is due to the lower flightpath angle with a subsequent reduction in altitude at the 3.5 n.mi. measuring point. This figure is included to illustrate the tradeoff between sideline and flyover noise as the power (jet velocity) is changed.

In conclusion, the following observations can be made with regard to the performance and sensitivity studies:

- The critical constraints on the vehicle are airport noise and landing field distance requirements.
- The turbofan engine characteristics allows meeting the noise requirements with a reasonable thrust-to-weight ratio and flexibility in off-mission performance (subsonic cruise).

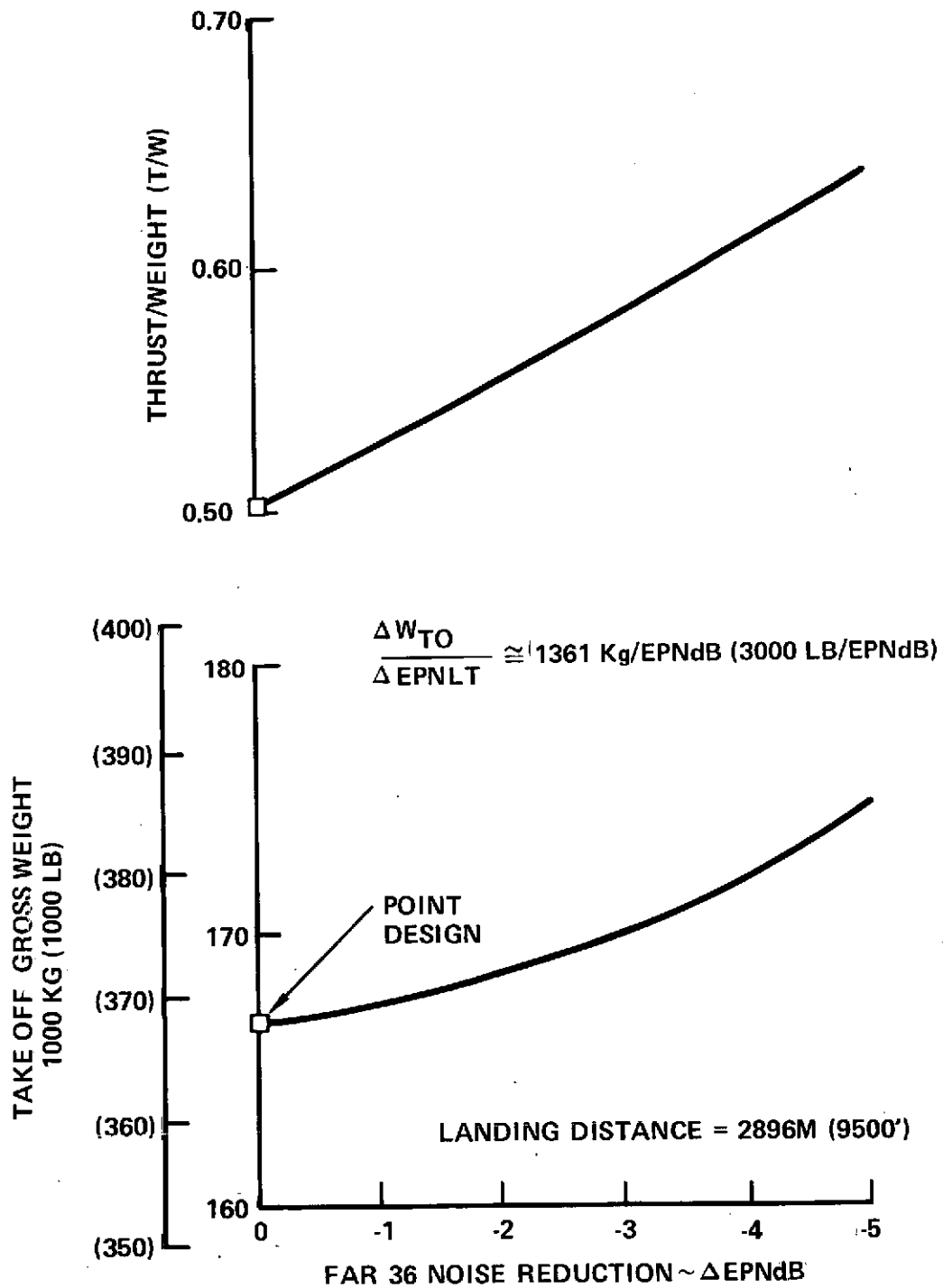


Figure 92. Gross Weight vs. Engine Noise

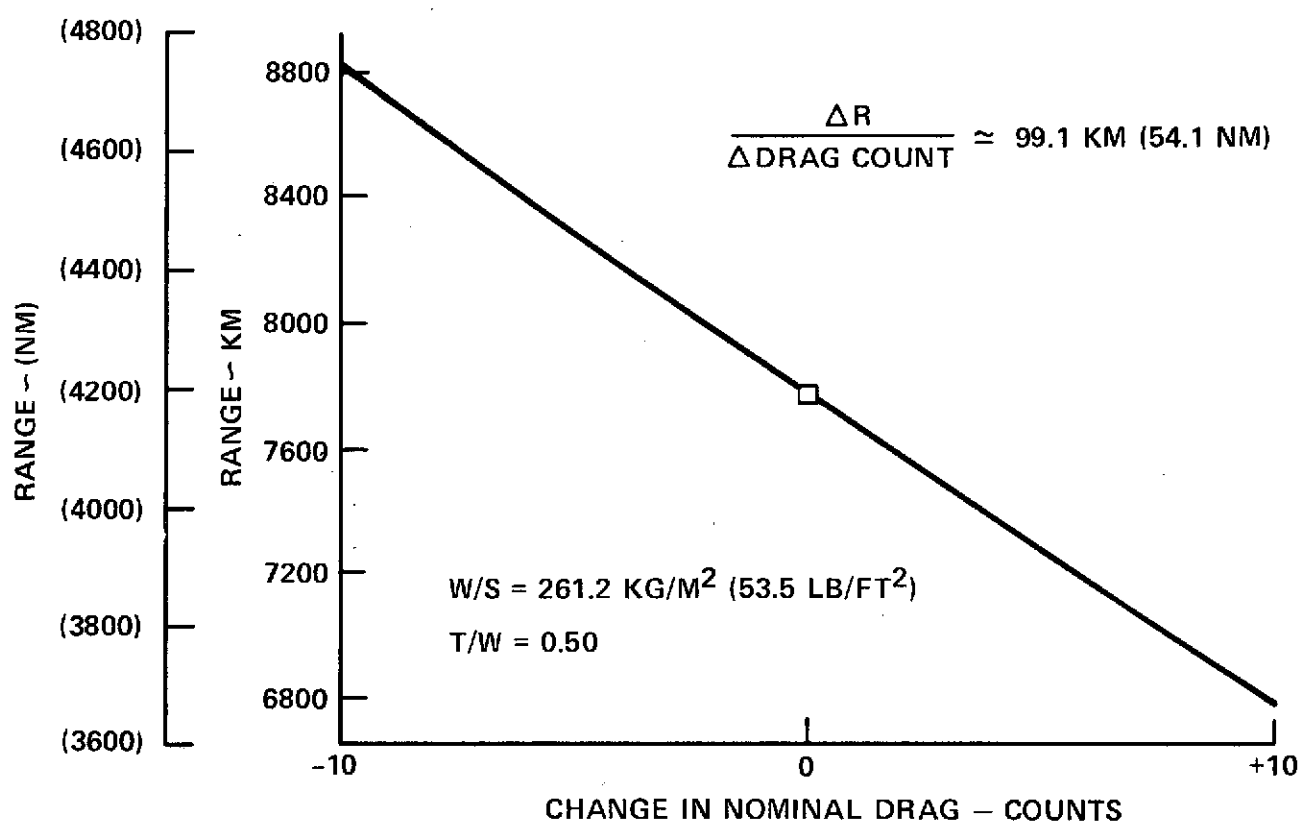


Figure 93. Range vs. Drag Level

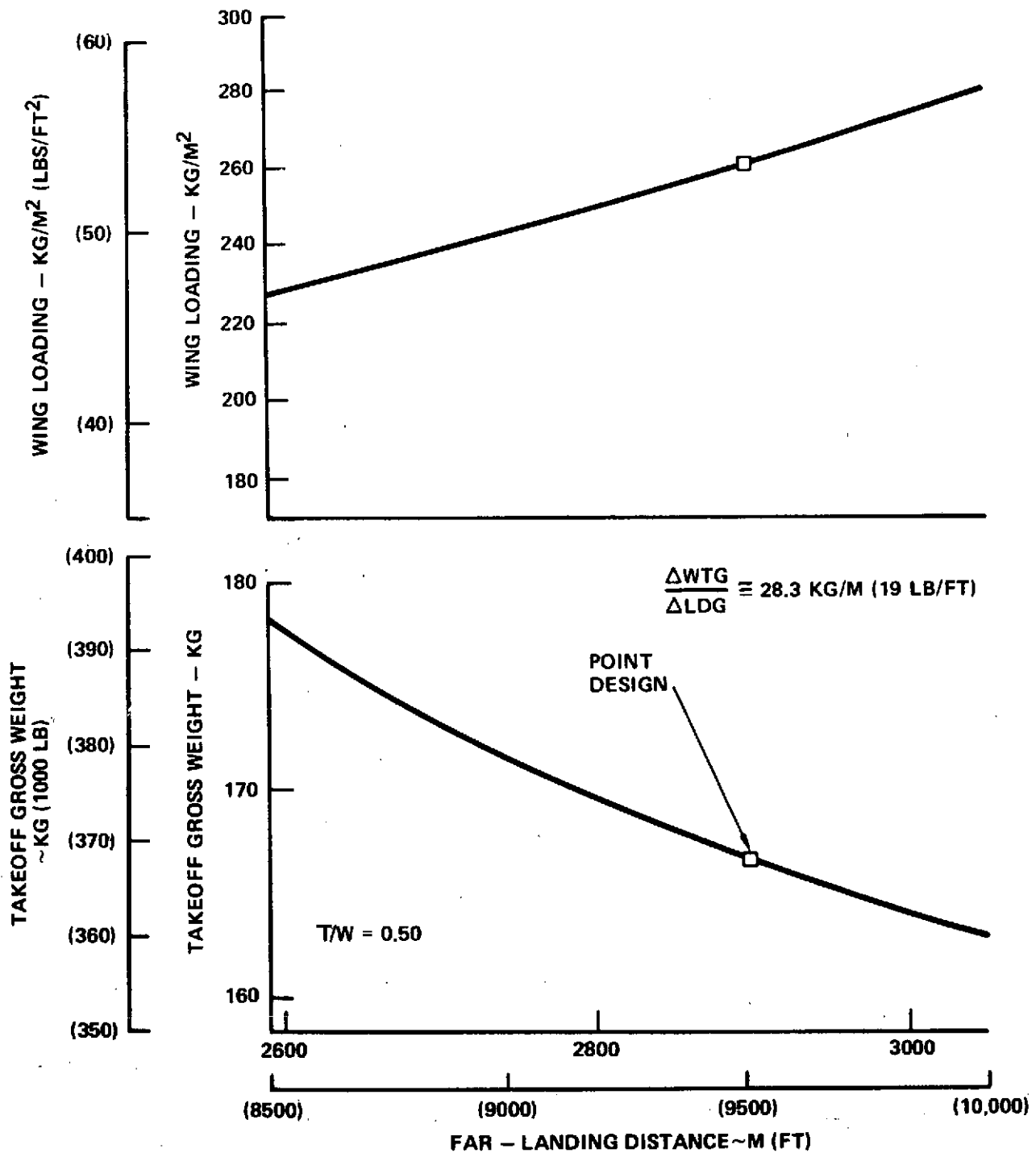


Figure 94. Gross Weight vs. Landing Field Length

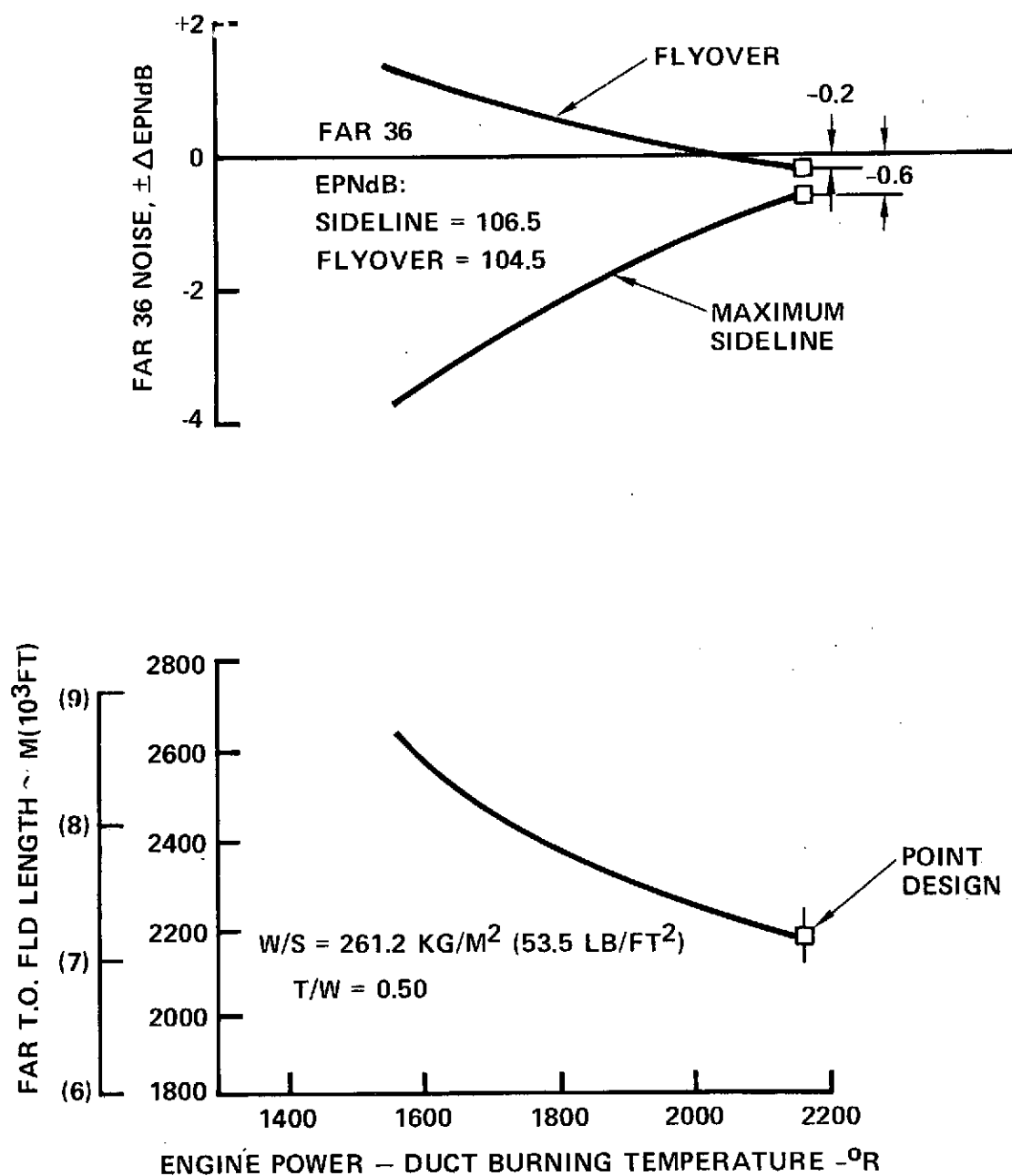


Figure 95. Engine Takeoff Power Setting vs. Takeoff Distance and Noise

- Ranges up to 10,000 km (5,400 n.mi.) can be achieved at a reasonable increase (23 percent) in the point design aircraft gross weight.
- Compared to the hydrocarbon fueled AST the hydrogen vehicle should be less sensitive (lower growth factors) to SFC, empty weight, and drag changes because of its lower fuel function (0.26 compared to 0.52 for the Jet A-1 airplane).

4.2.3 Environmental Summary

4.2.3.1 Airport Noise Footprint

An airport noise footprint for the selected aircraft was determined by computing noise levels for a complete gridwork consisting of 12 microphone locations along the flight path and at 9 different sideline distances. The resulting matrix of noise levels at each of these 108 points, shown on Table 19, is interpolated to determine the locus of points of fixed noise levels. A plot of these contour lines (footprint) is shown on Figure 96 for the selected point design aircraft. The takeoff gross weight for the aircraft is 166,946 kg (368,054 lbs). At this weight, FAR Part 36 specifies a sideline noise limit of 106.5 EPNdB at a distance of 648.6 m (2,128 ft) from centerline of the runway and a flyover value of 104.5 EPNdB (6.48 km (3.5 n.mi.) from brake release. Both of these constraint limits are greater than the actual values computed for the selected aircraft. The peak noise level of the specified sideline distance, 105.9 EPNdB, occurs at 2,533 m (8,310 ft) from brake release and contains 5,333 km² (1,318 acres) within this noise level contour. At the flyover measurement point 6.48 km (3.5 n.mi.) from brake release, a noise level of 104.3 EPNdB is calculated. The area within this contour line is 6,879 km² (1,700 acres). A plot of area contained within constant noise level contour lines versus effective perceived noise levels for the selected aircraft is shown on Figure 97.

4.2.3.2 Sonic Boom Signatures

The sonic boom overpressure signatures for selected points along a typical mission flight path ground track are presented in Figures 98 through 101.

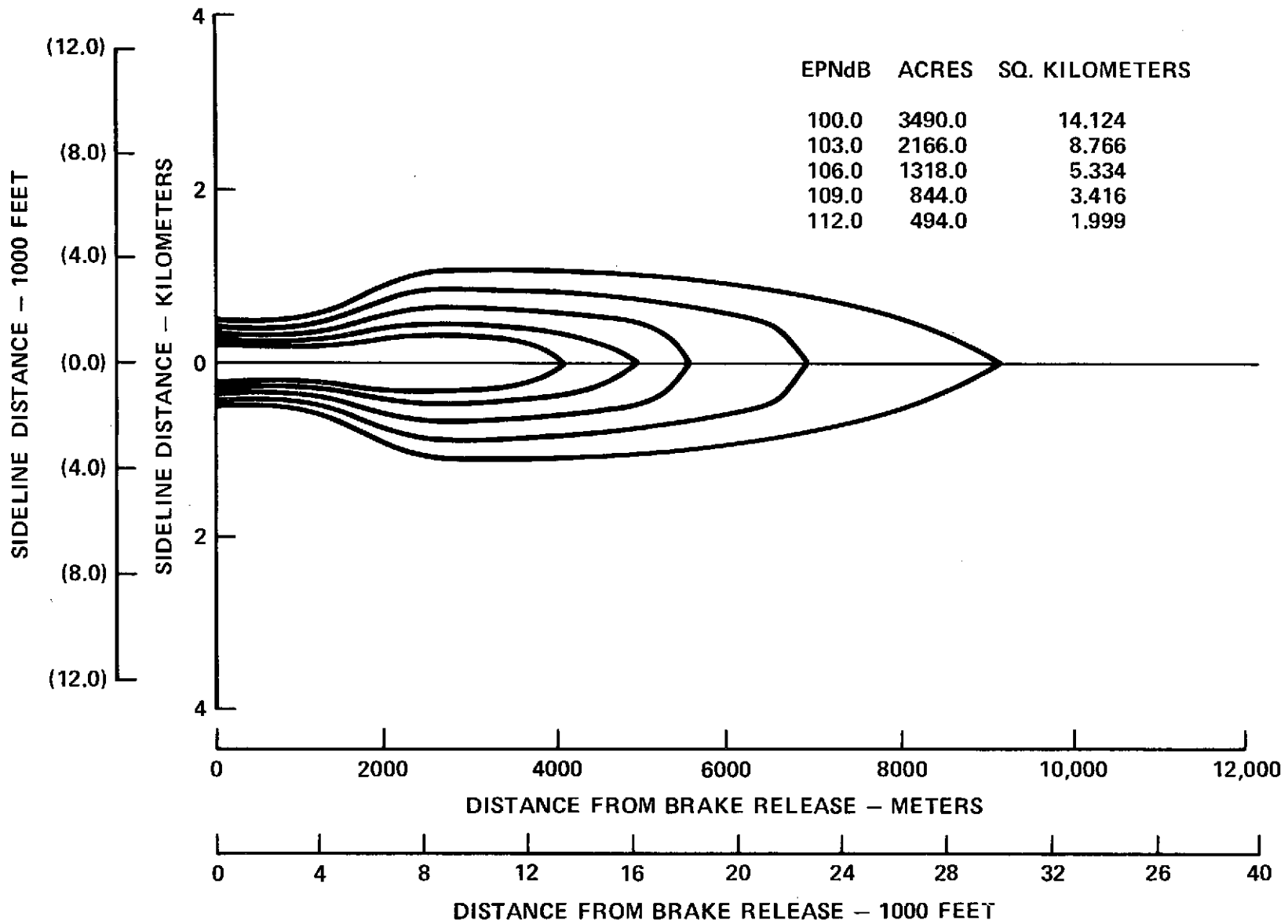


Figure 96. Takeoff Noise Contours

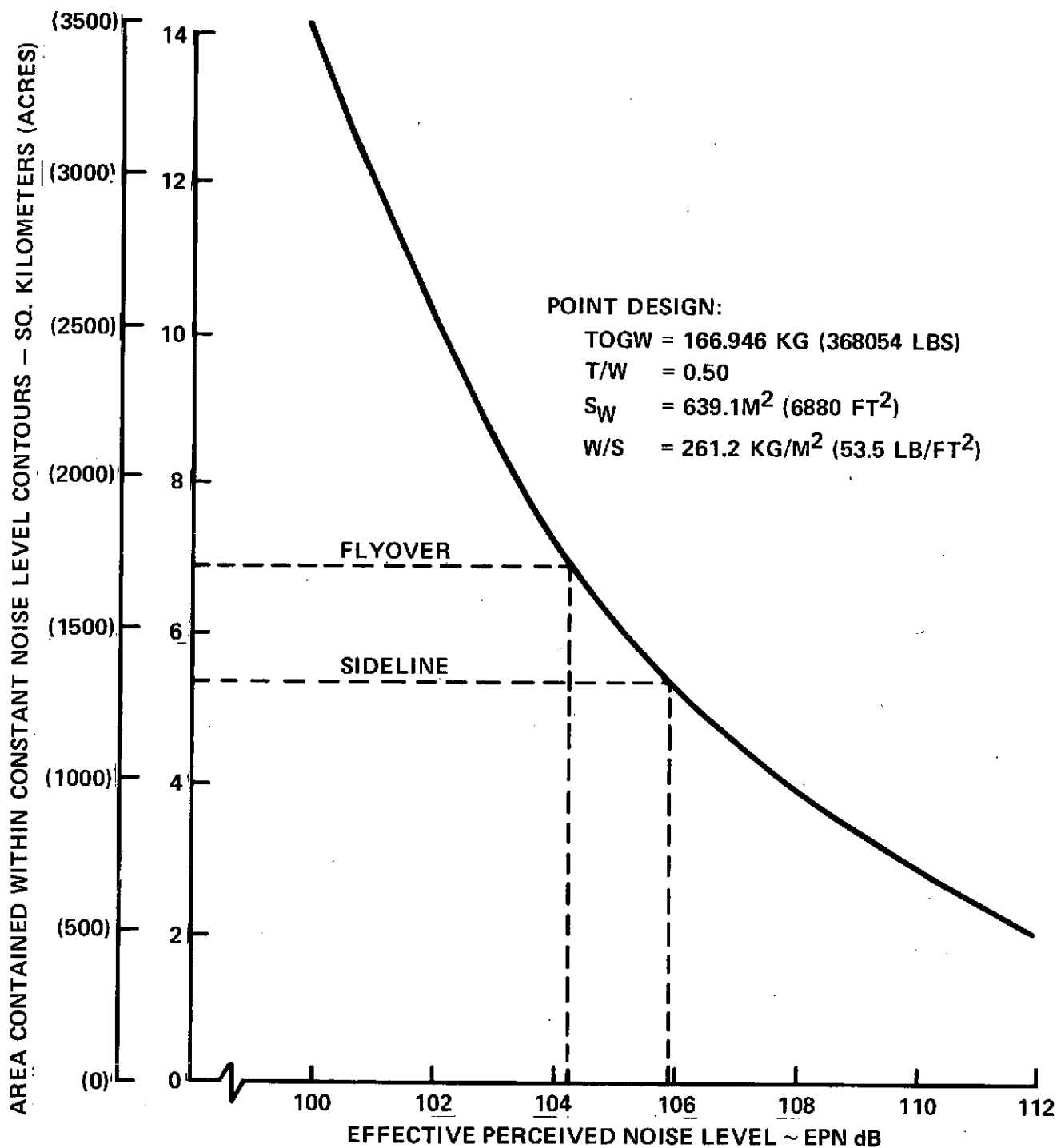


Figure 97. Area Contained Within Constant Noise Level Contour Lines vs. Effective Perceived Noise Levels

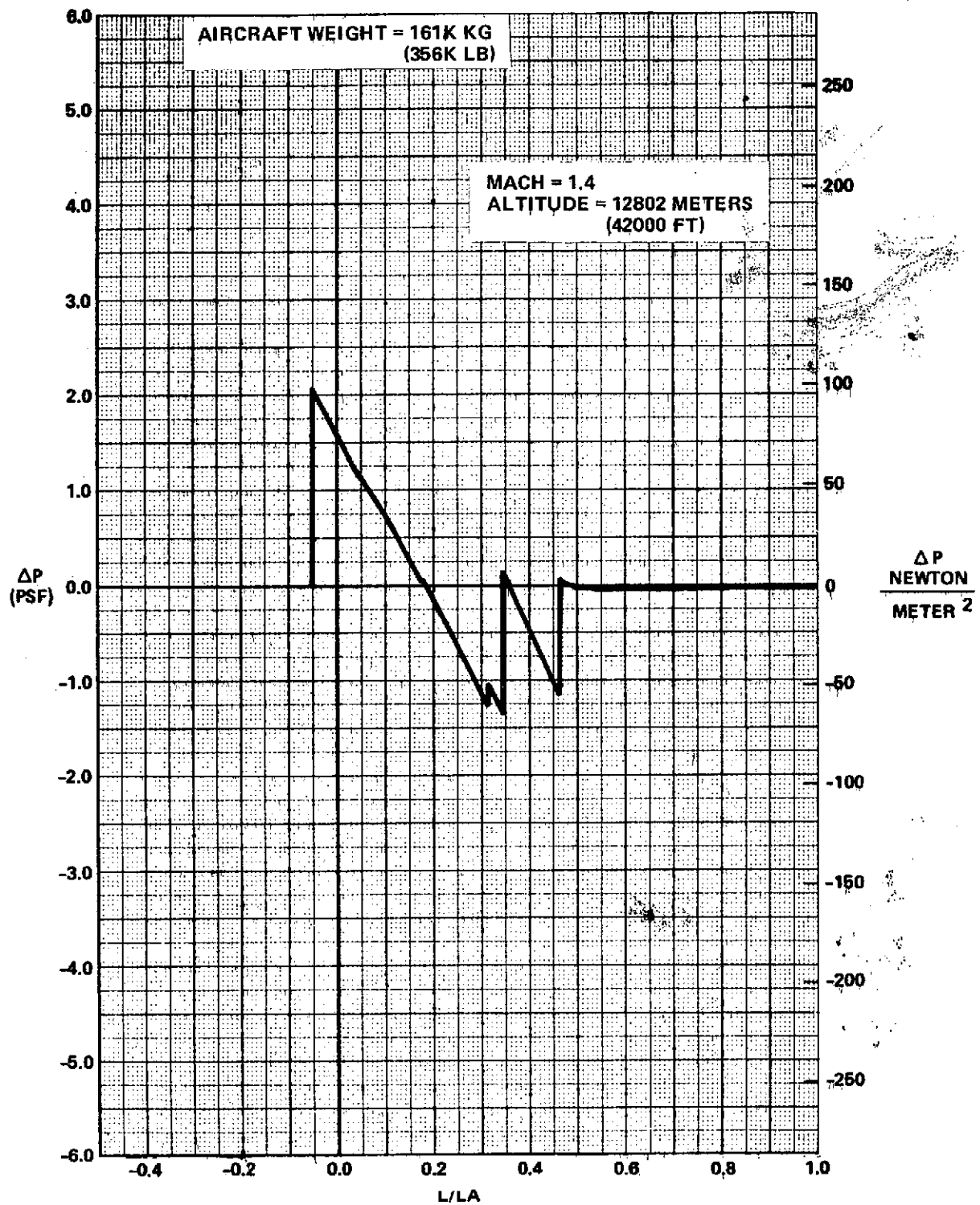


Figure 98. Sonic Boom Overpressure Signature, Aircraft Weight = 356K LB

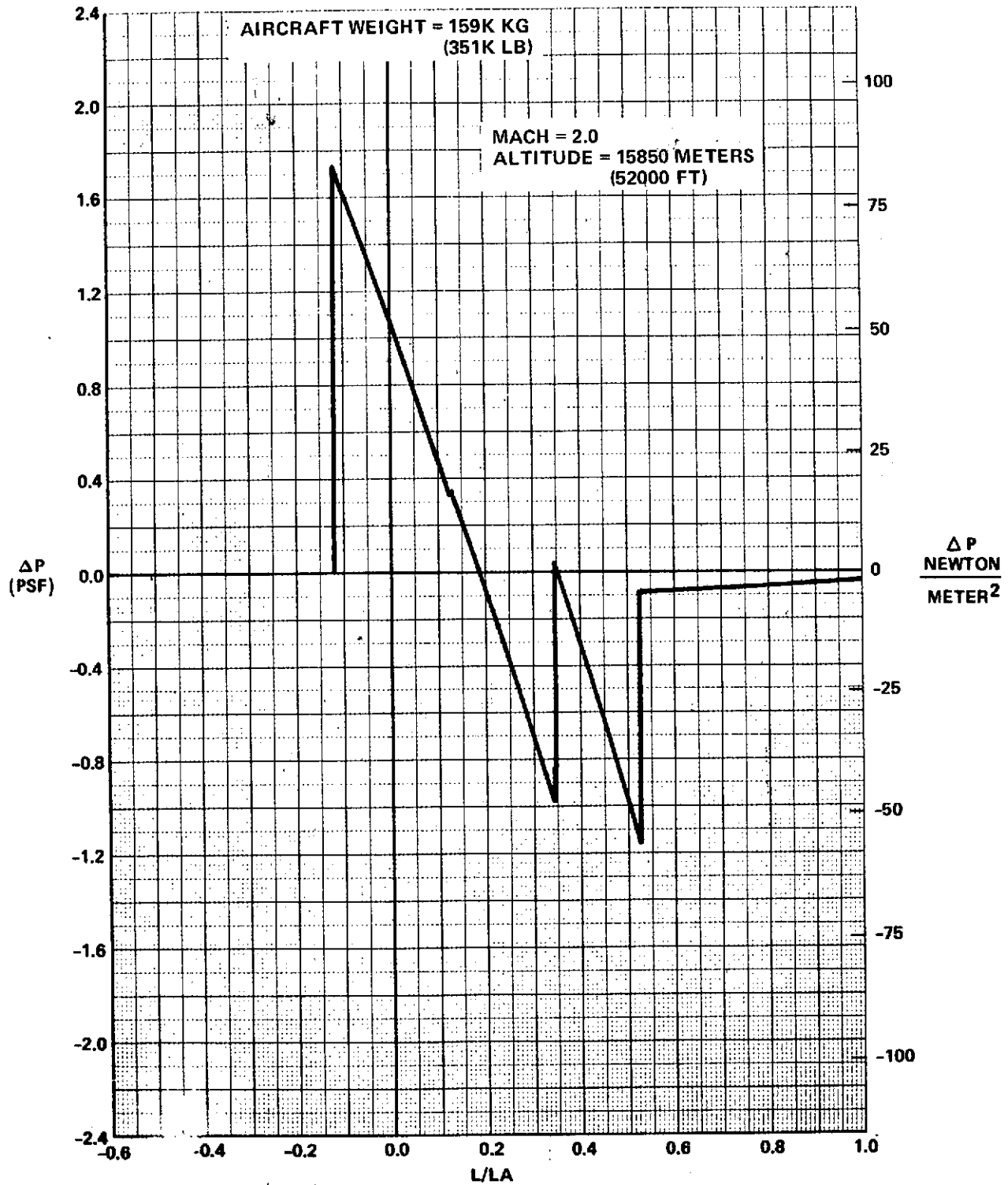


Figure 99. Sonic Boom Overpressure Signature - Aircraft Weight = 351K LB

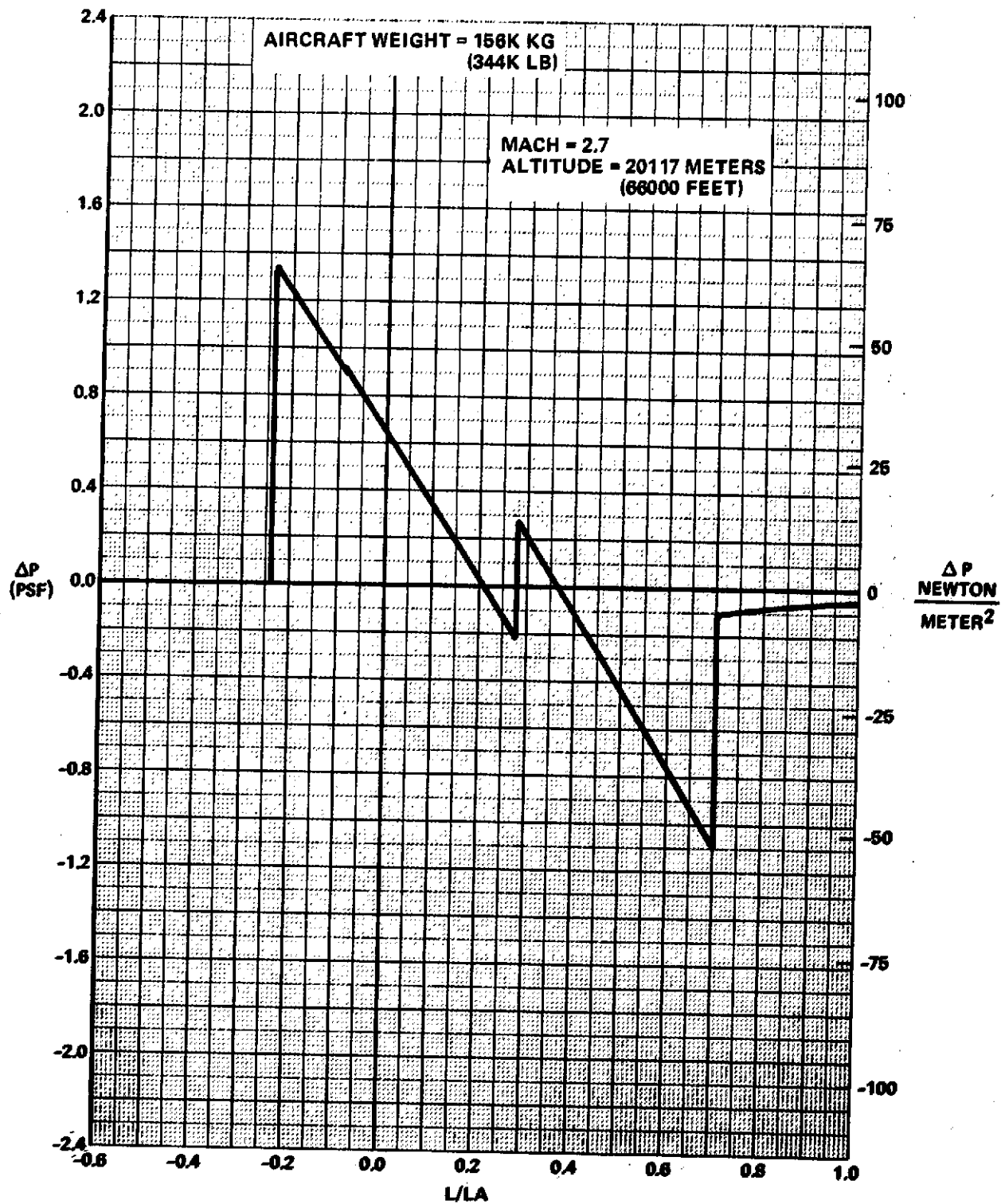


Figure 100. Sonic Boom Overpressure Signature - Altitude Weight = 344K LB

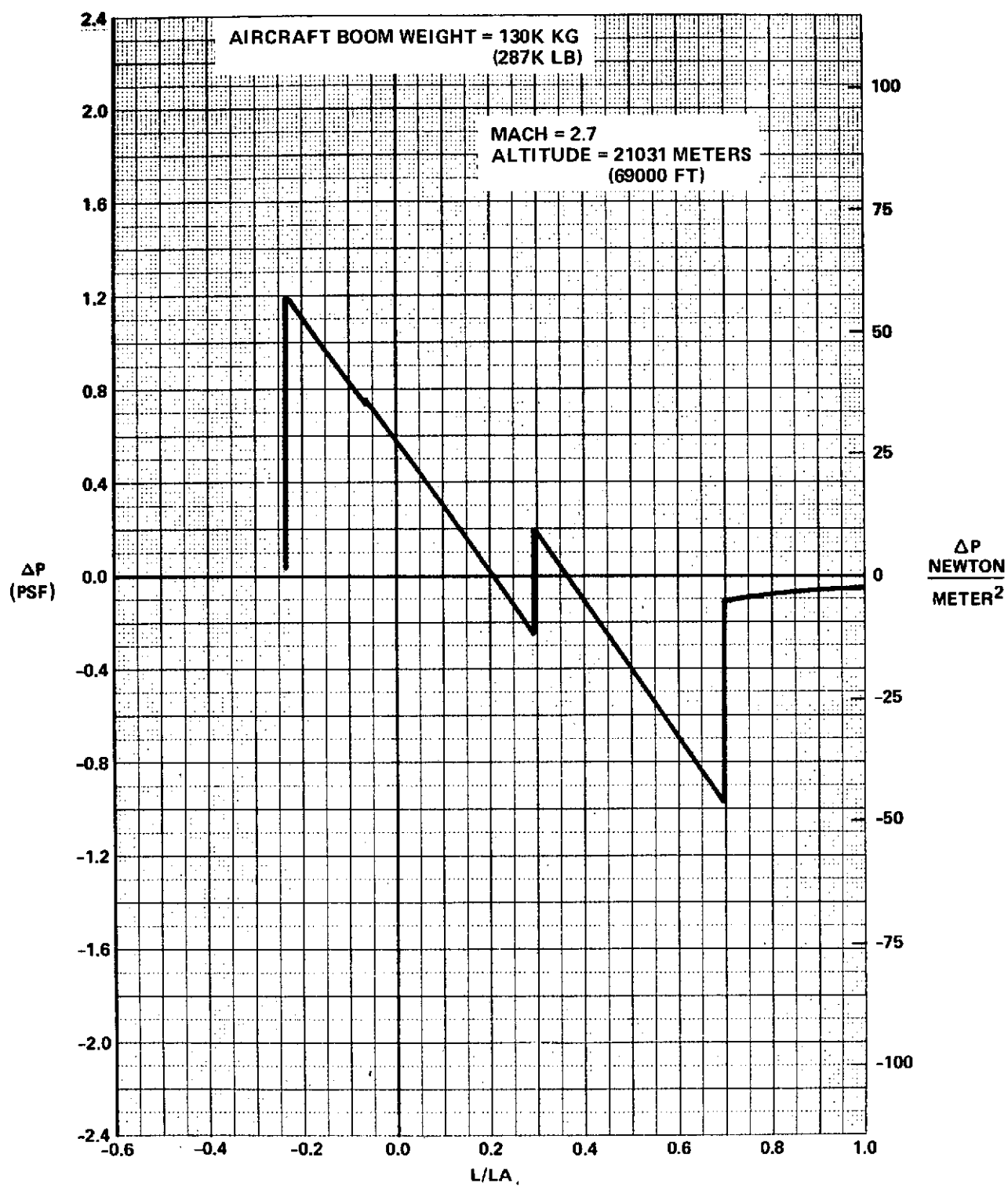


Figure 101. Sonic Boom Overpressure Signature - Aircraft Weight = 287K LB

TABLE 19. SIDELINE NOISE LEVEL MATRIX FOR PLOTTING FOOTPRINT CONTOURS

Sideline Distance m (feet)	Distance from Brake Release - m (feet)					
	30.5 (100.0)	1,219.0 (4,000.0)	2,438.0 (8,000.0)	3,048.0 (10,000.0)	3,658.0 (12,000.0)	4,420.0 (14,500.0)
0.0 (0.0)	95.9	122.9	118.6	117.7	114.1	110.5
76.2 (250.0)	121.8	121.0	120.2	117.1	113.8	110.3
152.4 (500.0)	116.4	115.7	117.0	115.3	112.9	109.9
304.8 (1,000.0)	108.4	108.7	112.3	111.7	110.5	108.5
457.2 (1,500.0)	101.2	103.1	109.1	108.7	108.1	106.8
648.6 (2,128.0)	93.8	97.9	105.8	105.8	105.4	104.6
914.4 (3,000.0)	87.8	93.1	101.8	102.0	101.9	101.5
1,219.0 (4,000.0)	83.4	89.9	97.6	97.9	97.9	97.5
2,438.0 (8,000.0)	73.4	79.8	85.2	85.9	86.1	86.2
	5,182.0 (17,000.0)	5,944.0 (19,500.0)	6,486.0 (21,280.0)	7,315.0 (24,000.0)	8,534.0 (28,000.0)	9,754.0 (32,000.0)
0.0 (0.0)	107.7	105.5	104.2	102.5	100.3	98.8
76.2 (250.0)	107.6	105.5	104.2	102.5	100.3	98.8
152.4 (500.0)	107.4	105.3	104.1	102.4	100.2	98.7
304.8 (1,000.0)	106.4	104.7	103.6	102.0	99.9	98.5
457.2 (1,500.0)	105.2	103.8	102.8	101.3	99.5	98.2
648.6 (2,128.0)	103.5	102.4	101.6	100.2	99.0	98.1
914.4 (3,000.0)	100.8	99.9	99.3	98.9	97.9	97.4
1,219.0 (4,000.0)	97.9	98.1	97.8	97.6	96.2	93.6
2,438.0 (8,000.0)	86.1	85.9	85.8	85.7	85.5	85.2

NOTE: Values in Table are noise levels in EPNdB

NASA/Langley program SONIC was used for this analysis. The flight conditions for the LH₂ point design configuration are summarized in Table 20 - no winds nor maneuvers were considered.

The overpressure and lift parameters calculated for these cases are also presented in Table 20. It should be noted that these parameters are basically far field terminology "left over" from the early days of sonic boom analyses. However, they are still quite useful for conducting tradeoff studies of closely-related configurations such as the present study, even though the calculated signatures clearly demonstrate near field effects.

TABLE 20. SONIC BOOM TABLE

Mach No.	Altitude ~ meter (ft)	Weight ~ kg (lbs)	Flight Condition	Overpressure Parameter	Lift Parameter	ΔP ~ $\frac{\text{newton}}{\text{m}^2}$ (lb/ft ²)
1.4	12,802 (42,000)	161,479 (356,000)	Climb	.0468	.0031	99.59 (2.08)
2.0	15,850 (52,000)	159,211 (351,000)	Climb	.0505	.0042	82.83 (1.73)
2.7	20,117 (66,000)	155,912 (343,728)	Start Cruise	.0588	.0064	63.20 (1.32)
2.7	21,031 (69,000)	130,343 (287,358)	End Cruise	.0589	.0062	56.98 (1.19)

The maximum overpressure calculated was 99.59 newtons/m² (2.08 psf). It occurred during the climb to cruise altitude at M = 1.4 and 12,802 meters (42,000 ft). During cruise, a maximum overpressure of 63.2 newton/m² (1.32 psf) was found to occur at start of cruise when the aircraft was heavy and at the lowest cruise altitude. At the end of cruise, sonic boom overpressure was reduced to 56.98 newtons/m² (1.19 psf).

4.2.3.3 Emissions

Table 21 compares the combustion of hydrogen with Jet A-1, a kerosene type hydrocarbon, in terms of exhaust products, and qualitatively forecasts the probability of being able to comply with standards anticipated for 1990. As can be seen, the hydrogen fuel, which has no carbon atoms, eliminates unburned hydrocarbons, carbon dioxide, carbon monoxide, and particulate carbon (smoke) from the engine exhaust. This allows the burner design efforts to be directed at reducing the NO_x emissions. Due to the differences in fuel boiling point the extremely high temperature combustor pilot zone which is needed in JP burners to provide good low-power efficiency for reduced carbon monoxide and unburned hydrocarbons, is not required for a hydrogen burner. Even though hydrogen burns stoichiometrically approximately 311°K (100°F) higher than Jet A-1, the improved reaction rates, mixing

TABLE 21. EMISSIONS - JET A-1 vs LH₂ FUEL

1990 CRITERIA

Emission Product	Compliance With Anticipated Standards	
	LH ₂	Jet A-1
CO	0	Difficult
CO ₂	0	Difficult
Unburned Hydrocarbons	0	Difficult
NO _x	Acceptable	Difficult
Smoke	0	Difficult
H ₂ O	Acceptable	Acceptable

characteristics, and the gaseous phase of hydrogen will permit burner designs to be tailored to reducing the time spent at peak temperature which is where NO_x is produced.

By properly designing a burner for hydrogen combustion, lower NO_x emissions in parts per million of engine exhaust will be attainable as compared to a JP engine. The vehicle analysis results show that the engine thrust requirement is reduced by almost one-half for a hydrogen fueled aircraft because of the TOGW reduction achieved with the reduced fuel weight. This thrust reduction further decreases the total NO_x emissions per flight.

Water vapor is the principal product of combustion of hydrogen. It is expected a hydrogen fueled AST will produce not quite twice the quantity of H₂O emitted by a conventionally fueled (Jet A-1) supersonic transport. During cruise the subject point design airplane uses 3.19 kg (7.03 lbs) of LH₂ per second. Assuming 100 percent combustion efficiency, this generates 28.5 kg (62.8 lbs) of H₂O per second. By contrast, an equivalent design of Jet A-1 fueled AST will use 11.6 kg (25.6 lbs) of fuel per second and, again assuming 100 percent combustion efficiency, will generate 15.1 kg (33.2 lbs) of H₂O per second.

4.3 VEHICLE COST

4.3.1 Summary of Vehicle Cost

The cost estimates provided for the liquid hydrogen AST include Development, Production and Operations. The summary of the development and production costs are presented in Table 22. The operations costs are presented, along with the system parameters in Tables 23 and 24. More detailed presentation of the development, production, and DOC/IOC/ROI are included in the computer printout for the point design in Appendix B. The development cost in Table 22 includes the production cost of the 4 vehicles used in the flight

TABLE 22. INVESTMENT COST SUMMARY (\$ - MILLIONS)

<u>Development</u>			
	Airframe	\$2661.51	
	Engine	\$ 658.98	
	Total	\$3320.49	
	Production Quantity	300 Aircraft	600 Aircraft
<u>Production</u>			
	Airframe	\$29.93	\$25.15
	Engines	8.55	7.69
	Avionics	.50	.50
	Profit	4.49	3.77
	Insurance and Taxes	2.99	2.52
	Warranty	1.50	1.26
	Total	\$47.96	\$40.89
<u>Other Investment</u>			
	Spares	7.20	6.23
	Special Support Equipment	2.40	2.05
	Production Tooling	1.41	.60
	Technical Data	.29	.25
	Total	\$11.30	\$ 9.13
	Grand Total Production	\$59.26	\$50.02

TABLE 23. SYSTEM COST SUMMARY (4200 n.mi. STAGE LENGTH)

	<u>300 Aircraft</u>	<u>600 Aircraft</u>
Passenger Capacity	234	234
Fleet Size	14+	14+
Utilization (block hours)	3600	3600
Stage Length Kilometers (n.mi.)	7778 (4200)	7778 (4200)
Revenue Passenger Miles (B)	7.24	7.24
Load Factor	.55	.55
DOC Cents/seat kilometer (cents/S n.mi.)	1.14 (2.06)	1.01 (1.87)
IOC Cents/seat kilometer (cents/S n.mi.)	.50 (.92)	.50 (.92)
ROI (percent) (after taxes)	6.04	10.93
Fare (\$/trip)	249	249

test program. Normally only one vehicle will remain in the development category after completion of the development test program and the other vehicles are converted to production status and sold. With one vehicle remaining in R&D status and the remaining three sold at the average cost of the production buy would mean a recoupment in the development program of \$143.9 million for the 300 aircraft production lot and \$122.7 million for the 600 production buy.

The cost for the LH₂ AST as used in the calculation of the DOC includes the total production cost, the production tooling, technical data, and the pro rate share of the total development cost. The airframe and engine cost breakdown with the inclusion of the items noted above is:

Airframe	\$49,983,000 (including avionics)
Engine	<u>\$10,744,000</u>
Total Cost	\$60,727,000

The costs and fare presented in Table 23 are calculated on the basis of a route stage length that is equal to the design range of the airplane. In actual operation the average stage length flown by an aircraft is considerable less than the design range and the productivity is reduced.

TABLE 24. SYSTEM COST SUMMARY (2200 n.mi. STAGE LENGTH)

Passenger Capacity	234
Fleet Size	9.+
Utilization (block hours)	3600
Stage Length Kilometers (n.mi.)	4074 (2200)
Revenue Passenger Miles (billions)	3.98
Load Factor	.55
DOC Cents/seat kilometer (cents/seat n.mi.)	1.38 (2.55)
IOC Cents/seat kilometer (cents/seat n.mi.)	.67 (1.24)
ROI (percent) (after taxes)	-3.16
Fare (\$/trip)	135

The ROI's shown in Table 23 are used primarily for comparative evaluation and selection of the point design aircraft rather than economic indicators that would be obtained from a total route simulation analysis. The ROI's shown in Table 23 are based on a route segment that is equal to the design range of the aircraft. The ROI for an off design range is determined also. The route chosen is the Los Angeles to Honolulu run. The passenger demand for this route is taken from the Phase II Market Analysis Study (Contract NAS1-11940). The system summary information for this route is provided in Table 24. The ROI as shown in Tables 23 and 24 are calculated by the gross method as used by the ASSET program, and described in paragraph 3.1.6.4. The ROI is also calculated by the model as described in Appendix A. The more detailed ROI model produces a ROI of 5.48 percent for the 7783 kilometer (4,200 n.mi.) stage length as compared to 6.04 percent for the ASSET calculation. The ROI for the 4,074 kilometer (2,200 n.mi.) stage length by the detailed method is -3.58 percent as compared to -3.16 percent by the ASSET program. The detailed output information for the economic ROI calculations are provided in Appendix B along with the other computer printouts for the Point Design Vehicle.

4.3.2 System Cost Sensitivities

The sensitivity analysis is designed to consider parametric variation of three scenario/operational parameters (stage length, utilization, and load factor) and three cost parameters (fare, fuel cost and aircraft quantity). Summary plots of the results are shown in Figure 102 through 108.

Utilization - The utilization is varied from the base point of 3,600 block hours to a low of 3,000 hours and a high of 4,000 hours. In all cases the passenger demand remains constant. The resultant sensitivity of DOC and ROI to utilization is shown in Figure 102. The change in DOC is not dramatic but the cascading effect on ROI is significant.

Load Factor - The load factor variation has no effect on DOC but does alter the IOC and the number of vehicles in the fleet. The change in the IOC is caused by the change in the number of passengers handled at each flight and the number of vehicles required is changed because the productivity of the airplane is changed while the total passenger demand remains constant. The change in ROI with a change in load factor ranging from .50 to .60 is shown in Figure 103.

Stage Length - Operating the AST at the off design ranges has a significant affect on the ROI (Figure 104). When the aircraft is flown a shorter stage lengths, the block speed is reduced but the flight frequencies are increased. This causes an increase in DOC and IOC. These increases override the decrease in investment due to the smaller number of vehicles required to accommodate the fixed passenger demand. The 4,200 n.mi. AST flying the Los Angeles to Honolulu route has a negative ROI when evaluated in terms of the assumptions used in this study. The ROI is extremely sensitive to fare level and a slight increase in fare would change the ROI from negative to positive for the LAX-HNL route, as shown in the fare sensitivity analysis that follows.

Fare Level - The effect of fare level on ROI is calculated for the basic design range of 7,778 kilometers (4200 n.mi.) and the off design range operation at 4,074 kilometers (2,200 n.mi.) (Figure 105). If the fare level is calculated in the same manner for both stage lengths ($\$9 + \$.03083/\text{passenger}$

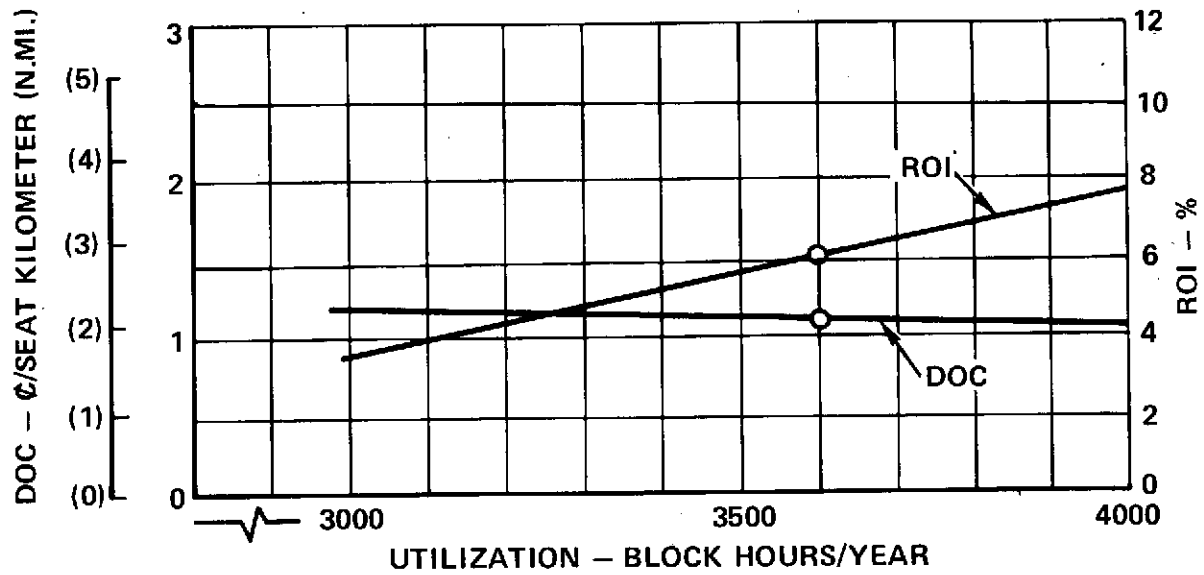


Figure 102. DOC/ROI vs. Utilization

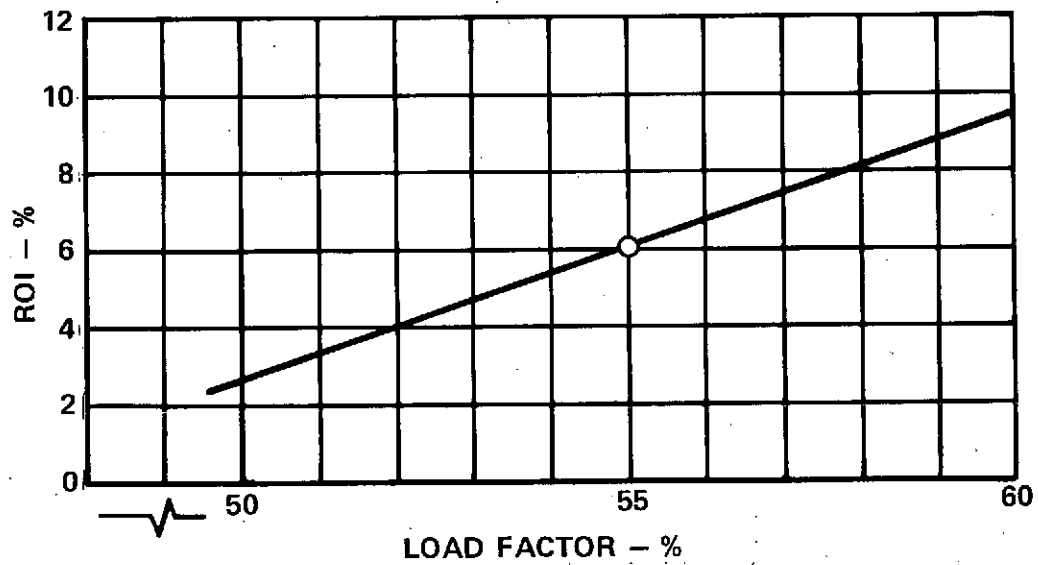


Figure 103. ROI vs. Load Factor

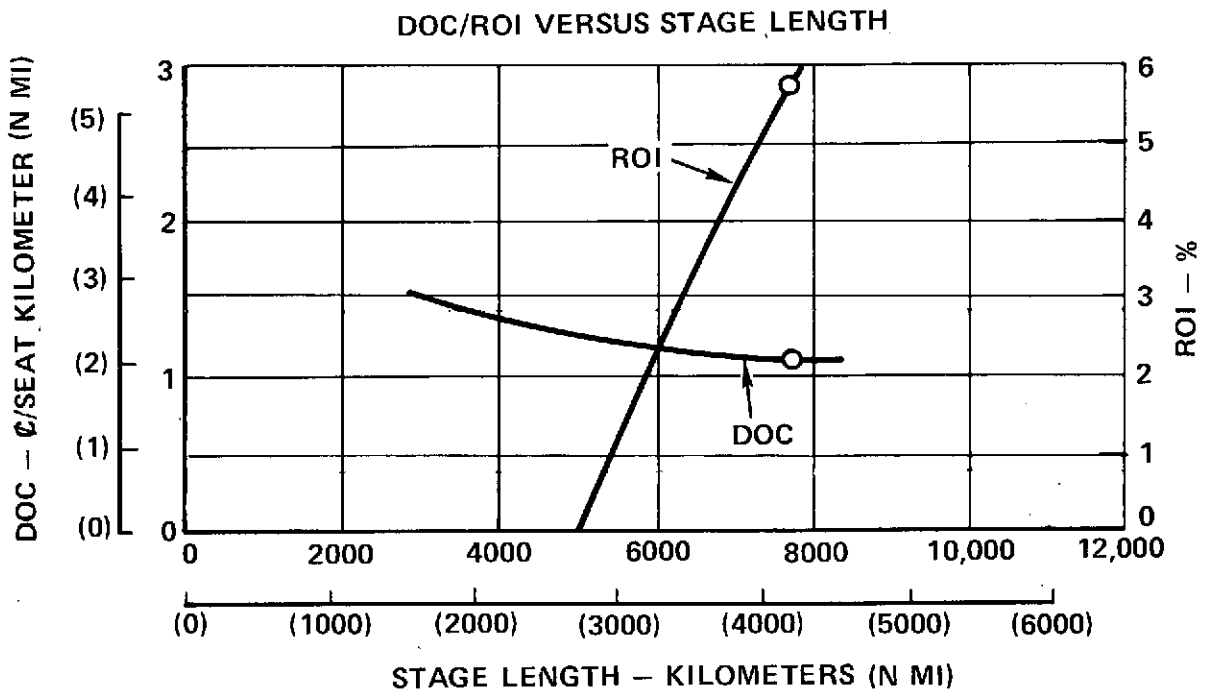


Figure 104. DOC/ROI vs. Stage Length

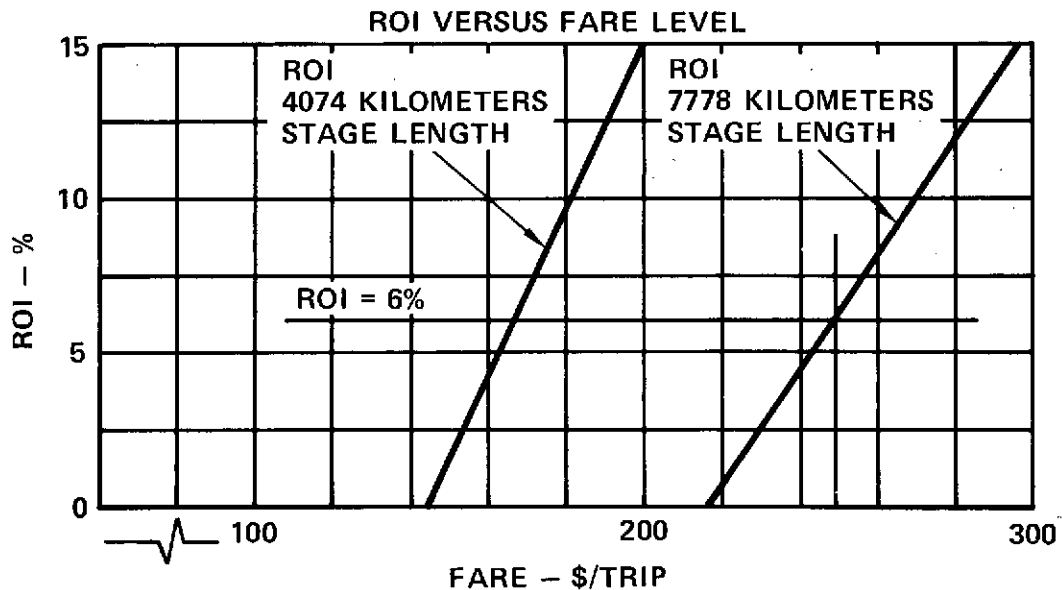


Figure 105. ROI vs. Fare Level

kilometer) the ROI for the 7,778 kilometer stage length is 6 percent and -3 percent for the 4,074 kilometer stage length. To have equal ROI's (6 percent) the fare level at the 4,074 kilometer stage length would have to be \$166 per trip. This fare is 27 percent above the current peak coach fare and 13 percent less than the first class fare from Los Angeles to Honolulu.

Fuel Cost - The DOC and ROI, as noted by Figure 106, are very sensitive to fuel cost. This is due to the fact that for the AST the fuel is a large percentage (41 percent) of the total DOC. A 50 percent increase in the fuel cost causes a drop in ROI from 6 percent to zero.

Production Quantity - The result of the sensitivity of production quantity on DOC and ROI is shown in Figure 107 and 108. Figure 107 shows the relationship between the production quantity and the production cost of the vehicle. The results are dependent upon the slopes of the learning curves chosen for the labor, material, engine and avionics. The values for the learning curve slopes are given in the input table included in Appendix A. The DOC and ROI are sensitive to the cost of the vehicle as the vehicle cost contributes approximately 32 percent to the DOC in terms of insurance and depreciation.

4.4 STRUCTURES

The point design LH₂ AST aircraft has been described in preceding sections. The size, weight, and performance which have been shown were based on structural designs established both by comparison with previous, similar aircraft designs, e.g., the Jet A-1 AST from references 1 and 4, and also as a result of specific analyses performed during the subject study. The highlights of the structural considerations related specifically to the hydrogen fueled airplane are outlined herein.

4.4.1 Design Load Conditions

Design conditions were analyzed to establish fuselage loads requirements for design of forebody and aftbody structure in the area of the LH₂ tanks. Conditions to be investigated were selected following review of loads analysis for the current Arrow Wing Structural Concept Study.

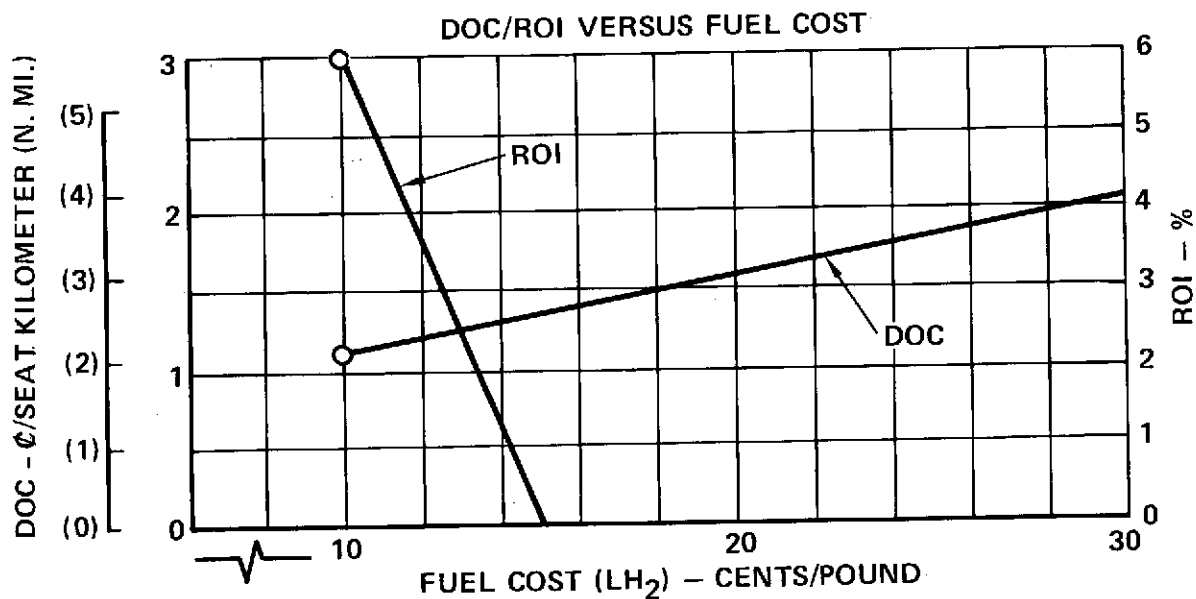


Figure 106. DOC/ROI vs. Fuel Cost

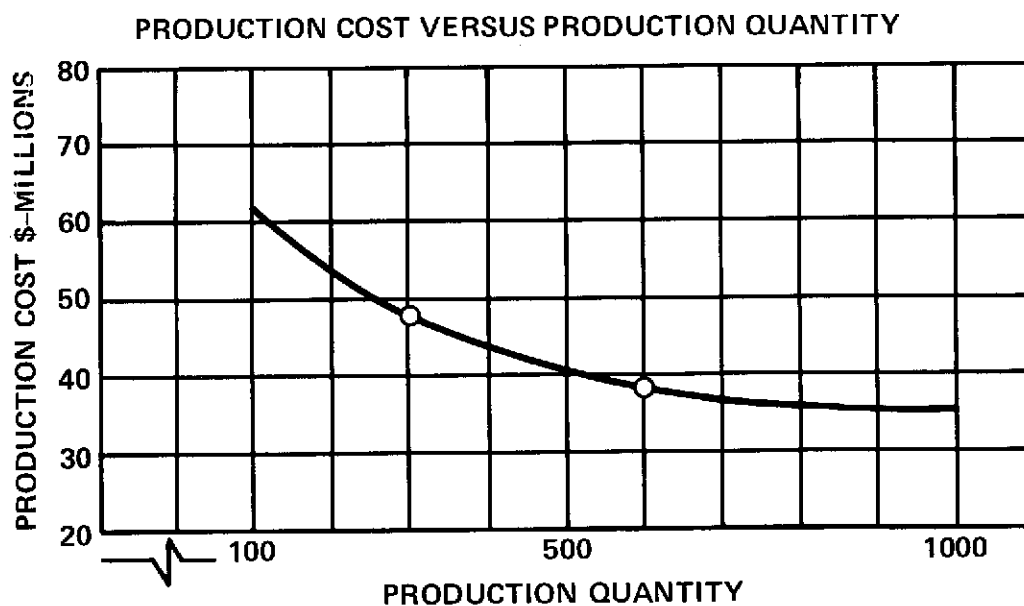


Figure 107. Production Cost vs. Production Quantity

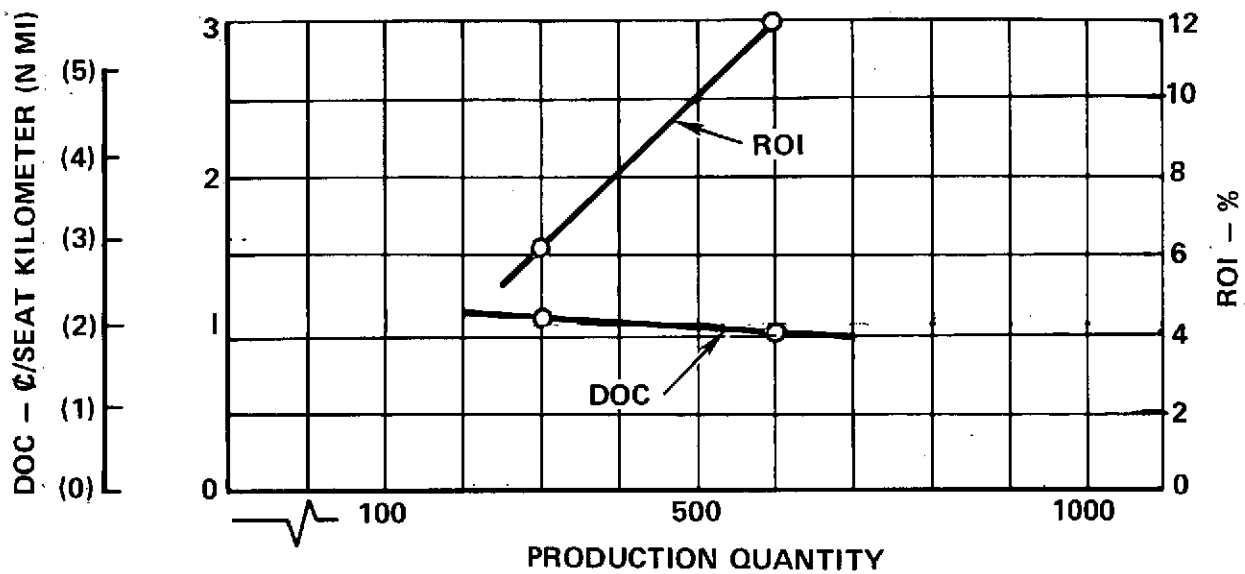


Figure 108. DOC/ROI vs. Production Quantity

Inertia data for fuselage and contents are shown on Figure 109. Conditions were analyzed at both light and heavy weights and produce the net shears and bending moments summarized in Table 25. Forebody loads are based on inertia loadings with possible aerodynamic loads relief conservatively omitted. The effect of balancing horizontal tail loads is included in afterbody loads. An arbitrary yaw condition at high speed is included for aftbody design to account for combined bending and torsion in this area. t

The maximum fuselage bending moments and shears are plotted on Figures 110 and 111. Most of the fuselage is designed by the 2.5 g positive maneuver, however the aft portion of the aft fuselage/tank is designed by negative maneuver.

TABLE 25. FUSELAGE LOADS - LH₂ AST

Forebody			Aftbody			
Condition	Positive Maneuver	Negative Maneuver	Condition	Positive Maneuver	Negative Maneuver	Arbitrary ¹ Yaw
V_E (keas)	200.6	167.2	V_E (keas)	200.6	200.6	270
V_E m/sec	(390)	(325)	V_E m/sec	(390)	(390)	(525)
n_z	2.5	-.15	n_z	2.5	-1.0	1.0
F.S.1000			F.S.2640			
$10^{-3}S_z$	-81.25	2.59	$10^{-3}S_z$	-217.45	123.0	6.46
$10^{-6}M_y$	-19.83	.83	$10^{-6}M_y$	124.47	-95.32	-26.15
F.S.1200			F.S.2900			
$10^{-3}S_z$	-123.75	3.34	$10^{-3}S_z$	-155.95	98.38	12.96
$10^{-6}M_y$	-40.33	1.47	$10^{-6}M_y$	93.82	-83.07	-33.41
F.S.1530			F.S.3300			
$10^{-3}S_z$	-190.5	4.68	$10^{-3}S_z$	-90.7	72.28	22.66
$10^{-6}M_y$	-92.72	2.81	$10^{-6}M_y$	55.03	-67.55	-41.38

1. Add $M_y = \pm 3.405 \times 10^6$ in-lbs.
2. All loads are limit.
3. + Bending moments (M_y) are nose-up.
4. Shear in lbs; moments in in-lbs.

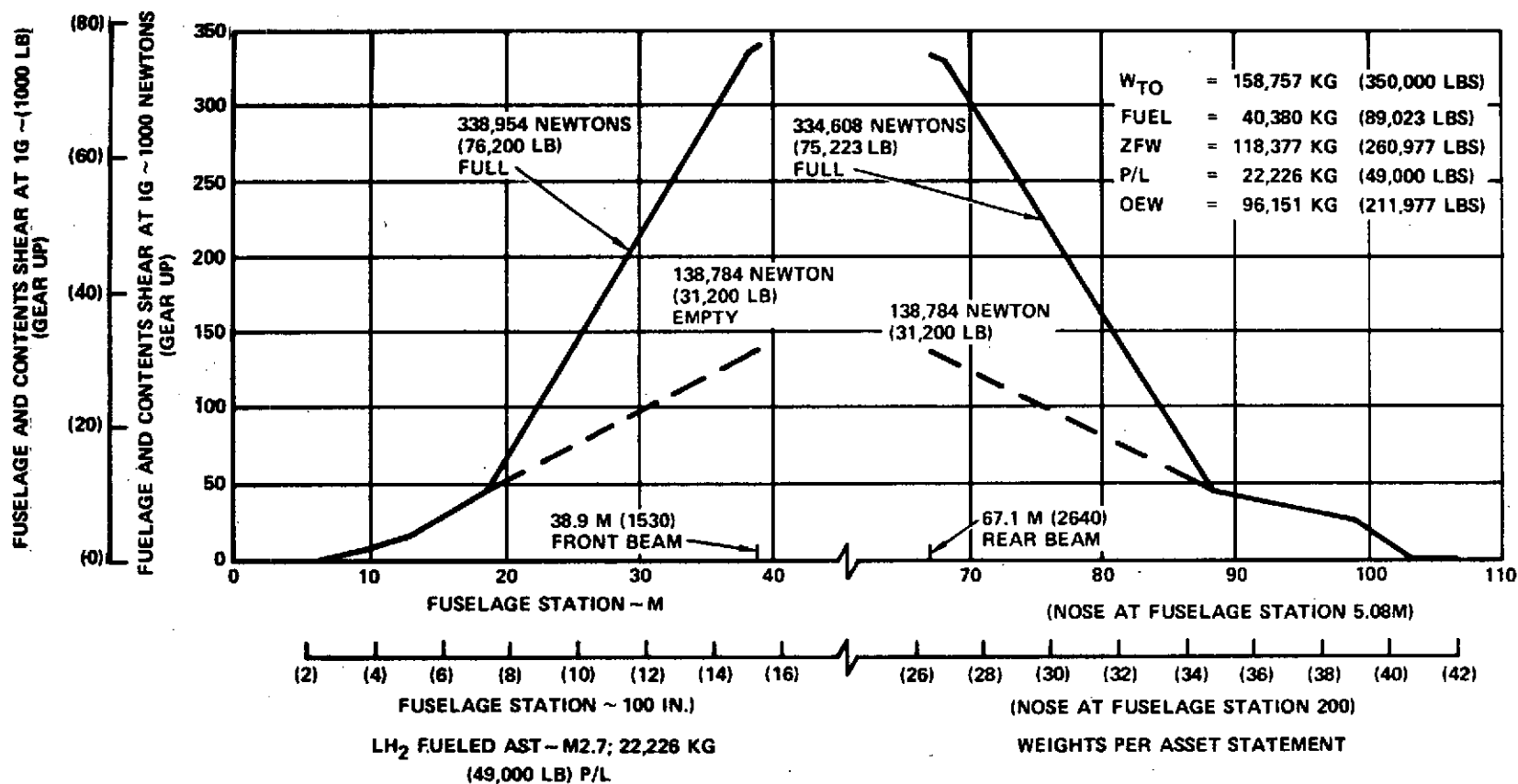


Figure 109. Fuselage and Contents Shear - Gear Up

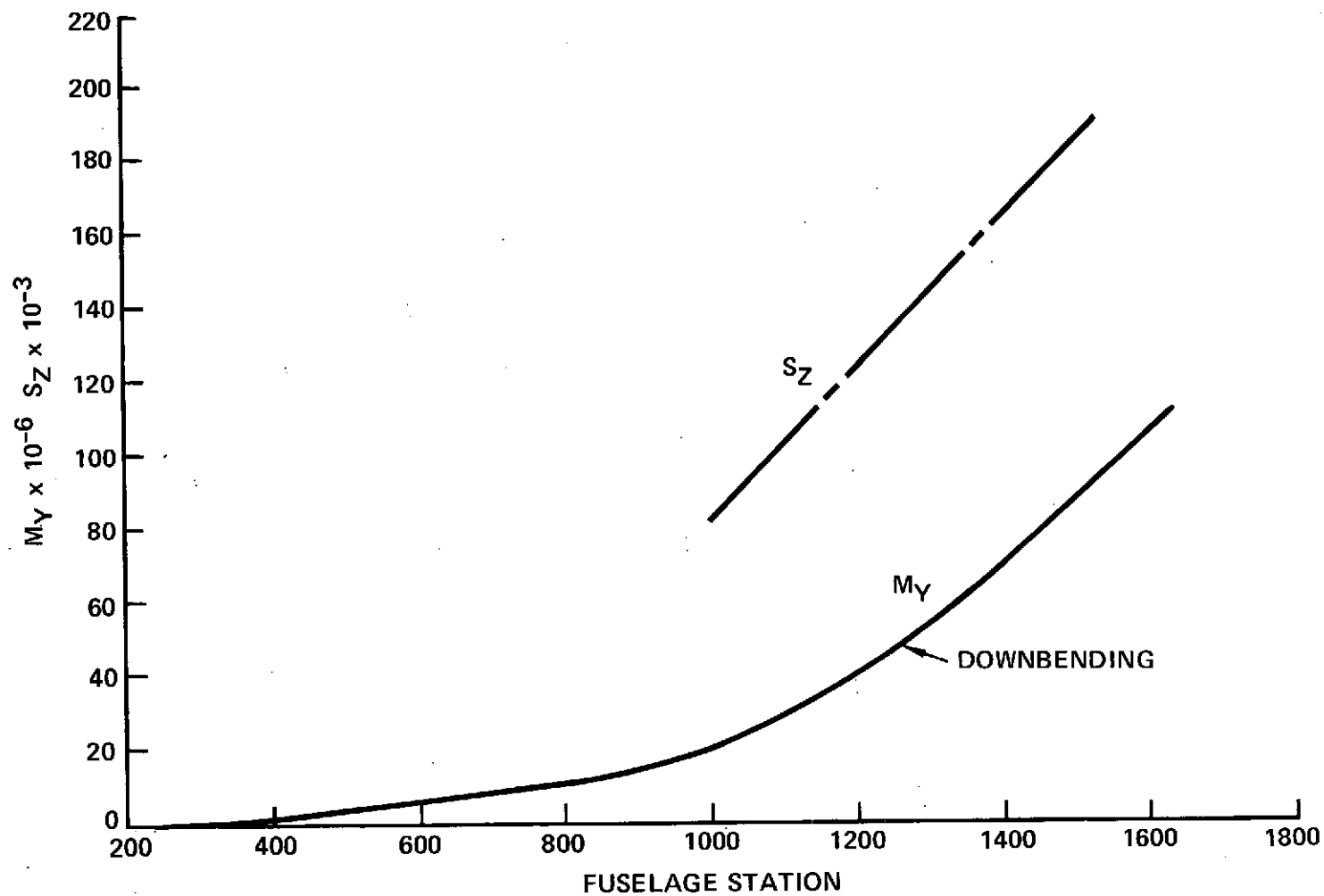
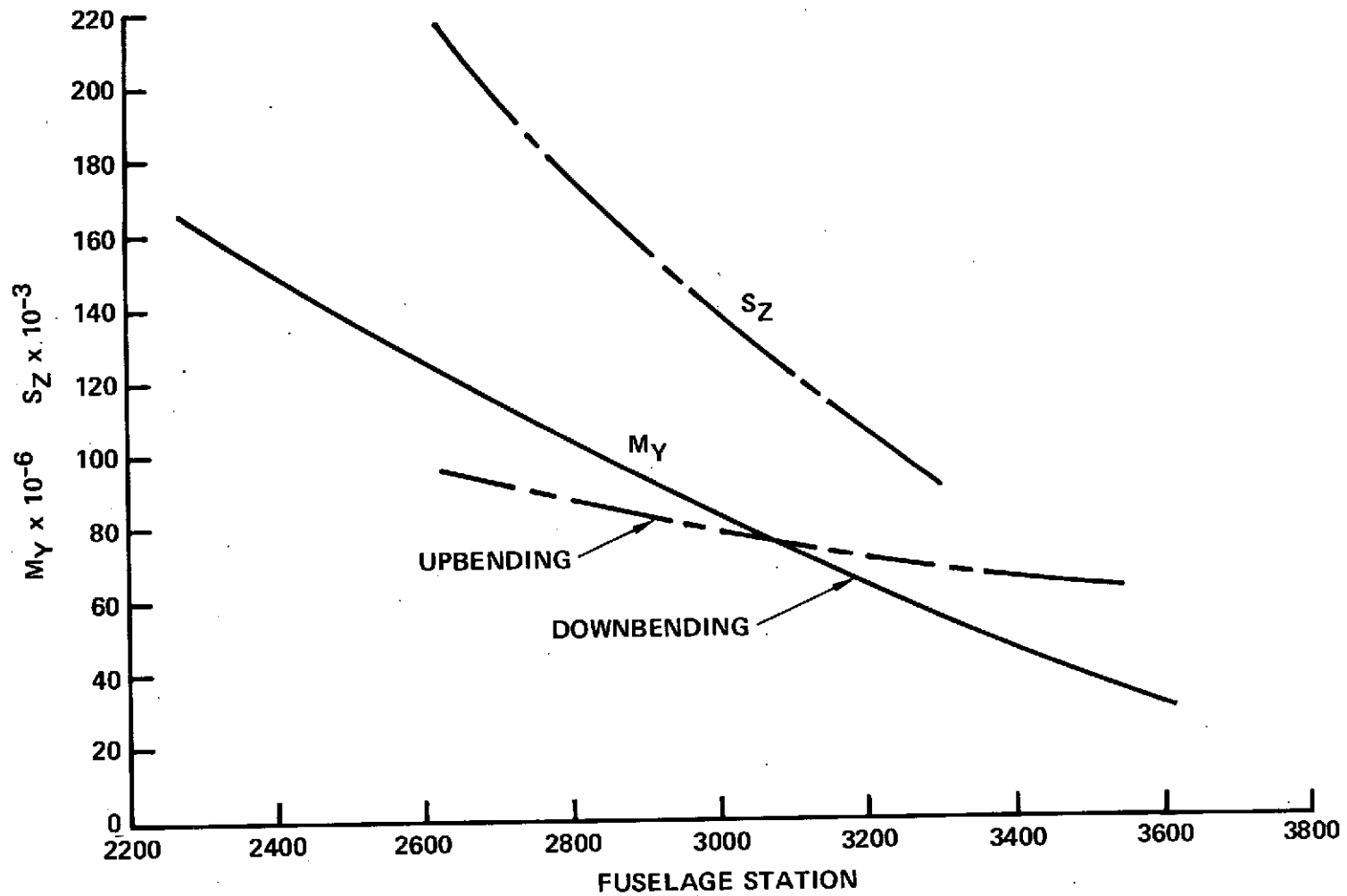


Figure 110. Forebody Shear and Bending Moments (Lim.)



AFT BODY SHEAR AND BENDING MOMENTS (Lim.)

Figure 111. Afterbody Shear and Bending Moments (Lim.)

Tank Pressures

Maximum absolute tank internal pressure is $158,579 \text{ newton/m}^2$ (23 psi).

$$\begin{array}{lcl} \text{Sea Level} & p = 158,579 - 101,353 = 57,226 \text{ newton/m}^2 \\ & (23.0 - 14.7 = 8.3 \text{ psig}) \end{array}$$

$$\begin{array}{lcl} \text{At 22,860 m} & p = 158,579 - 3,447 = 155,132 \text{ newton/m}^2 \\ (75,000 \text{ ft}) & (23.0 - .5 = 22.5 \text{ psig}) \end{array}$$

Pressure loads are multiplied by a factor of 2 for ultimate design. Fuselage shear and bending loads are multiplied by a factor of 1.5 for ultimate design.

4.4.2 Structural Analysis

The primary structure of the CL1701 airplane represents the application of the advanced technologies presumed to be available for near-term (1980-1981) start-of-design as identified in Reference 4.

The evaluation of various structural approaches was made based on the results of 1) the detail structural analysis of a spectrum of structural concepts and arrangements considering advanced materials and producibility methods, 2) the preliminary design drawing prepared for each structural arrangement showing the minimum weight structural concept, 3) the weight estimates of the wing and fuselage structure, and 4) the production and development costs determined for the candidate structural arrangements. Cost benefit trades were performed considering structural efficiency, initial costs, direct operating costs, and applied technology level. The trade studies identified the least weight and least cost homogeneous structural approach as the following:

- Chordwise stiffened wing structural arrangement
- Convex-beaded surface panels (Ti 6Al-4V annealed; weld bonded)
- Composite reinforced spar caps (Titanium alloy reinforced with Boron/Polymide; bonded)

The parametric sizing and costing evaluation process performed with the computational aid of the Lockheed ASSET computer program, however, identified the importance of minimizing structural weight. Thus, the structural

approach selected for the CL1701 airplane includes the minimum weight honeycomb core wing tip structure.

4.4.2.1 Wing Structure

The structural approach for the wing of the CL1701 airplane is shown in Figure 112 and identified by the three major areas which include the forward box, aft box and tip structure. The design concept is identical to that being developed in the ongoing Arrow-Wing Structures Study (Reference 4). The detail design for the LH₂ AST airplane is modified from that of its Jet A-1 fueled counterpart to account for the following differences:

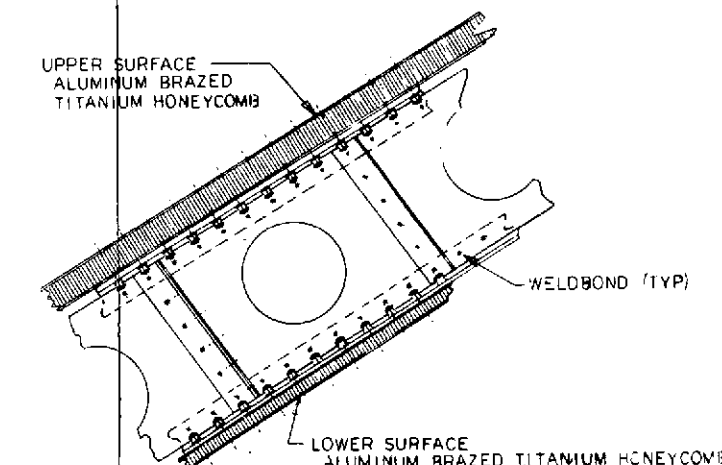
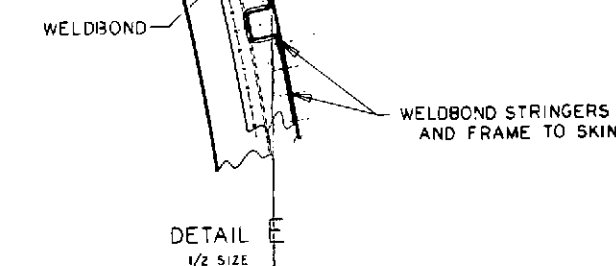
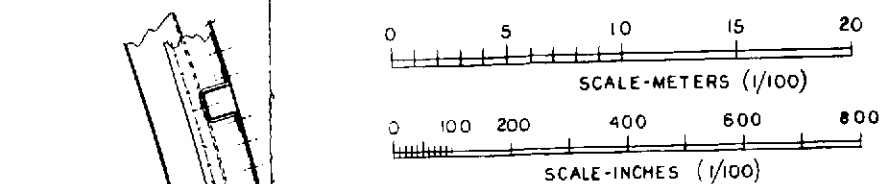
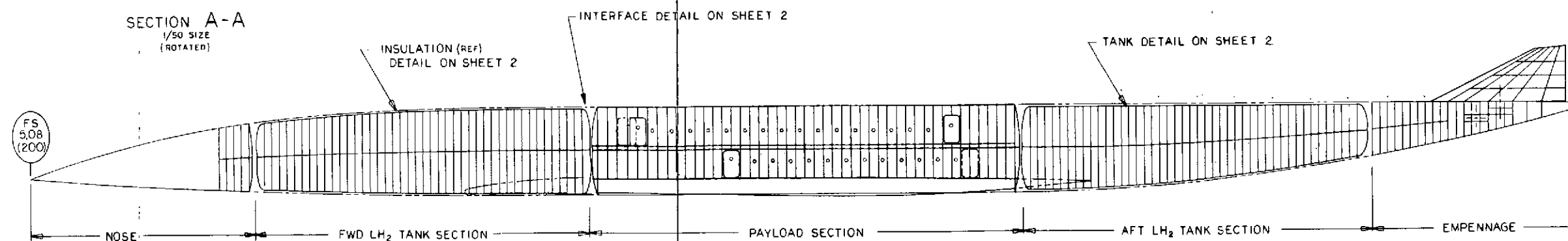
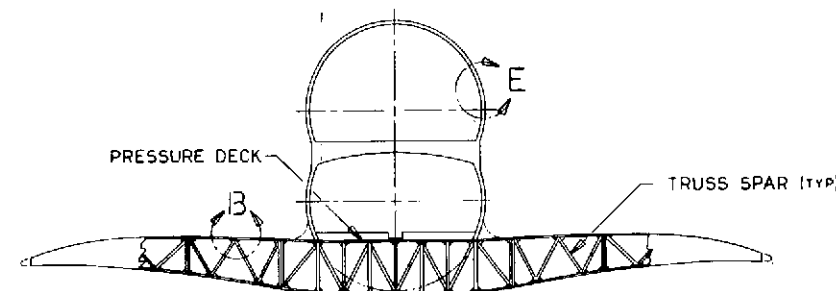
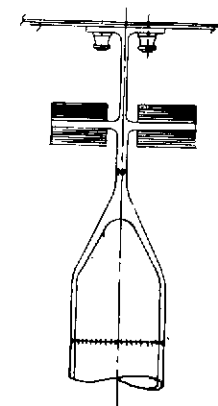
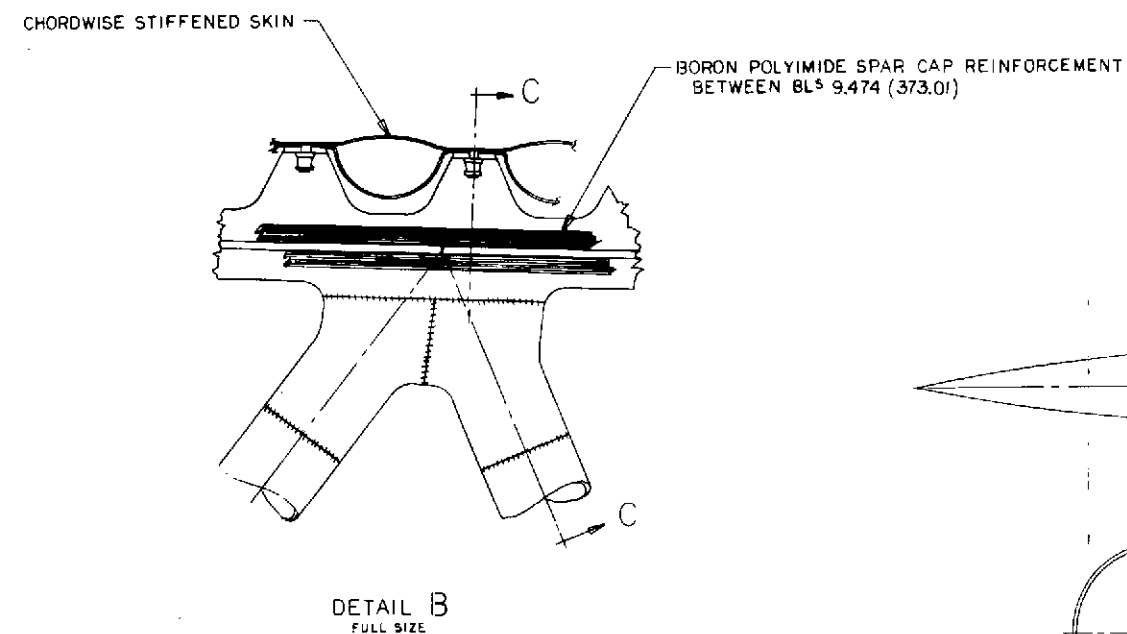
- Smaller wing area
- Lower wing loading
- No fuel containment

This latter point has both advantages and disadvantages: there is no need to modify an otherwise ideal load path to provide for tankage requirements; on the other hand, there is no load relief to apply at the design condition involving a 2.5g maneuver.

Forward and Aft Box Structure

The chordwise stiffened arrangement finds application to the forward and aft box structure which comprises the major portion of the basic wing. This arrangement is essentially a multispar structure with widely spaced ribs. The submerged spar caps of titanium alloy (Ti 6Al-4V annealed) are spaced approximately 20 inches on-center and are used to transmit the wing bending loads. These caps being submerged result in reduced temperatures, which in turn results in increased allowable stresses (fatigue) and also permits uncoupling of the spanwise and chordwise stiffness for vehicle flutter suppression.

Selective reinforcement of the basic metal structure is considered as the appropriate level of composite application for the near-term design. Composite reinforced spar cap details (Figure 112) show the application of unidirectional reinforcing with boron polyimide. Both truss-type and circular-arc corrugated webs are used as appropriate for access and manufacturing requirements.



ADVANCED DESIGN		CL1701-7
STRUCTURAL ARRANGEMENT- LH ₂ FUELED AST-POINT DESIGN		
DESIGNED BY	LOCKHEED - CALIFORNIA CO.	CL1701-7-3
CHECKED BY	LOCKHEED - CALIFORNIA CO.	CL1701-7-3
DATE	11-30-73	NOTES

Figure 112. Structural Arrangement - Sheet 1

NOTE:
1. ALL MATERIAL TITANIUM ALLOY
UNLESS SPECIFIED OTHERWISE

REPRODUCIBILITY OF THE
ORIGINAL PAGE IS POOR



The surface panel concepts for the forward and aft box in this arrangement have stiffening elements oriented in the chordwise direction. Structurally efficient circular-arc beaded-skin designs are used (Figure 112). These efficient circular-arc sections of sheet metal construction (Ti 6Al-4V annealed) provide effective designs when properly oriented in the airstream to provide acceptable aerodynamic performance as demonstrated on the NASA-Lockheed YF-12 airplane. The panel elements are weldbonded for improved fatigue life. The shallow protrusions provide smooth displacements under thermally induced strains and operational loads.

Tip Structure

The stiffness-critical wing tip structure utilized the monocoque construction (Figure 112) with biaxially stiffened panels which support the principal load in both the span and chord direction. The substructure is essentially a multispar design with full and partial ribs to provide support for the leading and trailing edge control surfaces and actuating system.

The monocoque construction has smooth-skinned aluminum brazed honeycomb sandwich panel (Figure 112) that result in minimum aerodynamic drag. Thermal stresses are absorbed with minimal relief but criticality, defined by flutter suppression requirement, produces a minimum weight structural design for the tip structure.

4.4.2.2 Fuselage Structure

The weather vision nose, payload and empennage sections of the CL1701 airplane are a conventional semimonocoque shell construction of titanium alloy material (Ti 6Al-4V annealed) with extensive use of weldbonding. The flight station enclosure tapers down from the constant cross-section of the forward tank and payload section which is formed by the intersection of two cylinders with a radius of 1.966 meters (77.4 inches). Structural continuity between the integral tank sections and the nose, payload, and empennage sections is provided by a truss arrangement, see Figure 113. Suitable longitudinal local reinforcements are used in truss member attachment areas to distribute the concentrated loads encountered. An analysis of a critical truss member is included in Appendix C.

Preceding page blank

Page intentionally left blank

The nose, payload and empennage structural arrangement is a uniaxial stiffened structure of skin and stringer with supporting frames. Weld bonding is utilized as shown in Figure 113 to improve the fatigue life of the structure. The skin and closed-hat stringers are supported by sheet metal frames that are spaced at approximately 0.508 meters (20-inch) intervals and aligned with the spars of the wing structure. Typical construction details of the frame and stringers are presented in Figure 113. A floor is provided at the intersection of the cylinders as well as above the wing box structure. Fore and aft intercostals are provided over the wing box to support the lower cabin floor. Transverse beams which are attached to each frame are provided to support the upper cabin floor. The pressure boundary is provided by the upper surface of the wing box and pressure bulkhead at each end. The main frames that distribute concentrated wing and gear loads into the fuselage structure are built-up from titanium forgings or extrusions. The fuselage aft of the hydrogen tankage contains structural provisions for mounting the fin and horizontal stabilizer. A skin-stringer-frame construction similar to that provided in the pressurized area of the fuselage is used. The main rings that distribute the fin loads into the fuselage are titanium forgings.

4.4.2.3 Empennage Structure

The empennage structure utilizes monocoque construction with a multispar substructure. The empennage structural concepts and arrangements are dictated by the high sonic environment to which it is subjected, as well as engine exhaust temperatures.

4.4.2.4 Fuel Tanks

In the course of the fuel tank investigations, three types of tanks were studied. The simplest of these is a thin skin aluminum non-integral tank supported at two fuselage stations. The second concept employs integrally stiffened aluminum skin which forms the fuselage structure as well as the tank wall. This is the integral tank concept. The third design utilized composite materials to also form an integral tank but the technology level required to fabricate such a tank, together with the internal cryogenic

Preceding page blank

insulation planned for the concept, is considered to be in the late nineteen eighties. For this reason most of the investigative effort was expended on the first two concepts.

As the investigation progressed it became apparent that the integral welded tank concept was superior to the non-integral. The integral tank has a higher volumetric efficiency, resulting in a weight saving. It has a greater structural efficiency resulting in further weight savings. In addition, the tank/fuselage structure as well as the insulation is more readily accessible for inspection purposes. The non-integral tank design would have to incorporate fuselage joints so that the tanks could be removed from the aircraft for periodic inspection of the fuselage structure and insulation. For these reasons the integral tank design is chosen for the subject design study.

From a cost standpoint, it is possible that some alternate design is preferable to the integrally stiffened shell design for the integral tanks. A brazed aluminum honeycomb sandwich structure is a possibility, as is a weldbonded skin stringer construction. This latter design requires an adhesive which is good for long time spans at cryogenic temperatures but it could result in a much less costly method of fabrication.

Non-Integral Tanks

The non-integral tanks are of a welded construction and are fabricated from 2219 aluminum alloy. The basic tank shell is of a monocoque design except for a few rings for baffles, tank shape maintenance, and tank support. The shell skin is chem milled to a thickness of .00127 m (0.050 inches) except for the sheet edges where it is .00203 m (0.080 inches) thick to account for the decreased material properties due to welding. The thin shell is supported against shear and compression buckling by the cryogenic insulation which is cemented to the external surface of the tank. In a monocoque structure such as this, shear and/or compressive buckling would result in tank failure.

The non-integral tanks are supported at two stations only so as to avoid loading of the tank by fuselage deflections. In addition, the aft support of the aft tank has a track and roller support arrangement to prevent

fuselage twist from torquing the tank. The four tank support points (two at each support station) consist of stainless steel pins which are recessed in the tank and surrounded by evacuated fittings to minimize the heat leak path. The tank crosssectional shape requires the same crosstie which is outlined in the integral tank description which follows. The design of this member is essentially the same for both tank concepts. The same holds true for the design of the baffle bulkheads for the two tank concepts.

Table 26 presents a breakdown of weights of structural components of a design of non-integral tanks for the LH₂ AST, plus a calculation of the fuel weight fraction (weight of tank structure divided by the weight of hydrogen it is to contain). Stress calculations are shown in Appendix C.

Integral Tanks

The integral tanks are of a welded construction and are fabricated from 2219 aluminum alloy (See Figure 113). The surfaces consist of integrally

TABLE 26. WEIGHT BREAKDOWN: NON-INTEGRAL TANKS
(INCLUDES BOTH TANKS)

Skin	$W_s = 2,087 \text{ kg (4,600 lb.)}$
Tank Ends	$W_e = 535 \text{ kg (1,180 lb.)}$
Support Structure	$W_f = 544 \text{ kg (1,200 lb.)}$
Baffle Bulkheads	$W_b = 367 \text{ kg (810 lb.)}$
Crosstie	$W_x = 408 \text{ kg (900 lb.)}$
Crack Stopper Straps	$W_c = 109 \text{ kg (240 lb.)}$
Total	4051 kg (8,930 lb.)
Add 10% for non-optimum and contingency factor:	
4,051 kg (8,930) x 1.10 = 4,459 kg (9,830) lb.	
Fuel Wt. Fraction	
$\frac{4,459 \text{ (9,830)}}{39,644 \text{ (87,400)}} = 0.113$	

stiffened skin with the stiffeners on the inside of the tank and with the outside surface of the tank smooth. This outside surface is .117 m (4.6 in) below contour, and the space between is occupied by insulation. The thermal protection system consists of two different types of insulations (see Section 4.5 for details). Generally, the cryogenic insulation is a closed cell foam type material which is bonded to the smooth tank surface. The high temperature insulation is a fiberglass mat faced with a thin layer of polyimide resin. Heat shield panels of sandwich construction made up of fiberglass filler faced with graphite polyimide comprise the aircraft external surface. The heat shield panels are supported by low conductance fiberglass standoffs which are fastened to the tank surface.

The integrally stiffened tank skin carries fuselage bending and shear loads as well as tank internal pressure loads. As in the case of the non-integrated tanks, the cryogenic insulation performs the function of stabilizing the tank skin against shear and compression buckling. The skin-stringers are machined from a basic extruded shape, and the stringers are tapered to provide sufficient material to resist fuselage bending moments at any given station. The 2219 alloy chosen for the tank structure is tough, weldable, and is highly resistant to stress corrosion cracking. It is an excellent cryogenic material, since it retains good ductility and has much improved strength at liquid hydrogen temperature. Weld joints in the tank are appropriately beefed up to account for the reduced material properties through the weld area and to provide for fatigue strength. An ultimate tension stress limit of $27.58 \times 10^6 \text{ n/m}^2$ (40,000 psi) is imposed on the tank structure for fatigue considerations. This stress level is also the approximate column/crippling allowable stress for the compression surfaces.

The surfaces are stabilized by "floating" rings on the inside of the tank. These rings are spaced at 0.508 m (20 in.) and are fastened to the cross tee flange of each of the integral stringers. They are formed channel shaped and are fabricated from 2219-T87 aluminum alloy sheet. The ring cross-sectional geometry varies along the length of the tanks, being a function of the surface load per inch. In addition to the shell stabilizing rings, there are baffle bulkheads every 5.08 m (200 in.) of the tank length.

These are provided to dampen fuel slosh and to resist fuel pressure

generated by a forward acting crash load factor. These bulkheads consist of a thin aluminum membrane supported by a peripheral ring which also acts as a surface stabilizing ring for flight loads.

Since the fuselage (tank) cross section consists of two intersecting circles arranged vertically, there is an unbalanced pressure load at the cusps formed by the intersection points. This load will be self-reacting if a load path is provided to the cusp on the opposite side of the fuselage. This continuous crosstie can perform two functions; in addition to providing the aforementioned load path, it can act as a walkway for internal ground inspection/maintenance of the tank. Accordingly, the crosstie is designed as a continuous honeycomb sandwich panel which support loads in the vertical direction as well as transmitting lateral tension loads. Holes are provided in the panel to allow LH_2 flow from the top half of the tank to the bottom half.

Table 27 presents a weight breakdown of structure components for the integral tanks of the LH_2 AST, plus a calculation of its fuel weight fraction. Stress calculations are shown in Appendix C.

The transition from the integral tank structure to the conventional fuselage structure is made through tubular truss members which are positioned around the periphery of the transition area. The truss members are made from fiberglass reinforced with boron filaments so as to afford maximum rigidity and a minimum heat leak rate. See analysis in Appendix C.

Integral Composite Tanks

If materials technology advances to the point where tanks can be fabricated from composites, it is clear that significant weight reductions can be realized. This would require development of composites which are impervious to and unaffected by liquid and gaseous hydrogen. In addition, methods of making gas and liquid tight joints in the composites would have to be perfected.

At the present time the most promising candidate for a composite tank structure is boron-aluminum, refer to Table 8 and Section 3.1.4. This material has the advantage of having an impervious aluminum surface which

TABLE 27. WEIGHT BREAKDOWN: INTEGRAL TANKS
(INCLUDES BOTH TANKS)

Shell	$W_s = 3,946 \text{ kg (8,700 lb.)}$
Tank Ends	$W_e = 612 \text{ kg (1,350 lb.)}$
Rings	$W_r = 894 \text{ kg (1,970 lb.)}$
Baffle Bulkheads	$W_b = 367 \text{ kg (810 lb.)}$
Crosstie	$W_x = 408 \text{ kg (900 lb.)}$
Transition Trusses	$W_t = 1,134 \text{ kg (2,500 lb.)}$
Crack Stopper Straps	$W_c = 109 \text{ kg (240 lb.)}$
Total	$7,7471 \text{ kg (16,470 lb.)}$

Add 10% non-optimum and contingency factor: $7,471 \text{ (16,470)}$
 $\times 1.10 = 8,224 \text{ kg (18,130 lb.)}$

$$\text{Fuel Wt. Fraction} = \frac{8,224 \text{ (18,130)}}{41,989 \text{ (92,570)}} = 0.196$$

NOTE: Fuel Weight is greater because of higher volumetric efficiency with integral tank.

satisfies at least one of the requirements. A great deal of work would have to be done to develop methods of fabrication and joining of large structural components. This concept is considered to be beyond the capabilities forecast for the 1981 design freeze date.

4.5 INSULATION EVALUATION

4.5.1 Approach

The fundamental key to the development of a hydrogen-fueled supersonic transport aircraft is a thermal protection system that has the desired mechanical and thermodynamic properties to enable it to operate in a commercial environment for the required life span with a minimum of maintenance.

A commercially acceptable thermal protection system would use insulation materials that are:

- Impervious to air so as not to require purging to prevent cryopumping.
- Not reliant on the maintenance of a high vacuum.
- Not susceptible to ageing or cracking under repeated thermal stresses.
- Able to withstand the exterior temperatures associated with supersonic flight.
- Capable of being repaired or replaced readily.

Existing materials are not known to have met these requirements. However, this analysis has been based on known properties of existing materials to: (1) provide data for the present conceptual analysis of the capabilities of an LH₂ AST; (2) reveal the areas offering maximum potential for improvement through research and development; and (3) provide a basis for judging the magnitude of future improvements which might be made as a result of properly directed development.

Consequently, the weights and thickness of components of the thermal protection system reported in this section should be regarded as conservative estimates of the corresponding values which might result from use of insulants that could be available by 1981 which will meet these requirements.

4.5.2 Design Configuration

Evaluation of insulation performance was restricted to external insulation concepts. External insulation systems have demonstrated reasonable success in current aerospace applications and appear to have greater potential for

satisfying airline operational requirements within the 1981 time constraint. The use of systems requiring purge gas or CO₂ frost were not considered realistic in an air transport environment.

The properties of the materials used to represent the three elements of the thermal protection system in the analysis are listed in Table 28. These include the cryogenic insulation, a high temperature insulation, and a heat shield -- the latter used only in the integral tank concept.

Integral and non-integral fuselage tankage configurations with two-layer external insulation systems were investigated. The two-layer concept consists of an outer layer of high temperature insulation, assumed for purposes mentioned to be fibrous quartz, applied over a cryogenic insulation, represented by polyurethane foam. The high temperature insulation is required to limit the foam temperature to the maximum of 422°K (300°F) assumed for the study.

The basic tankage design and flight profile requirements are as described in Sections 4.1.2 and 4.2.1, respectively. Briefly, the design mission consists of Mach 2.7 cruise at an altitude of approximately 21,000 m (68,000 ft) with a design range of 7800 km (4200 n.mi.). All fuel is contained in fuselage forward and aft tanks. Because of equivalent boundary conditions, only the forward tank was analyzed.

The tank design is of the "double lobe" configuration shown in Figure 113. The tank length was increased for the non-integral configuration to obtain the same tank volume as the integral configuration for comparative analysis. Each tank was originally sized to carry 20,200 kg (44,500 lb) of fuel for the 7800 km (4200 n.mi.) basic mission plus a 480 km (260 n.mi.) reserve mission. During simulation of the mission, however, 680 to 1360 kg (1500 to 3000 lb) of fuel becomes unusable due to boiloff. Within the scope of the present work, the required tank volume was not solved iteratively, and so the data presented are for a system which completes the basic mission, but carries a reduced reserve quantity. Tank nominal working pressure was not optimized, but held constant at 138,000 newton/m² (20 psia).

TABLE 28. INSULATION THERMODYNAMIC PROPERTIES

Avg Temp (°F)	$\rho = 2 \text{ lb/ft}^3$ Polyurethane Foam (Low-Temp)		$\rho = 4.5 \text{ lb/ft}^3$ Fibrous Quartz (Hi-Temp)		Graphite/Kevlar/ Polyimide Heat Shield	
	k $\frac{\text{BTU}}{\text{hr ft } ^\circ\text{F}}$	C_p $\frac{\text{BTU}}{\text{lb } ^\circ\text{F}}$	k $\frac{\text{BTU}}{\text{hr ft } ^\circ\text{F}}$	C_p $\frac{\text{BTU}}{\text{lb } ^\circ\text{F}}$	k $\frac{\text{BTU}}{\text{hr ft } ^\circ\text{F}}$	C_p $\frac{\text{BTU}}{\text{lb } ^\circ\text{F}}$
-460	0	0.287	0	0.143		0.0936
-400	0.002		0.01			
-300	0.008		0.017			
-200	0.0114	0.30	0.023	0.20		
-100	0.0132		0.028		0.0248	
0	0.0142		0.033			0.25
200	0.0154	0.32	0.04	0.225	0.0536	
400	0.0163		0.045		0.0835	
700	0.018		0.051		0.145	0.488
1200	~0.02		~0.07			

4.5.3 Thermal Environment

Ambient Temperatures - Standard day design ambient temperatures were used in all mission calculations. It was assumed that on a hot day the vehicle cruise Mach number would be reduced to maintain the same total temperature.

Skin Temperatures - Previous analysis of AST skin temperatures has indicated a maximum variation of ± 10 degrees F along the aircraft fuselage in the area of the LH_2 tanks. The longitudinal variation of skin temperature is, therefore, assumed negligible. Actual skin temperatures were calculated in two stages. The first was to generate external heat transfer coefficients and recovery temperatures for the LH_2 tank regions using a standard utility computer program. The second stage consisted of using an insulation optimization computer program to combine the coefficients and recovery temperatures with calculated internal and external radiation and convective heat fluxes to obtain radiation equilibrium skin temperatures.

4.5.4 Analysis Method

The initial insulation optimization consisted of determining the minimum combined insulation system weight plus boiloff weight while maintaining acceptable materials temperatures. Boiloff quantity is produced by dry tank wall heat flux, wetted tank wall heat flux, ullage gas to liquid heat flux, and internal heat loads. These quantities, in turn, are dependent on fuel depth and ambient conditions which are functions of mission profile. The thermal analyzer transient temperature program was modified to provide simulation of these interrelated factors.

Computer program input consists of converting the physical system into an analogous electrical resistance - capacitance network (thermal model). Boundary conditions and temperature - dependent materials data are input in tabular form. The program uses a finite time interval approach to solve for temperature distributions and time histories. During each computing interval, the tank simulation routines are executed to obtain required ullage space and liquid volume heat transfer and boiloff conditions. These calculations and conditions are summarized as follows:

Ullage Space

- Heat flux - Radiation to LH_2
 - Free convection to LH_2
 - Free convection to Dry Wall
- Boiloff flow into ullage space from LH_2
- Pressure work due to fuel flow
- Final pressure, temperature and volume

Liquid Volume

- Heat flux - Boiling or free convection to wet wall
 - Radiation to Dry wall, GH_2
- Boiloff due to heat flux, boost pumps and misc. items (service hatch, supports, plumbing, etc.)
- Boiloff due to tank pressure fluctuations
- Final fuel temperature and volume

Ambient/Outer Skin

- Radiation equilibrium skin temperature
 - Radiation to space
 - Radiation to earth
 - Aeroheating

Temperature Distribution

- Materials properties versus temperature data (density, specific heat, thermal conductivity, etc.)

Air Gap

- Free convection heat transfer coefficients
- Radiation heat flux

The thermal model was constructed to obtain one-dimensional temperature distributions between the internal tank wall and the external skin at five points (actually, ten points due to symmetry) of equal heat transfer around the tank. Mission profile calculations were started after the tank was pressurized to the scheduled 20 psia tank pressure. The insulation system, tank and aircraft structure were assumed thermally stabilized before start of takeoff. Computer calculations did not include analysis of liquid or gas stratification, fuel sloshing, initial fuel subcooling due to pressurization, or variable insulation thicknesses from tank top to tank bottom.

4.5.5 Results

Boiloff quantities, insulation system weights and interface temperatures are shown on Figures 114 through 117 for the non-integral and Figures 118 through 120 for the integral tank system. Basic mission cumulative boiloff and boiloff rate for two sets of insulation thicknesses are shown on Figure 114 for the non-integral tank configuration. The irregular evaporation rates are due to the cumulative effects of varying fuel flow, wetted and dry tank areas, aircraft Mach nos., and altitude.

Preliminary analysis predicted that significant tank pressure slumps would occur during periods of high fuel flow due to insufficient boiloff. Preliminary work, however, assumed an average boost pump heat rejection rate over

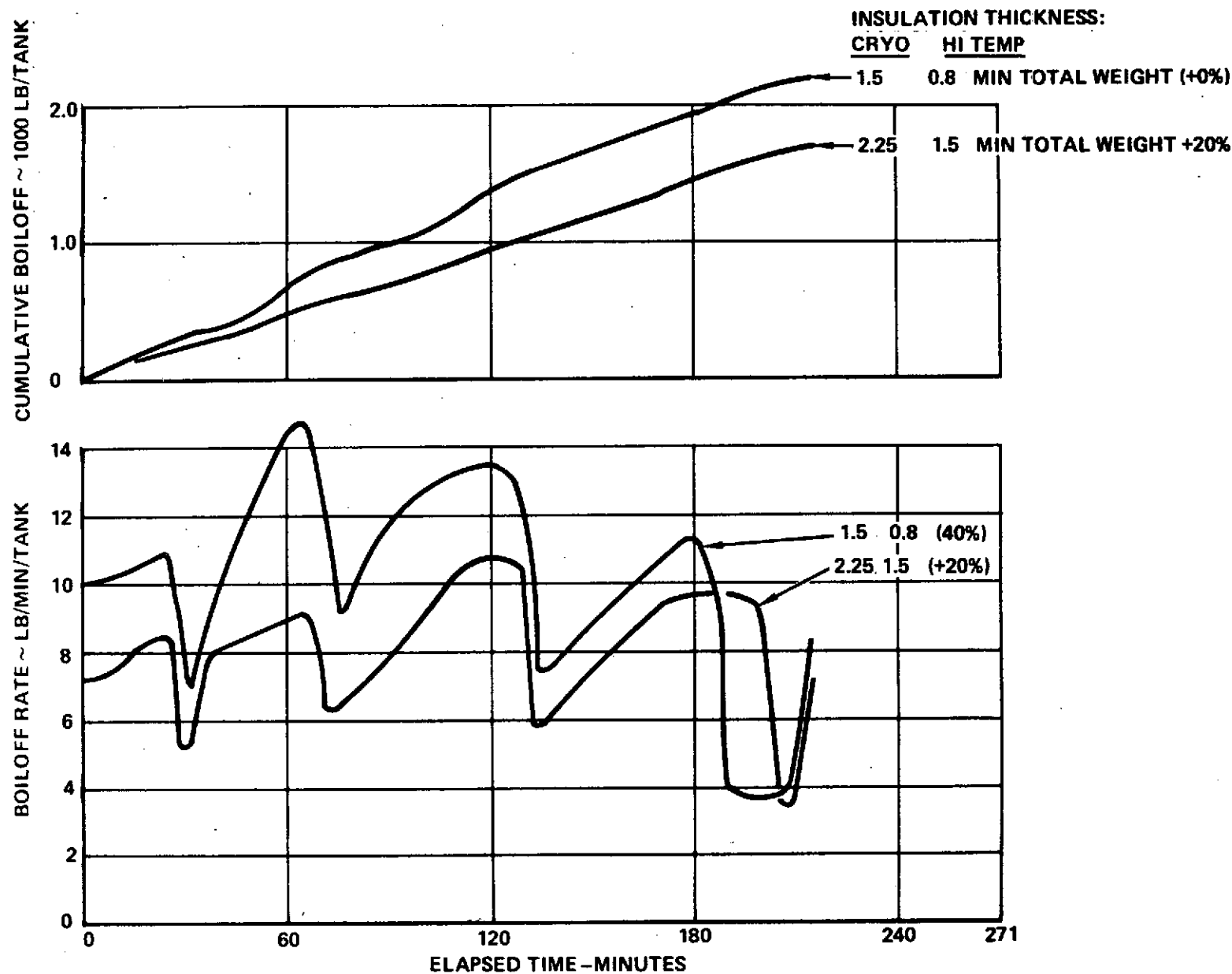


Figure 114. Boiloff Summary for Non-Integral AST LH₂ Tankage

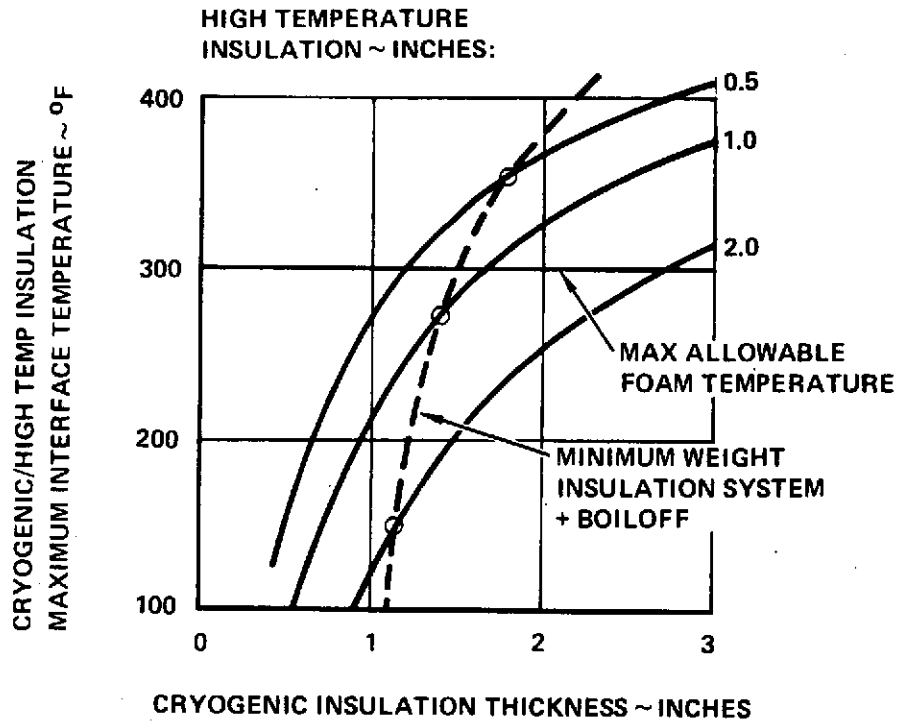


Figure 115. Non-Integral Tank - Interface Temperature

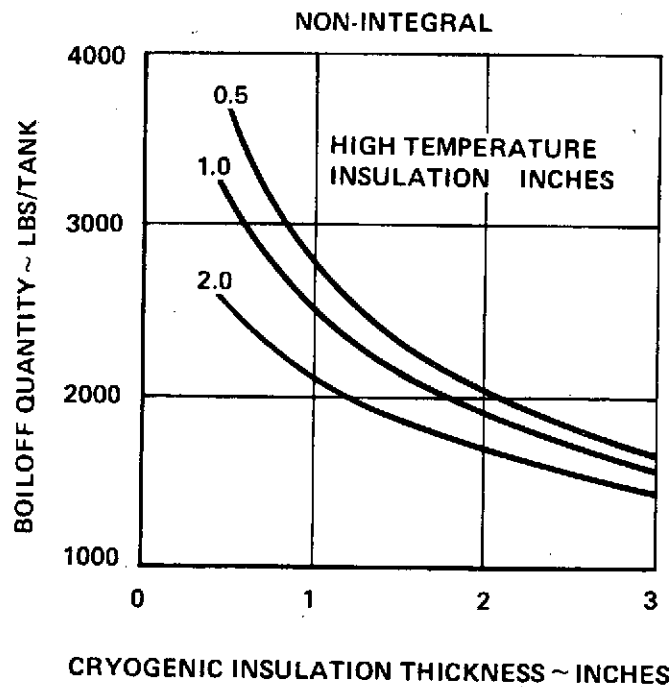


Figure 116. Non-Integral Tank - Mission Boiloff

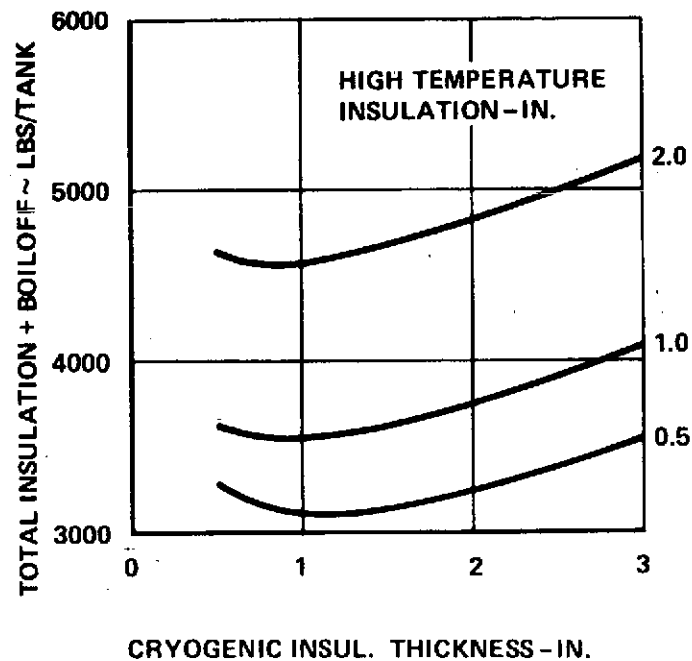


Figure 117. Non-Integral Tank - Total Insulation + Boiloff

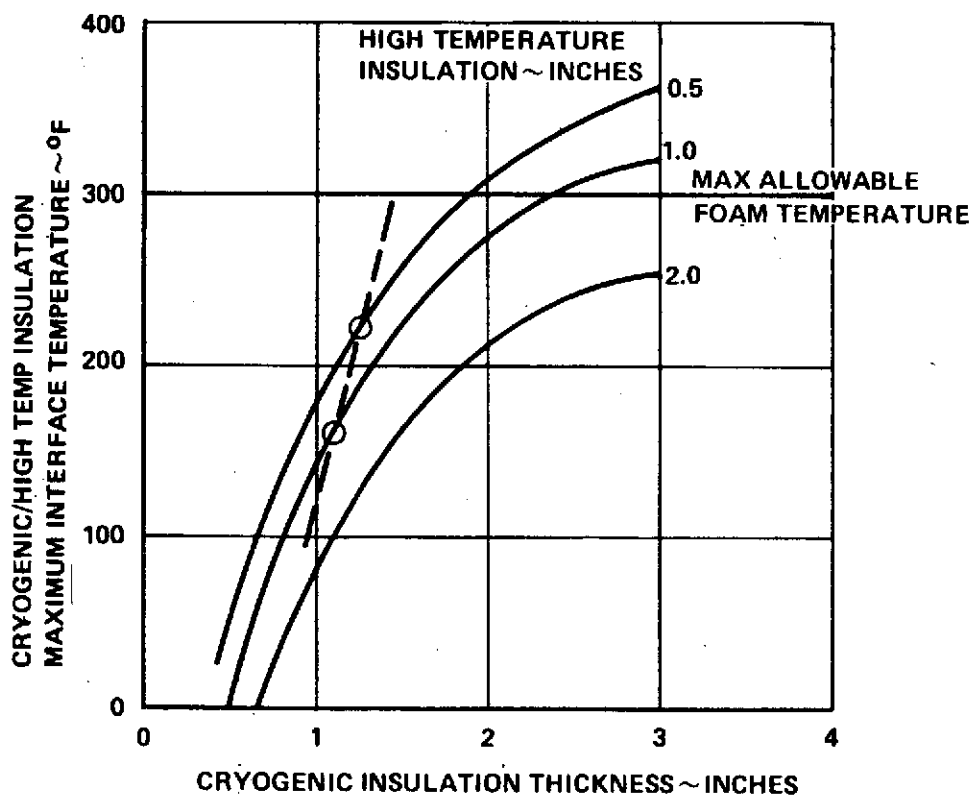


Figure 118. Integral Tank - Interface Temperature

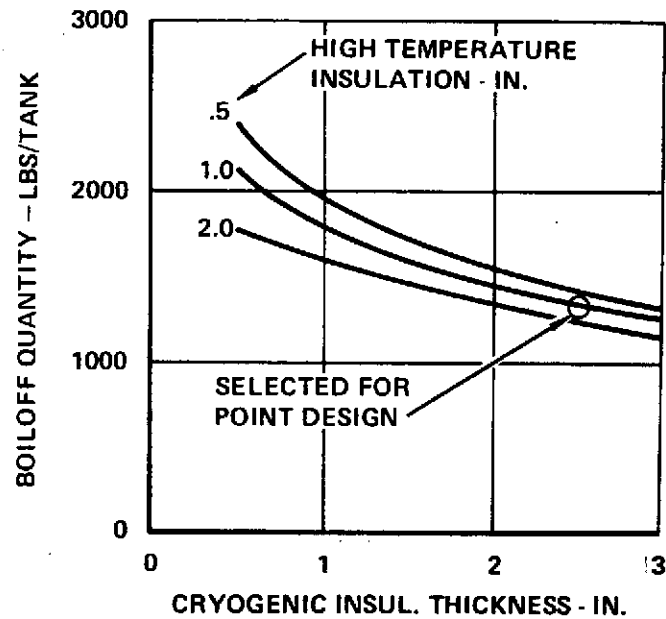


Figure 119. Integral Tank - Mission Boiloff

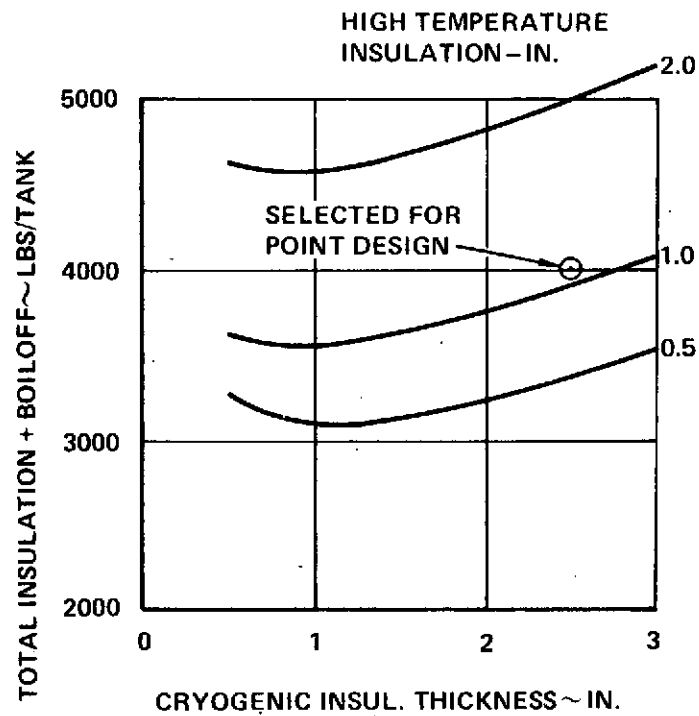


Figure 120. Integral Tank - Total Insulation + Boiloff

the entire flight profile, did not include radiation from the dry tank wall to the liquid surface, and did not account for additional fuel surface boiling when tank pressure was less than saturation pressure. Detailed analysis of these factors in the present study shows that boiloff is sufficient to maintain the 138,000 newton/m² (20 psia) pressure schedule throughout the mission profile. Boiloff for the basic mission typically represents from 3 to 7 percent of the initial fuel weight.

Examination of the curves illustrates the following well known trends for cryogenic insulation systems:

1. Increasing cryogenic insulation thickness decreases boiloff losses, but also increases the maximum cryogenic/high temperature insulation interface temperature (or peak foam temperature).
2. The higher peak foam temperature may require additional high temperature insulation, which in turn, increases total insulation system weight.

The minimum weight insulation system is determined by cross-plotting the locuses of minimum boiloff plus insulation weight points with maximum interface temperature as shown on Figures 115 and 118. Note that insulation system weights shown on all of the enclosed curves do not include the metal tank weight, and neither the external skin and structure weight (non-integral) nor the graphite/kevlar polyimide heat shield weight (integral).

The previous discussion has used the term minimum weight system as a criteria. This represents only the inflight losses and does not attempt to evaluate the system with regard to the following considerations:

1. The effect of ground hold on losses
2. Sufficient insulation to prevent excessive frost formation on the exterior surface.
3. The economic considerations of initial insulation weight and cost vs. the total cumulative boil-off over the life of the airplane.

While item 3 is of real consideration, it is beyond the scope of the present study particularly in view of the uncertain cost of hydrogen. Items 1 and 2 were investigated however and were found to place limitations on realizing

the "minimum weight" system. The most severe limitation was found to be the avoidance of frost formation on the bottom of the fuselage on a hot day with an assumed 5 mph wind. While it is realized that the maximum build up of frost will be limited due to the inherent insulating properties of the frost itself a minimum skin temperature of 40°F was selected for conservatism. A comparison of the non-integral and integral systems selected based on this limitation is shown in Table 29. The weight fractions shown here were used in the weight inputs to generate the integral tank point design vehicle.

The results of this study are summarized as follows:

1. The use of a heat shield of low conductance in the integral tank concept is lighter than the non-integral system.
2. Exterior fuselage temperature is the limiting factor in reducing the total boiloff and insulation weight to a minimum.
3. Variations in insulation thickness, top to bottom, may provide a more optimum system.

TABLE 29
COMPARISON OF NON-INTEGRAL VS INTEGRAL INSULATION SYSTEMS

	<u>Non-Integral</u>		<u>Integral</u>	
Max. Foam Temp. °K (R)	427	(760)	427	(760)
Min. Ground Hold Ext.				
Surface Temp. °K (R)	278	(500)	280	(504)
Foam Thickness cm. (in.)	6.35	(2.5)	6.35	(2.5)
Hi Temp Thickness cm. (in.)	4.57	(1.8)	2.85	(1.12)
Wt. Fractions: (Wt./Wt.H ₂)				
Low Temp. Insul.	0.0301		0.0301	
High Temp. Insul.	0.0487		0.0299	
Total Insulation	<u>0.0788</u>		<u>0.0600</u>	
Boiloff	<u>0.0355</u>		<u>0.0300</u>	
Total Boiloff & Insul.	<u>0.1143</u>		<u>0.0900</u>	

5.0 CONCEPT VIABILITY

The purpose of the study was to determine the feasibility of using liquid hydrogen as the fuel for commercial supersonic transport aircraft. In this section the results are reviewed to provide conclusions regarding the matter.

5.1 CRITICAL EVALUATION

Four bases of critical evaluation are considered in the following paragraphs to provide insight as to the viability of the LH_2 fueled AST aircraft.

5.1.1 Comparison with Equivalent Jet A-1 Vehicle

One of the overriding objectives of the Phase II effort was to provide a design of LH_2 fueled AST which could be compared directly with a hydrocarbon (Jet A-1) fueled version. The payload and original ground rules of the subject study were modified to provide a comparable basis for design with the Jet A-1 fueled AST being developed under Contract NAS1-12288 (Reference 4). Table 30 presents a number of relevant factors to compare characteristics of aircraft designed to use each of the fuels. Both aircraft are designed to carry a payload of 49,000 lb. (234 passengers) 4200 n.mi. and cruise at Mach 2.7. They are designed to the same technology state-of-the-art, defined by the work of Reference 4 as that which is presumed to be available for start of hardware development in 1981.

As seen in the table, the LH_2 AST gross weight is less than half that of the Jet A-1 fueled design. This leads to lower airline operating costs for a variety of reasons, e.g., wheels, tires, and brakes, all sized as functions of gross weight, are among the most significant maintenance cost items. Low gross weight also minimizes ground handling problems and cost of equipment.

In addition, low gross weight also means smaller engines since engines basically are sized to provide the thrust/weight ratio needed to meet takeoff field length requirements, modified as needed to also meet noise limitations. Smaller engines mean lower initial cost as well as lower maintenance costs.

Operating empty weight is 72 percent that of the Jet A-1 vehicle. This reflects a significant reduction of inert weight which need not be either

Preceding page blank

TABLE 30
COMPARISON OF JET A-1 AND LH₂ FUELED SUPERSONIC TRANSPORTS
OF ADVANCED DESIGN

Fuel			JET A-1		LH ₂	
Payload	(lb)	kg.	(49,000)	22,226	(49,000)	22,226
Range	(n.mi.)	km.	(4,200)	7,778	(4,200)	7,778
Cruise Speed	Mach		2.7		2.7	
Takeoff Gross Weight	(lb)	kg.	(750,000)	340,194	(368,000)	166,922
Operating Empty Weight	(lb)	kg.	(309,700)	140,478	(223,100)	101,196
Fuel Weight, Mission	(lb)	kg.	(326,000)	147,871	(81,440)	36,941
Total	(lb)	kg.	(391,300)	177,491	(95,900)	43,500
Fuel Volume	(ft ³)	m ³	(8,290)	234.7	(21,700)	614.5
Wing Area	(ft ²)	m ²	(10,822)	1005.4	(6,880)	639.2
Wing Loading (W/S) Takeoff	(lb/ft ²)	kg/m ²	(69.3)	338.4	(53.5)	261.2
Landing	(lb/ft ²)	kg/m ²	(39.1)	190.9	(41.7)	203.6
Span	(ft)	m	(132.5)	40.39	(105.6)	32.19
Overall Length	(ft)	m	(297)	90.5	(328)	100.0
Lift/Drag (cruise)			8.5		6.99	
Specific Fuel Consumption (cruise)	((lb/hr)/lb)	kg/hr/daN	(1.51)	1.54	(0.561)	.572
Thrust/Weight (SLS)			0.477		0.50	
Thrust Per Engine	(lb)	kg.	(89,500)	40,597	(46,000)	20,865
Weight Fractions	Percent					
Fuel			52.2		26.1	
Payload			6.5		13.3	
Structure			25.3		33.5	
Propulsion			10.0		15.8	
Equipment and Operating Items			6.0		11.3	
Energy/Seat. Mi.	(BTU/seat n.mi)	joule/seat m	(6102)	3,479	(4274)	2,437

manufactured (at an average cost of about \$109/kg (\$240/lb) for typical supersonic transport aircraft structure), or lifted and accelerated to cruise conditions on every flight for the life of the aircraft. These results also lead to airline operating economies.

One of the most interesting items observed in the table is the fact that there is a factor of 4.08 difference in the total fuel weight required by the two aircraft. However, the ratio of the average specific fuel consumption (SFC) values during cruise listed in the table is only 2.69. It might be expected that the same ratio should apply for both parameters. The fact that there is a higher ratio for the fuel weights than there is for the SFC's, is largely accounted for by the greatly reduced weight which must be lifted and accelerated by the hydrogen fueled aircraft. This reduced weight consists of not only the inert weight factor mentioned above, but also the much lighter fuel load. The reduced fuel load is mainly attributable to the SFC ratio; however, it is also favorably affected by the consideration that because the vehicle is lighter to begin with, for a given L/D it will require less thrust to overcome drag, therefore it will consume proportionately less fuel. It is seen that the L/D for the LH₂ aircraft is lower by almost 18 percent, but its average weight in cruise is lower by approximately 48 percent, thus leading to the favorable effect on fuel required during the flight.

Examination of the physical characteristics of the aircraft shows the LH₂ AST to be longer, have a shorter span and a much smaller wing. The wing loading is much lower at takeoff but virtually the same at landing. The thrust per engine is almost half that of the Jet A-1, but the thrust loading (uninstalled total thrust, sea level static, standard day condition, divided by gross weight) is higher.

Another factor of interest to compare the relative desirability of the two aircraft is energy expended per available seat mile. The Jet A-1 AST uses 43 percent more BTU/available seat mile than does the LH₂ AST, viz., 6102 BTU vs. 4274 BTU per seat mile. It should be noted that neither of these numbers includes the energy required to produce the fuels, nor to transport them to the airport. Both values represent just the energy contained in the fuel required by the respective aircraft to accomplish the given mission.

Table 31 lists some pertinent cost data for comparison of the two types of aircraft. The costs are expressed in terms of 1973 dollars, calculated on the bases noted. The LH₂ AST aircraft is almost \$20 million cheaper than the comparable Jet A-1 airplane in production, and development is estimated to cost

TABLE 31
COST COMPARISON: JET A-1 VS. LH₂ AST's
(Refer to Table 30 for vehicle data)

Costs*		Aircraft	
		Jet A-1	LH ₂
RDT&E	\$10 ⁶		
Engine		950	659
Airframe		<u>3,327</u>	<u>2,661</u>
Total		4,277	3,320
Production Aircraft, each	\$	67,328,000	47,967,000
Return On Investment (ROI) (After taxes)	Percent	2.24	6.04
Direct Operating Cost (DOC)	¢/SM		
Flight Crew		0.088	0.098
Fuel and Oil		0.568	0.735
Insurance		0.181	0.137
Depreciation		0.583	0.441
Maintenance		<u>0.468</u>	<u>0.376</u>
Total		1.888	1.787
Indirect Operating Cost (IOC)	¢/SM	0.888	0.801

* Basis for Costs:

- production of 300 aircraft
- Fare = \$9 + 0.0496 x Range (statute miles)
- passenger load factor = 0.55
- aircraft utilization = 3600 hrs/year
- fuel cost: Jet A-1 = 1.97¢/lb
LH₂ = 10¢/lb

almost a billion dollars less due largely to the lower airframe weight and use of smaller engines. Direct Operating Cost (DOC) and Return On Investment (ROI) are both strongly influenced by the cost of the fuel. The values of DOC and ROI shown in the table are based on fuel costs which are artificially low for both fuels. In September 1973, Jet A-1 sold for approximately 12¢/gal. (1.78¢/lb. or 97¢ per 10⁶ BTU). By early January 1974, the price had risen

to 23¢/gal. (3.42¢/lb. or \$1.86 per 10^6 BTU) and airlines were quoting future contracts with fuel suppliers at double that price (Reference 11). In the same reference, the Chairman of the Civil Aeronautics Board was quoted as saying the airlines may be conservative -- fuel prices may increase as much as 500 percent. The cost of LH_2 produced in large quantities from coal is variously quoted at prices from \$2.50 to \$5.00 per 10^6 BTU (12.9 to 25.8¢/lb.) delivered to the airport (Reference 12 and 14).

Figure 121 presents a plot of DOC for each type of aircraft as a function of the cost of its fuel. The data of Figure 121 shows a hydrogen fueled AST can be competitive on the basis of DOC when LH_2 costs approximately 1.75 times the price of Jet A-1. In other words, when Jet A-1 costs \$2.00 per 10^6 BTU (3.68¢/lb.), airline operators could afford to pay \$3.50 per 10^6 BTU (18.5¢/lb.) for LH_2 . It is significant that this comparison, favorable as it is to the hydrogen aircraft, does not include consideration of cost advantages resulting from the lower maintenance requirements and the longer life anticipated for components on engines fueled with liquid hydrogen.

5.1.2 Community Acceptance

Community acceptance is herein considered in terms of noise, sonic boom overpressure, and exhaust emissions. Table 32 lists values of these factors for both LH_2 and Jet A-1 fueled AST aircraft.

The LH_2 aircraft is more attractive in all aspects with the sole exception of water vapor in the exhaust. That particular item may or may not be a disadvantage. It has not yet been decided by authorities whether the exhaustion of quantities of H_2O in the stratosphere due to SST fleet operation will produce harmful effects.

Although there are no governmental restrictions concerning odors emitted by kerosene fueled aircraft, the completely odor-free operation resulting from use of LH_2 fuel would be a positive factor in community relations in the vicinity of airports.

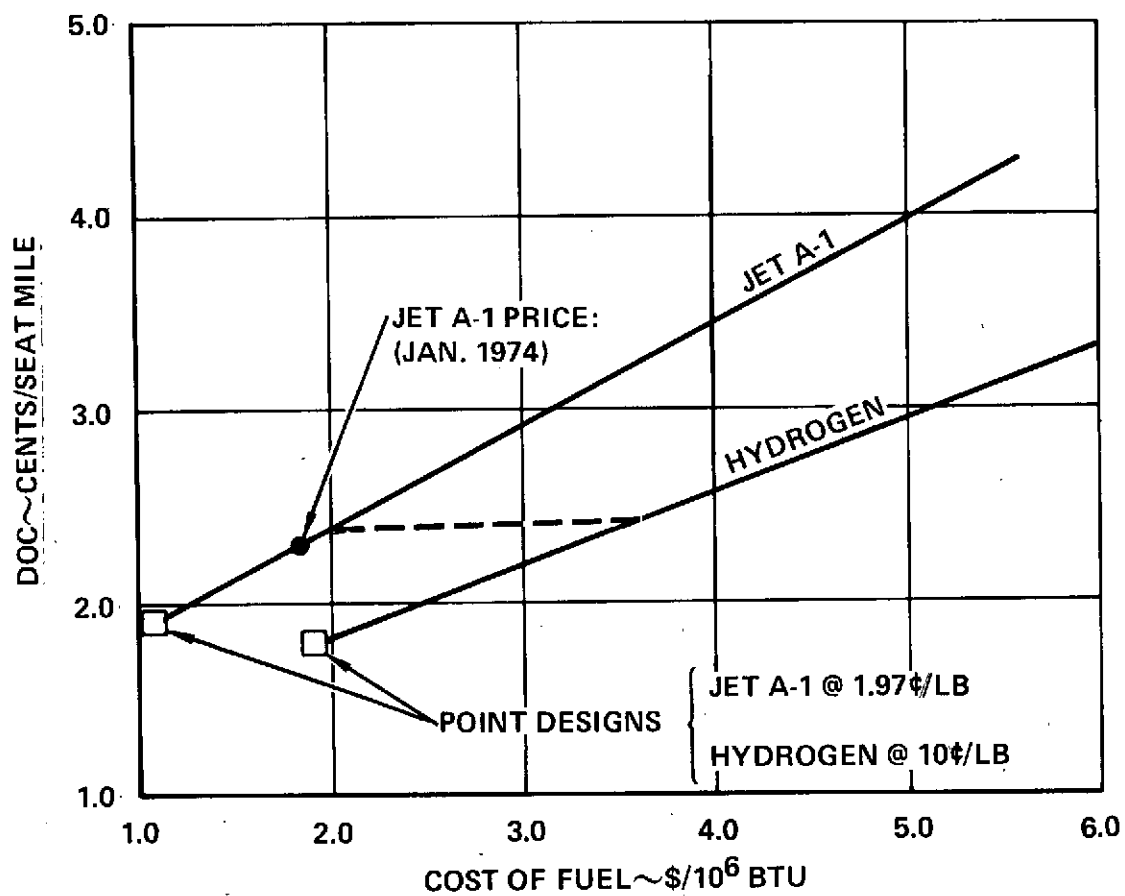


Figure 121. DOC vs. Cost of Fuel

TABLE 32
COMMUNITY ACCEPTANCE PARAMETERS

		Jet A-1 AST	LH ₂ AST
Noise	EPNdB		
Sideline		108	105.9
Flyover		108	104.3
Sonic Boom Overpressure	n/m ² (psf)		
Start of Cruise		89.5 (1.87)	63.2 (1.32)
End of Cruise		67 (1.40)	57 (1.19)
Maximum Encountered (during climbout)		120 (2.50)	99.6 (2.08)
Exhaust Emissions			
NO _x	gm/kg	3.7*	low
CO	gm/kg	90*	None
Unburned Hydrocarbons	gm/kg	0.5*	None
H ₂ O	kg/sec	15.05	28.5
Odors		Objectionable	None

*Data from Reference 13 for GE-J85, simulated flight at Mach 1.6, 55000 ft.

5.1.3 Level of Technical Risk

Technology development required to permit start of development of LH₂ fueled AST aircraft can be considered in two categories: minimum and desirable. The "minimum" category consists of those items which are necessary to accommodate the requirements of operating, handling, and maintaining aircraft of the subject design with its cryogenic fuel in a safe, economical manner; the "desirable" category includes additional items which can be seen will lead to further significant improvement in the operation or cost of LH₂ fueled AST aircraft. Table 33 presents the items of technology development required for both categories.

TABLE 33
MAJOR TECHNOLOGY DEVELOPMENT REQUIRED
FOR LH₂ FUELED AST AIRCRAFT

Minimum (necessary for the point design aircraft)

- Duct-burning turbofan engines designed to operate efficiently on hydrogen fuel.
- Lightweight cryogenic insulation, e.g., PVC or polyurethane foam, which is impervious to air, which can be bonded to an aluminum tank and can demonstrate an acceptable effective useful life.
- Lightweight high temperature insulation, e.g., fiberglass mat, surface sealed with polyimide, impervious to air, satisfactory for exposure to temperatures from 0°F to +400°F.
- Lightweight heat shield structural material having low thermal conductivity, e.g., fiberglass core, graphite/Kevlar/polyimide faced honeycomb sandwich, which is satisfactory for airline service.
- Lightweight aluminum tankage, capable of withstanding airline service, plus exposure to cryogenic temperatures and attendant thermal stresses.
- A satisfactory vent system for the LH₂ fueled aircraft.
- An aircraft fuel feed system including pumps, valves, quantity sensors, heat exchanger, pressurization system and control, and vacuum-jacketed lines acceptable for airline service.
- A ground supply and fuel handling system for use at airline terminals.
- An acceptable specification and set of standards for handling liquid hydrogen in routine airline operation.

-continued-

Table 33 Major Technology Development Required For LH₂ Fueled
AST Aircraft (Continued)

Desirable (improvements for additional advantage)

- Cryogenic insulation material which is impervious to gaseous or liquid hydrogen and can be used inside the aircraft fuel tanks. Alternatively, development of a barrier film which can be applied over a cryogenic insulation to prevent permeation by gaseous hydrogen into the insulation.
- Composite materials satisfactory for use as structure for an integral cryogenic tank.
- Heat shield material and design which serves efficiently as a high temperature insulation for application over the integral tank structure.

None of the items listed under the "Minimum" heading are considered to represent high technical risk. It is felt that with proper development effort, by 1981, all technology required for start of final design of a liquid hydrogen fueled supersonic transport aircraft could be available.

5.1.4 FAA Regulation Compatibility

One of the ground rules for the subject design study was that the LH₂ AST should be compatible with FAA regulations. The following regulations actively figured in establishing the configuration and performance characteristics of the point design LH₂ AST airplane:

- | | |
|--------------------|---------------|
| ○ FAR Part 25 | Certification |
| ○ FAR Part 36 | Noise |
| ○ FAR Part 121.648 | Fuel Reserves |
| ○ FAR Part 25 | Runway Length |

No exceptions to any of these regulations were found to be required for the point design LH₂ AST.

5.2 MAJOR TECHNOLOGY DEVELOPMENT REQUIRED

Figure 122 is a conceptual view of a program which could be undertaken to develop liquid hydrogen supersonic transport aircraft. The complete program is represented to indicate the general correlation and phasing of all major events. The major technology development items listed in Table 33 under the "Minimum" heading should be undertaken and completed before "go-ahead" for final design in 1981.

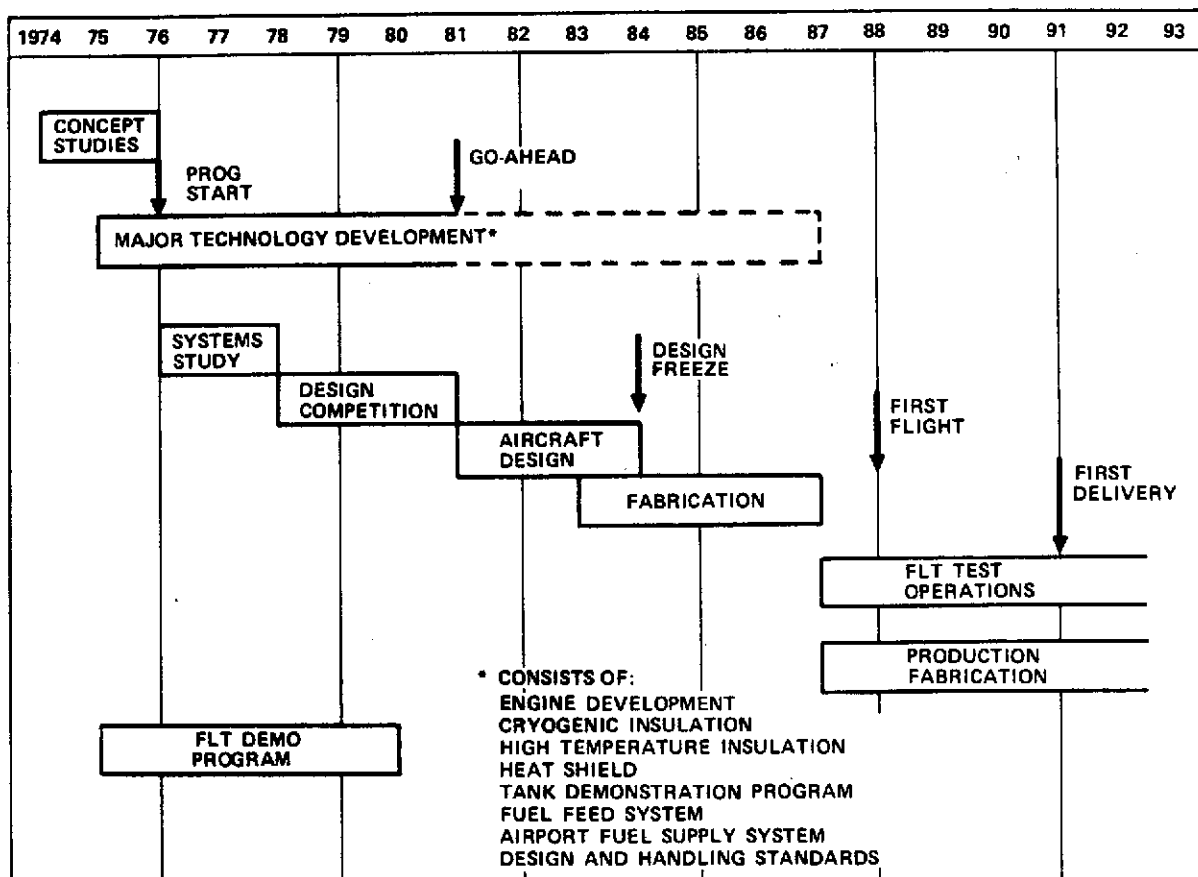


Figure 122 . LH₂ AST Conceptual Development Schedule

5.3 CONCLUSIONS

Use of liquid hydrogen for fuel in a supersonic transport of advanced design has many attractive advantages. The advantages to the air transport industry of using a synthetic fuel which is completely independent of the supply of petroleum are apparent, particularly in view of the dramatic developments of the past two months (since the Arab oil embargo started in October, 1973).

On the basis of the cost analysis presented herein, the case for hydrogen fueled supersonic transport aircraft is very clear: it is less costly to develop; less costly to fabricate; and, given a price of LH_2 per unit of energy only 1.75 times that of Jet A-1, less costly to operate.

Aside from consideration of economics and the availability of fuel, the LH_2 fueled AST offers advantages in being more acceptable to the community. Environmental pollution is drastically reduced. Noise is lower and sonic boom overpressures are lower along the flight path.

Energy expenditure per passenger mile is significantly lower than for a Jet A-1 aircraft of comparable design.

In addition, and undoubtedly one of the strongest reasons for recommending use of hydrogen as the fuel for an American supersonic transport, it avoids what would otherwise be a very significant increase in demand for petroleum-based fuel, thereby not adding to the burdens of society in the 1990 era.

6.0 RECOMMENDATIONS

In view of the many attractive advantages, it is recommended that development of technology for LH_2 fueled supersonic transport aircraft be actively pursued. The following actions are recommended to further explore the potential of such aircraft and to establish technology feasibility:

- Study alternate configuration concepts of LH_2 AST'S which appear to have advantage e.g., the wide-body version (CL-1701-4-1) discussed at the Mid Term Oral Review, and an actively-cooled aluminum skin version of the point design aircraft.
- perform additional studies of the point design aircraft to establish better definition of the design, including windtunnel testing.
- build and test insulated model cryogenic tanks to determine their capability for withstanding thermal cycling under simulated structural loading conditions.
- investigate thermal protection system concepts.
- study aircraft ground handling and refueling operations to establish specifications for equipment and procedures to assure safe, economical practices.
- initiate a flight demonstration program based on conversion of existing subsonic aircraft to LH_2 fuel, to learn the practical aspects of handling hydrogen in simulated airline operations (Reference 13).

Preceding page blank

REFERENCES

1. Contract NAS 1-11940, "Studies of the Impact of Advanced Technologies Applied to Supersonic Transport Aircraft, "NASA-Langley Research Center to Lockheed-California Company, September 11, 1972.
2. Contract NAS 1-11939, "Studies of the Impact of Advanced Technologies Applied to Supersonic Transport Aircraft," McDonald Douglas Corporation
3. Contract NAS 1-11938, "Studies of the Impact of Advanced Technologies Applied to Supersonic Transport Aircraft," The Boeing Company.
4. Contract NAS 1-12288, "Study of Structural Design Concepts for an Arrow-Wing Supersonic Transport Configuration," NASA-Langley Research Center to Lockheed-California Company, May 21, 1973.
5. Transportation Energy Panel, "Research and Development Opportunities for Improved Transportation Energy Usage," Department of Transportation, DOT - TSC - OST-73-14, September 1972.
6. Hubbert, M.K., "The Resources of the Earth," Scientific American, September 1972, pp. 61-70.
7. Synthetic Fuels Panel, "Hydrogen and Other Synthetic Fuels," prepared for the Federal Council on Science and Technology R&D Goals Study under the cognizance of the U.S. Atomic Energy Commission, September 1972.
8. ANON, "Supersonic Transport Development Program" Phase III Proposal Volume II-E Propulsion Report, Book I or III, submission to the Federal Aviation Agency IFASS-66-7, Lockheed-California Company, September, 1966, LR 19841.
9. Konesck, J.L., and Syberg, J. "Transonic and Supersonic test of a Mach 2.65 Mixed-Compressor Axisymmetric Intake," CR, 1971 NASA.
10. Tjonneland, E., "The Design, Development and Testing of a Supersonic Transport Inlet System," AGARD Paper 18 presented at the 38th meeting of the Propulsion and Energetics Panel, Oslo, Norway, Sept. 1971.

Preceding page blank

REFERENCES (Continued)

11. "The Airlines Face a Rough Ride, "Business Week, Jan. 19, 1974, p.23.
12. Johnson, John E., "The Economics of Liquid Hydrogen Supply for Air Transportation," Union Carbide Corporation, presented at Cryogenic Engineering Conference, August 10, 1973.
13. "The Energy Dilemma and its Impact on Air Transportation," The 1973 Summer Faculty Fellowship Program in Engineering Systems Design, NASA - Langley Research Center, ASEE, and Old Dominion University.
14. Wentorf, R.H. Jr., and Hanneman, R.E., "Thermochemical Hydrogen Generation," General Electric Company, Report 73 CRD 222, July 1973.
15. Harris, R.V., "An Analysis and Correlation of Aircraft Wave Drag," NASA TMX-947, 1964.
16. Lamb, Milton; and McLean F. Edward, "Evaluation of Techniques for Numerical Representation and Prediction of the Longitudinal Characteristics of Supersonic Fighters." NASA TMX-2283, 1971.
17. Combs, Henry, et al, "CL-400 Hydrogen Fueled Airplane," Appendices - Proposal Summary Report, Lockheed-California Company, LR 12296, June 13, 1958.
18. Brewer, G. Daniel, "Hypersonic Scramjet Vehicle Study" (U), Lockheed-California Company, LR 21137, Volumes I through V, 3 January 1968, (Secret).
19. Morris, R.E. and Williams, N.B., "Study of Advanced Airbreathing Launch Vehicles with Cruise Capability," Lockheed-California Company, Reports NASA CR 73194 - 73199, Feb.-April 1968.

APPENDIX A

COST MODEL DESCRIPTION

The cost models used in the evaluation of the Liquid Hydrogen AST consists of subroutines to the ASSET program, plus a separate model on the CPS (Conversational Programming System) terminal for calculating returns on investment (ROI).

Development Cost Model

The cost estimates for the primary elements of development cost are determined by cost estimating relationships (CER's) which are determined by statistical analysis of historical data from military programs. The basic equations used to estimate the development cost for the airframe and engine are modified versions of the CER's developed by the RAND Corporation (references A-1 and A-2). The RAND equations are modified to reflect airframe and engine manufacturer's experience. The engine equations are modified by information obtained from P&W and GE for liquid hydrogen engines. The airframe engineering hour estimates by the RAND CER's are modified to reflect a Lockheed in-house estimate. The Lockheed estimate is provided by a methodology that has been developed through a detailed analysis of Lockheed programs. The modifications to the RAND equations are provided by the application of K factors to the basic equations.

The development cost model includes the following elements:

Prototype Aircraft	Development Tooling
Design Engineering	Special Support Equipment
Development Test Articles	Development Spares
Flight Test	Technical Data
Engine Development	Avionics Development

The equations for determining the cost for each of the above elements are shown in the Development Cost Model that follows.

The cost for the prototype aircraft is determined from the flyaway cost model and input to the development model. The prototype aircraft are costed on the basis of the first few vehicles produced.

Development Cost Model

Prototype Aircraft

TPROT=TFLCO * XNYO

Design Engineering

RFDE = .0396 * WAMPR ** .791 * SS ** 1.526 * CXNYO ** .183
DIH = RFDE * XKE - SELHO = (Design Engineering hours less sustaining)
DIEC = DIH (DER + OER) * (1 + APRFF) = (design engineering cost)

Tooling

DTHB = 4.0127 * WAMPR ** .764 * SS ** .899 * CXNYO ** .178 *
DRT ** .066
DHT = DTHB * XKT - PTLHO = (Design tooling hours less sustaining)
DTC = DTH (DTR + OTR) * (1 + APRFF) = (Design tooling cost)

Development Test Articles

DSTA = (TAFCO/CXNYO) * XNSTA = (Cost for static test article)
DFTA = (TAFCO/CXNYO) * XNFTA = (Cost for fatigue test article)
DMTS = (TAFCO/CXNYO) * XMFSF = (Cost for systems test articles)
DART = (DSTA + DFTA + DMTS) * (1 + APRFF)

Flight Test

RFFT = .001244 * WAMPR ** 1.16 * SS ** 1.371 * CXNYO ** 1.281
DFT = RFFT (1 + APRFF) * XKFT = (Flight test cost including profit)

Engine Development

CEDCM = XMAX ** .62 [(CXNY10+CXNYO)*XNENG] ** .10
DCENG = CEDCF * [(TCE/1000)/XNENG] ** CEDCE * CEDCM

Avionics

DAV = DPAVD * WAVUN + FAVDC

Spares

$$\text{DSPAR} = \text{ADSF} * \text{TAFCO} + \text{EDSF} * \text{TENCO} + \text{AVDSF} * \text{TAVCO}$$

Special Support Equipment

$$\text{DSSE} = \text{DSSEF} * \text{TFLCO}$$

Technical Data

$$\text{DDATA} = \text{DTDF} (\text{TFLCO} + \text{DIEC} + \text{DTC} + \text{DART} + \text{DFT} + \text{DCENG} + \text{DLENG} + \text{DAV} + \text{DSPAR} + \text{DSSE} + \text{DOT} + \text{DMT})$$

The description of the inputs and the factors for the development model are included along with the description of the inputs for the production model that follows.

Investment Cost Model

The Investment Cost Models includes subroutines to provide the cost for the aircraft, the aircraft spares, and the special support equipment. The primary element of investment is the aircraft and it is given the most attention in terms of detail and consideration of the labor and material cost factors. The spares and special support equipment cost are treated as percentages of the flyaway cost of the aircraft. The production cost estimate is made to the same general level of detail as the airplane group weight statement. The production cost input format includes the following elements:

- Material Cost Factors
- Labor Cost Factors
- Labor rates
- Sizing and Learning Curve Factors
- Sustaining Engineering
- Sustaining Tooling
- Engineering Change Orders
- Quality Assurance
- Miscellaneous Costs
- Warranty
- Insurance and Taxes
- Profit

An illustrative example of the elements of the airframe and their representative cost factors is shown in Table A-1. How these factors are applied is illustrated in the schematic of the flyaway cost model shown in Figure A-1.

Airframe Material Cost

As shown by Table A-1, the material cost factors include representative cost factors for various types of material for the structural elements of the airframe. The airframe production cost model has space for material cost factor inputs for aluminum, titanium, steel, composites, and other. The various types of materials are listed across the top of the input sheet (Table A-1). A material cost factor is assigned to each type of material. The material cost factors are applied to the amount of each type of material as determined from the sizing program. The ASSET program determines the total weight of each element from the performance and configuration input data. After the total weight of the component is determined, the amount of each type of material is obtained by applying percentage factors to the total. The percentage factors for each type of material are established through previous analysis and input to the program.

Airframe Labor Cost

The same procedure as used in the materials is used in the labor subroutine, except that the labor is in hours. After the total number of hours are determined the labor rate is applied to arrive at the total labor cost.

The labor rates shown in Table A-1 include the rates for design engineering, tooling, manufacturing, quality assurance, and miscellaneous. Only the labor rates for manufacturing and quality assurance are used for development engineering and tooling.

Non-Structural Elements Cost Factors

The cost factors for these elements includes both labor and material. This category includes the installation cost for the systems and equipments noted as well as their manufacturing cost with the exception of the engine and avionics. The installation costs for the engine and avionics are included here but the purchased costs for these items are shown separately.

After the labor hours, labor rates and material cost factors are applied to each material type, the elements are summed to arrive at a total airframe labor and material cost. These sums are then adjusted for quantity and size.

Sizing and Learning Curve Factors

The sizing factors are included to account for scaling of the labor and material cost due to aircraft size. The learning curve factor accounts for cost change due to quantity produced. The labor and material cost factors shown in Table A-1 are normalized to a particular vehicle weight and production quantity. The scaling factors modify the labor and material cost according to the size of the vehicle being analyzed and the number of aircraft in the production program. The sizing and learning curve factors include:

- Material Sizing Factor
- Labor Sizing Factor
- Material Learning Curve
- Labor Learning Curve
- Engine Learning Curve
- Avionics Learning Curve

As noted by Figure A-1 the adjustment factors for quantity are applied to the engine and avionics as well as the labor and material.

Miscellaneous Factors

There are cost items which must be included in the production cost of the aircraft that are not part of the labor and material costs directly associated with the manufacturing of the vehicle. These are such items as quality assurance engineering changes, tool maintenance, sustaining engineering, warranty, taxes, insurance and miscellaneous costs. The costs for these items is added to the cost for the structural and non-structural elements to arrive at a total airframe cost. These factors are applied against the total airframe labor cost to arrive at the cost of each item. Costs are summed to obtain a total airframe cost.

Engine Cost

The engine cost estimate is provided by a production cost equation, or supplied by engine manufactures, and input to the model. The equation is

A-6

REPRODUCIBILITY OF THE
ORIGINAL PAGE IS POOR

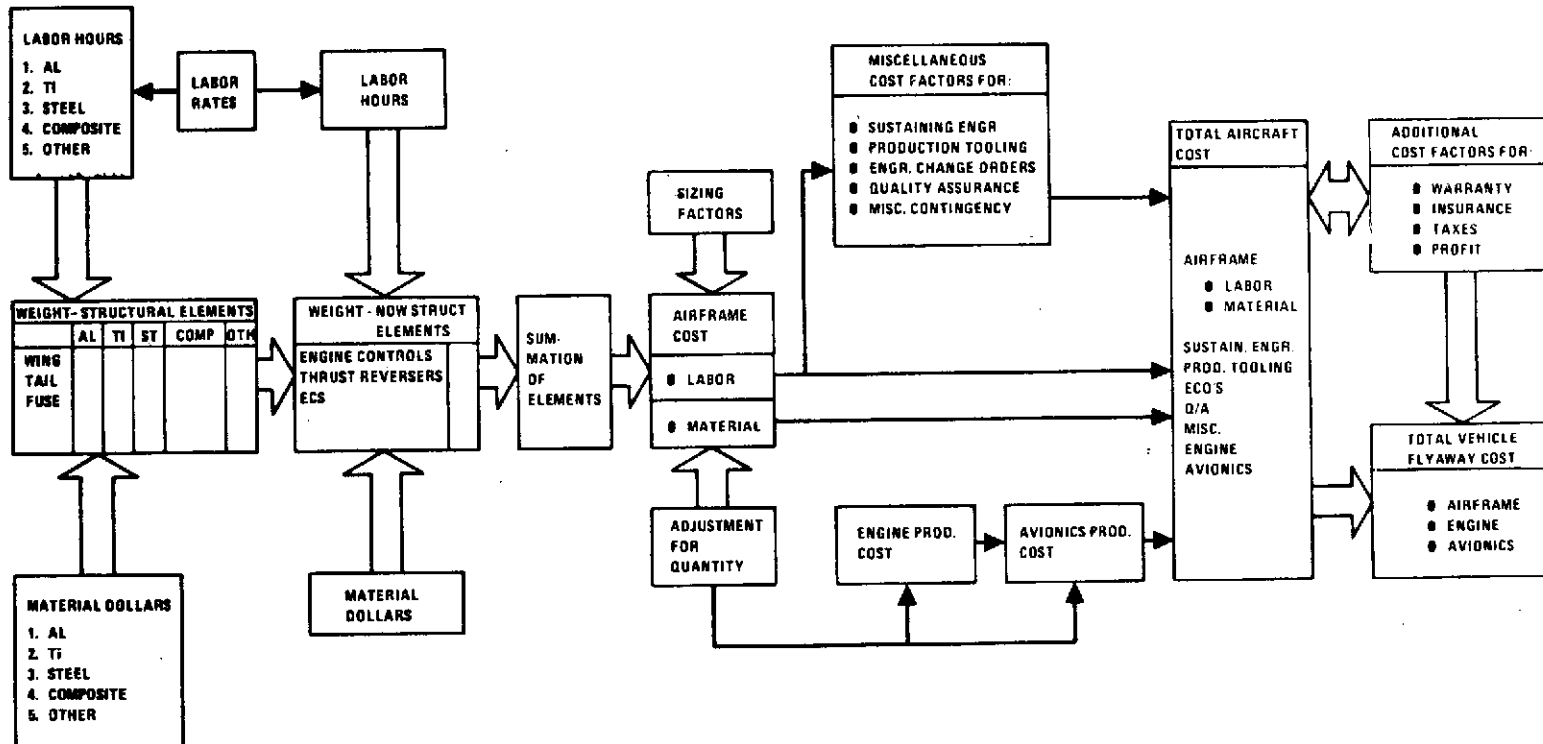


Figure A-1. Aircraft Flyaway Cost Model



TABLE A-1
ASSET COST INPUT

Flags and Misc Inputs	CSTPRT	0	PASP	1.0					1	
	XMMAX	2.7	XMMIN	0.25						
	XNENGL	0	TMAXLE	0	XNAVS	1.0	TMR	1.73	3	
Production Schedule (300 A/C)	XNY1	12	XNY2	18	XNY3	24	XNY4	30		
	XNY7	36	XNY8	36	XNY9	36	XNY10	36	5	
Material Type	AL		TI		Steel		Composite	Other		
Material Cost Factors - \$/lb	DPWIAL	12.72	DPWITI	52.35	DPWIST	15.90	DPWIC0	114.48	DPWIST	12.72
	DPTAAL	12.72	DPTATI	38.90	DPTAST	15.90	DPTAC0	106.08	DPTAST	12.72
	DPFUAL	12.72	DPFUTI	25.55	DPFUST	15.90	DPFUC0	114.48	DPFUST	12.72
	DPLGAL	37.10	DPLGTI	47.23	DPLGST	42.41	DPLGC0	125.40	DPLGST	37.10
	DPNAAL	15.90	DPNATI	21.35	DPNAST	19.88	DPNAC0	127.20	DPNAST	15.90
	DPAIAL	37.14	DPAITI	60.62	DPAIST	42.45	DPAIC0	109.56	DPAIST	37.14
	DPSCAL	127.20	DPSCTI	134.96	DPSCST	129.36	DPSCC0	208.61	DPSCST	127.20
										Wing Tail Fuselage Landing Gear Nacelle Air Induction Surface Controls
Labor Cost Factors - hr/lb	HPWIAL	4.80	HPWITI	8.023	HPWIST	7.20	HPWIC0	7.50	HPWIST	4.80
	HPTAAL	4.80	HPTATI	13.20	HPTAST	10.60	HPTAC0	7.50	HPTAST	4.80
	HPFUAL	6.00	HPFUTI	9.00	HPFUST	7.20	HPFUC0	9.00	HPFUST	6.00
	HPLGAL	0.12	HPLGTI	0.12	HPLGST	0.12	HPLGC0	0.12	HPLGST	0.12
	HPNAAL	4.80	HPNATI	10.00	HPNAST	8.00	HPNAC0	6.00	HPNAST	4.80
	HPAIAL	5.40	HPAITI	11.20	HPAIST	9.00	HPAIC0	7.50	HPAIST	5.40
	HASCAL	4.80	HPSCTI	11.50	HPSCST	8.00	HPSCC0	6.00	HPSCST	4.80
										Wing Tail Fuselage Landing Gear Nacelle Air Induction Surface Controls
Non-Structural Element Cost Factors	DPEC	175.00	FXECMC		HPEC	2.50	FXECLH			
	DPTR	0	FXTRMC		HPTR	0.14	FXTRLH			
	DPES	51.62	FXESMC		HPES	2.58	FXESLH			
	DPXI	215.00	FXXIMC		HPXI	3.50	FXXILH			
	DPHY	161.23	FXHYMC		HPHY	9.20	FXHYLH			
	DPEL	95.43	FXELMC		HPPEL	7.30	FXELLH			
	DPES	15.90	FXSSMC		HPES	4.80	FXSSLH			
	DPFE	42.46	FXFEMC		HPFE	3.27	FXFELH			
	DPAM	0	FXAMMC		HPAM	0	FXAMLH			
	DPAG	44.54	FXAGMC		HPAG	0.12	FXAGLH			
	DPET	0	FXELMC		HPET	0.14	FXEILH			
	DPAV	13.88	FXAVMC		HPAV	4.20	FXAVLH			
	DPSI	0.50	FXSILC		HPSI	0.67	FXSILH			
	DPVC	0	FXVCMC		HPVC	0	FXVCLH			
	DPFS	27.70	FXFSMC		HPFS	3.51	FXFSLH			
										Engine Controls Thrust Reverser ECS Instruments Hydraulics Electrical Engine Section Furn. & Equip. Armament Auxiliary Gear Eng. Installation Avionics Install. Systems Integr. Vector Control Fuel System
Manufacturing Support Factors	QAPO	0.20	ECPO	0	PTMPO	0.25	SEPO	0.15	RMRO	0.35
	QAP	0.20	ECP	0	PTMP	0.12	SEP	0.10	RMR	0.35
Eng & Avionics Prod Cost Factors	CERCP	631,000	CEPCE	0.60	XLEPCF	0	XLEPCE	1.0	DPAVP	0
Tax Insurance, Warranty, and Profit Cost Factors	ATAIF	0.10	ETAIF	0	AVTAIF	0	AWAF	0.05	EMAF	0
	APRFF	0.15	EPFRFF	0	AVPRFF	0			AVWAF	0
Sizing and Learning Curve Factors	WEMTM	213,058	XMCS	0.99						
	WEMBL	227,064	XHCS	0.96						
	XMMB	100	XMICS	0.95						
	XNHB	100	XHLCS	0.80						
	XNCEB	1.0	XCEICS	0.90						
	XNLEB	1.0	XLEICS	0.90						
	XNAB	1.0	XAVICS	1.00						

A-7

ORIGINAL PAGE IS POOR
REPRODUCIBILITY OF THE



TABLE A-1
ASSET COST INPUT (Continued)

Material Type	AL	TI	Steel	Composite	Other		
Labor Rates	DER 8.17 ØER 9.20 DEGR 0 ØEGR 0 XMGR 0	DTR 6.09 ØTR 12.36 DTGR 0 ØTGR 0 XAGR 0	DMR 5.12 ØMR 10.72 DMGR 0 ØMGR 0 XEMR 0	DQAR 6.29 ØQAR 10.72 DQAGR 0 ØQAGR 0	DMISC 5.12 ØMISC 10.72		51
RDTE Cost Factors	XKE 0.80 XNSTA 1.0 GEDCF 21.3x10 ⁶ DRT 1.0 DSSEF 0.02	XKT 0.88 SNFTA 1.0 CEDCE 0.55 ADSF 0.15 DTDF 0.005	XKFT 0.37 XMTSF 0.30 XLEDCE 0 EDSF 0.50 DMT 0	ETSMR 0 XLEDCE 0 AVDSF 0.30 DMT 0	EFTMR 0 DPAVD 0	FAVDC 0	56
Investment Cost Factors	PET 3.0 PSSEF 0.05	PECF 0 PTDF 0.005	PECE 1.0 POT 0	APSF 0.15 PMT 0	EPSF 0.30	AVPSF 0.30	58
Operational (Military) Cost Factors							65
Direct Operating Cost (DOC) Factors	XNRITE 12.0 SSPB 15.0 U 3600	YEAR 1973 IFB 20.0 IRA 0.0222	XNCREW 3.0 PCSIR 0.7 PERIOD 14.0	XNPASS 234 MNPLIR 0.05 CPT 0.10	XNATT 8.0 TG 15.0 COT 0.945	XLF 0.55 MBF 1.90	68
Indirect Operating Cost (IOC) Factors	REVPAS 1.81x10 ⁶ XKSE .0206 XKPH 12.0	AVCARG 2000 XKLE 2.87 XKCH 96.0	XKCP 58.0 XKCP .0061	XKAT 27.0 XKCP .0065	XKPB 0.58 XKGA 0.064		71
Return on Investment (ROI) Factor	CFARE .0496	XKFARE 9.0	XKFACC 0	TAXR 0.48	CARGF 0.30		72

taken from the latest RAND revision (Reference A-2) of their analysis of turbojet and turbofan production cost. The RAND equation has been modified by estimates provided by P&W and GE for the AST. The production cost equation for the duct burning turbofan is of the form:

$$\text{Engine Production Cost} = 631,000 \left(\frac{\text{TCE}}{1000} \right)^{.6} (\text{XNENG C})^{-.152}$$

Where

TCE = maximum seal level static thrust

XNENG C = number of engines in the production program.

The constant in the equation is changed to 546,000 for costing the turbojet engine.

Avionics

The avionics estimates are provided by vendors or in-house analysis and input to the model.

Additional Factors

The total summation of cost elements up to this point produces the flyaway cost of the aircraft without profit and costs for warranty, taxes, and insurance. The cost for these items is obtained by applying factors for each to the total aircraft cost. These costs are incorporated into the total aircraft production cost to arrive at the total vehicle flyaway cost except for the amortized R&D.

DEVELOPMENT AND PRODUCTION MODEL SYMBOL DEFINITIONS

TFLCO	=	Cost of prototype
CSTRT	=	Print Indicator (1 = detail, 0 = summary)
FAST	=	Indicator if AST or other
XMMAX	=	Maximum Mach number
XMIN	=	Minimum Mach Number - Stall Speed
XNENGL	=	Number of lift engines
TMAXLE	=	Maximum thrust of lift engines
XNAVS	=	Number of avionics suites

TMR	= Tooling material rate
XNY1-XNY	= Number of aircraft delivered per year
XNYO	= Number of aircraft in the development program
QAPO/QAP	= Quality assurance factor for development/and production
ECPO/ECP	= Engineering change order factor for development/and production
PTMPO/PTMP	= Tool maintenance factor for development/and production
SEPO/SEP	= Sustaining engineering factor for development/and production
RMRO/RMR	= Raw material rate for development and production
XMISCO/XMISC	= Miscellaneous cost factor for development/and production
CEPCF	= Constant value for engine production cost formula - cruise engine
CEPCE	= Value of coefficient in engine production cost formula - cruise engine
XLEPCF	= Constant value for engine production cost formula - lift engines
XLEPCE	= Value of coefficient in engine production cost formula - lift engine
DPAVP	= Avionics production cost factor
FAVPC	= Production cost for avionics
ATAIF	= Airframe insurance factor
ESTAIF	= Engine insurance factor
AVTAIF	= Avionics insurance factor
AWAF	= Airframe warranty factor
EWAF	= Engine warranty factor
AVWAF	= Avionics warranty factor
APRFF	= Airframe profit factor
EPRFF	= Engine profit factor
AVPRFF	= Avionics profit factor
WEMTBM	= Weight empty of aircraft being evaluated
WEMTBL	= Weight empty of base line vehicle from which the cost factors were developed
XNMB	= Quantity at which the material factors were developed
XNHB	= Quantity at which the labor factors were developed
XNCEB	= Base quantity for cruise engines
XNLEB	= Base quantity for lift engines

XNAB	=	Base quantity for avionics
XMCS	=	Material cost sizing coefficient
XHCS	=	Labor cost sizing coefficient
XMLCS	=	Material learning curve slope
XHLCS	=	Labor learning curve slope
XCELCS	=	Cruise engine learning curve slope
XLELCS	=	Lift engine learning curve slope
DER	=	Engineering labor rate (direct)
ØER	=	Engineering overhead rate (indirect)
DEGR	=	Growth rates - not used
ØEGR	=	
XMGR	=	
DTR	=	Tooling labor rate (direct)
ØTR	=	Tooling overhead (indirect)
DTGR	=	Growth rates - not used
ØTGR	=	
XAGR	=	
DMR	=	Manufacturing labor rate (direct)
ØMR	=	Manufacturing overhead rate (indirect)
DMGR	=	Growth rates - not used
ØMGR	=	
XEGR	=	
DQAR	=	Quality assurance labor rate (direct)
ØQAR	=	Quality assurance overhead rate (indirect)
DQAGR	=	Growth rates - not used
ØQAGR	=	
DMISC	=	Labor rate for miscellaneous items
ØMISC	=	Overhead rate for miscellaneous items
XKE	=	Complexity factor for engineering
XKT	=	Complexity factor for tooling
XKFT	=	Complexity factor for flight test
XNSTA	=	Number of test articles for structural tests
XNFTA	=	Number of test articles for fatigue tests

XMTSF	=	Number of test articles for systems test
ETSMR	=	Engineering test material rate
EFTMR	=	Flight material rate
CEDCF	=	Constant value for cruise engine development cost equation
CEDCE	=	Value of coefficient for development cost formula for cruise engines
XLEDCE	=	Constant value for lift engine development equation
XLEDCE	=	Value of coefficient for development cost formula for lift engines
DPAVD	=	Development cost factor for avionics
FAVDC	=	Development cost for avionics
DRT	=	Production rate for development
ADSF	=	Airframe spares factor for development
EDSF	=	Engine spares factor for development
AVDSF	=	Avionics spares factor development
DSSEF	=	Special support cost factor for development
DTDF	=	Technical data cost factor for development
DØT	=	Operator trainer cost factor for development
DMT	=	Maintenance trainer cost factor for development
PRT	=	Maximum monthly production rate
PECF	=	Constant term for production engineering cost formula
PECE	=	Value of coefficient for production engineering cost formula
APSF	=	Spares factor for production airframes
EPSF	=	Spares factor for production engines
AVPSF	=	Spares factor for production avionics
PSSEF	=	Special support equipment cost factor for production
PTDF	=	Technical data cost factor for production
PØT	=	Cost for operator trainers
PMT	=	Cost for maintenance trainers

OPERATING COST MODELS

The operating cost includes the standard elements normally found in the direct and indirect operating cost (DOC/IOC) as reported by the airlines. The DOC model is a modified version of the 1967 ATA method (Reference A-3). The modifications to the DOC equations in the ATA method consists of: 1) combining the crew cost equations into a general expression for any number of crew members and 2) expanding the maintenance equations into greater detail. The more detailed maintenance equations are obtained from (Reference A-4). The IOC model consists of set of expression derived through the combined efforts of Lockheed and Boeing (Reference A-5). The indirect expense factors are those experienced by the international carriers (Reference A-6).

DOC MODEL

Flight Crew $[3.0*(45+SSFB)+35(XNCREW-3)+IFB] * (1.0+FCSIR)^{XNYR} * U$

Fuel and Oil $1.02*U*(FB/TB*CFT+XNENG* COT*.135)$

Insurance $IRA*TUACC$

Depreciation $(TUACC+SPARES)/PERIOD$

Maintenance Equipment and Furnishings

Labor = $[.5TF+1.0+(4.5TF+18)*WAF/10^6]*U/TB*MNTLR$

Material = $[.4TF+1.20+(14TF+42)*WAF/10^6]*U/TB$

Landing Gear

Labor = $(1.0+10*WAF/10^6)*U/TB*MNTLR$

Material = $(2.4+1.50*TUAFC/10^6)*U/TB$

Tires and Brakes

Material = $(1.2+7.0*WAF/10^6)U/TB$

Other Systems

Labor = $(15TF+3.3)*(WAF/10^6)^{.5} *XMAX^{.5}*U/TB*MNTLR$

Material = $(1.4TF+.8)+(2.3TF+.7)*(TUAFC/10^6) *XMAX^{.5}*U/TB$

Structures

$$\begin{aligned}\text{Labor} &= (1.0 + 50 \cdot \text{WAF} / 10^6) \cdot \text{XMMAX}^5 \cdot \text{U} / \text{TB} \cdot \text{MNTLR} \\ \text{Material} &= (.3 + .8 \cdot \text{TUAFC} / 10^6) \cdot \text{XMMAX}^5 \cdot \text{U} / \text{TB}\end{aligned}$$

Other Power Plant

$$\begin{aligned}\text{Labor} &= (19.0 \cdot \text{TF} + .8) \cdot (\text{WAF} / 10^6)^{.5} \cdot \text{XMMAX}^5 \cdot \text{U} / \text{TB} \cdot \text{MNTLR} \\ \text{Material} &= .3 \cdot \text{TF} + .1 + (.8 \cdot \text{TF} + .1) \cdot (\text{TUAFC} / 10^6) \cdot \text{XMMAX}^5\end{aligned}$$

Engine

$$\begin{aligned}\text{Labor} &= [.4 \cdot \text{TF} + .2 + (.018 \cdot \text{TF} + .012) \cdot \text{TCE} / \text{XNENG} / 10^3] \cdot \text{U} / \text{TB} \cdot \text{MNTLR} \cdot \text{XNENG} \\ \text{Material} &= (3.8 \cdot \text{TF} + 2.40) \cdot (\text{ENG} / 10^5) \cdot \text{U} / \text{TB} \cdot \text{XNENG}\end{aligned}$$

The above formulas calculate the DOC in terms of dollars per aircraft year. This is converted to cents per seat mile by converting the dollars to cents and dividing each element by the seat miles flown per year.

IOC MODEL

Item I System Expense

$$\text{System Expense} = \text{XKSE} \times \text{direct maintenance labor dollar}$$

Item II Local Expense

$$\text{Local Expense} = \text{XKLØE} \times \frac{\text{maximum takeoff weight}}{1000} \times \text{departures}$$

Item III Aircraft Control

$$\text{Aircraft Control Expense} = \text{XKCØ} \times \text{departures}$$

Item IV Cabin Attendant Expense

$$\text{Cabin Attendant Expense} = \text{XKAT} \times \text{Cabin attendant block hours}$$

Item V Food and Beverage Expense

$$\text{Food and Beverage Expense} = \text{XKFB} \times \text{weighted revenue passenger block hours}$$

Item VI Passenger Handling Expense

$$\text{Passenger Handling Expense} = \text{XKPH} \times \text{Passengers enplaned}$$

Item VII Cargo Handling

$$\text{Cargo Handling Expense} = \text{XKCH} \times \text{Total tons carried}$$

Item VIII Other Passenger Expense

Other Passenger Expense = $XK\emptyset P \times \text{Revenue Passenger miles}$

Item IX Other Cargo Expense

Other Cargo Expense = $XK\emptyset C \times \text{Revenue Freight ton miles}$

Item X General and Administrative Expense

G&A Expense = $XKGA \times \text{Direct plus indirect Operating expense less depreciation and insurance}$

DOC & IOC MODEL SYMBOL DEFINITIONS

XNWRITE	=	Symbol for selecting the range
YEAR	=	Year input for calculating costs in the proper year's dollars
XNCREW	=	Number of personnel in the flight crew
XNPASS	=	Passenger capacity of the aircraft
XNATT	=	Number of cabin crew
XLF	=	Load factor
SSFB	=	Flight crew supersonic flight bonus
IFB	=	Flight crew international flight bonus
FCSIR	=	Flight crew salary inflation rate
ENG C	=	Engine cost per engine
MNTLIR	=	Maintenance labor inflation rate
TG	=	Ground time in minutes
U	=	Utilization
IRA	=	Insurance rate
PERIOD	=	Depreciation period
CFT	=	Cost of fuel (\$/LB)
COT	=	Cost of oil (\$/LB)
MBF	=	Maintenance burden factor
REVPAS	=	Number of revenue passengers per year
AVCARG	=	Average pounds of cargo per flight
XKSE	=	System expense IOC factor
XKLDE	=	Local expense IOC factor

XKCØ	= Aircraft control IOC factor
XKAT	= Cabin attendant IOC factor
XKFB	= Food and beverage IOC factor
XKPH	= Passenger handling IOC factor
XKCH	= Cargo handling IOC factor
XKØP	= Other passenger expense IOC factor
XKØC	= Other cargo expense IOC factor
XKGA	= G&A expense IOC factor
CFARE	= Fare cost factor - (function of distance)
XKFARE	= Constant portion of the fare - (function of no. of revenue passengers)
XKFACC	= Facilities cost (dollar input)
TAXR	= Income tax rate (decimal)
CARGF	= Revenue per cargo ton mile
FB	= Block fuel
TB	= Block time
WAF	= Weight of airframe (weight empty - engines)
TUAFc	= Total airframe cost
TF	= Flight time
TNACC	= Total aircraft flyaway cost including R&D

Return on Investment (ROI) Model

The return on investment (ROI) for the AST is calculated by two methods for two purposes. The method incorporated into the ASSET program is a simplified method used for comparative analysis or screening. The second method is established as a separate Computer program and provides a more detailed accounting of the economic factors involved in a realistic ROI.

The ROI model has the capability of calculating the DOC and IOC or accepting them as inputs. The DOC is calculated by the standard ATA method and by the modified ATA method as incorporated into the ASSET program (more detailed breakdown of the maintenance cost). The ROI model listing is included here for information purposes. The input listing and definitions is also included. The number in parenthesis indicates the input location in the program listing.

ROI INPUT SYMBOL DEFINITIONS

1. (16.5) GT = gate time
2. (17) K = K factors for IOC equations
3. (18) MF = factors for modifying maintenance equations
4. (19) U = annual utilization
5. (19) TB = block time
6. (19) FB = block fuel
7. (19) CFA = flyaway cost of the airplane
8. (19) XNPASS = aircraft passenger size
9. (19) RANGE = stage length flown
10. (19) LF = load factor
11. (19) YRDP = number of years of depreciation
12. (20) AFST = airframe spares factor
13. (20) ENSF = engine spares factor
14. (20) SSE = special support equipment cost factor
15. (20) REV 1 = zero range fare constant
16. (20) REV 2 = fare cost as a function of range
17. (20) DBTR = debt to equity ratio
18. (20) IR = interest rate
19. (20) TXRATE = tax rate
20. (20) AVCARG = average amount of cargo
21. (20) REV 3 = revenue rate for cargo (\$/ton mi)
22. (21) DSQ = number of aircraft in each quarter for a 10 year period
23. (22) AVAIL = number of aircraft available for operations from fleet buy (decimal fraction of total fleet)
24. (31) WAF = weight of airframe (WE-engine wt)
25. (31) TOGW = take off gross weight
26. (31) SSFB = supersonic flight bonus for crew
27. (31) XNCREW = number in flight crew
28. (31) XNENG = number of engines
29. (31) THRUST = maximum sea level static thrust of the engine

- 30. (31) IFB = international flight bonus for flight crew
- 31. (31) FCSIR = flight crew inflation rate
- 32. (31) MNTLIR = maintenance labor inflation rate
- 33. (31) XNYR = number of years for inflation (1967 to time period
of study)
- 34. (31) IRA = insurance rate
- 35. (31) PCTSAL = percent salvage
- 36. (31) CAF = cost of the airframe
- 37. (31) XMMAX = maximum cruise Mach number
- 38. (31) CE = cost of the engine
- 39. (31) XNATT = number of cabin attendants
- 40. (31) CFT = cost of fuel (\$/lb)
- 41. (31) COT = cost of oil (\$/lb)
- 42. (31) MBF = maintenance burden factor

*K factor inputs required if IOC is to be calculated. If IOC is available (\$/year) then input per line 188 of program.

**All of inputs on line 31 are required if DOC is to be calculated here.
If DOC is available (\$/year), then input per line 188 of the program.

The final calculation of the ROI is of the form:

$$\text{ROI} = \frac{(\text{REVENUE} - \text{EXPENSE} - \text{INTEREST}) (1 - \text{TAX RATE}) + \text{INTEREST}}{\text{AVERAGE VALUE OF INVESTMENT}}$$

```

1.      /*Program name is ROI AST.  Program calculates the ret
2.      urn on investment of a fleet of AST type aircraft.*//;
3.      /*The program either calculates the DOC and IOC, give
4.      n the proper inputs, or it uses the input values of D
5.      OC and IOC*/;
6.      /*Contact LOU VAUGHN, DICK KINSMAN, DEPT 67/10, EXT 7553
7.      6*/;
8.      DECLARE TB(5) DEC(6), FB(5) DEC(6), RANGE(5) DEC(6);
9.      DECLARE DOCFO(5) DEC(6), DOC(5) DEC(6), DOCMT(5) DEC(6)
10.     ;
11.     DECLARE MC(30,5) DEC(6) CTL, MCG(12,5) DEC(6) CTL, DOCE
12.     L(10,5) DEC(6), K(12) DEC(6), MF(28) DEC(6), IOCEL(10,5)
13.     DEC(6);
14.     DECLARE TMFHC(5) DEC(6), TMFCC(5) DEC(6), TLABN(5) DEC(
15.     6), TLABMB(5) DEC(6), TMATH(5) DEC(6);
16.     DECLARE IOC(5) DEC(6), IOCSUB(5) DEC(6);
17.     DECLARE TITLE1(10) CHAR(25) VAR, TITLE2(6) CHAR(14) VA
18.     R;
19.     DECLARE ACY(0:10) DEC(6), ACYAV(10) DEC(6), ACYAVL(10)
20.     DEC(6);
21.     DECLARE DSAV(10) DEC(6), DSY(10) DEC(6);
22.     DECLARE DSQ(10,4) DEC(6), REV(10) DEC(10), ROI(10) DEC(
23.     6), REVPAS(10) DEC(6), REVCAR(10) DEC(6);
24.     DECLARE INVAV(10) DEC(6), DEPR(10) DEC(6), INT(10) DEC(
25.     6), EXP(10) DEC(6), INC(10) DEC(6);
26.     DECLARE BKVAL(10) DEC(6), DEPRS(0:10) DEC(6), CASH(10)
27.     DEC(6);
28.     DECLARE TOTDBT(0:10) DEC(6), NEWDBT(10) DEC(6), AVDBT(1
29.     0) DEC(6);
30.     GET LIST(TITLE1, TITLE2);
31.     GET LIST(GT);
32.     GET LIST(K);
33.     GET LIST(MF);
34.     GET LIST(U, TB, FB, CFA, XNPASS, RANGE, LF, YRDP);
35.     GET LIST(AFSF, ENSF, SSE, REV1, REV2, DBTR, IR, TXRATE, AVCAR
36.     G, REV3);
37.     GET LIST(DSQ);
38.     GET LIST(AVAIL);
39.     /*SET L=0 IF DOC AND IOC ARE TO BE CALCULATED, L=1 IF
40.     ONLY ROI IS REQ'D.  SET M=0 IF DETAILED MAINT CALCS A
41.     RE DESIRED*/;
42.     GET LIST(L, M);
43.     /*m=FIRST RANGE FOR WHICH ROI CALCULATION IS DESIRED,
44.     n=LAST RANGE.  IF ALL FIVE ARE DESIRED, m=1, n=5*/;
45.     GET LIST(m, n);
46.     IF L=0 THEN GO TO SKIP2;
47.     GET LIST(WAF, TOGW, SSFB, XNCREW, XNENG, THRUST, IFB, FCSIR,
48.     MNTLIR, XNYR, IRA, PCTSAL, CAF, XMMA, CE, XNATT, CFT, COT, MBF
49.     );
50.     DOCFCR=(3*(45+SSFB)+35*(XNCREW-3)+IFB)*(1+FCSIR)**XNY
51.     R*U;

```



```

33.      DOCI=IRA*CFA;
34.      DOCD=(CFA+CAF*AFSF+CE*XNENG*ENSF)/YRDP*(1-PCTSAL);
35.      DO I=1 TO 5;
36.          DOCFO(I)=1.02*U*(FB(I)/TB(I)*CFT+XNENG*COT*.135);
37.      END ;
38.      MNTLR=4*(1+MNTLIR)**XNYR;
39.      IF M=0 THEN GO TO GROSS;
40.      /*EQUIPMENT AND FURNISHINGS LABOR*/;
41.      ALLOCATE MC;
42.      DO I=1 TO 5;
43.          MC(1,I)=(.5+4.5*WAF/10**6)*MF(1)*MNTLR*(TB(I)-GT)*U
              /TB(I);
44.          MC(2,I)=(1+18*WAF/10**6)*MF(2)*MNTLR*U/TB(I);
45.          MC(3,I)=MC(1,I)+MC(2,I);
46.          /*EQUIPMENT AND FURNISHINGS MATERIAL*/;
47.          MC(4,I)=(.4+14*WAF/10**6)*MF(3)*(TB(I)-GT)*U/TB(I);
48.          MC(5,I)=(1.2+42*WAF/10**6)*MF(4)*U/TB(I);
49.          MC(6,I)=MC(4,I)+MC(5,I);
50.          /*LANDING GEAR LABOR*/;
51.          MC(7,I)=(1+18*WAF/10**6)*MF(5)*MNTLR*U/TB(I);
52.          /*LANDING GEAR MATERIAL*/;
53.          MC(8,I)=(2.4+1.5*CAF/10**6)*MF(6)*U/TB(I);
54.          MC(9,I)=(1.2+70*WAF/10**6)*MF(6)*U/TB(I);
55.          MC(10,I)=MC(8,I)+MC(9,I);
56.          /*OTHER SYSTEMS LABOR*/;
57.          MC(11,I)=.015*(WAF*XMMAX)**.5*MF(7)*MNTLR*(TB(I)-GT)
              *U/TB(I);
58.          MC(12,I)=.0033*(WAF*XMMAX)**.5*MF(8)*MNTLR*U/TB(I);
59.          MC(13,I)=MC(11,I)+MC(12,I);
60.          /*OTHER SYSTEMS MATERIAL*/;
61.          MC(14,I)=(1.4+2.3*CAF/10**6)*XMMAX**.5*MF(9)*(TB(I)
              -GT)*U/TB(I);
62.          MC(15,I)=(.8+.7*CAF/10**6)*XMMAX**.5*MF(10)*U/TB(I)
              ;
63.          MC(16,I)=MC(14,I)+MC(15,I);
64.          /*STRUCTURES LABOR*/;
65.          MC(17,I)=(1+50*WAF/10**6)*XMMAX**.5*MF(11)*MNTLR*U/
              TB(I);
66.          /*STRUCTURES MATERIAL*/;
67.          MC(18,I)=(.3+.8*CAF/10**6)*XMMAX**.5*MF(12)*U/TB(I)
              ;
68.          /*OTHER POWER PLANT LABOR*/;
69.          MC(19,I)=.009*(WAF*XMMAX)**.5*MF(13)*MNTLR*(TB(I)-G
              T)*U/TB(I);
70.          MC(20,I)=.0008*(WAF*XMMAX)**.5*MF(14)*MNTLR*U/TB(I)
              ;
71.          MC(21,I)=MC(19,I)+MC(20,I);
72.          /*OTHER POWER PLANT MATERIAL*/;
73.          MC(22,I)=(.3+.8*CAF/10**6)*XMMAX**.5*MF(15)*(TB(I)-
              GT)*U/TB(I);
74.          MC(23,I)=(.1+.1*CAF/10**6)*XMMAX**.5*MF(16)*U/TB(I)
              ;

```

```
75.      MC(24,1)=MC(22,1)+MC(23,1);
76.      /*ENGINE LABOR*/;
77.      MC(25,1)=(.4+.018*THRUST/10**3)*MF(17)*XNENG*MNTLR*
      (TB(1)-GT)*U/TB(1);
78.      MC(26,1)=(.2+.012*THRUST/10**3)*MF(18)*XNENG*MNTLR*
      U/TB(1);
79.      MC(27,1)=MC(25,1)+MC(26,1);
80.      /*ENGINE MATERIAL*/;
81.      MC(28,1)=3.8*CE*XNENG/10**5*MF(19)*(TB(1)-GT)*U/TB(
      1);
82.      MC(29,1)=2.4*CE*XNENG/10**5*MF(20)*U/TB(1);
83.      MC(30,1)=MC(28,1)+MC(29,1);
84.      /*TOTAL MAINTENANCE FLIGHT HOUR COST*/;
85.      TMFHC(1)=(MC(1,1)+MC(4,1)+MC(11,1)+MC(14,1)+MC(19,1
      )+MC(22,1)+MC(25,1)+MC(28,1))/U;
86.      /*TOTAL MAINTENANCE FLIGHT CYCLE COST*/;
87.      TMFCC(1)=(MC(2,1)+MC(5,1)+MC(7,1)+MC(10,1)+MC(12,1)
      +MC(15,1)+MC(17,1)+MC(18,1)+MC(20,1)+MC(23,1)+MC(26
      ,1)+MC(29,1))*TB(1)/U;
88.      /*TOTAL MAINTENANCE LABOR*/;
89.      TLABM(1)=MC(3,1)+MC(7,1)+MC(13,1)+MC(17,1)+MC(21,1)
      +MC(27,1);
90.      /*TOTAL MAINTENANCE BURDEN*/;
91.      TLABMB(1)=MBF*TLABM(1);
92.      /*TOTAL MAINTENANCE MATERIAL*/;
93.      TMATM(1)=MC(6,1)+MC(10,1)+MC(16,1)+MC(18,1)+MC(24,1
      )+MC(30,1);
94.      END ;
95.      FREE MC;
96.      IF M=0 THEN GO TO SKIP1;
97.      GROSS:  ALLOCATE MCG;
98.      DO I=1 TO 5;
99.      /*AIRFRAME LABOR*/;
100.     MCG(1,1)=(.05*WAF/10**3+6-630/(WAF/10**3+120))*MF(2
      1)*MNTLR*XNMAX*.5*U/TB(1);
101.     MCG(2,1)=.59*MCG(1,1)*(TB(1)-GT)*MF(22);
102.     MCG(3,1)=MCG(1,1)+MCG(2,1);
103.     /*AIRFRAME MATERIAL*/;
104.     MCG(4,1)=3.08*CAF/10**6*MF(23)*(TB(1)-GT)*U/TB(1);
105.     MCG(5,1)=6.24*CAF/10**6*MF(24)*U/TB(1);
106.     MCG(6,1)=MCG(4,1)+MCG(5,1);
107.     /*ENGINE LABOR*/;
108.     MCG(7,1)=(.6+.027*THRUST/10**3)*XNENG*MF(25)*MNTLR*
      (TB(1)-GT)*U/TB(1);
109.     MCG(8,1)=(.3+.03*THRUST/10**3)*XNENG*MF(26)*MNTLR*U
      /TB(1);
110.     MCG(9,1)=MCG(7,1)+MCG(8,1);
111.     /*ENGINE MATERIAL*/;
112.     MCG(10,1)=K(11)*XNENG*CE/10**5*MF(27)*(TB(1)-GT)*U/
      TB(1);
113.     MCG(11,1)=K(12)*XNENG*CE/10**5*U/TB(1)*MF(28);
```

```

114.      MCG(12,1)=MCG(10,1)+MCG(11,1);
115.      /*TOTAL MAINTENANCE FLIGHT HOUR COST*/;
116.      TMFHC(1)=(MCG(4,1)+MCG(2,1)+MCG(7,1)+MCG(10,1))/U;
117.      /*TOTAL MAINTENANCE FLIGHT CYCLE COST*/;
118.      TMFCC(1)=(MCG(5,1)+MCG(1,1)+MCG(8,1)+MCG(11,1))*TB(
119.      1)/U;
120.      /*TOTAL MAINTENANCE LABOR*/;
121.      TLABM(1)=MCG(3,1)+MCG(9,1);
122.      /*TOTAL MAINTENANCE BURDEN*/;
123.      TLABMB(1)=MBF*TLABM(1);
124.      /*TOTAL MAINTENANCE MATERIAL*/;
125.      TMATM(1)=MCG(6,1)+MCG(12,1);
126.      END ;
127.      FREE MCG;
128.      SKIP1: DO I=1 TO 5;
129.          DOCMT(1)=TLABM(1)+TLABMB(1)+TMATM(1);
130.          DOC(1)=DOCFR+DOCFO(1)+DOCI+DOCD+DOCMT(1);
131.      END ;
132.      DO I=1 TO 5;
133.          DOCEL(1,1)=DOC(1)/U;
134.          DOCEL(2,1)=DOCEL(1,1)/(RANGE(1)/TB(1));
135.          DOCEL(3,1)=DOCEL(2,1)/XNPASS;
136.          DOCEL(4,1)=DOCEL(3,1)/LF;
137.          DOCEL(5,1)=DOCFR/(U/TB(1)*RANGE(1));
138.          DOCEL(6,1)=DOCFO(1)/(U/TB(1)*RANGE(1));
139.          DOCEL(7,1)=DOCI/(U/TB(1)*RANGE(1));
140.          DOCEL(8,1)=DOCD/(U/TB(1)*RANGE(1));
141.          DOCEL(9,1)=DOCMT(1)/(U/TB(1)*RANGE(1));
142.          DOCEL(10,1)=DOC(1)/(U/TB(1)*RANGE(1));
143.      END ;
144.      PUT LIST('          SYSTEM DIRECT OPERATING COSTS (DO
145.      LLARS/MILE)');
146.      PUT LIST(1f(1));
147.      PUT EDIT('RANGE (ST MI)',RANGE(1),RANGE(2),RANGE(3),R
148.      ANGE(4),RANGE(5))(A(19),(5) (F(9)));
149.      PUT EDIT('BLOCK TIME(HOURS)',TB(1),TB(2),TB(3),TB(4),
150.      TB(5))(A(19),(5) (F(9,3)));
151.      PUT EDIT('BLOCK FUEL(LBS)',FB(1),FB(2),FB(3),FB(4),FB
152.      (5))(A(19),(5) (F(9)));
153.      PUT LIST(1f(1));
154.      DO I=5 TO 10;
155.          IF I=10 THEN PUT LIST(1f(.5));
156.          PUT EDIT(TITLE2(I-4),DOCEL(1,1),DOCEL(1,2),DOCEL(1,
157.      3),DOCEL(1,4),DOCEL(1,5))(A(19),(5) (F(9,3)));
158.      END ;
159.      PUT LIST(1f(2));
160.      DO I=1 TO 5;
161.          IOCEL(1,1)=K(1)*TLABM(1)/(RANGE(1)*U/TB(1));
162.          IOCEL(2,1)=K(2)*(TOGW/10**3)/RANGE(1);
163.          IOCEL(3,1)=K(3)/RANGE(1);
164.          IOCEL(4,1)=K(4)*U*XNATT/(RANGE(1)*U/TB(1));

```

```

159.      IOCEL(5,1)=K(5)*U*XNPASS*LF/(RANGE(1)*U/TB(1));
160.      IOCEL(6,1)=K(6)*XNPASS*LF/RANGE(1);
161.      IOCEL(7,1)=K(7)*AVCARG/(2*10**3*RANGE(1));
162.      IOCEL(8,1)=K(8)*XNPASS*LF;
163.      IOCEL(9,1)=K(9)*AVCARG/(2*10**3);
164.      END ;
165.      DO J=1 TO 5;
166.        IOCSUB(J)=0;
167.        DO I=1 TO 9;
168.          IOCSUB(J)=IOCSUB(J)+IOCEL(I,J);
169.        END ;
170.      END ;
171.      DO I=1 TO 5;
172.        IOCEL(10,I)=K(10)*(DOC(I)-DOCD-DOCI)/(RANGE(1)*U/TB
(I))+K(10)*IOCSUB(I);
173.      END ;
174.      DO J=1 TO 5;
175.        IOC(J)=0;
176.        DO I=1 TO 10;
177.          IOC(J)=IOC(J)+IOCEL(I,J);
178.        END ;
179.      END ;
180.      PUT LIST('          SYSTEM INDIRECT OPERATING COSTS (DO
LLARS/MILE)');
181.      PUT LIST(1f(1));
182.      DO I=1 TO 10;
183.        PUT EDIT(TITLE1(I),IOCEL(I,1),IOCEL(I,2),IOCEL(I,3)
,IOCEL(I,4),IOCEL(I,5))(A(19),(5) (F(9,3)));
184.        IF I=10 THEN PUT LIST(1f(.5));
185.      END ;
186.      PUT EDIT('TOTAL IOC',IOC(1),IOC(2),IOC(3),IOC(4),IOC(
5))(A(19),(5) (F(9,3)));
187.      IF L=0 THEN GO TO SKIP3;
188.      SKIP2: GET LIST(DOC,IOC);
189.      SKIP3: DEPRS,ACY(0),INCSUM,BKVLSM,INTSUM,TOTDBT(0)=0;
190.      COST=CFA*(1+SSE)+AFSF*CAF+ENSF*CE*XNENG;
191.      DO I=m TO n;
192.        IF L=0 THEN IOC(I)=IOC(I)*RANGE(1)*U/TB(1);
193.        PUT LIST(1f(2));
194.        NWDTSM=0;
195.        DO J=1 TO 10;
196.          DSAV(J)=(4*DSQ(J,1)+3*DSQ(J,2)+2*DSQ(J,3)+DSQ(J,4
))/4;
197.          DSY(J)=DSQ(J,1)+DSQ(J,2)+DSQ(J,3)+DSQ(J,4);
198.          ACY(J)=ACY(J-1)+DSY(J);
199.          ACYAV(J)=ACY(J-1)+DSAV(J);
200.          ACYAVL(J)=ACYAV(J)*AVAIL;
201.          REVPAS(J)=(REV1+REV2*RANGE(1))*XNPASS*LF*U/TB(1)*
ACYAVL(J);
202.          REVCAR(J)=AVCARG/2000*U/TB(1)*RANGE(1)*ACYAVL(J)*
REV3;

```

```

203.      REV(J)=REVPAS(J)+REVCAR(J);
204.      INVAV(J)=ACYAV(J)*COST;
205.      DEPR(J)=INVAV(J)/YRDP;
206.      DEPRS(J)=DEPRS(J-1)+DEPR(J);
207.      NEWDBT(J)=DBTR*DSY(J)*COST;
207.5     NWDTSM=NWDTSM+NEWDBT(J);
208.      TOTDBT(J)=TOTDBT(J-1)+NEWDBT(J)-.1*NWDTSM;
209.      AVDBT(J)=TOTDBT(J-1)+DBTR*DSAV(J)*COST;
211.      INT(J)=IR*AVDBT(J);
212.      EXP(J)=(DOC(I)+IOC(I))*ACYAVL(J);
213.      BKVAL(J)=INVAV(J)-DEPRS(J);
214.      IF REV(J)-EXP(J)-INT(J)<0 THEN INC(J)=REV(J)-EXP(
J); ELSE INC(J)=REV(J)-EXP(J)-TXRATE*(REV(J)-EXP(
J)-INT(J));
215.      CASH(J)=INC(J)+DEPR(J)-INT(J);
216.      ROI(J)=INC(J)/BKVAL(J);
217.      INCSUM=INCSUM+INC(J);
218.      BKVLSM=BKVLSM+BKVAL(J);
219.      END ;
220.      ROI AV=INCSUM/BKVLSM;
221.      PUT EDIT('          RATE OF RETURN ON INVES
TMENT FOR',RANGE(1),' STATUTE MILE RANGE AIRCRAFT
')(A,F(8),A);
222.      PUT LIST(1f(.5));
223.      PUT LIST('YEAR      AVG NO  AIRCRAFT  AVERAGE      CUMUL
A-  AVERAGE  REVENUE  INTEREST  OPERATING      CAS
H    ROI');
224.      PUT LIST('          AIRCRAFT  ADDED      INVESTMENT      T
IVE    BOOK          EXPENSE  EXPENSE      INFL
OW');
225.      PUT LIST('          DURING  DURING  DURING  DEPRE
-  VALUE OF');
226.      PUT LIST('          YEAR    YEAR      YEAR      CIA
TION COMPANY');
227.      PUT LIST('          $M      $M      $M      $M      $M
          %');
228.      PUT LIST(1f(.5));
229.      T=1/10**6;
230.      DO J=1 TO 10;
231.      PUT EDIT(J,ACYAV(J),DSY(J),INVAV(J)*T,DEPRS(J)*T,
BKVAL(J)*T,REV(J)*T,INT(J)*T,EXP(J)*T,CASH(J)*T,R
OI(J)*100)(X(3),F(2),X(3),F(6,2),X(5),F(5,2),X(2)
,(7)(X(2),F(8,2)),X(3),F(6,2));
232.      END ;
233.      PUT LIST(1f(.5));
234.      PUT EDIT('          AVERAGE ROI OVER THE TEN YEAR
PERIOD=',ROI AV*100,'%')(A,F(5,2),A);
235.      END ;
236.      PUT LIST(1f(.5));

```

*ROI AST, VAUGHN 15,636 BYTES 203 SYMBOLS CREATED 73.241 BY D6710
LAST SAVED 74.016 LAST LOAD 74.018



REFERENCES

- A-1 "Cost-Estimating Relationships for Aircraft Airframes"
R-761-PR (abridged) February 1972.
- A-2 "Estimating Aircraft Turbine Engine Costs" RM-6384/1-PR,
September 1970.
- A-3 Standard Method of Estimating Comparative Direct Operating
Costs of Turbine Powered Transport Airplanes, Air Transport
Association, December 1967.
- A-4 "More Realism in a Standard Method for Estimating Airline
Operating Expense", Lockheed California Company, Report
OEA/SST/179, March 1966.
- A-5 "Revisions to 1964 Lockheed/Boeing Indirect Operating Expense
Method", Lockheed California Company, Report COA2061,
December 1969.
- A-6 Indirect Operating Expense Coefficients years 1963 through
1972, Lockheed California Company, COA/1277, June 1973.

APPENDIX B

COMPUTER PRINTOUT
ASSET PARAMETRIC ANALYSIS

CL-1701-6

LH2-AST

D-B TURBOFAN ENGINES



SUMMARY ID NO. 201

ASSET PARAMETRIC ANALYSIS

JANUARY 15 1974

AIRCRAFT MODEL --CL 1701-6

ENGINE 1.D. -- 1000

WING QUARTER CHORD SWEEP = 68.63 DEG

1.D.C. DATE --1990

SLS SCALE 1.0 = 81330

WING TAPER RATIO = 0.0

DESIGN SPEED --SUPERSONIC

NUMBER OF ENGINES = 4.

1 W/S	53.5	0.0	0.0	0.0	0.0	0.0	0.0	0.0	0.0	0.0	0.0	0.0	0.0	0.0	0.0	0.0	0.0
2 T/W	0.500	0.0	0.0	0.0	0.0	0.0	0.0	0.0	0.0	0.0	0.0	0.0	0.0	0.0	0.0	0.0	0.0
3 AR	1.62	0.0	0.0	0.0	0.0	0.0	0.0	0.0	0.0	0.0	0.0	0.0	0.0	0.0	0.0	0.0	0.0
4 T/C	3.00	0.0	0.0	0.0	0.0	0.0	0.0	0.0	0.0	0.0	0.0	0.0	0.0	0.0	0.0	0.0	0.0
5 RADIUS N. M1	4200	0	0	0	0	0	0	0	0	0	0	0	0	0	0	0	0
6 GROSS WEIGHT	368054	0	0	0	0	0	0	0	0	0	0	0	0	0	0	0	0
7 FUEL WEIGHT	95959	0	0	0	0	0	0	0	0	0	0	0	0	0	0	0	0
8 OP. WT. EMPTY	223094	0	0	0	0	0	0	0	0	0	0	0	0	0	0	0	0
9 ZERO FUEL WT.	272094	0	0	0	0	0	0	0	0	0	0	0	0	0	0	0	0
10 THRUST/ENGINE	48006	0	0	0	0	0	0	0	0	0	0	0	0	0	0	0	0
11 ENGINE SCALE	0.566	0.0	0.0	0.0	0.0	0.0	0.0	0.0	0.0	0.0	0.0	0.0	0.0	0.0	0.0	0.0	0.0
12 WING AREA	6880.	0.	0.	0.	0.	0.	0.	0.	0.	0.	0.	0.	0.	0.	0.	0.	0.
13 WING SPAN	105.6	0.0	0.0	0.0	0.0	0.0	0.0	0.0	0.0	0.0	0.0	0.0	0.0	0.0	0.0	0.0	0.0
14 P. TAIL AREA	5271.8	0.0	0.0	0.0	0.0	0.0	0.0	0.0	0.0	0.0	0.0	0.0	0.0	0.0	0.0	0.0	0.0
15 V. TAIL AREA	296.5	0.0	0.0	0.0	0.0	0.0	0.0	0.0	0.0	0.0	0.0	0.0	0.0	0.0	0.0	0.0	0.0
16 BODY LENGTH	326.1	0.0	0.0	0.0	0.0	0.0	0.0	0.0	0.0	0.0	0.0	0.0	0.0	0.0	0.0	0.0	0.0
COST DATA																	
17 RDTL - BIL.	3.320	0.0	0.0	0.0	0.0	0.0	0.0	0.0	0.0	0.0	0.0	0.0	0.0	0.0	0.0	0.0	0.0
18 FLYAWAY - MIL.	67.94	0.0	0.0	0.0	0.0	0.0	0.0	0.0	0.0	0.0	0.0	0.0	0.0	0.0	0.0	0.0	0.0
19 INVESTMENT-BIL.	1.014	0.0	0.0	0.0	0.0	0.0	0.0	0.0	0.0	0.0	0.0	0.0	0.0	0.0	0.0	0.0	0.0
20 LCC - C/SM	1.767	0.0	0.0	0.0	0.0	0.0	0.0	0.0	0.0	0.0	0.0	0.0	0.0	0.0	0.0	0.0	0.0
21 ICC - C/SM	0.801	0.0	0.0	0.0	0.0	0.0	0.0	0.0	0.0	0.0	0.0	0.0	0.0	0.0	0.0	0.0	0.0
22 RDI A.T. - 0/0	1.04	0.0	0.0	0.0	0.0	0.0	0.0	0.0	0.0	0.0	0.0	0.0	0.0	0.0	0.0	0.0	0.0
CONSTRAINT OUTPUT																	
23 TAKEOFF LST(1)	7141	0	0	0	0	0	0	0	0	0	0	0	0	0	0	0	0
24 CLIMB GRAD(1)	0.2007	0.0	0.0	0.0	0.0	0.0	0.0	0.0	0.0	0.0	0.0	0.0	0.0	0.0	0.0	0.0	0.0
25 TAKEOFF LST(2)	6988	0	0	0	0	0	0	0	0	0	0	0	0	0	0	0	0
26 CLIMB GRAD(2)	0.0660	0.0	0.0	0.0	0.0	0.0	0.0	0.0	0.0	0.0	0.0	0.0	0.0	0.0	0.0	0.0	0.0
27 LIDL ENDB D(1)	9239	0	0	0	0	0	0	0	0	0	0	0	0	0	0	0	0
28 AP SPEED-KT(1)	153.5	0.0	0.0	0.0	0.0	0.0	0.0	0.0	0.0	0.0	0.0	0.0	0.0	0.0	0.0	0.0	0.0
29 LIDL ENDB D(2)	9365	0	0	0	0	0	0	0	0	0	0	0	0	0	0	0	0
30 AP SPEED-KT(2)	154.6	0.0	0.0	0.0	0.0	0.0	0.0	0.0	0.0	0.0	0.0	0.0	0.0	0.0	0.0	0.0	0.0
31 LIDL ENDB D(3)	9491	0	0	0	0	0	0	0	0	0	0	0	0	0	0	0	0
32 AP SPEED-KT(3)	156.1	0.0	0.0	0.0	0.0	0.0	0.0	0.0	0.0	0.0	0.0	0.0	0.0	0.0	0.0	0.0	0.0

B-2



MISSIO SUMMARY

CL 1701-6 LM2-AS1 D-B TURBOFAN ENGINES

SEGMENT	INIT ALTITUDE (FT)	INIT MACH NO	INIT WEIGHT (LB)	SEGMENT FUEL (LB)	TOTAL FUEL (LB)	SEGMENT DIST (N MI)	TOTAL DIST (N MI)	SEGMENT TIME (MIN)	TOTAL TIME (MIN)	EXTERN STORE TAB ID	ENGINE THRUST TAB ID	EXTERN F TANK TAB ID	AVG L/D RATIO	AVG SFC (FF/T)	MAX OVER PRES
TAKEOFF POWER 1	0.	0.0	366054.	457.	457.	0.	0.	10.0	10.0	0.	-1101.	0.	0.0	0.149	0.0
POWER 2	0.	0.300	367597.	696.	1153.	0.	0.	0.5	10.5	0.	1209.	0.	6.35	0.359	0.0
CLIMB	0.	0.300	366901.	941.	2094.	5.	54	1.2	11.7	0.	1209.	0.	8.38	0.377	0.0
CRUISE	5000.	0.414	365960.	583.	2676.	0.	5.	4.0	15.7	0.	-1101.	0.	9.01	0.215	0.0
ACCEL	5000.	0.414	365377.	202.	2879.	4.	9.	0.7	16.4	0.	1101.	0.	9.89	0.233	0.0
CLIMB	5000.	0.539	365175.	4552.	7431.	103.	112.	13.7	30.1	0.	1101.	0.	9.84	0.336	0.0
CLIMB	34000.	0.989	366623.	16451.	23882.	447.	559.	24.0	54.2	0.	1206.	0.	6.20	0.558	0.0
CLIMB	63000.	2.760	344172.	444.	24326.	21.	560.	0.6	55.0	0.	1206.	0.	6.92	0.574	0.0
CRUISE	66000.	2.700	343727.	55622.	80148.	3420.	4000.	132.3	187.3	0.	-1201.	0.	6.99	0.561	0.0
DECEL	69000.	2.700	287906.	21.	80169.	32.	4031.	1.3	188.6	0.	1501.	0.	6.99	-0.209	0.0
DESCENT	69000.	2.282	267884.	193.	80363.	132.	4163.	11.9	200.5	0.	1501.	0.	7.97	-0.124	0.0
CRUISE	70000.	2.700	287691.	548.	80910.	36.	4200.	1.4	201.9	0.	-1201.	0.	6.97	0.566	0.0
CRUISE	5000.	0.414	287143.	531.	81441.	0.	4200.	5.0	206.9	0.	-1101.	0.	9.80	0.218	0.0
RESET	0.	0.0	286612.	0.	81441.	0.	4200.	0.0	206.9	0.	0.	0.	0.0	0.0	0.0
RESET	0.	0.0	286612.	0.	81441.	-4200.	0.	*****	0.0	0.	0.	0.	0.0	0.0	0.0
RESERVE	0.	0.0	286612.	5701.	87142.	0.	0.	0.0	0.0	0.	0.	0.	0.0	0.0	0.0
CLIMB	0.	0.200	280912.	578.	87720.	3.	3.	0.7	0.7	0.	1209.	0.	8.41	0.375	0.0
CLIMB	1500.	0.505	260333.	3343.	91064.	102.	105.	13.4	14.2	0.	1101.	0.	9.10	0.304	0.0
CRUISE	36000.	0.900	276990.	1457.	92521.	90.	195.	10.5	24.6	0.	-1201.	0.	9.67	0.293	0.0
DESCENT	36000.	0.900	275532.	119.	92640.	50.	245.	7.1	31.7	0.	1501.	0.	9.07	-0.169	0.0
CRUISE	36000.	0.900	275413.	248.	92888.	15.	260.	1.6	33.5	0.	-1201.	0.	9.66	0.292	0.0
CRUISE	15000.	0.503	275165.	3072.	95960.	0.	260.	30.0	63.5	0.	-1101.	0.	9.96	0.224	0.0
TUGWT= 366054.0 FUEL A= 95959.6 FUEL R= 95960.3															

B-3

REPRODUCIBILITY OF THE
ORIGINAL PAGE IS POOR



CL 1701-6 LH2-AST D-B TURBOFAN ENGINES

T/C AR W/S T/W
3.00 1.62 53.5 0.500

WEIGHT STATEMENT

	WEIGHT (POUNDS)	WEIGHT FRACTION	(PERCENT)
TAKE-OFF WEIGHT	(368054.)		
FUEL AVAILABLE	95960.	FUEL	26.07
ZERO FUEL WEIGHT	(272094.)		
PAYLOAD	49000.	PAYLOAD	13.31
OPERATING WEIGHT	(223094.)		
OPERATING ITEMS	5358.	OPERATING ITEMS	2.73
STANDARD ITEMS	4678.		
EMPTY WEIGHT	(213058.)		
WING	47205.		
TAIL	6913.		
BODY	44646.	STRUCTURE	39.51
LANDING GEAR	17201.		
SURFACE CONTROLS	4620.		
NACELLE AND ENGINE SECTION	2734.		
PROPULSION	(57996.)	PROPULSION	15.76
WEIGHT OF LIFT ENGINES	0.		
VECTOR CONTROL SYSTEM	0.		
ENGINES	24690.		
THRUST REVERSAL	0.		
AIR INDUCTION SYSTEM	9654.		
FUEL SYSTEM	21927.		
ENGINE CONTROLS + STARTER	1324.		
INSTRUMENTS	1092.		
HYDRAULICS	2797.		
ELECTRICAL	4593.		
AVIONICS	1900.	EQUIPMENT	8.62
FURNISHINGS AND EQUIPMENT	11500.		
ENVIRONMENTAL CONTROL SYSTEM	7860.		
AUXILIARY GEAR	1960.		
A.M.P.W.	(175618.)	TOTAL	(100.00)
EXCESS FUEL CAPACITY - BODY	-0.		
EXCESS FUEL CAPACITY - WING	0.		
EXCESS BODY LENGTH - FT	0.0		
STRUCTURE ALUMINUM			

B-4



WEIGHTS MATRIX

ELEMENT / MATERIAL	AL	TIT.	STEEL	COMP.	OTHER	TOTAL
WING	2171.	40407.	944.	2927.	755.	47205.
TAIL	311.	6423.	69.	0.	111.	6913.
FUSEL	14554.	22948.	804.	1116.	5224.	44646.
L. C.	17.	4300.	6605.	0.	6279.	17201.
NACELLE	52.	406.	909.	0.	0.	1367.
AIR INDUCT	453.	8731.	99.	0.	572.	9654.
S. CILS	1109.	208.	970.	69.	2264.	4620.
TOTALS	18668.	83423.	10400.	4112.	15203.	131607.



B-6

COST SUMMARY

RDT AND E		INVESTMENT			DIRECT OPERATIONAL COST (DOC)		
	TOTAL*		TOTAL*	PER PROD A/C**		C/SM***	PERCENT
PROTOTYPE AIRCRAFT	644.57	PRODUCTION AIRCRAFT	14390.07	47966.91	FLIGHT CREW	0.09816	5.49389
DESIGN ENGINEERING	803.61	PRODUCTION ENGINEERING	0.0	0.0	FUEL AND OIL	0.73470	41.11995
DEVELOPMENT TEST ARTICLES	293.33				INSURANCE	0.13702	7.66855
FLIGHT TEST	89.64				DEPRECIATION	0.44085	24.67360
ENGINE DEVELOPMENT CRUISE	656.96				MAINTENANCE	0.37600	21.04401
ENGINE DEVELOPMENT LIFT	0.0				TOTAL DOC	1.76671	100.000
AVIONICS DEVELOPMENT	0.0						
MAINTENANCE TRAINER DEVEL	0.0	MAINTENANCE TRAINERS	0.0	0.0	INDIRECT OPERATIONAL COST (IOC)		
OPERATOR TRAINER DEVELOP	0.0	OPERATOR TRAINERS	0.0	0.0		C/SM***	PERCENT
DEVELOPMENT TOOLING	700.86	PRODUCTION TOOLING	421.57	1405.23	SYSTEM	0.00316	0.39730
SPECIAL SUPPORT EQUIPMENT	12.89	SPECIAL SUPPORT EQUIPMENT	719.50	2396.34	LOCAL	0.09340	11.66091
DEVELOPMENT SPARES	100.08	PRODUCTION SPARES	2160.90	7203.00	AIRCRAFT CONTROL	0.00513	0.64028
TECHNICAL DATA	16.52	TECHNICAL DATA	88.46	294.87	CABIN ATTENDANT	0.07064	8.81928
TOTAL RDT E	3320.49	TOTAL INVESTMENT	17780.50	59268.34	FOOD AND BEVERAGE	0.02441	3.04780
					PASSENGER HANDLING	0.13656	17.04900
MISC. DATA		RETURN ON INVESTMENT (ROI)			CARGO HANDLING	0.00849	1.05977
RANGE (ST. MILES)	4833.04	TOTAL REVENUE PER YEAR *	469.73		OTHER PASSENGER EXPENSE	0.33550	41.88589
BLOCK SPEED (MPH)	1306.71	TOTAL EXPENSE PER YEAR *	410.84		OTHER CARGO EXPENSE	0.00278	0.34680
FARE (1)	246.72	TOTAL INVESTMENT *	1014.47		GENERAL + ADMINISTR.	0.12089	15.09296
FLEET SIZE	14.42	INCL. FACILITIES ROI BEFORE TAXES	11.61		TOTAL IOC	0.80098	100.000
PRODUCTION BASIS	300.00	ROI AFTER TAXES	6.04				
REV. PASSENG. (MIL. PER YR)	1.81						
AVER. CARGO PER FLIGHT	2000.00						
FLIGHT PER A/C PER YEAR	973.33						

* - MILLIONS OF DOLLARS

** - 1000 OF DOLLARS PER PRODUCTION A/C

*** - CENTS PER SEAT MILE



RESEARCH DEVELOPMENT TEST AND EVALUATION (RDTE)

	DEVELOPMENT AND DESIGN	CONTRACTOR TEST AND EVALU	DEVELOPMENT AIRCRAFT	TOTAL RDT AND E
AIRFRAME	1308.24	333.02	443.60	2084.86
ENGINEERING				
HOURS	40230.	7508.	2210.	49948.
LABOR RATE	8.17	8.17	6.17	8.17
OVERHEAD RATE	9.20	9.20	9.20	9.20
TOTAL	698.79	130.42	38.39	867.59
TOOLING				
HOURS	30201.	1842.	3683.	35726.
LABOR RATE	6.09	6.09	6.09	6.09
OVERHEAD RATE	12.36	12.36	12.36	12.36
TOTAL	609.45	33.98	67.96	711.38
MANUFACTURING				
HOURS		7367.	14733.	22100.
LABOR RATE		5.12	5.12	5.12
OVERHEAD RATE		10.72	10.72	10.72
TOTAL		116.69	233.38	350.06
QUALITY CONTROL				
HOURS		1473.	2947.	4420.
LABOR RATE		6.29	6.29	6.29
OVERHEAD RATE		10.72	10.72	10.72
TOTAL		25.06	50.12	75.18
MATERIAL				
RAW AND PRCHSD		7.77	15.55	23.32
PURCHASED EQUIP		14.44	26.87	43.31
TOTAL		22.21	44.42	66.63
MISCELLANEOUS				
HOURS		295.	589.	884.
LABOR RATE		5.12	5.12	5.12
OVERHEAD RATE		10.72	10.72	10.72
TOTAL		4.67	9.34	14.00
ENGINES	658.98		65.89	724.86
AVIONICS	0.0		2.00	2.00
PROFIT (AIRFRAME)	196.24	49.95	66.54	312.73
INSUR.+TAXES			44.36	44.36
WARRANTY			22.18	22.18
SUBTOTAL	2163.45	382.98	644.57	3190.99
OTHER ITEMS				129.50
TOTAL (RDTE)				3320.49

B-7

REPRODUCIBILITY OF THE
ORIGINAL PAGE IS POOR



B-8

	PRODUCTION										TOTAL
	PRODUCTION YEARS										
	1	2	3	4	5	6	7	8	9	10	
AIRFRAME	862.27	601.06	681.57	966.23	1048.35	970.96	916.47	875.06	842.02	814.74	8978.73
ENGINEERING											
HOURS	3103.	2673.	2829.	3006.	3177.	2879.	2671.	2514.	2368.	2285.	27525.
LABOR RATE	8.17	8.17	8.17	8.17	8.17	8.17	8.17	8.17	8.17	8.17	
OVLKHEAD RATE	9.20	9.20	9.20	9.20	9.20	9.20	9.20	9.20	9.20	9.20	
TOTAL	53.90	46.43	49.13	52.21	55.18	50.01	46.40	43.66	41.49	39.70	478.11
TOOLING											
HOURS	3724.	3206.	3394.	3607.	3612.	3455.	3205.	3016.	2866.	2742.	33030.
LABOR RATE	6.09	6.09	6.09	6.09	6.09	6.09	6.09	6.09	6.09	6.09	
OVLKHEAD RATE	12.36	12.36	12.36	12.36	12.36	12.36	12.36	12.36	12.36	12.36	
TOTAL	68.71	59.18	62.62	66.55	70.33	63.75	59.14	55.65	52.68	50.80	609.40
MANUFACTURING											
HOURS	31033.	26731.	26286.	30058.	31768.	28793.	26710.	25135.	23883.	22854.	275251.
LABOR RATE	5.12	5.12	5.12	5.12	5.12	5.12	5.12	5.12	5.12	5.12	
OVLKHEAD RATE	10.72	10.72	10.72	10.72	10.72	10.72	10.72	10.72	10.72	10.72	
TOTAL	491.56	423.42	448.05	476.12	503.20	456.07	423.09	398.14	378.31	362.01	4359.97
QUALITY CONTROL											
HOURS	6207.	5346.	5657.	6012.	6354.	5759.	5342.	5027.	4777.	4571.	55050.
LABOR RATE	6.29	6.29	6.29	6.29	6.29	6.29	6.29	6.29	6.29	6.29	
OVLKHEAD RATE	10.72	10.72	10.72	10.72	10.72	10.72	10.72	10.72	10.72	10.72	
TOTAL	105.57	90.94	96.23	102.26	108.07	97.95	90.67	85.51	81.25	77.75	936.40
MATERIAL											
RAW AND PURCH	43.00	57.45	72.67	87.52	102.00	99.73	98.02	96.66	95.54	94.57	847.16
PURCHASED EQUIP	79.66	106.70	134.95	162.53	189.43	165.21	182.04	179.52	177.42	175.64	1573.29
TOTAL	122.66	164.15	207.62	250.04	291.43	264.93	260.06	276.18	272.96	270.21	2420.45
MISCELLANEOUS											
HOURS	1241.	1069.	1131.	1202.	1271.	1152.	1068.	1005.	955.	914.	11010.
LABOR RATE	5.12	5.12	5.12	5.12	5.12	5.12	5.12	5.12	5.12	5.12	
OVLKHEAD RATE	10.72	10.72	10.72	10.72	10.72	10.72	10.72	10.72	10.72	10.72	
TOTAL	19.66	16.94	17.92	19.04	20.13	18.24	16.92	15.93	15.13	14.48	174.40
ENGINES	167.27	196.53	235.07	272.19	307.64	293.71	283.49	275.47	268.91	263.37	2563.64
AVIONICS	6.00	9.00	12.00	15.00	18.00	18.00	18.00	18.00	18.00	18.00	150.00
PROFIT	129.34	120.16	132.24	144.93	157.25	145.64	137.47	131.26	126.30	122.21	1346.81
INSUR.+TAXES	86.23	80.11	88.16	96.62	104.83	97.10	91.65	87.51	84.20	81.47	897.87
WARRANTY	43.11	40.05	44.08	48.31	52.42	48.55	45.82	43.75	42.10	40.74	448.94
TOTAL FLYAWAY	1294.22	1246.90	1393.12	1543.29	1668.50	1573.96	1492.90	1431.05	1381.53	1344.63	14390.07



RATE OF RETURN ON INVESTMENT FOR 4074 Kilometer (2200 n.mi.) MILE RANGE

YEAR	AVG NO AIRCRAFT DURING YEAR	AIRCRAFT ADDED DURING YEAR	AVERAGE INVESTMENT DURING YEAR \$M	CUMULA- TIVE DEPRE- CIATION \$M	AVERAGE BOOK VALUE OF COMPANY \$M	REVENUE \$M	INTEREST EXPENSE \$M	OPERATING EXPENSE \$M	CASH INFLOW \$M	ROI %
1	0.65	1.04	46.79	3.34	43.45	15.79	2.25	17.01	-0.11	-2.79
2	1.69	1.04	121.65	12.03	109.62	41.07	5.48	44.21	0.06	-2.87
3	2.73	1.04	196.52	26.07	170.45	66.34	8.35	71.42	0.60	-2.98
4	3.77	1.04	271.38	45.45	225.93	91.61	10.87	98.63	1.49	-3.11
5	4.81	1.04	346.25	70.19	276.06	116.88	13.03	125.84	2.74	-3.25
6	5.85	1.04	421.11	100.26	320.85	142.15	14.82	153.05	4.36	-3.40
7	6.89	1.04	495.98	135.60	360.28	167.42	16.26	180.26	6.33	-3.56
8	7.93	1.04	570.84	176.47	394.37	192.69	17.34	207.47	8.66	-3.75
9	8.97	1.04	645.70	222.50	423.12	217.96	18.06	234.67	11.35	-3.95
10	10.01	1.04	720.57	274.06	446.51	243.23	18.42	261.88	14.40	-4.18

AVERAGE ROI OVER THE TEN YEAR PERIOD=-3.58%



RATE OF RETURN ON INVESTMENT FOR 7778 Kilometer (4200 n.mi.) MILE RANGE

YEAR	AVG NO AIRCRAFT DURING YEAR	AIRCRAFT ADDED DURING YEAR	AVERAGE INVESTMENT DURING YEAR \$M	CUMULA- TIVE DEPRE- CIATION \$M	AVERAGE BOOK VALUE OF COMPANY \$M	REVENUE \$M	INTEREST EXPENSE \$M	OPERATING EXPENSE \$M	CASH INFLOW \$M	ROI %
1	1.00	1.60	71.98	5.14	66.84	29.30	3.46	25.63	5.25	5.34
2	2.60	1.60	187.16	18.51	168.65	76.18	8.43	66.64	13.95	5.34
3	4.20	1.60	302.34	40.11	262.23	123.06	12.85	107.64	22.93	5.41
4	5.80	1.60	417.51	69.93	347.58	169.94	16.72	148.65	32.20	5.49
5	7.40	1.60	532.69	107.98	424.71	216.82	20.04	189.65	41.75	5.59
6	9.00	1.60	647.86	154.25	493.61	263.70	22.80	230.66	51.60	5.70
7	10.60	1.60	763.04	208.76	554.28	310.58	25.02	271.67	61.73	5.82
8	12.20	1.60	878.22	271.49	606.73	357.46	26.67	312.67	72.15	5.95
9	13.80	1.60	993.39	342.44	650.95	404.34	27.78	353.68	82.85	6.10
10	15.40	1.60	1108.57	421.63	686.94	451.22	28.33	394.68	93.85	6.26

AVERAGE ROI OVER THE TEN YEAR PERIOD= 5.84%

APPENDIX C

STRESS ANALYSIS
OF
CANDIDATE TANK DESIGNS

TABLE OF NOMENCLATURE

APPENDIX C

C	= Distance from neutral axis to outer shell
C_f	= Stability constant 62.5×10^{-6}
D	= Fuselage diameter
D_{eff}	= Effective diameter
E	= Young's modulus
F_{TU}	= Ultimate allowable stress
f	= Applied stress
f_b	= Bending stress
f_{ALT}	= Tank stress at maximum altitude
f_c	= Compressive stress
f_{CCR}	= Compressive buckling stress
f_s	= Shear stress
$f_{S.L.}$	= Tank stress at sea level
f_{SCR}	= Shear buckling stress
f_t	= Tension stress
f_{t_L}	= Longitudinal tension stress
I	= Moment of inertia
Kt	= Quality factor for fatigue
L	= Ring spacing
LIM	= Limit
M	= Bending Moment
M.S.	= Margin of safety
n_z	= Vertical load factor
p	= Pressure
P	= Load
P_T	= Tension load per inch
R	= Radius
ρ	= Radius of gyration
S.L.	= Sea level
Sa	= Alternating stress
Sm	= Mean stress

TABLE OF NOMENCLATURE (Continued)

APPENDIX C

t	=	Skin thickness
t_e	=	Effective thickness of shell
ULT	=	Ultimate
W_{n_z}	=	Load
w	=	Distributed load

APPENDIX C
STRESS ANALYSIS OF CANDIDATE TANK DESIGNS

NON-INTEGRAL TANKS

At maximum tank dia.

Tank Press. = 23 psia

at S.L.

$$\Delta P + 23.0 - 14.7 = 8.3 \text{ psi}$$

at 75,000'

$$\Delta P = 23.0 - 0.5 + 22.5 \text{ psi}$$

For tank shell

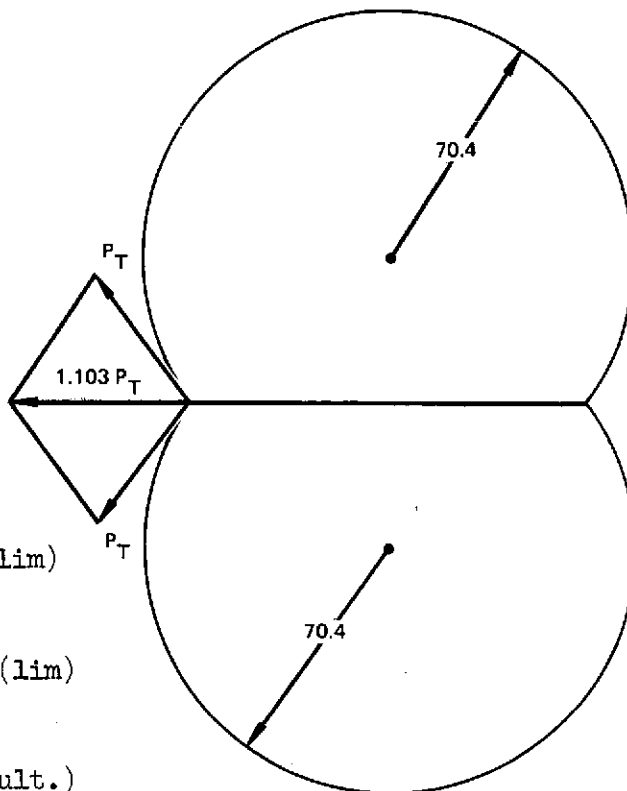
$$t = 0.05$$

$$f_{S.L.} = \frac{8.3 \times 70.4}{0.050} = 11,700 \text{ psi (lim)}$$

$$f_{ALT.} = \frac{22.5 \times 70.4}{0.050} = 31,700 \text{ psi (lim)}$$

$$f_{S.L.} = 2 \times 11,700 = 23,400 \text{ psi (ult.)}$$

$$f_{ALT} = 2 \times 31,700 = 63,400 \text{ psi (ult.)}$$

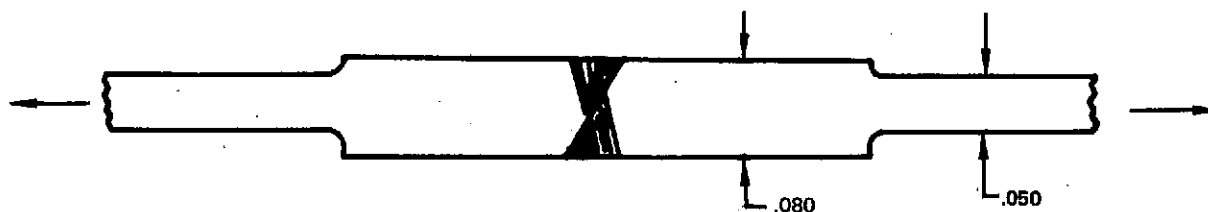


For 2219-T87 aluminum alloy

$$F_{TU} = 64,000 \text{ psi (Mil Hndbk 5)}$$

$$M.S. = 64,000/63,400 - 1 = \underline{\underline{0.01}}$$

For welded joints:



$$f_t = \frac{22.5 \times 2 \times 70.4}{0.080} = 39,600 \text{ psi}$$

Strength Across Welds

$$F_{tu} = 41,000 \text{ psi (Ref. Aerospace Structural Metals Hndbk. Code 3205 Pg.5)}$$

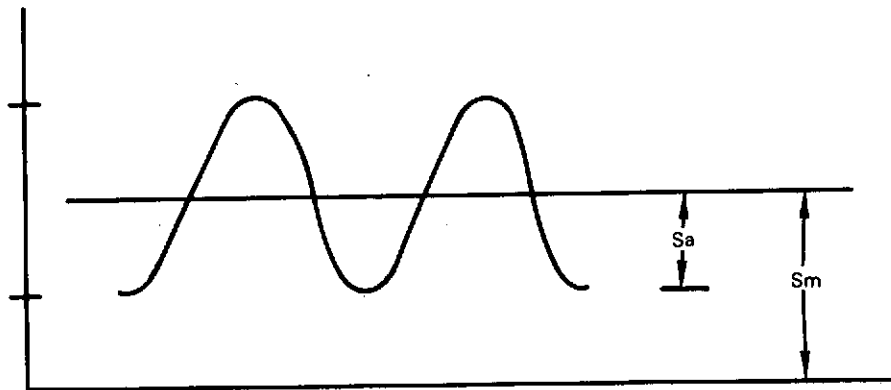
$$\text{M.S.} = 41,000/39,600 - 1 = \underline{\underline{0.03}}$$

FATIGUE CONSIDERATIONS FOR BASIC SHELL

For the following refer to Lockheed Engineering "Structural Life-Assurance Manual."

For 50,000 hr. life assume average flight at 3 hr.

$$\text{No. cycles} = 50,000/3 = 16,700$$

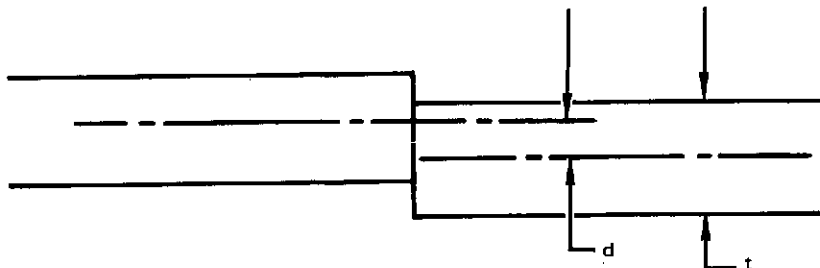


(Ref. SIM #4 Pg. 5)

$$\text{Mean Stress, } S_m = \frac{31,700 + 11,700}{2} = 21,700 \text{ psi}$$

$$\text{Alternating Stress, } S_a = \frac{31,700 - 11,700}{2} = 10,000 \text{ psi}$$

For mismatched welded joints in a cylindrical pressure vessel (Ref. SLM 7b Pg. 73)



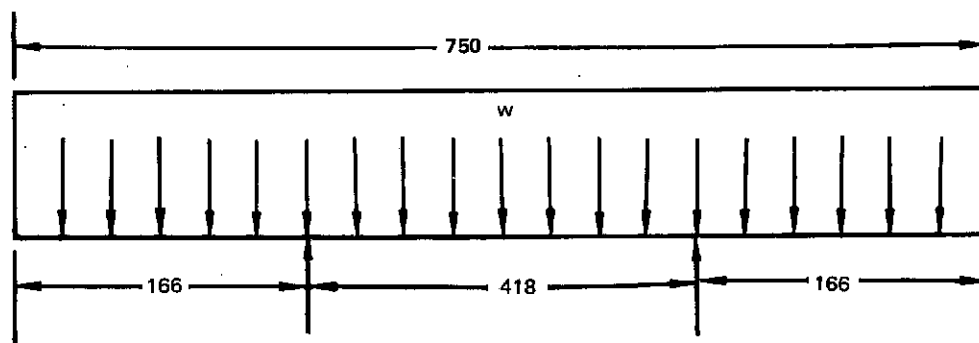
Assume $d/t = 0.30$

$K_t = 2$ for longitudinal joints (SLM 7b Pg. 72)

For this K_t and the above stress values the life exceeds 100,000 cycles for standard aluminum alloy. (Ref. SLM No. 16b, Pg. 5)

The above is based on the basic shell stresses and fatigue properties since they are not available for the welded material, but it is felt that it represents a good approximation. The scatter factor of 6 and the disregarding of the beneficial effects of the cryogenic temperatures serve to give confidence of a safe life for the tank.

TANK SHEAR AND BENDING



Dimensions For Front Tank (approximate)

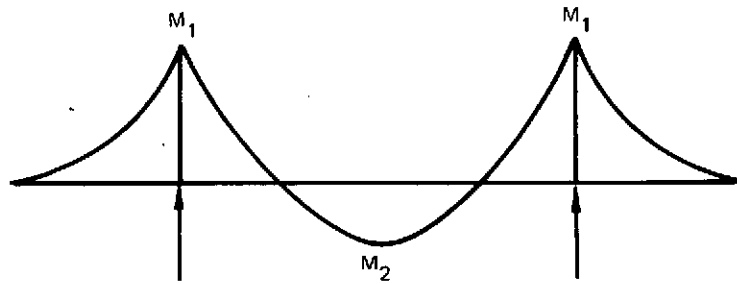
Tank and insulation is 19.1 percent of fuel weight.

Volume of forward tank = 10,479 ft.³

$$hz = 2.5 \text{ g}$$

$$W_{nz} = 10,479 \times 1.191 \times 4.42 \times 2.5 \times 1.5 = 207,000 \text{ lb (ult)}$$

$$w = 207,000/750 = 276 \text{ lb/in.}$$



$$M_1 = 3.81 \times 10^6 \text{ in.lb}$$

$$M_2 = -2.23 \times 10^6 \text{ in.lb}$$

FORWARD TANK

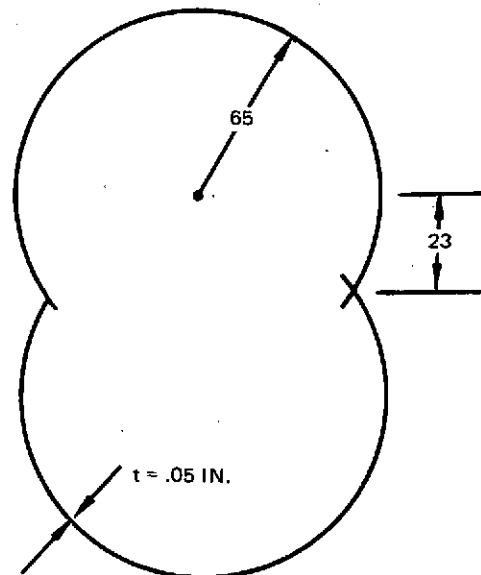
Approximate dimensions at forward mount

$$I = 0.808 \times 10^5 \text{ in.}^4$$

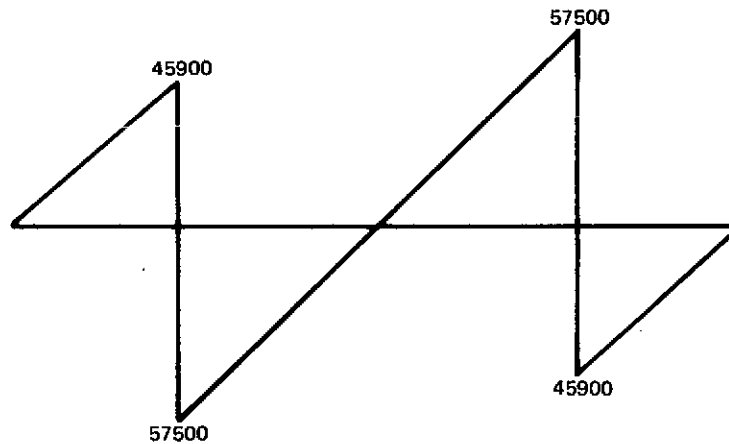
$$f_c = \frac{mc}{I}$$

$$= \frac{3.81 \times 10^6 \times 88}{0.808 \times 10^5}$$

$$= 4,150 \text{ psi}$$



TANK SHEAR



$$f_s = \frac{57,500}{2 \times 0.785 \times 176 \times 0.05} = 4,160 \text{ psi}$$

COMPRESSION BUCKLING STRESS

$$f_{CCH} = \frac{0.3Et}{R} = \frac{0.3 \times 10^7 \times 0.05}{65}$$
$$= 2,300 \text{ psi}$$

SHEAR BUCKLING STRESS

$$f_{SCR} = \frac{0.1Et}{R} = \frac{0.1 \times 10^7 \times 0.05}{65}$$
$$= 770 \text{ psi}$$

The shear and compressive buckling stresses are below the applied stresses but the shell will be supported by the insulation applied to the surface. The shell will also be stabilized by the internal pressure and it is not anticipated that there will be a loss of pressure and insulation at the same time.

INTEGRAL TANK

A typical section is at F.S. 2710 -
near the forward end of the aft tank.

$$I = 3.14 \times 10^6 \text{ in.}^4$$

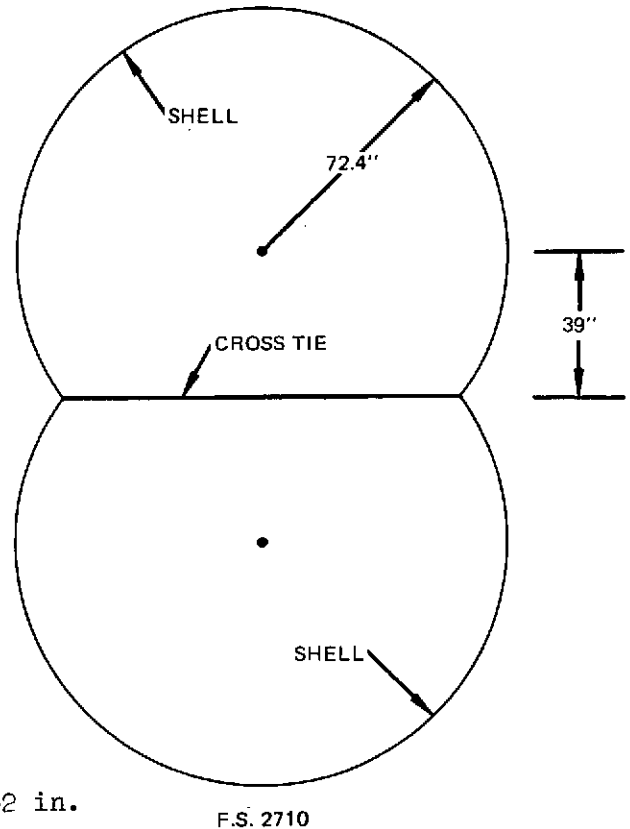
For this station

$$M = 114 \times 10^6 \text{ in.-lb (Ref. Pg.)}$$

Maintaining a tension and compression
stress level of 40,000 psi

$$\frac{Mc}{I} = 40,000 \text{ psi}$$

$$t_e = \frac{114 \times 10^6 \times 1.5 \times 111.4}{3.14 \times 10^6 \times 40,000} = 0.152 \text{ in.}$$



Additional thickness is required on the upper surface to take pressure induced
longitudinal tension loads.

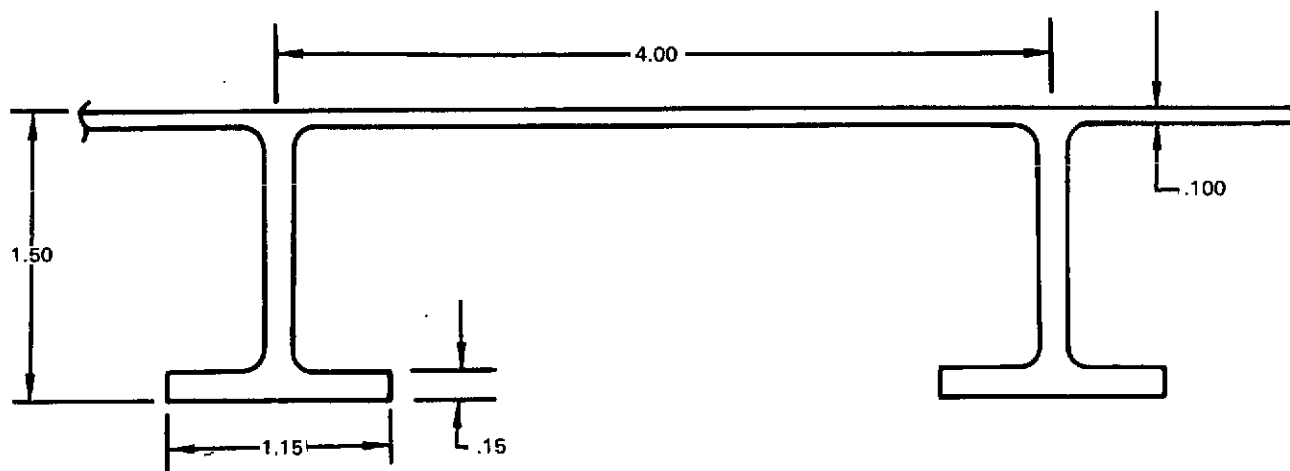
$$f_{t1} = \frac{PR}{2t} = \frac{22.5 \times 1.5 \times 72.4}{2t} = 40,000 \text{ psi}$$

$$t = \frac{72.4 \times 22.5 \times 1.5}{2 \times 40,000} = 0.031$$

Note: When bending and pressure stresses are added, a multiplying factor of
1.5 instead of 2 is used for the pressure.

$$\text{Total Upper Surface Effective Thickness} = 0.152 + 0.031 = 0.183 \text{ in.}$$

TYPICAL UPPER SURFACE INTEGRALLY STIFFENED SKIN SECTION



INTERNAL SUPPORT RINGS

To ensure against general instability of the load carrying surfaces the following ring stiffness is required:

$$(EI)_{\text{RING}} = \frac{C_f MD^2}{L}$$

M = Bending Moment

D = Fuselage Diameter

L = Ring Spacing

C_f = A Constant $\approx 62.5 \times 10^{-6}$

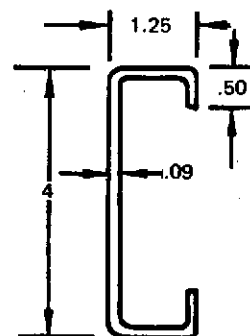
At F.S. 2710

$M = 114 \times 10^6$ $D_{\text{eff}} = 200 \text{ in.}$

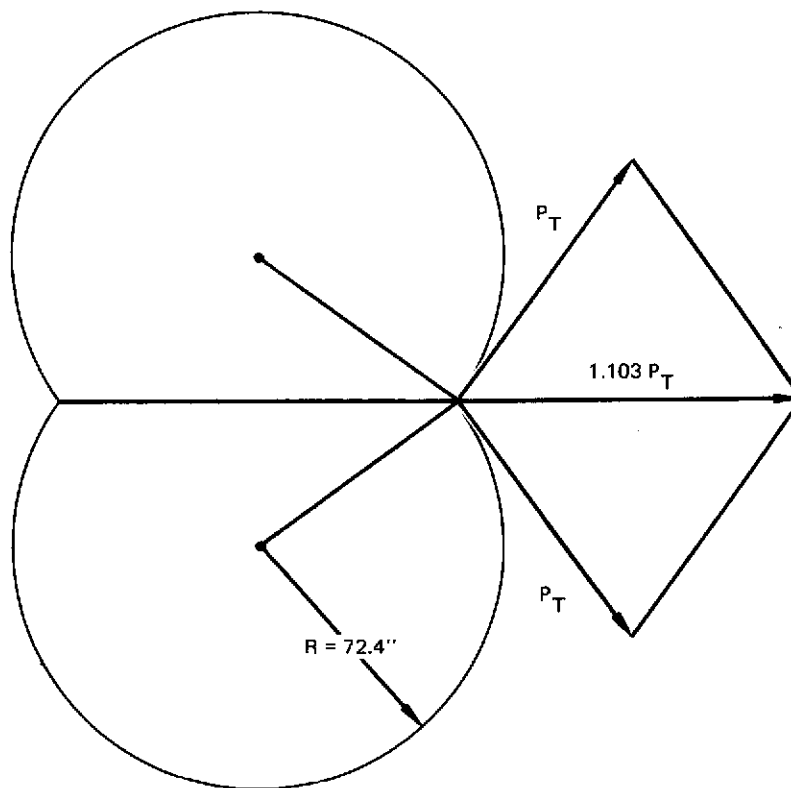
$L = 20 \text{ in.}$

$$I_{\text{RING}} = \frac{62.5 \times 10^{-6} \times 114 \times 10^6 \times 200^2}{20 \times 10.5 \times 10^6} = 1.36 \text{ in.}^4$$

A ring cross section as shown fulfills this requirement.



CROSS TIE



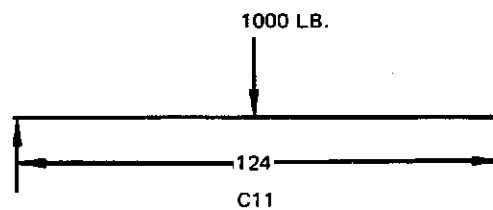
SECTION AT F.S. 2710

For $\Delta P = 22.5$ psi

$$P_T = 22.5 \times 2 \times 72.4 = 3,260 \text{ lb/in.}$$

$$\text{Cross tie load} = 1.103 \times 3260 = 3600 \text{ lb/in.}$$

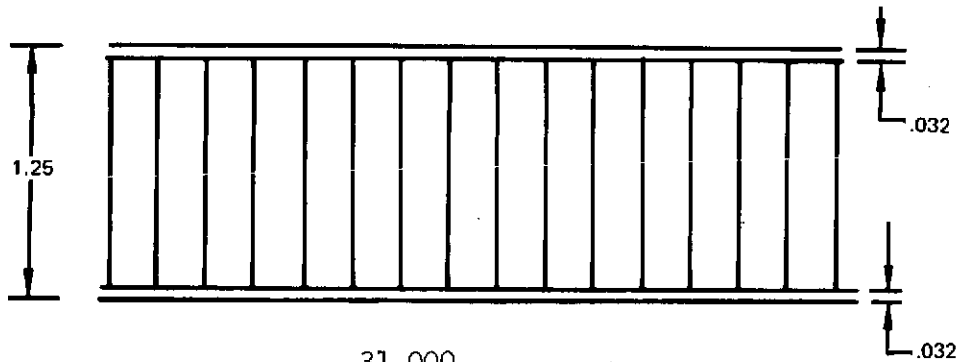
The cross tie member acts as a walkway in addition to transmitting the above load:



$$M = \frac{PL}{4} = \frac{1,000 \times 124}{4} = 31,000 \text{ in.-lb.}$$

C-11

This bending moment is spread over 12 inches of sandwich panel.



$$f_b = \frac{31,000}{12 \times 1.25 \times 0.032} = 65,000 \text{ psi}$$

$$f_t = \frac{3,600}{2 \times 0.032} = 56,000 \text{ psi}$$

For 2024-T861

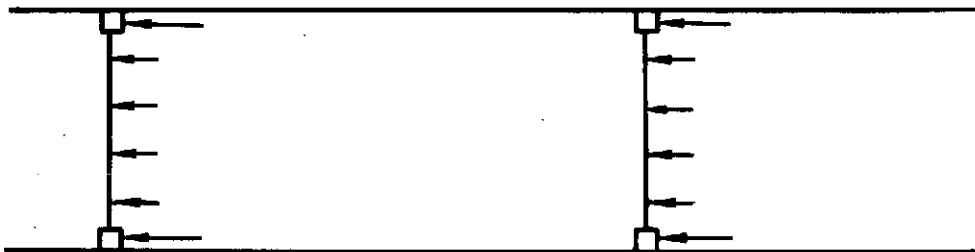
$$FTU = 65,000 \text{ psi}$$

(Ref. Mil Hndbk 5,
Table 3.2.3.0(e))

$$M.S. = \frac{65,000}{65,000} - 1 = 0.00 \text{ (Bending)}$$

$$M.S. = \frac{65,000}{56,000} - 1 = 0.16 \text{ (Tension)}$$

BAFFLES



Baffles are spaced at 200 inches and are designed by 9 g(n_x) crash condition

$$p = \frac{4.42 \times 9 \times 200}{1,728} = 4.60 \text{ psi}$$

Baffles are 0.020 aluminum membrane.

Edge Stress:

$$f_t = 0.328 \sqrt[3]{\frac{EP^2 R^2}{t^2}} \quad (\text{Ref. Roark, Pg. 215})$$

$$= 0.328 \sqrt[3]{\frac{10.5 \times 10^6 \times 4.6^2 \times 72.4^2}{0.02^2}}$$

$$= 46,900 \text{ psi}$$

Peripheral Ring Axial Load

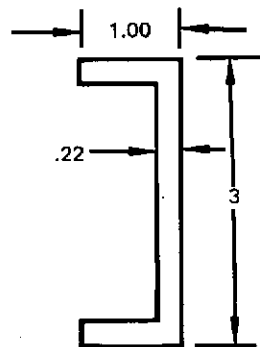
$$P_A = 46,900 \times 0.02 \times 72.4 = 67,900 \text{ lb.}$$

Stiffness Requirement

$$E_I = \frac{PR^3}{3} \quad (\text{Ref. Roark, Pg. 306})$$

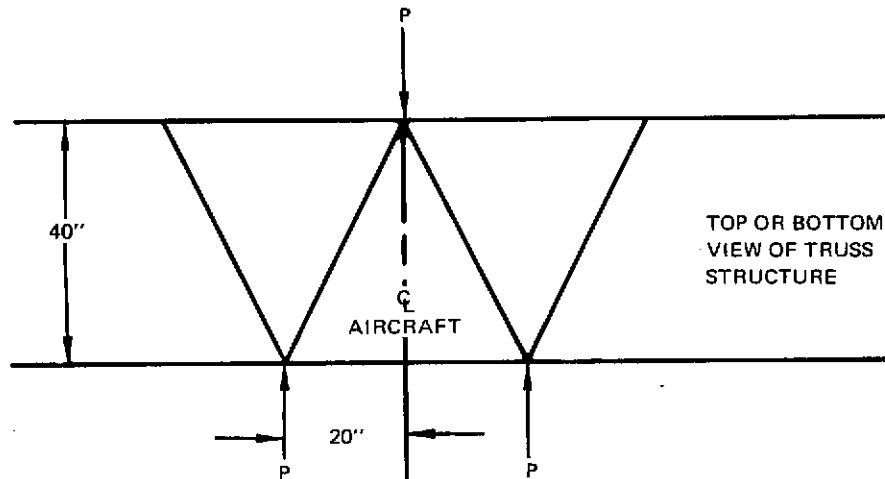
$$I = \frac{46,900 \times 0.02 \times 72.4^3}{3 \times 10.5 \times 10^6} = 1.13 \text{ in.}^4$$

A ring of the following dimensions fulfills the requirements



TRANSITION STRUCTURE (For Integral Tanks)

Forward Transition of Aft Tank



F.S. 2710

$$I = 3.14 \times 10^6 \text{ te} \quad C = 111.4 \text{ in.}$$

$$M = 114 \times 10^6 \text{ in.-lb (lim)}$$

$$f = \frac{Mc}{I} = \frac{1.5 \times 114 \times 10^6 \times 111.4}{3.14 \times 10^6 \text{ te}}$$

$$w = fte = \frac{1.5 \times 114 \times 10^6 \times 111.4}{3.14 \times 10^6}$$

$$w = 6,070 \text{ lb/in.}$$

$$P = 40 \times 6,070 = 242,500 \text{ lb}$$

Load In Strut

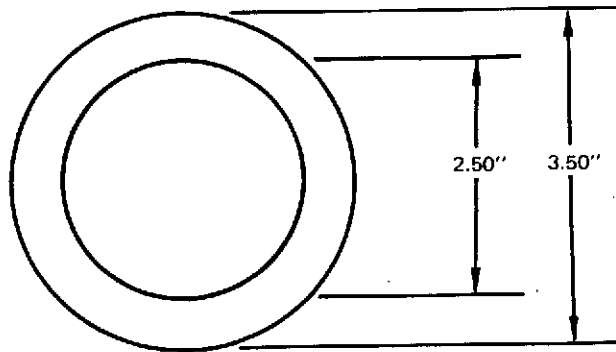
$$P_s = \frac{242,500}{2 \cos 25.66} = 134,500 \text{ lb}$$

STRUT SIZE (MAXIMUM)

The strut design is based on the configurations depicted in the report "Fiberglass Supports for Cryogenic Tanks," NASA CR-120937, IMSC-D281476. The strut stress is limited to 30,000 psi (ult) for fatigue considerations.

$$\text{Length} = 40 / \cos 25.66^\circ = 44.4 \text{ in.}$$

CROSS SECTION



$$A = 4.712 \text{ in.}^2$$

$$\rho = 1.056 \text{ in.}$$

$$E = 6.5 \times 10^6$$

$$f = 140,000 / 4.712 = 29,700 \text{ psi}$$

$$\text{Tension M.S.} = 30,000 / 29,700 - 1 = \underline{\underline{0.01}}$$

$$P_{\text{COL}} = \frac{\pi^2 EA}{(L/\rho)^2} = \frac{9.85 \times 6.5 \times 10^6 \times 4.717}{(44.4/1.056)^2} = 171,000 \text{ lb}$$

$$\text{Compression M.S.} = 171,000 / 140,000 - 1 = \underline{\underline{0.22}}$$